

INFORMATION TO USERS

This manuscript has been reproduced from the microfilm master. UMI films the text directly from the original or copy submitted. Thus, some thesis and dissertation copies are in typewriter face, while others may be from any type of computer printer.

The quality of this reproduction is dependent upon the quality of the copy submitted. Broken or indistinct print, colored or poor quality illustrations and photographs, print bleedthrough, substandard margins, and improper alignment can adversely affect reproduction.

In the unlikely event that the author did not send UMI a complete manuscript and there are missing pages, these will be noted. Also, if unauthorized copyright material had to be removed, a note will indicate the deletion.

Oversize materials (e.g., maps, drawings, charts) are reproduced by sectioning the original, beginning at the upper left-hand corner and continuing from left to right in equal sections with small overlaps. Each original is also photographed in one exposure and is included in reduced form at the back of the book.

Photographs included in the original manuscript have been reproduced xerographically in this copy. Higher quality 6" x 9" black and white photographic prints are available for any photographs or illustrations appearing in this copy for an additional charge. Contact UMI directly to order.

U·M·I

University Microfilms International
A Bell & Howell Information Company
300 North Zeeb Road, Ann Arbor, MI 48106-1346 USA
313/761-4700 800/521-0600

Order Number 9325173

The effect of ultrasound on polycyclic aromatic hydrocarbons in aqueous media

Wheat, Patrick E., Ph.D.

University of Alaska Fairbanks, 1992

Copyright ©1992 by Wheat, Patrick E. All rights reserved.

U·M·I
300 N. Zeeb Rd.
Ann Arbor, MI 48106

Vertical line of text on the right side of the page.

THE EFFECT OF ULTRASOUND ON
POLYCYCLIC AROMATIC HYDROCARBONS IN AQUEOUS MEDIA

A
Thesis

Presented to the Faculty
of the University of Alaska Fairbanks

In Partial Fulfillment of the Requirements
for the Degree of:

DOCTOR OF PHILOSOPHY

By
Patrick E. Wheat, B.A., M.Sc.

Fairbanks, Alaska

October, 1992

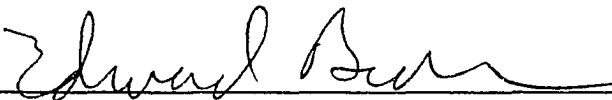
(C) Copyright 1992 Patrick E. Wheat

THE EFFECT OF ULTRASOUND ON
POLYCYCLIC AROMATIC HYDROCARBONS IN AQUEOUS MEDIA

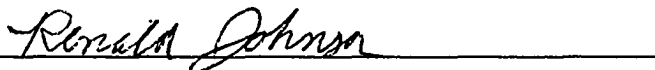
By

Patrick E. Wheat

Recommended:



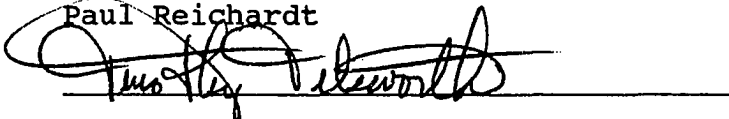
Edward Brown



Ronald Johnson



Paul Reichardt



Timothy Tilsworth



Mark Tumeo - Advisory Committee Chair




Robert Carlson - Department Head

Approved:

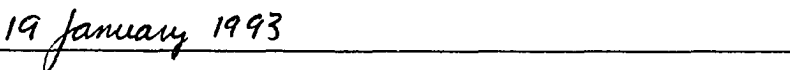


Frank Williams, Dean - School of Engineering

Dean of Graduate School



Date:



Abstract

Polycyclic aromatic hydrocarbons (PAHs) are common environmental contaminants which pose a potential threat to human health and environmental quality. An investigation to determine the ability of ultrasonic radiation to desorb PAHs adsorbed on solid substrates and to chemically alter these chemicals in aqueous solutions and suspensions has been conducted. The data indicate that enhanced transport of adsorbed PAH from a glass surface can be induced by treatment with ultrasonic radiation of varying intensities. Furthermore, chemical alteration can be induced under intense (147 watts/cm^2) ultrasonic treatment. The extent of reaction is a function of irradiation time at this ultrasonic intensity.

Reaction products from ultrasonic treatment of aqueous solutions of biphenyl, analysed by gas chromatography (GC) and mass spectrometry (MS), include ortho-, meta-, and para-[1,1 biphenyl]-ol. The principal product from ultra-sonic treatment of aqueous phenanthrene appears to be a phenanthrenediol.

The use of ultrasound to treat PAH contaminated aqueous solutions in tandem with other methodologies appears promising. However, the toxicity of reaction product mixtures produced by ultrasonic treatment remains to be determined.

Patrick E. Wheat

October, 1992

Environmental Quality Engineering
and Science Program

University of Alaska, Fairbanks
Dr. Mark Tumeo, advisor

Table of Contents

| | Page |
|--|------------|
| Signature page | i |
| Title page | ii |
| Abstract | iii |
| Table of Contents | iv - viii |
| List of Figures | ix - xvi |
| List of Tables | xvii - xxi |
| Acknowledgements | xxii |
| Dedication | xxiii |
| Chapter 1: Introduction | 1 |
| 1.1 Environmental concerns | 1 |
| 1.1.1 Alternative treatment methods | 3 |
| 1.2 Ultrasound | 5 |
| 1.3 Objectives | 7 |
| Chapter 2: Literature Review | 8 |
| 2.1 Characteristics of ultrasound | 8 |
| 2.2 Ultrasound induced chemical change | 9 |
| 2.2.1 Historical Perspective | 9 |
| 2.2.2 Cavitation | 10 |
| 2.2.3 Dissolved gas | 11 |
| 2.2.4 Free radical formation | 12 |
| 2.2.5 Single electron transfer (SET) agents | 14 |
| 2.3 Ultrasound induced desorption - extraction | 16 |

Table of Contents

| | Page |
|---|------|
| Chapter 3: Experimental Methods | 20 |
| 3.1 Materials | 20 |
| 3.2 Preparative methods | 20 |
| 3.2.1 General | 20 |
| 3.2.2 Preparation of pentane | 21 |
| 3.2.3 Preparation of active carbon (AC) for fragmentation experiments. Sieve gradation - general method. | 22 |
| 3.2.4 Preparation of AC for desorption experiments | 23 |
| 3.2.5 Preparation of sand (Tanana Valley alluvium) for desorption experiments | 24 |
| 3.2.6 Preparation of glass beads for desorption experiments | 26 |
| 3.2.7 Preparation of Isotope for desorption experiments | 28 |
| 3.3 Experimental Methods | 29 |
| 3.3.1 Fragmentation experiments: active carbon and sand | 29 |
| 3.3.2 Chemical alteration experiments - general method | 31 |
| 3.3.2.1 Gas Chromatography (GC) and combined Gas Chromatography/Mass Spectrometry (GC/MS) Analysis | 37 |
| 3.3.3 Desorption experiments - general methods | 37 |
| 3.3.3.1 Overview of desorption experiments | 37 |
| 3.3.3.2 Radiation experiment #1 - sonication of 9- ¹⁴ -C- phenanthrene on active carbon | 39 |

Table of Contents

| | Page |
|--|------|
| 3.3.3.3 Sonication of 9- ¹⁴ C phenanthrene adsorbed on Tanana Valley alluvial sand | 43 |
| 3.3.3.4 Sonication of UL- ¹⁴ C biphenyl and biphenyl on glass beads | 48 |
| Chapter 4 Results and Discussion | 53 |
| 4.1 Fragmentation | 53 |
| 4.1.1 Active carbon fragmentation | 53 |
| 4.1.2 Tanana Valley sand fragmentation | 58 |
| 4.2 Chemical Alteration | 61 |
| 4.2.1 Volatility | 66 |
| 4.2.2 Hydrophobicity | 68 |
| 4.2.3 Contribution of Iron (III) | 70 |
| 4.2.4 Gas Chromatography/Mass Spectrometry | 71 |
| 4.2.5 Toxicity considerations | 78 |
| 4.3 Desorption | 79 |
| 4.3.1 Active carbon/phenanthrene desorption experiment | 79 |
| 4.3.2 Sand/ ¹⁴ C-phenanthrene desorption experiments | 82 |
| 4.3.3 Glass beads/ ¹⁴ C-biphenyl desorption experiments | 88 |
| 4.3.4 Hypothetical mechanism of desorption | 93 |
| Chapter 5 Summary & Conclusion | 98 |
| 5.1 Conclusions | 98 |
| 5.1.1 Fragmentation | 98 |
| 5.1.2 Chemical alteration of adsorbed contaminants | 99 |

Table of Contents

| | Page |
|--|---------|
| 5.1.3 Desorption | 100 |
| 5.2 Future work | 101 |
| Bibliography | 104-112 |
| Appendix A: Materials & Methods - Supplemental Information | 113 |
| A.1 Instrumentation | 113 |
| A.2 Solvents | 114 |
| A.3 Chemicals | 115 |
| A.4 Gases | 117 |
| Appendix B: Supplemental experimental data - active carbon and Tanana Valley Sand Fragmentation | 118 |
| Appendix C: GC and GC/MS Data | 133 |
| C.1 Gas chromatography programs | 134 |
| C.2 GC/MS data | 137 |
| Appendix D: Supplemental experimental data - chemical alteration | 150 |
| Appendix E: Supplemental Experimental Data - Radioisotope Studies | 175 |
| E.1 Data from Active Carbon/ $9\text{-}^{14}\text{C}$ Phenanthrene Experiment (Radiation Experiment #1 - Rad #1) | 176 |
| E.2 Data from Tanana Valley Sand/ $9\text{-}^{14}\text{C}$ Phenanthrene Experiments (Radiation Experiments #2 & #3 - Rad #2 and #3) | 180 |
| E.3 Data from Glass Beads/ $UL\text{-}^{14}\text{C}$ Biphenyl Experiments (Radiation Experiments #4 thru #8 - Rad #2 through #8) | 186 |

Table of Contents

| | Page |
|--|------|
| E.4 Linear Regression Analysis of Plotted Data from Radiation | 201 |
| Experiments Number Four Through Eight (Rad #4 Through Rad #8) | |
| E.5 Method Development for Glass Beads/ ^{14}C Biphenyl | 203 |
| Experiments | |
| E.6 Conversion from disintegrations per minute to mass | 208 |
| measure | |

LIST OF FIGURES

| Figure | Description | Page |
|--------|--|------|
| (1) | Fragmentation Experimental Apparatus | 29 |
| (2) | Structure of Biphenyl and Phenanthrene | 32 |
| (3) | Chemical Alteration Experimental Apparatus | 33 |
| (4) | Desorption Experimental Apparatus | 40 |
| (5) | Cold Trap Apparatus | 49 |
| (6) | Sieve Analysis of Active Carbon Subjected To 43 Watts/Cm ² for 5 Minutes in a 50 mL Reactor | 54 |
| (7) | Sieve Analysis of Active Carbon Subjected To 85 Watts/Cm ² for 5 Minutes in 50 mL Reactor | 55 |
| (8) | Sieve Analysis of Active Carbon Subjected To 138 Watts/Cm ² for 5 Minutes in 50 mL Reactor | 55 |
| (9) | Sieve Analysis of Active Carbon Subjected to 50 Watts/Cm ² for 30 Minutes in 310 mL Reactor | 56 |
| (10) | Sieve analysis of Active Carbon Subjected to 85 Watts/Cm ² for 5 Minutes in a 310 mL Reactor | 56 |
| (11) | Sieve Analysis of Active Carbon Subjected to 150 Watts/Cm ² for 30 minutes in 310 mL Reactor | 57 |
| (12) | Sieve Analysis of Active Carbon Subjected to 190 Watts/Cm ² for 50 minutes in 310 mL Reactor Single Trial - No Control | 57 |
| (13) | Sieve Analysis of Tanana Valley Sand - Single Trial - Untreated Starting Material | 59 |
| (14) | Sieve Analysis of Tanana Valley Sand Subjected to 156 Watts/Cm ² for 50 Minutes in 310 mL Reaction Vessel - Single Trial | 60 |
| (15) | Average Biphenyl Gas Chromatography Peak Area vs Total Reaction Time (90% Confidence Interval Data) - Fe ³⁺ /Air Infusion | 61 |

LIST OF FIGURES

| Figure | Description | Page |
|--------|--|------|
| (16) | Average Phenanthrene Gas Chromatography Peak Area vs Total Reaction Time (90% Confidence Interval Data) - Fe ³⁺ /Air Infusion | 62 |
| (17) | Average Total Biphenyl Reaction Product Gas Chromatography Peak Area vs Total Reaction Time (90% Confidence Interval Data) - Fe ³⁺ /Air Infusion | 63 |
| (18) | Average Total Phenanthrene Reaction Product Gas Chromatography Peak Area vs Total Reaction Time (90% Confidence Interval Data) Fe ³⁺ /Air Infusion | 63 |
| (19) | Average Ratio of Biphenyl GC Peak Area to Total Biphenyl Reaction Product Gas Chromatography Peak Area vs Total reaction Time (90% Confidence Interval Data) - Fe ³⁺ /Air Infusion | 64 |
| (20) | Average Ratio of Phenanthrene GC Peak Area to Total Phenanthrene Reaction Product Gas Chromatography Peak Area vs Total Reaction Time (90% Confidence Interval Data) Fe ³⁺ /Air | 65 |
| (21) | Total Ion Chromatogram of Biphenyl Reaction Mixture | 73 |
| (22) | Total Ion Chromatogram of Phenanthrene Reaction Mixture | 74 |
| (23) | Mass Spectrum of Phenanthrene Reaction Product | 76 |
| (24) | Radiation Experiment #1 (rad #1) - First Trial - Phenanthrene/Active Carbon - Sonic Treatment Background Corrected Disintegrations/Minute/Milliliter vs Cumulative Sample Volume Collected at Indicated Probe Energy Level | 80 |
| (25) | Radiation Experiment #2 (Rad #2) - Phenanthrene/Tanana Valley Sand - Duplicate Averaged Disintegrations/Minute/Milliliter vs Cumulative Sample Volume Collected at Indicated Probe Tip Energy Level | 83 |

LIST OF FIGURES

| Figure | Description | Page |
|--------|--|------|
| (26) | Radiation Experiment #3 (Rad #3) - Phenanthrene/Tanana Valley Sand Duplicate Average Disintegrations/Minute/Milliliter vs Cumulative Sample Volume Collected at Indicated Probe Tip Energy Level | 83 |
| (27) | Radiation Experiment #3 - Liquid Scintillation Count of Residual Radioactivity on Surface of Sand After Sonic Treatment - Surface Dried Sand Samples | 86 |
| (28) | Radiation Experiment #7 (Rad #7) Biphenyl/Glass Beads Averaged DPM/mL vs Cumulative Sample Volume Collected | 89 |
| (29) | Radiation Experiment #5 (Rad #5) Control (No Sonic) Biphenyl Glass Beads - Duplicate Averaged DPM/mL vs Cumulative Sample Volume Collected | 90 |
| (30) | Comparison of Calculated Desorption Linear Regression Slope Estimates for Sonic and Control (No Sonic) Experiments - 99% Confidence Interval | 91 |
| (B1) | Active Carbon Sieve Analysis - 1/16/91 - Untreated Starting Material | 118 |
| (B2) | Active Carbon Sieve Analysis - 2/1/91 Untreated Starting Material | 120 |
| (B3) | Active Carbon Sieve Analysis - 2/28/91 Untreated Starting Material | 121 |
| (B4) | Sieve Analysis of Active Carbon Subjected To 43 Watts/Cm ² for 5 Minutes in a 50 mL Reaction Vessel | 122 |
| (B5) | Sieve Analysis of Active Carbon Subjected To 85 Watts/Cm ² for 5 Minutes in 50 mL Reaction Vessel | 123 |
| (B6) | Sieve Analysis of Active Carbon Subjected To 138 Watts/Cm ² for 5 Minutes in 50 mL Reaction Vessel | 124 |
| (B7) | Sieve Analysis of Active Carbon Subjected to 50 Watts/Cm ² for 30 Minutes in 310 mL Reactor | 125 |

LIST OF FIGURES

| Figure | Description | Page |
|--------|--|------|
| (B8) | Sieve Analysis of Active Carbon Subjected to 85 Watts/Cm ² for 5 Minutes in a 310 mL Reactor | 126 |
| (B9) | Sieve Analysis of Active Carbon Subjected to 85 Watts/Cm ² for 25 Minutes in 310 mL Reactor | 127 |
| (B10) | Sieve Analysis of Active Carbon Subjected to 100 Watts/Cm ² for 30 Minutes in 310 mL Reactor | 128 |
| (B11) | Sieve Analysis of Active Carbon Subjected to 150 Watts/Cm ² for 30 minutes in 310 mL Reactor | 129 |
| (B12) | Sieve Analysis of Active Carbon Subjected to 190 Watts/Cm ² for 50 minutes in 310 mL Reactor Single Trial - No Control | 130 |
| (B13) | Sieve Analysis of Tanana Valley Sand - Single Trial - Untreated Starting Material | 131 |
| (B14) | Sieve Analysis of Tanana Valley Sand Subjected to 156 Watts/Cm ² for 50 Minutes in 310 mL Reaction Vessel - Single Trial | 132 |
| (C1) | Gas Chromatography Plot of Biphenyl Control (No Sonic) Reaction Mixture - FID Detector | 137 |
| (C2) | Gas Chromatography Plot of Biphenyl Ultrasonic Reaction Mixture - FID Detector | 138 |
| (C3) | Total Ion Chromatogram of Biphenyl Ultrasonic Reaction Mixture | 139 |
| (C4) | Mass Spectrum of ortho-Hydroxy Biphenyl - Peak at Time 30.33 Minutes in Total Ion Chromatogram (See Figure #C3) | 140 |
| (C5) | Mass Spectra of meta- & para-Hydroxy Biphenyl - Peaks with Retention Times of 35.93 and 36.20 Minutes in Ion Chromatogram (See Figure #C3) | 142 |

LIST OF FIGURES

| Figure | Description | Page |
|--------|--|------|
| (C6) | Sample Gas Chromatography Plot of a Phenanthrene Control (No Sonic) Reaction Mixture - FID Detector | 145 |
| (C7) | Sample Gas Chromatography Plot of Phenanthrene Ultrasonic Reaction Mixture - FID Detector | 146 |
| (C8) | Total Ion Chromatogram of Phenanthrene Ultrasonic Reaction Mixture | 147 |
| (C9) | Mass Spectrum of Phenanthrene Ultrasonic Reaction Product at 40.28 Minutes (Figure #C8) | 148 |
| (D1) | Gas Chromatography Plot of Biphenyl Control (No Sonic) Reaction Mixture - (FID) Detector | 152 |
| (D2) | Gas Chromatography Plot of Biphenyl Ultrasonic Reaction Mixture - (FID) Detector | 153 |
| (D3) | Gas Chromatography Plot of Phenanthrene Control (No Sonic) Reaction mixture - (FID) Detector | 154 |
| (D4) | Gas Chromatography Plot of Phenanthrene Ultrasonic Reaction Mixture - (FID) Detector | 155 |
| (D5) | Average Biphenyl Gas Chromatography Peak Area vs Total Reaction Time (90% Confidence Interval Data) - Air Infusion | 157 |
| (D6) | Average Biphenyl Gas Chromatography Peak Area vs Total Reaction Time (90% Confidence Interval Data) - No Gas Infusion | 158 |
| (D7) | Average Biphenyl Gas Chromatography Peak Area vs Total Reaction Time (90% Confidence Interval Data) - Fe ³⁺ /Air Infusion | 159 |
| (D8) | Average Total Biphenyl Reaction Product Gas Chromatography Peak Area vs Total Reaction Time (90% Confidence Interval Data) - Air Infusion | 160 |
| (D9) | Average Total Biphenyl Reaction Product Gas Chromatography Peak Area vs Total Reaction Time (90% Confidence Interval Data) - No Gas Infusion | 161 |

LIST OF FIGURES

| Figure | Description | Page |
|--------|---|------|
| (D10) | Average Total Biphenyl Reaction Product Gas Chromatography Peak Area vs Total Reaction Time (90% Confidence Interval Data) - Fe ³⁺ /Air Infusion | 162 |
| (D11) | Average Ratio of Biphenyl GC Peak Area to Total Biphenyl Reaction Product Gas Chromatography Peak Area vs Total Reaction Time (90% Confidence Interval Data) - Air Infusion | 163 |
| (D12) | Average Ratio of Biphenyl GC Peak Area to Total Biphenyl Reaction Product Gas Chromatography Peak Area vs Total reaction Time (90% Confidence Interval Data) - No Gas Infusion | 164 |
| (D13) | Average Ratio of Biphenyl GC Peak Area to Total Biphenyl Reaction Product Gas Chromatography Peak Area vs Total reaction Time (90% Confidence Interval Data) - Fe ³⁺ /Air Infusion | 165 |
| (D14) | Average Phenanthrene Gas Chromatography Peak Area vs Total Reaction Time (90% Confidence Interval Data) - Air Infusion | 166 |
| (D15) | Average Phenanthrene Gas Chromatography Peak Area vs Total Reaction Time (90% Confidence Interval Data) - No Gas Infusion | 167 |
| (D16) | Average Phenanthrene Gas Chromatography Peak Area vs Total Reaction Time (90% Confidence Interval Data) - Fe ³⁺ /Air Infusion | 168 |
| (D17) | Average Total Phenanthrene Reaction Product Gas Chromatography Peak Area vs Total Reaction Time (90% Confidence Interval Data) - Air Infusion | 169 |
| (D18) | Average Total Phenanthrene Reaction Product Gas Chromatography Peak Area vs Total Reaction Time (90% Confidence Interval Data) - No Gas Infusion | 170 |
| (D19) | Average Total Phenanthrene Reaction Product Gas Chromatography Peak Area vs Total Reaction Time (90% Confidence Interval Data) - Fe ³⁺ /Air Infusion | 171 |

LIST OF FIGURES

| Figure | Description | Page |
|--------|---|------|
| (D20) | Average Ratio of Phenanthrene GC Peak Area to Total Phenanthrene Reaction Product Gas Chromatography Peak Area vs Total Reaction Time (90% Confidence Interval Data) - Air Infusion | 172 |
| (D21) | Average Ratio of Phenanthrene GC Peak Area to Total Phenanthrene Reaction Product Gas Chromatography Peak Area vs Total Reaction Time (90% Confidence Interval Data) - No Gas Infusion | 173 |
| (D22) | Average Ratio of Phenanthrene GC Peak Area to Total Phenanthrene Reaction Product Gas Chromatography Peak Area vs Total Reaction Time (90% Confidence Interval Data) - Fe ³⁺ /Air Infusion | 174 |
| (E1) | Radiation Experiment #1 (Rad #1) - First Trial - Phenanthrene/Active Carbon - Sonic Treatment - Background Corrected Disintegrations/Minute/Milliliter vs Cumulative Sample Volume Collected at Indicated Probe Energy Level | 176 |
| (E2) | Radiation Experiment #1 (Rad #1) Second Trial Phenanthrene/Active Carbon - Sonic Treatment - Background Corrected Disintegrations/Minute/Milliliter vs Cumulative Sample Volume Collected at Indicated Probe Tip Energy Level | 179 |
| (E3) | Radiation Experiment #2 (Rad #2) - Phenanthrene/Tanana Valley Sand - Duplicate Averaged Disintegrations/Minute/Milliliter vs Cumulative Sample Volume Collected at Indicated Probe Tip Energy Level | 180 |
| (E4) | Radiation Experiment #3 (Rad #3) -Phenanthrene/Tanana Valley Sand Duplicate Average Disintegrations/Minute/Milliliter vs Cumulative Sample Volume Collected at Indicated Probe Tip Energy Level | 182 |
| (E5) | Radiation Experiment #3 - Liquid Scintillation Count of Residual Radioactivity on Surface of Sand After Sonic Treatment - Wet Sand Samples | 184 |

LIST OF FIGURES

| Figure | Description | Page |
|--------|---|-----------|
| (E6) | Radiation Experiment #3 - Liquid Scintillation Count of Residual Radioactivity on Sand Surface After Sonic Treatment - Surface Dried Sand Samples | 185 |
| (E7) | Radiation Experiment #4 (Rad #4)- Biphenyl/Glass Beads - Averaged DPM/mL vs Cumulative Sample Volume Collected | 186 & 205 |
| (E8) | Radiation Experiment #5 (Rad #5) Control (No Sonic) Biphenyl Glass Beads - Duplicate Averaged DPM/mL vs Cumulative Sample Volume Collected | 189 & 206 |
| (E9) | Radiation Experiment #6 (Rad #6) Sonic Treatment Biphenyl Glass Beads - Duplicate Averaged DPM/mL vs Cumulative Sample Volume Collected at Indicated Probe Tip Energy Level | 192 |
| (E10) | Radiation Experiment #7 (Rad #7) Biphenyl/Glass Beads Duplicate Averaged DPM/mL vs Cumulative Sample Volume Collected at Indicated Probe Tip Energy Level | 195 |
| (E11) | Radiation Experiment #8 (Rad #8) - Control (No Sonic) Biphenyl Glass Beads - Duplicate Averaged DPM/mL vs Cumulative Sample Volume Collected | 198 & 207 |
| (E12) | Comparison of Calculated Desorption Linear Regression Slope Estimates for Sonic and Control (No Sonic) Experiments - 99% Confidence Interval | 202 |

LIST OF TABLES

| Table | Description | Page(s) |
|-------|--|---------|
| (1) | Preparation of Glassware | 20 |
| (2) | Glass Bead Analysis | 28 |
| (3) | Overview of Desorption Experiments | 38 |
| (4) | Values of Measured and Calculated Physical Parameters for First Sand/9- ¹⁴ C Phenanthrene Desorption Experiment | 47 |
| (5) | Values of Measured and Calculated Physical Parameters for Second Sand/9- ¹⁴ C Phenanthrene Desorption Experiment (Rad #3) | 47 |
| (B1) | Active Carbon Sieve Analysis - 1/16/91 - Untreated Starting Material | 119 |
| (B2) | Active Carbon Sieve Analysis - 2/1/91 Untreated Starting Material | 120 |
| (B3) | Active Carbon Sieve Analysis - 2/28/91 Untreated Starting Material | 121 |
| (B4) | Sieve Analysis of Active Carbon Subjected To 43 Watts/Cm ² for 5 Minutes in a 50 mL Reaction Vessel | 122 |
| (B5) | Sieve Analysis of Active Carbon Subjected To 85 Watts/Cm ² for 5 Minutes in 50 mL Reaction Vessel | 123 |
| (B6) | Sieve Analysis of Active Carbon Subjected To 138 Watts/Sq Cm for 5 Minutes in 50 mL Reaction Vessel | 124 |
| (B7) | Sieve Analysis of Active Carbon Subjected to 50 Watts/Cm ² for 30 Minutes in 310 mL Reactor | 125 |
| (B8) | Sieve Analysis of Active Carbon Subjected to 85 Watts/Cm ² for 5 Minutes in a 310 mL Reactor | 126 |
| (B9) | Sieve Analysis of Active Carbon Subjected to 85 Watts/Cm ² for 25 Minutes in 310 mL Reactor | 127 |
| (B10) | Sieve Analysis of Active Carbon Subjected to 100 Watts/Cm ² for 30 Minutes in 310 mL Reactor | 128 |
| (B11) | Sieve Analysis of Active Carbon Subjected to 150 Watts/SqCm for 30 minutes in 310 mL Reactor | 129 |

LIST OF TABLES

| Table | Description | Page(s) |
|-------|--|---------|
| (B12) | Sieve Analysis of Active Carbon Subjected to 190 Watts/Sq for 50 minutes in 310 mL Reactor Single Trial - No Control | 130 |
| (B13) | Sieve Analysis of Tanana Valley Sand - Single Trial - Untreated Starting Material | 131 |
| (B14) | Sieve Analysis of Tanana Valley Sand Subjected to 156 Watts/Sq Cm for 50 Minutes in 310 mL Reaction Vessel - Single Trial | 132 |
| (C1) | Gas Chromatography Program for Perkin Elmer Gas Chromatograph With FID Detector - Biphenyl | 134 |
| (C2) | Gas Chromatography Program for Perkin Elmer Gas Chromatograph With FID Detector Phenanthrene | 135 |
| (C3) | Data Acquisition and Operating Parameters for Hewlett Packard Gas Chromatograph With Mass Selective Detector - Biphenyl and Phenanthrene | 136 |
| (C4) | Mass Spectrum of Biphenyl Reaction Product With Retention Time of 30.33 Minutes (Figure #C3); o-Hydroxy Biphenyl | 141 |
| (C5) | Mass Spectrum of Biphenyl Reaction Product With Retention Time of 35.93 Minutes (Figure #C3) m- or p-Hydroxy Biphenyl | 143 |
| (C6) | Mass Spectrum of Biphenyl Reaction Product With Retention Time of 36.20 Minutes (Figure #C3) m- or p-Hydroxy Biphenyl | 144 |
| (C7) | Mass Spectrum of Phenanthrene Reaction Product With Retention Time of 40.28 Minutes | 149 |
| (D1) | Average Biphenyl GC Peak Area As a Function of Reaction Time 90% Confidence Interval Data - Air Infusion | 157 |
| (D2) | Average Biphenyl Peak Area As a Function of Reaction Time - 90% Confidence Interval Data - No gas Infusion | 158 |
| (D3) | Average Biphenyl GC Peak Area As a Function of Reaction Time 90% Confidence Interval Data - Fe ³⁺ /Air Infusion | 159 |
| (D4) | Average Total Biphenyl Reaction Product Area As a Function of Reaction Time - 90% Confidence Interval Data - Air Infusion | 160 |

LIST OF TABLES

| Table | Description | Page(s) |
|-------|---|---------|
| (D5) | Average Total Biphenyl Reaction Product Peak Area As a Function of Reaction Time - 90% Confidence Interval Data - No Gas Infusion | 161 |
| (D6) | Average Total Biphenyl Reaction Product Peak Area As a Function of Reaction Time - 90% Confidence Interval Data - Fe ³⁺ /Air Infusion | 162 |
| (D7) | Average Ratio of Biphenyl Peak Area To Corrected Total Product Peak Area as a Function of Reaction Time - 90% Confidence Interval Data - Air Infusion | 163 |
| (D8) | Average Ratio of Biphenyl Peak Area To Corrected Total Product Peak Area as a Function of Reaction Time - 90% Confidence Interval Data - No Gas Infusion | 164 |
| (D9) | Average Ratio of Biphenyl Peak Area To Corrected Total Product Peak Area as a Function of Reaction Time - 90% Confidence Interval Data - Fe ³⁺ /Air Infusion | 165 |
| (D10) | Average Phenanthrene Peak Area As a Function of Total Reaction Time - 90% Confidence Interval - Air Infusion | 166 |
| (D11) | Average Phenanthrene Peak Area As a Function of Total Reaction Time - 90% Confidence Interval - No Gas Infusion | 167 |
| (D12) | Average Phenanthrene Peak Area As a Function of Total Reaction Time - 90% Confidence Interval - Air/Fe ³⁺ Infusion | 168 |
| (D13) | Average Phenanthrene Product Peak Area As a Function of Total Reaction Time - 90% Confidence Interval - Air Infusion | 169 |
| (D14) | Average Phenanthrene Product Peak Area As a Function of Total Reaction Time - 90% Confidence Interval - No Gas Infusion | 170 |
| (D15) | Average Phenanthrene Product Peak Area As a Function of Total Reaction Time - 90% Confidence Interval - Fe ³⁺ /Air Infusion | 171 |
| (D16) | Average Ratio of Phenanthrene Peak Area to Total Reaction Product Area As Function of Total Reaction Time - 90% Confidence Interval Data - Air Infusion | 172 |

LIST OF TABLES

| Table | Description | Page(s) |
|-------|---|---------|
| (D17) | Average Ratio of Phenanthrene Peak Area to Total Reaction Product Area As Function of Total Reaction Time - 90% Confidence Interval Data - No Gas Infusion | 173 |
| (D18) | Average Ratio of Phenanthrene Peak Area to Total Reaction Product Area As Function of Total Reaction Time - 90% Confidence Interval Data - Fe ³⁺ /Air Infusion | 174 |
| (E1) | Overview of Desorption Experiments | 175 |
| (E2) | Radiation Experiment #1 (Rad #1) - First Trial - Phenanthrene/Active Carbon - Sonic Treatment - Background Corrected Disintegrations/Minute/Milliliter vs Cumulative Sample Volume Collected at Indicated Probe Energy Level | 177-178 |
| (E3) | Radiation Experiment #1 (Rad #1) - Second Trial - Phenanthrene/Active Carbon Sonic Treatment - Background Corrected Disintegrations/Minute/Milliliter vs Cumulative Sample Volume Collected at Indicated Probe Tip Energy Level | 179 |
| (E4) | Radiation Experiment #2 (Rad #2) - Phenanthrene/Tanana Valley Sand - Duplicate Averaged Disintegrations/Minute/Milliliter vs Cumulative Sample Volume Collected at Indicated Probe Tip Energy Level | 181 |
| (E5) | Radiation Experiment #3 (Rad #3) - Phenanthrene/Tanana Valley Sand Duplicate Average Disintegrations/Minute/Milliliter vs Cumulative Sample Volume Collected at Indicated Probe Tip Energy Level | 182-183 |
| (E6) | Radiation Experiment #3 - Liquid Scintillation Count of Residual Radioactivity on Surface of Sand After Sonic Treatment - Wet Sand Samples | 184 |
| (E7) | Radiation Experiment #3 - Liquid Scintillation Count of Residual Radioactivity on Sand Surface After Sonic Treatment - Surface Dried Sand Samples | 185 |
| (E8) | Radiation Experiment #4 (Rad #4) Biphenyl/Glass Bead - Duplicate Averaged Data - Liquid Scintillation Counting Results | 186-187 |

LIST OF TABLES

| Table | Description | Page(s) |
|--------|--|---------|
| (E9) | Radiation Exp #4 (Rad #4) Sonic Treatment - Glass Beads/Biphenyl - Experimental Parameters and Recovery Data | 188 |
| (E10) | Radiation Experiment #5 (Rad #5) Biphenyl/Glass Beads - Duplicate Averaged Data - Liquid Scintillation Counting Results | 189-190 |
| (E11) | Radiation Exp #5 (Rad #5) Control (No Sonic) - Glass Beads/Biphenyl - Experimental Parameters and Recovery Data | 191 |
| (E12): | Radiation Experiment #6 (Rad #6) Sonic Treatment Biphenyl/Glass Beads - Duplicate Averaged Data - Liquid Scintillation Counting Results | 192-193 |
| (E13) | Radiation Exp #6 (Rad #6) Sonic Treatment - Glass Beads/ Biphenyl - Experimental Parameters and Recovery Data | 194 |
| (E14) | Radiation Experiment #7 (Rad #7) Biphenyl/Glass Beads - Sonic Treatment - Duplicate Averaged Data - Liquid Scintillation Counting Results | 195-196 |
| (E15): | Radiation Exp #7 (Rad #7) Sonic Treatment - Glass Beads/Biphenyl - Experimental Parameters and Recovery Data | 197 |
| (E16) | Radiation Experiment #8 (Rad #8) - Control (No Sonic) Biphenyl/Glass Beads Duplicate Averaged Data - Liquid Scintillation Counting Results | 198-199 |
| (E17) | Radiation Exp #8 (Rad #8) Control (No Sonic) - Glass Beads/Biphenyl - Experimental Parameters and Recovery Data | 200 |
| (E18) | 99% Confidence Intervals of Calculated Desorption Linear Regression Slope Data - Sonic and Control (No Ultrasound) Sonic Interval Data | 202 |

Acknowledgements

The author gratefully acknowledges the contribution of several people without whose continued support and encouragement completion of this project would not have been possible. First, my gratitude is extended to Dr. Mark Tumeo for his unswerving belief in my abilities which I perceive through a glass, darkly.

Second, I would like to express my gratitude and devotion to my wife Mary E. Wheat and my children Erin M. Wheat and Ethan T. Wheat, to my parents Doris M. and David S. Wheat, and to my brothers D. Michael and Steven J. Wheat who endured the slings and arrows of my outrageous fortune.

Third, I must acknowledge the aid and support of my friends and colleagues at the University of Alaska. Their contributions were invaluable; and, while I cannot name all of them here, certain individuals need to be singled out and individually acknowledged. These include Larry Hinzman, Lily Young, Kevin Curtis, Debendra Das, Dan Holleman, Mohammad Saccharide, Tamar Stephens, Joseph Reuter, William Krause, Howard Fruhwirth, Stephen Winch, and those members of my graduate research committee whose names appear on the signature page of this document.

Special thanks are extended to Douglas McIntosh for his aid in GC/MS analyses, to Pham Quang for his aid in statistical analyses, and to Steven Hage for his help in preparing this manuscript.

Dedication

In Memory of:

Leona Faughnan

(1898-1992)

and

John McGuire

(1921-1992)

Chapter #1: Introduction:

1.1 Environmental concerns

Sludges and slurries, directly discharged or formed from contaminants and natural sediments, pose challenging treatment, storage, and disposal problems. These materials are produced by domestic and industrial activities and have traditionally been disposed of using a number of currently unacceptable methodologies including dilution and discharge, storage in unlined retention basins, and incorporation into other waste streams. Utilization of these inadequate methods has resulted in many of the historical environmental problems by which we are challenged today. Furthermore, attempts to alleviate the detrimental effects of these problems and administer clean-ups have met with limited success for a number of technical, economic, legal and political reasons. The magnitude of the problem is global in scope (Holoubek et al., 1990; Krahn et al., 1991; Fernandez et al., 1992).

Recent work (Short and Lowson, 1988; McCarty and Zachara, 1989 & 1990; Champ, 1990; Looney et al., 1990; Gschwend, 1990; Germann, 1990; Fogler, 1990; Penrose et al., 1990; Jardine et al., 1990; Raloff, 1990; Kile and Chiou, 1990)

has suggested that actinide elements and organic contaminants adsorbed on colloidal material, in surfactant emulsions, and within micelles can undergo dramatic translations in a groundwater aquifer. This transport enhancement is of particular importance when the fate of colloidal material suspended in wastewater generated by remediation efforts is considered. The intent of hazard remediation efforts is to provide amelioration of the risk potential of an existing condition while supplying safety assurances to workers and other affected parties during treatment. However, water reinjected into an aquifer after soil washing, solvent flushing, air stripping and/or other treatment schemes may act as a carrier of contaminated colloidal material and micro-emulsions, enhancing the rate of contaminant spread and their subsequent hazard potential.

The presence of contaminated particulate material less than 70 micrometers in diameter has been demonstrated to be a serious hindrance to effective treatment of many wastes (Kostecki and Calabrese, 1989; & Esposito et al., 1989). Nunno et al. (1989), in their review of European hazardous waste remediation sites, have indicated that this material is highly refractory to solvent washing and, once isolated, requires disposal as a hazardous waste, often in landfills. In the United States, however, landfilling of hazardous moist or wet contaminated sludges is banned by law (40 CFR

264.314b). For this reason various types of incineration may represent the only viable form of satisfactory treatment for this material.

1.1.1 Alternative treatment methods

Groundwater and sediments contaminated by the discharge of wastewater, slurries, and sludges present a major treatment challenge because of the volume and hazardous nature of this material. The discharged material results from domestic and industrial activities and exhibits diverse size, texture, chemical properties, and toxicity. Because of these characteristics the amelioration of the hazard potential of the discharged material, and the groundwater and sediments it contacts, have made each treatment task unique in both scope and complexity.

Various demonstration and emerging technologies have been designed and implemented for treatment of these contaminated materials and many more are currently under development (EPA, 1991a; 1991b). These technologies include biological, chemical, and physical methods of treatment as well as many of the imaginable hybrids of two or more of these approaches. Given the wide variety of treatment methodologies it is of interest to note that many types of contaminated material remain untreatable.

Sediments contaminated with polycyclic aromatic hydrocarbons (PAHs) and polychlorinated biphenyls (PCBs) cannot be effectively treated using current technologies (Fernandez et al., 1992; Tanabe et al., 1987). Because of the volume of contaminated material, effective treatment using available techniques (incineration, landfilling, solidification, and soil washing, etc.) is considered prohibitively expensive.

The use of natural and acclimated microbial agents on large scale superfund sites, such as PCB contaminated sediments in the Hudson River, has been conducted with limited success. The refractory nature of PCBs towards biodegradation and the fact that natural degradation in sediments appears to be mediated by the slow action of anaerobic organisms (Brown et al., 1987; Lake et al., 1992) make the rate of treatment by this method less than satisfactory.

The treatment of PCB contaminated sediments by chemical means has also been attempted with little success (Heylin, 1991). Recent work (Sedlak and Andren, 1991) suggests that chlorinated polycyclic aromatic hydrocarbons (PCBs and others) may be susceptible to reaction under free radical reaction conditions similar to those present during treatment with Fenton's reagent ($\text{FeSO}_4 - \text{H}_2\text{O}_2$). These findings can be utilized to anticipate the nature of

reaction products formed when aqueous solutions of PCBs are treated with high intensity ultrasound either in the presence or absence of single electron transfer agents (SETs).

1.2 Ultrasound

At the outset of this project, the possibility that contaminated aqueous solutions and mixtures could be treated with high intensity ultrasonic fields to decrease their hazard potential was considered, and appeared likely. This decrease in hazard potential was anticipated based on the high probability for chemical alteration of contaminants under intense sonication (Parke and Taylor, 1956; Fitzgerald et al., 1956).

A review of the literature indicated that the surfaces of natural particles are not smooth even though they may appear so from a macroscopic viewpoint (Marshall, 1987). Furthermore, surface roughness features such as craters and crevices are considered to be likely sites of hydrophobic contaminant adsorption at high solution concentrations.

Harvey et al. (1944) and others (Atchley and Crum, 1988; Crum, 1982) have investigated the role of craters and crevices in the formation of cavitation bubbles and have found that these locations represent favorable points of

bubble nucleation in high intensity ultrasonic fields. Furthermore, there is ample evidence (Suslick, 1985; Henglein, 1987) that forcing reaction conditions can be expected when cavitation bubbles are created in organic and aqueous solutions by the action of intense ultrasound.

When these bodies of information were joined together it became apparent that a combination of crevice contaminant buildup, crevice bubble nucleation, and forcing reaction conditions, (Lindley and Mason, 1987; Boudjouk, 1988) under the influence of intense ultrasound, could provide the necessary requirements for ultrasonically stimulated high energy reactions. Furthermore, the concentration of energy at the site of contaminant adsorption could potentially yield a high rate of effective energy transfer and utilization, making this treatment method applicable where heating of the bulk matrix to destroy a contaminant in low concentration is impractical.

Further review of the literature indicated that localized velocity currents could be expected in the proximity of solid-liquid interfaces under the influence of moderate to intense ultrasonic stimulation and that enhanced transport of contaminant away from solid surfaces could be expected (Nyborg and Jackson, 1958; Nyborg and Gould, 1959; Sprich and Lewandos, 1983).

1.3 Objectives

The intent of this investigation was twofold: first, to determine whether desorption of an adsorbed organic contaminant would occur in the presence of an ultrasonic field of varying intensity; and, second, to ascertain whether chemical alteration of an organic contaminant in aqueous solution would occur under similar conditions.

In order to accomplish this goal the manner in which aqueous mixtures of adsorbed and soluble contaminants interact with the water and an applied ultrasonic field had to be described, at least qualitatively.

It was anticipated that a successful outcome from these experiments would provide the necessary information required to design a system that would exhibit broad applicability when used alone or in conjunction with other treatment technologies and would enlarge the scope of effective alternatives in remediation efforts.

Chapter 2 Literature Review

2.1 Characteristics of Ultrasound

Ultrasonic radiation spans a range of frequencies from approximately 20 kilohertz (20KHz) to 10 megahertz (10MHz). Ultrasound propagates through fluids as a series of longitudinal vibrations that occur as a travelling series of pressure pulses. Perhaps the best example is a displacement pulse travelling in an outstretched "Slinky". Because of its physical character ($\lambda = 7.45$ cm) ultrasonic radiation cannot act directly on adsorbed or soluble molecular species to induce chemical change (Suslick, 1988; Lorimer and Mason, 1987b). However, aggregations of organic molecules adsorbed onto solid surfaces immersed in liquids are susceptible to thermodynamic activation under selected conditions (Alben and Kaczmarczyk, 1986; Grimalt et al., 1984; Marcus et al., 1988; Sprich and Lewandos, 1983). Some factors of importance are the dissolved gases present in solution and their characteristics, the temperature of the reaction mixture and the vapor pressure of the liquid medium at that temperature, the presence of metal ions in the reaction mixture, the time of reaction, the intensity of the radiation, and whether the radiation is delivered to the reaction mixture as pulsed or continuous energy.

2.2 Ultrasound Induced Chemical Change

2.2.1 Historical Perspective

The use of ultrasound to induce chemical alteration in homogeneous aqueous solutions of contaminants is supported by the early work of Wood and Loomis (1927) and others (Parke and Taylor, 1956; Weissler et al., 1950; Weissler, 1953; Griffing, 1950 & 1952; Fitzgerald et al., 1956; Zechmeister and Magoon, 1956). These early investigators correctly described many of the chemical, physical, and biological implications of ultrasonics and ultrasound induced cavitation phenomena and set the stage for many future investigations. Strong interest in the field continued for a number of years but studies were restricted by the inability of researchers to generate fields of sustained intensity and homogeneous frequency. The tools for serious, systematic investigations in the field of high intensity ultrasound became widely available in the late 1970's as a result of the commercialization of lead-zirconate-titanate crystalline piezoelectric ultrasonic transducers based on the formulations of Jaffe et al. (1955). After this time the field of ultrasound utilization and investigation blossomed (Suslick, 1989).

2.2.2 Cavitation

The vehicle of chemical change in solutions exposed to ultrasonic radiation is the cavitation event (Fitzgerald et al., 1956; Weissler, 1953; Henglein, 1987). Cavitation results when the vapor pressure of a liquid exceeds the restraining pressure of the surroundings and a cavity (bubble) is spontaneously formed. The high intensity ultrasonic cavitation event is characterized by the initiation of bubble formation, high localized temperatures, and high localized pressures (Suslick, 1985 & 1990). The onset of the cavitation event is believed to be a complex function of a number of variables including solvent vapor pressure, hydrostatic pressure, solution contamination (gas, solid, liquid), surface characteristics of solid contaminants (smooth, cratered, etc.), the ratio of heat capacities (C_p/C_v) of the dissolved gas, and the ambient solution temperature (Lorimer and Mason, 1987b). Under the influence of high intensity ultrasonic radiation, violent cavitation can be produced in liquids, inducing chemical and physical change (Suslick, 1989; Boudjouk, 1988). Furthermore, in liquids undergoing transient cavitation, characterized by the growth and implosive collapse of bubbles over one or a few acoustic cycles, many micro bubbles can be formed to serve as nucleation sites for the

next cycle and to enhance the overall reaction process (Suslick, 1986b). At very high acoustic pressures cavitation can be inhibited by bubble shrouding of the sonic horn and rapid bubble growth, causing bubbles to become too large for recompression and to be bouyed to the surface of the liquid (Suslick, 1986b).

2.2.3 Dissolved Gas

Dissolved gases, cavitation phenomena and free radical formation in an applied ultrasonic field have all been linked (Mead, 1976) and the continuous presence of gas within the reaction solution is therefore important (Suslick, 1981). Ultrasound, however, has a tendency to degas solutions (Brown, 1965) and dissolved gas content will decrease after prolonged sonication if not replenished in some manner. The introduction of gas into the medium can help to restore the dissolved gas concentration in the reaction mixture, especially if the sonic treatment is performed in a pulsed mode allowing the partial pressure of the gas in the reaction mixture to increase in the intervals between active sonication.

2.2.4 Free Radical Formation

Many authors have presented evidence that the nature of the dissolved gas plays an important part in free radical formation accompanying acoustic cavitation (Kruus, 1987; Makino et al., 1982; Margulis and Didenko, 1986; Mead et al., 1976; Rozin and Rozina, 1986; Sokol'skaya, 1978). Purdhomme (1957) and others (Griffing, 1952; Hart and Henglein, 1987; Henglein and Kormann, 1985) have presented evidence that free radical species can combine to form hydrogen peroxide (H_2O_2) upon sonication of aqueous solutions saturated with various gases. Hydrogen peroxide formation is important because it can subsequently decompose to form additional free radicals, increasing the chemical activity of the system.

The rate of free radical formation is related to the maximum pressure and temperature obtained in the collapsing cavity and is strongly dependent on the polytropic ratio (C_p/C_v) and the thermal conductivity of the ambient gas (Fitzgerald et al., 1956). The polytropic ratio (C_p/C_v) helps define the amount of energy released as heat during the adiabatic compression of a gas.

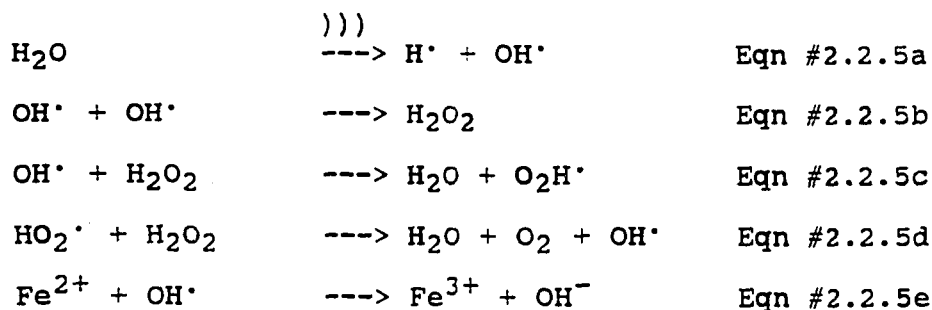
The formation of free radical species (i.e. H^\cdot , OH^\cdot , O_2H^\cdot , N^\cdot , NO^\cdot , NO_2^\cdot) in response to applied high intensity ultrasound has also been proposed by a number of researchers

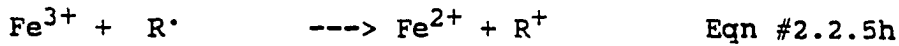
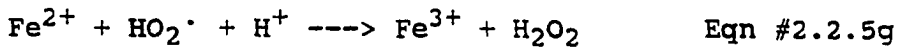
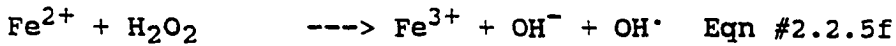
(Sokol'skaya, 1978; Weissler, 1960; Mead et al., 1976; Hart and Henglein, 1987; Henglein, 1987). These studies indicate that a variety of nitrogen, hydrogen, and hydroxyl substituted chemical species may occur in ultrasonic reactions in which nitrogen gas (or air) is present. The formation of (H[•]) and (OH[•]) radicals in aqueous solutions subjected to high intensity ultrasonic fields has been definitively demonstrated by Riesz and co-workers (1990) through the use of spin trapping and electron spin resonance. Henglein and Kormann (1985) has provided evidence that the efficiency with which a solute reacts with hydroxyl radicals is related to its hydrophobicity. The greater the hydrophobicity the more efficiently the solute acts as a radical scavenger. From these studies it can be hypothesized that hydrophobic polycyclic aromatic hydrocarbons (PAHs) may undergo free radical substitution reactions in an applied high intensity ultrasonic field. Furthermore, according to the work of Henglein and Kormann (1985), the efficiency with which PAHs react with hydroxyl radicals produced in high intensity ultrasound fields should increase as a function of their hydrophobicity.

2.2.5 Single Electron Transfer (SET) Agents

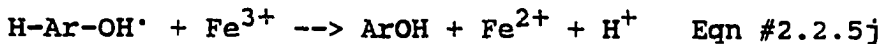
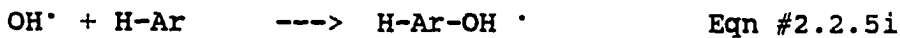
The similarity between ultrasound, pulsed radiolysis and high energy photolysis with respect to the formation of free radical species (Suslick, 1986a & 1986b) has led to the expectation that free radical substitution reactions may be expected to occur upon sonication of aqueous solutions of PAHs. Furthermore, participation by transition metals in single electron transfer (SET) processes can be expected based on the work of Hart and Henglein (1987) and the extensive studies of Fenton's reaction by Walling and co-workers (1971 & 1975), Jefcoate and Norman (1968), and Smith and Norman, (1963).

Iron in the +2 or +3 oxidation state (iron II, iron III) can act as a single electron transfer agent, donating or receiving an electron from a free radical generated in the solution. The combined formulations of Walling (1971) Henglein (1987) and Hart and Henglein (1987) lead to the following set of equations to explain the mechanism of electron transfer:





Either Fe^{2+} or Fe^{3+} , linked through these reactions, may participate when an organic free radical species is formed in solution. The initial hydrogen and hydroxyl free radicals ($\text{OH}\cdot$) come from cavitation caused by the ultrasonic field {}))) and can react with a polycyclic aromatic hydrocarbon in the following manner (Walling and Johnson, 1975)



Where "H-Ar" is an aromatic or polycyclic aromatic compound.

From this formulation the presence of iron (II or III) in solution may be expected to promote formation of the phenol (ArOH) among other products (Smith and Norman, 1963; Walling and Johnson, 1975). As long as a source of free radicals is present (equation 2.2.5a) an equilibrium can exist between Fe^{2+} and Fe^{3+} under these reaction conditions and the continuous presence of available Fe^{3+} is expected to favor the formation of phenols from PAHs. In a similar fashion, other chemical species which exist in two oxidation states

separated by a single electron may be expected to promote this type of product formation (i.e. $\text{Cr}^{+2} \leftrightarrow \text{Cr}^{+3}$, $\text{Hg}^{+1} \leftrightarrow \text{Hg}^{+2}$, $\text{Cu}^{2+} \leftrightarrow \text{Cu}^{+}$, $\text{Ti}^{+3} \leftrightarrow \text{Ti}^{+2}$, and in general $\text{R}^{+x} \leftrightarrow \text{R}^{+(x-1)}$).

The use of other single electron transfer (SET) agents may also be expected to cooperate in this type of reaction. Examples of these other SET agents include heterogeneous suspensions of group IA metals and, perhaps, some polymer species. These factors hold additional promise for enhanced treatment of organic contaminants while simultaneously changing the oxidation state of alkali and transition metal species in hazardous waste site effluent streams.

2.3 Ultrasound Induced Desorption - Extraction

Activated carbon (AC) has been used to remove both inorganic and organic contaminants from water, wastewater, contaminated groundwater, and industrial product streams by physical adsorption of the contaminants onto its surface (Perrich, 1981). When the carbon's adsorption capacity is achieved the material requires regeneration or disposal; options which may carry adverse health, legal and economic aspects for generators and users. Similarly, naturally occurring sediments acting as repositories of adsorbed contaminants (Grimalt et al., 1984; Marcus et al., 1988;

Holoubek et al., 1990) can present a major health threat to users of resources associated with the sediments and a significant legal challenge to entities responsible for the contamination. A methodology to treat contaminated sediments and active carbon to remove adsorbed contaminants that is effective, economical and can be conveniently performed at the point of contaminant generation is currently unavailable. Ultrasound may hold promise as an effective treatment in some of these situations.

The ability of ultrasound to enhance extraction of inorganic and organic contaminants adsorbed on solid substrates in the presence of aqueous and organic solvents has been demonstrated in recent studies (Ackay et al., 1989; Alben and Kaczmarczyk, 1986; Bellar et al., 1980; Holoubek et al., 1990; Harper et al., 1983; Grimalt et al., 1984; Krahn et al., 1991; Marcus et al., 1988). These investigations have demonstrated that ultrasound can be utilized to enhance mass transport of an adsorbed contaminant from the surface of a solid substrate under a variety of conditions. In general, ultrasound enhanced extraction has focused on organic contaminant extraction into organic solvents and inorganic contaminant extraction into various aqueous solutions. The ability of ultrasound to enhance transport of organic contaminants into purely

aqueous media and inorganic contaminants into organic media, however, has not been fully investigated.

Intense ultrasound should provide sufficient energy to effect transport of a hydrophobic contaminant into a polar medium if the radiation can be coupled to the adsorbed contaminant, but problems associated with readsorption can ultimately impair the efficiency of treatment. Ackay et al. (1989) have addressed this concern by pointing out that under ultrasound induced cavitation conditions the redistribution and readsorption of dissolved elements is unlikely. Extension of this hypothesis to the extraction of adsorbed hydrophobic organic contaminants from solid substrates into aqueous media seems to indicate that continuous sonication, perhaps at high energy levels, should minimize readsorption phenomena. Under these conditions the solubilized or suspended contaminant should be effectively carried by the effluent from the high energy environment of the reactor leaving the "cleaned" substrate behind.

The efficiency with which organic contaminants are extracted from the surface of solid substrates into organic media using ultrasound has been characterized as being consistently less effective than soxhlet extraction (Bellar, 1980). However, because the ultrasonic procedure is rapid and easy to perform its use as a method to rapidly assay sediment samples for aromatic hydrocarbon content has

recently been investigated (Krahn et al., 1991). The loss of contaminant due to chemical alteration, under intense ultrasonic extraction conditions, was not addressed in these studies. Masking of chemical alteration by clean-up procedures, utilized in this work and in other ultrasound enhanced extraction methods (EPA 1986a, 1986b, and 1986c), is likely but has not yet been fully investigated. Research proposals to identify chemical alteration as a loss mechanism during ultrasonic extraction have been submitted by Dr. Tumeo of this laboratory, and approval for funding is pending.

The use of ultrasonic fields to enhance extraction, induce both thermodynamic and chemical changes, and address environmental concerns is accelerating (Boudjouk, 1988; Lindley and Mason, 1987; Lorimer et al. 1987a, Lorimer and Mason 1987b; Hart and Henglein, 1987; Henglein, 1987; Kotronarou et al., 1992; Petrier et al., 1992). However, the use of high intensity ultrasound to facilitate hazardous waste site remediation has yet to be fully addressed.

Chapter #3: Experimental Section

3.1 Materials A list of chemicals, solvents, gases and instrumentation utilized without significant preparation are presented in Appendix A

3.2 Preparative Methods:

3.2.1 General

Table #1: Preparation of Glassware

| Designation | Preparation Steps |
|---------------------|---|
| "Prcleaned" | washed with liquinox/water solution, rinsed with reverse osmosis (RO) water, washed and reacted with hydrofluoric acid (5%) for a period of 10 to 15 minutes (mins) (all except volumetric ware), rinsed with Type I, organic free water, dried at 105°C in a constant temperature oven for at least one (1) hour (hr), and loosely sealed with aluminum foil prior to shelf storage. |
| "Prcleaned" "GC" | glassware to be used for procedures requiring gas chromatographic analysis were precleaned, rinsed 2 times with 2 - 10 Milliliters (mLs) of "Omni-Solv" acetone, 2 times with 2 - 10 mLs of resi-analyzed dichloromethane (CH ₂ Cl ₂), and dried in a constant temperature oven at 150°C for a minimum of one (1) hr |
| "Volumetric" | cleaned with liquinox/water solutions, rinsed with RO water, deionized (DI) water, organic free DI water, "Omni-Solv" acetone (2 times with 2-10 mLs), "Resi-Analyzed" dichloromethane (2 times with 2-10 mLs), and dried at 150°C for at least one (1) hr prior to use. |

Liquid scintillation samples were prepared by adding scintillation cocktail, shaking vigorously, and allowing to stand overnight prior to determination of radioactivity. Representative controls and blanks were used throughout to ascertain the presence of contamination and background levels of radioactivity. Reported levels of radioactivity are corrected for background and counting efficiencies are determined by comparison with quenched liquid scintillation counting efficiencies.

All temperatures are uncorrected (no thermometer stem correction performed).

Boiling points were recorded under ambient conditions and are uncorrected.

3.2.2 Preparation of Pentane:

Pentane (C_5H_{12} - reagent grade) was prepared for use, as a solvent for polycyclic aromatic hydrocarbons (PAHs) in the following multi-step process. Approximately 2500 mLs of reagent grade pentane was placed into a 3000 mL separatory funnel equipped with a Teflon stopcock and ground glass stopper and was successively washed and separated from:

- (a) alkaline potassium permanganate solution (100 mLs);
- (b) Type I organic free water (200 mLs);
- (c) concentrated H_2SO_4 (50 mLs); and

(d) type I organic free water (200 mLs).

The moist pentane resulting from this treatment was then dried over anhydrous sodium sulfate (Na_2SO_4), placed into a precleaned Pyrex distillation apparatus and refluxed for 30 mins over CaH_2 . The dry pentane was distilled into a receiving flask maintained at 0°C with an ice-water bath. The pentane boiling point range was $36.5\text{--}37.5^\circ\text{C}$. The redistilled pentane was stored over previously prepared (see appendix A: section A2.2i) type 4A activated molecular sieves in a brown bottle with a Teflon lined screw cap.

3.2.3 Preparation of Active Carbon (AC) for Fragmentation Experiments. Sieve Gradation - General Method.

Active carbon (approximately 100 grams (g)) was placed on a brass eight (8) inch diameter, 1000 micron (μ) mesh American Standard sieve fitted with a brass cover and pan. The sieve cluster was placed in a Ro-Tap testing sieve shaker and shaken vigorously, with tapping, for a period of five (5) mins. At the end of this time the sieve cluster was opened and the $+1000 \mu$ active carbon was removed to a precleaned Pyrex beaker. The $+1000 \mu$ material was stored in a desiccator equipped with Drierite prior to further use.

Sieve gradations of material resulting from various experimental procedures were obtained in the same manner except that a set of three (3) inch American Standard sieves were used with the same testing sieve shaker and the sieve cluster contained 1000, 500, 250, and 125 μ sieves, as well as a pan and an aluminum cover.

In all cases the dry samples were shaken for a period of five (5) mins.

3.2.4 Preparation of Active Carbon for Desorption

Experiments

Active carbon (presieved to +1000 μ as described above - ca 1500 g) was placed into a precleaned 3000 mL round bottom flask and organic free water was added until the level of the liquid was even with the top of the material. An additional 500 mLs of organic free water was then added and the mixture was shaken vigorously. The carbon was allowed to settle and the opaque supernatant was decanted and discarded. This procedure was repeated nine (9) times with 500+ mL aliquots of organic free water until the supernatant was clear. The flask was then inverted over a coarse fritted glass filter fitted to a vacuum filter flask. A vacuum was applied and the carbon was allowed to drain until no further water passed through the filter. The round

bottom flask containing the moist carbon was fitted to a rotary evaporator and the water was removed over a hot water bath (85°C) with rotation and applied vacuum until the carbon flowed freely in the flask. The carbon was placed in a precleaned 3000 mL Pyrex glass beaker and dried for 48 hrs at 105°C. The carbon was removed from the oven and placed hot into a desiccator equipped with a supply of indicating Drierite.

Five samples of the carbon were sieved (5 mins - Ro-Tap) through a stack of sieves (1000, 500, 250, 125 μ) and the sieve analysis recorded (see appendix B). The remaining active carbon was stored in a vacuum desiccator, equipped with Drierite, prior to use in subsequent experiments.

3.2.5 Preparation of Sand (Tanana Valley Alluvium) for Desorption Experiments

A pit run sample [ca 100 kilograms (kg)] was obtained from Fairbanks Sand and Gravel by Bret Davidson, a graduate student at the University of Alaska Fairbanks. The pit run material was dried in an oven at 105°C and the large (+3/4 inch) material was removed by hand sieving on a 3/4 inch brass American Standard sieve. The remaining (-3/4 inch) material was placed onto a set of two sieves, a pan, and a cover. The topmost sieve had a mesh opening of 2000 μ and

the second sieve had openings of 1180 μ . The material was shaken for a period of five (5) mins with tapping. At the end of this time the sieve was removed from the shaker and the plus 2000 μ and minus 1180 μ material were retained and set aside. The remaining +1180 μ material was transferred to a porcelain crucible and placed into a muffle furnace at 600°C for a period of one (1) hr. At the end of this time the material was removed from the furnace, stirred while still hot with a stainless steel spatula, and reheated to 600°C for an additional period of 15 mins. The material was removed from the oven, placed on a wire rack to cool slightly and then transferred to a vacuum desiccator equipped with Drierite.

Pre-tests with this material indicated that a large amount of fine particulate material was adsorbed on the surface of the granules. Because this would presumably result in contaminant impregnated particulate material being discharged from the reaction flask during experimental runs, the sand was further treated by placing approximately 20 g of this -2000 to +1180 μ material into a precleaned, tear drop shaped Pyrex flask equipped with a ground glass joint. Enough organic free water was added to cover the sand. The water/sand mixture was shaken vigorously and the excess water decanted off and discarded. This procedure was repeated (6 times) until the effluent water remained clear.

Enough organic free water was then added to cover the sand, and the flask was immersed in a boiling water bath for a period of 2 mins. At the end of this time a vacuum adapter was fitted to the flask and a vacuum rapidly imposed on the system. This caused the water in the flask to boil explosively, and the fine particulate matter which had not been removed by rinsing was ejected into the water. The water was decanted and discarded, and the sand was then rinsed three (3) times with 20 mLs of organic free water. This vacuum "dusting" procedure was repeated twice more (total of three times) and the sand was finally rinsed until no further fine particulate matter appeared in solution. The sand was removed from the flask and dried at 90°C prior to use as a desorption substrate.

3.2.6 Preparation of Glass Beads for Desorption Experiments:

Glass beads were inspected visually under a 60x microscope and were found to be roughly spherical in shape and to have relatively smooth exteriors. In order to increase the surface roughness, and the associated contaminant adsorption area, approximately 100 g of glass beads were placed into a polypropylene container with 100+ g of medium coarse, dry, Tanana Valley alluvial sand and enough water added to submerge the mixture and provide about

1/2 inch of liquid cover. A motor driven impeller was inserted into the mixture and stirring was initiated at approximately 100 revolutions per minute. The mixture was stirred for 24 hrs with infrequent additions of water to maintain submergence of the material. At the end of the 24 hrs, stirring was discontinued and the crude mixture was filtered to remove the sand and water. The resulting glass beads (now translucent) were compared with an untreated bead under the 60x microscope. The surface of the treated beads appeared appreciably rougher than that of the untreated bead.

The beads were washed thoroughly with deionized water and were then treated with a 10% solution of hydrofluoric acid for a period of 30 mins. At the end of this time the beads were again thoroughly rinsed with deionized water and then with organic free water. The beads were placed in a precleaned porcelain crucible and dried at 150°C overnight. The next morning the beads were removed from the oven, allowed to cool to room temperature, rinsed 2 times with approximately 20 mLs of reagent grade acetone, followed by two rinses with resi-analyzed dichloromethane and dried in the oven at 150°C for a period of 72 hrs. At the end of this time the beads were removed from the oven, allowed to cool to room temperature, and placed into a precleaned glass bottle equipped with a ground glass joint and stopper.

Thirty (30) roughly spherical glass beads were measured to ascertain their average diameters. The results of that evaluation are presented in table #2.

Table #2: Glass Bead Analysis*

| Property | Value |
|--------------------------------|-------------------------|
| Average diameter (d) | 0.296 centimeter (cm) |
| Average volume ($1/6 d^3$) | 0.014 cm ³ |
| Average surface area (d^2) | 0.275 cm ² |
| Total mass of 30 beads | 0.9733 g |
| Average mass/bead | 0.0324 g |
| Average density of bead | 69.52 g/cm ³ |

* Spherical glass bead shape assumed

3.2.7 Preparation of Isotope for Desorption Experiments

Individual samples of radiolabeled ¹⁴C-phenanthrene and ¹⁴C-biphenyl were placed into separate 100 mL volumetric flasks and diluted to volume with pentane which had been previously prepared (Section #3.2.2). This solution was assayed by liquid scintillation counting in 10 mL of Bio-Safe II scintillation solution to ascertain the radioactivity/mL of solution. These stock solutions were then used to prepare solutions utilized to load contaminant (phenanthrene or biphenyl) onto solid substrates.

3.3 Experimental Methods

3.3.1 Fragmentation Experiments: Active Carbon and Sand

The response of active carbon (AC) and Tanana Valley alluvial sand to an applied ultrasonic field was investigated to ascertain the extent of fragmentation that would occur. Both ultrasonic treated (sonic) and control (no sonic treatment) trials were performed. For the fragmentation experiments active carbon or sand (3.000 g +/- 0.01 g) was weighed, and added to the reaction flask.

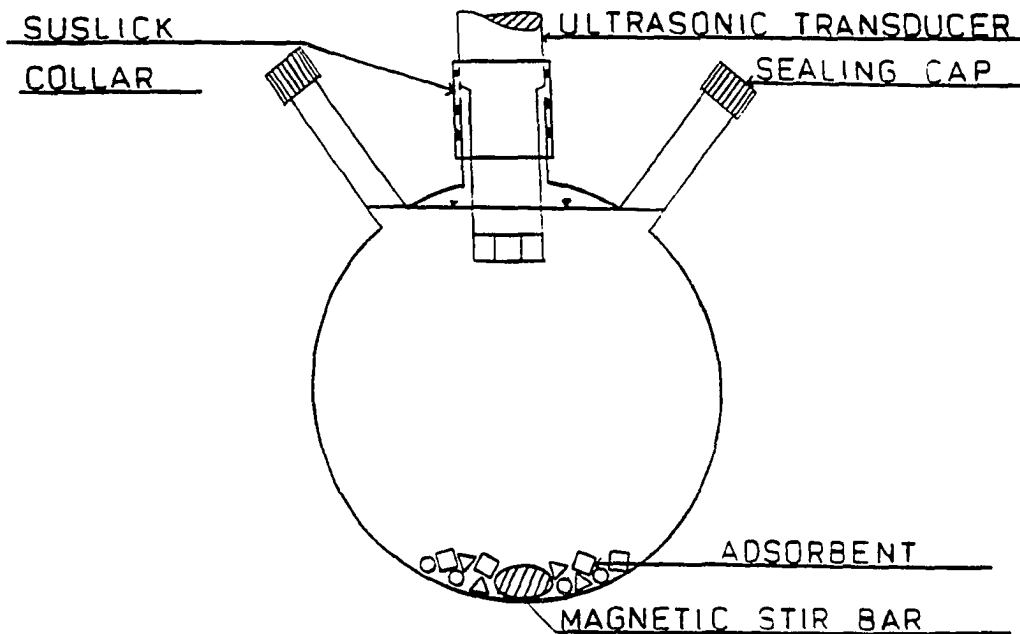


Figure #1: Fragmentation Experimental Apparatus

A magnetic stir bar was added and the reaction vessel was then fitted to the ultrasonic horn with the aid of the stainless steel (SS) Suslick collar. The reaction vessel was then immersed in an external cooling bath, and cooling water flow was initiated. Sufficient deionized (DI) water was added to fill the flask to the top of the side arms and magnetic stirring was initiated. Continuous sonication was performed at the indicated probe tip energy level and for the indicated time (see appendix B). Control samples were stirred but were not subjected to ultrasonic energy. Probe tip energy levels were supplied as a percent of full meter scale (475 Watts/cm^2) from the XL-2020 ultrasonic generator. At the end of the experimental run the carbon or sand was rinsed from the flask with DI water onto a preweighed medium porosity (5-14 μ) sintered glass funnel and vacuum filtered. No fine particulate material appeared to pass the filter by visual inspection of the filtrate. The surface dry material was removed from filter, placed into a preweighed liquid scintillation vial and the filter with fine adsorbed particulate matter and the scintillation vial with the carbon or sand sample was dried at 90°C for a period of approximately 12 hrs (filter) and 24 hrs (scintillation vial and sample). The filter with adsorbed material was removed from the oven, cooled to room

temperature in a vacuum desiccator equipped with Drierite, and weighed on an analytical balance to the nearest mg. The sample weights in the preweighed scintillation vials were determined, after cooling to room temperature, and the sample material was then placed into a set of 3 inch brass American Standard Sieves containing one each, from top to bottom a 1000, 500, 250, and 125 μ sieve. This three (3) inch sieve pack, with the sample, was placed into a tall American Standard sieve and packed in with Styrofoam packing beads. At the end of five (5) mins of shaking and tapping the sieve package was removed from the shaker and the mass retained on each sieve was determined on the analytical balance to three (3) significant decimal places. After weighing, the fractions were recombined in the original LSC vial and retained in a desiccator. Samples subjected to ultrasound and control samples (no sonic treatment) were treated in a similar fashion.

3.3.2 Chemical alteration experiments - general method

Two polycyclic aromatic hydrocarbons (phenanthrene and biphenyl) were chosen as contaminants to study in this project.

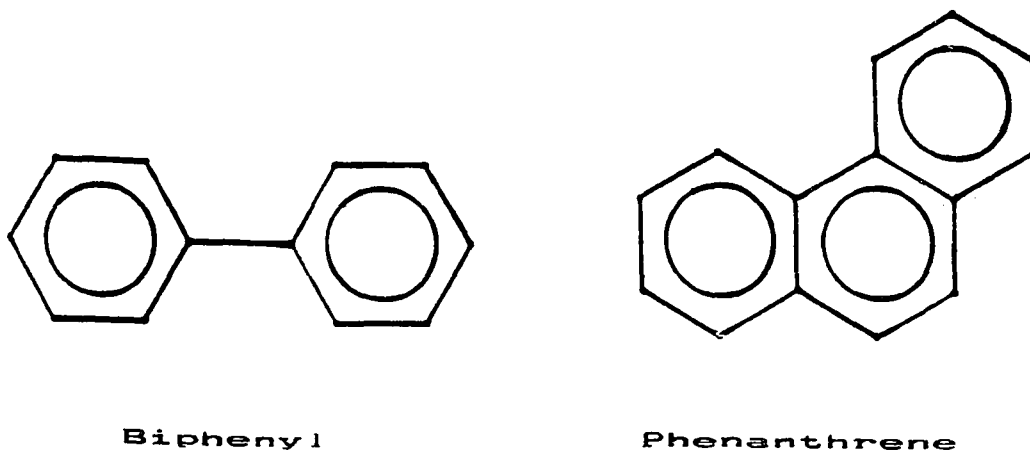


Figure #2: Structure of Biphenyl and Phenanthrene

Phenanthrene and Biphenyl were chosen for study because both exhibit hazardous properties (Windholz, 1976) and are readily available as radioactively labelled compounds. Phenanthrene is a fused ring compound exhibiting low water solubility [ca 1.28 milligrams/liter (mg/L)], and a common contaminant associated with slag and casting sand deposits from aluminum smelting, residue from coal combustion, and fly ash deposits. Biphenyl, a central nervous system depressant, is slightly soluble in water (ca. 7.0 mg/L) and represents the hydrocarbon skeleton of the polychlorinated biphenyl (PCB) family of congeners.

A modified reaction vessel, after the design of K.S. Suslick (1989) was constructed from a 300 mL borosilicate (Pyrex) round bottom boiling flask with a one (1) inch O.D.

neck and three (3) access ports for: additions; gas infusion; and a thermometer. The reaction apparatus is depicted in figure #3. The third access port has been deleted for visual clarity.

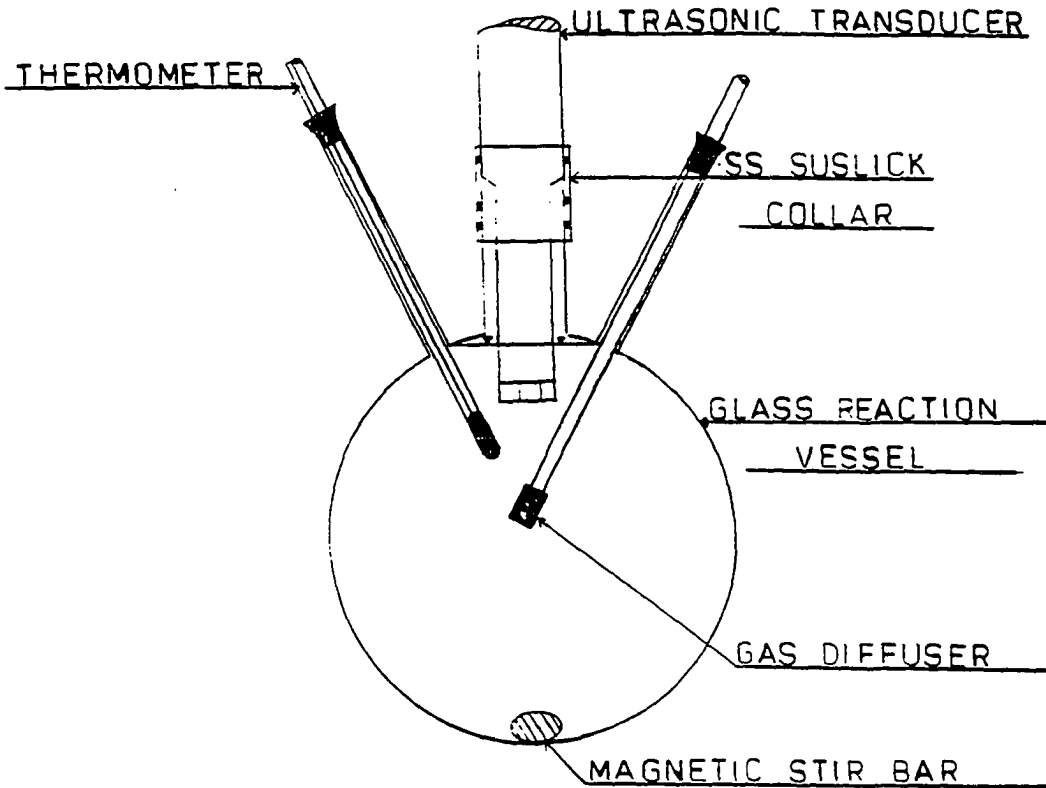


Figure #3: Chemical Alteration Experimental Apparatus

The non-radioactive compound of interest (phenanthrene or biphenyl - 0.390 mg) was transferred to the "precleaned GC" reaction vessel in a pentane solution and the pentane was removed under a stream of N_2 gas. Both biphenyl and phenanthrene appeared to form crystalline precipitates on

the walls of the reactor using this method of addition. For reactions requiring the addition of metal salts $\text{FeCl}_3 \cdot 6\text{H}_2\text{O}$ ($0.0179 \text{ g} \pm 0.0005 \text{ g}$; ca 6.63×10^{-5} mole) was added as a crystalline solid after evaporation of the pentane solvent. A Teflon stir bar was added and the reaction vessel was fitted to the ultrasonic horn with the SS Suslick collar. The o-rings of the Suslick collar were wrapped with Teflon tape to minimize the chance of contamination with o-ring extracts. The reactor was immersed in an external cooling water bath supplied with an inlet and outlet tube, filled with 310 mLs of organic free water, and a flow of house water was initiated to the external cooling bath at approximately 485 mLs/min. A thermometer was fitted to the reaction vessel and sealed in place with a rubber stopper. In experiments requiring gas infusion a precleaned coarse fritted glass aerator was introduced into the reaction vessel in the same manner. In reactions which required no gas infusion the aerator port was sealed with a rubber stopper. The rubber stopper was not allowed to contact the solution at any time during or after reaction. The temperature in the reaction flask varied from 21°C to 27°C during the experimental procedure. An initial temperature rise from 21°C to approximately 24°C accompanied the onset of sonic exposure. The reaction mixture temperature rise

during a one (1) min active probe pulse was approximately 2°C .

The addition neck was open to atmospheric pressure but was loosely covered with aluminum foil to exclude airborne contaminants. The gas flow to the reactor varied from 10 to 100 mLs/min. A tank mounted pressure regulator was used to control gas flow rate. The ultrasonic intensity was adjusted to:

- (1) 0 Watts/cm² at probe tip for control runs; and
- (2) approximately 147 Watts/cm² at probe tip {10 on dial, 31% on meter (XL-2020)} - pulsed (alternating one (1) min active probe and one (1) min inactive probe) with a total active probe time of one half (1/2) the total indicated reaction time (see Appendix D). Controls were also subjected to the same length of treatment but no sonic energy was applied to these reaction mixtures.

At the end of the reaction the gas infusion and cooling water were discontinued and the liquid contents of the flask were placed into a precleaned 500 mL separatory funnel fitted with a Teflon stopcock and a ground glass stopper. The gas diffuser, thermometer and Teflon stir bar were each rinsed two times with approximately one (1) mL of reagent grade dichloromethane (CH_2CL_2) and an additional 8 mLs of CH_2CL_2 was used to rinse the reaction flask. This rinse was added to the previous thermometer, diffuser and stir bar

rinses in the separatory funnel with the reaction mixture water. The reaction flask was rinsed with an additional 11 mLs of CH_2CL_2 and this rinse was again placed into the separatory funnel. The total volume of CH_2CL_2 used to clean the reactor and reaction hardware was 25 mLs. The mixture was shaken and the layers separated. The organic layer was removed and placed into a 50 mL Erlenmeyer flask. The flask was immersed into a warm water bath and evaporation of the CH_2CL_2 was initiated under a stream of N_2 gas. The reaction mixture was extracted twice more with 25 mL aliquots of CH_2CL_2 and the extracts were combined in the Erlenmeyer flask and evaporated to approximately 10 mLs total volume. At this point the flask was removed from the water bath and evaporation was continued at or below room temperature by hand. At the end of this evaporation stage the flask was cold to the touch in the region of the evaporating solution and frequently the water drops on the outside of the flask changed to ice due to the reduced temperature caused by heat loss during evaporation of the CH_2CL_2 . The volume of CH_2CL_2 extracts was reduced to approximately 2.0 mLs using this method at which point extracts were transferred to a small precleaned conical vial with a single rinse of 1.0 mL of CH_2CL_2 . The extracts in the small vial were hand evaporated to dryness at below room temperature, capped with a Teflon

lined screw cap and stored at -20°C (freezer), under N_2 gas, prior to GC analysis.

3.3.2.1 Gas Chromatography and Combined Gas Chromatography/Mass Spectrometry Analysis

Extracts to be analyzed by gas chromatography (GC) were removed from the freezer and 100 microliters (μL) of CH_2Cl_2 was added to the cold sample. The vial and sample were warmed to room temperature and a one (1.0) μL injection was made directly onto the 0.53 millimeter megabore column without splitting.

GC analyses with flame ionization detection (FID) were performed on a Perkin Elmer 8410 gas chromatograph. The Perkin Elmer GC programs are presented in Appendix C.

GC analyses with mass spectral detection were performed on a Hewlett Packard gas chromatograph fitted with a mass selective detector. See Appendix C for GC/MS details.

3.3.3 Desorption Experiments - General Methods

3.3.3.1 Overview of desorption experiments

A brief overview of desorption experiments performed in this investigation is presented in table #3, below. Table #3 lists the experimental designator, the identity of the

contaminant studied, and the substrate on which it was adsorbed in that particular experiment.

Table #3 : Overview of Desorption Experiments

| Experiment # | Contaminant ID | Substrate ID |
|--|----------------------------------|---------------|
| Radiation Experiment #1 Trial #1 (Rad #1 - Trial #1) | Phenanthrene (Sonic) | Active Carbon |
| Radiation Experiment #1 Trial #2 (Rad #1 - Trial #2) | Phenanthrene (Sonic) | Active Carbon |
| Radiation Experiment #2 (Rad #2) | Phenanthrene (Sonic) | Sand |
| Radiation Experiment #3 (Rad #3) | Phenanthrene (Sonic) | Sand |
| Radiation Experiment #4 (Rad #4) | Biphenyl (Sonic) | Glass Beads |
| Radiation Experiment #5 (Rad #5) | Biphenyl (No Sonic-Control) | Glass Beads |
| Radiation Experiment #6 (Rad #6) | Biphenyl (Sonic) | Glass Beads |
| Radiation Experiment #7 (Rad #7) | Biphenyl (Sonic) | Glass Beads |
| Radiation Experiment #8 (Rad #8) | Biphenyl (No Sonic - Control) | Glass Beads |

3.3.3.2 Radiation Experiment #1 - Sonication of 9-¹⁴C-
Phenanthrene on Active Carbon

Active carbon (0.9995 g) prepared in the manner described previously (Section #3.2.4) was placed into a tear drop shaped Pyrex glass flask equipped with a ground glass joint. To this carbon was added an assayed pentane solution (25 mLs total) of phenanthrene (2.2717 mg) and ¹⁴C- labelled phenanthrene [0.228 mg; 16.77 microcuries (μ Ci) - 17,237,392 disintegrations per minute (DPM)] in small (ca 1.5 mL) aliquots with evaporation under a stream of nitrogen (N₂) gas. The volumetric flask used to hold the pentane solution of isotope and the pipette used to transfer the solution were rinsed thoroughly with pentane and these washes were also added to the flask containing the active carbon. After all of the pentane had been evaporated, 1.5 mLs of organic free water was added to submerge the active carbon with adsorbed phenanthrene. The flask was then covered with aluminum foil and allowed to stand (at 2°C - refrigerator) until the sonication reaction was performed.

Assays were performed on the volumetric flask used to hold the pentane solution of isotope and on the pipette used to transfer the solutions. The amount of radioactivity remaining on the transfer glassware was negligible compared with the amount loaded on the carbon (i.e. total background corrected radioactivity remaining on transfer glassware = 14

DPM).

The mixture of active carbon/phenanthrene was equilibrated at 2°C for 50 days prior to sonication. The mixture was removed from the refrigerator and transferred to a modified, Pyrex glass, 50 mL Suslick reaction vessel (reactor). The reactor has an inlet tube equipped with a Teflon stopcock and a short outlet tube which is compatible with a specially constructed fraction collector. The assembled apparatus is depicted below.

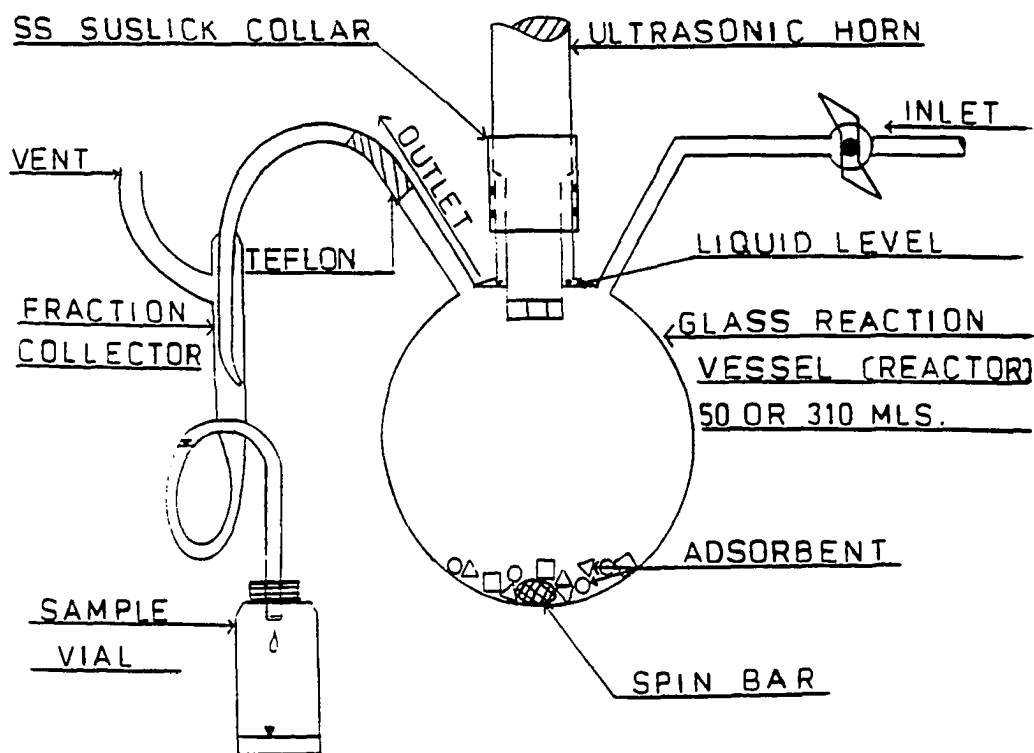
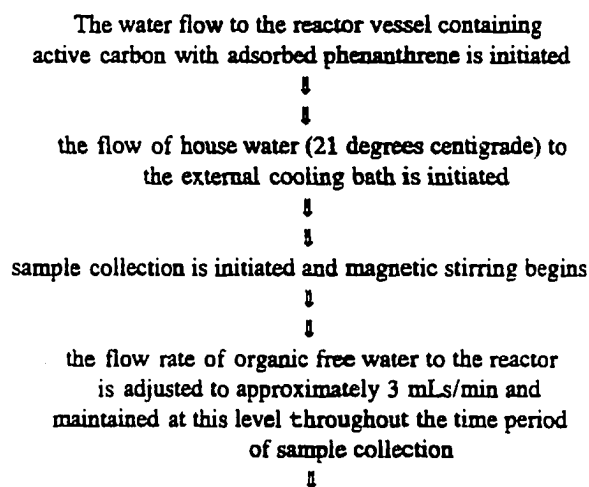


Figure #4: Desorption Experimental Apparatus

The tear drop flask which had contained the carbon, phenanthrene, and water mixture was assayed for residual radioactivity. The assay indicated negligible radioactivity remaining in the flask (39 DPM - 0.0002% of original radioisotope load amount). A magnetic stirrer was added and the reactor containing the carbon, phenanthrene, water, and stir bar was attached to the ultrasonic transducer with the SS Suslick collar. The reaction apparatus was immersed in an external cooling bath filled with water at 21°C. A source of organic free water was connected to the reactor inlet tube and the outlet tube was connected to the fraction collector with a short section of Teflon tubing. The reactor was filled with organic free water and allowed to equilibrate for a period of 2 hrs prior to initiation of the experimental protocol.

The following flow chart describes the experimental steps performed in Radiation Experiment #1 (rad #1).



five (5) probe tip energy levels are investigated in the order 0 watts/sq cm, 24 watts/sq cm, 48 watts/sq cm, 67 watts/sq cm, 81 watts/sq cm, and 0 watts/sq cm

↓

↓

samples were obtained in preweighed sample containers as indicated below:

- (a) 2.0 mLs in liquid scintillation vial;
- (b) 2.0 mLs in liquid scintillation vial - duplicate of first sample;
- (c) 3.0 mLs in a Pyrex test tube with Teflon lined cap;
- (d) 3.0 mLs in a second Pyrex test tube with Teflon lined cap;
- (e) 3.0 mLs in a third Pyrex test tube with Teflon lined cap; and
- (f) 3.0 mLs in a fourth Pyrex test tube with Teflon lined cap;

↓

↓

Volumes were determined by preweighing vial (or tube) prior to experiment and weighing vial and sample at end of experiment. Weight differential yielded the mass of the sample collected. Masses were then converted to volume measure at weighing temperature (Weast, 1987).

↓

↓

After weighing, the samples were stored at 2 degrees centigrade in a refrigerator prior to analysis.

↓

↓

At the end of the experimental protocol the flow of water to the reactor was discontinued, the magnetic stirrer was stopped, and the flow of cooling water to the external bath was terminated.

The active carbon was allowed to stand in the reactor under water for 84 hrs, at room temperature (ca. 23°C) and was then treated in the following manner (Radiation Experiment #1, Trial #2):

The flow of organic free water was reinitiated to the reactor at 3 mLs/min and magnetic stirring was resumed the cooling water to the external water bath was resumed and three samples alpha1, alpha2, and alpha3 were collected during reactor flow adjustment

↓

↓

four (4) two (2) mL LSC vial counting samples and eight (8) ten (10) mL tube samples were then taken at each successive energy level (0 Watts/sq cm, 24 Watts/sq cm , 48 Watts/sq cm, 67 Watts/sq cm, 81 Watts/sq cm, and 0 Watts/sq cm) in preweighed sample containers

↓

↓

The mass and volume of the samples were determined as described above

Liquid scintillation counting of all active carbon/ $9-^{14}\text{C}$ phenanthrene samples was conducted in 17 mLs of Biosafe II liquid scintillation counting solution with 30 g of (Cab-O-Sil - M5) fumed silicon dioxide thixotropic gelling agent.

The outcome of the first and second sonic treatment of the active carbon/phenanthrene system are presented in appendix E: section E1.

3.3.3.3 Sonication of $9-^{14}\text{C}$ phenanthrene adsorbed on Tanana Valley alluvial sand

Replicate sand experiments were performed to evaluate the ability of an ultrasonic field to desorb an adsorbed PAH (phenanthrene) in aqueous media (radiation experiments #2 and #3 - rad #2 & #3). The general protocol was similar for

both experiments and is presented below. Individual variations for the two experiments are noted in this section and in tables #4 and #5 below.

A pentane solution of ^{14}C -phenanthrene was prepared and assayed. No additional neutral compound was added since the available area of adsorption was anticipated to be quite low compared with that of active carbon, and a high specific activity was required to obtain measurable quantities of radioactivity in the approximately two (2) mL effluent fractions. The sand (prepared previously - section #3.2.4) was placed into a suitable glass vessel - i.e. tear drop shaped - to concentrate the solution in the proximity of the sand in the final stages of evaporation. The pentane solution was then added in small aliquots (1.5 mLs) to the sand, and the pentane from each aliquot was evaporated until the sand was surface dry prior to addition of the next aliquot. Evaporation generally occurred at below room temperature with a buildup of condensation on the outside of the glass walls of the vessel. The flask containing the pentane solution of radioisotopic phenanthrene was rinsed three (3) times with approximately two (2) mLs of pentane and these washings are added to the sand sample and evaporated as before. The sand/ ^{14}C -phenanthrene was then covered with organic free water (ca 1.5 mLs) and allowed to

equilibrate at 2°C and/or room temperature for the time period indicated in tables #4 & #5 below.

At the end of the equilibration time the sand/9-¹⁴C phenanthrene/water was transferred to the reaction vessel and the water used for transfer and washing of the equilibration flask was combined with the sand/9-¹⁴C phenanthrene/water in the reaction vessel. The 50 mL reactor was utilized for the sand/9-¹⁴C phenanthrene experiments. A magnetic stir bar was added to the reaction vessel and the reactor was carefully fitted to the ultrasonic horn with the aid of the stainless steel Suslick collar, engaging both of the o-ring seals. A source of organic free water was connected to the inlet of the reactor and a fraction collector was connected to the outlet (see figure #4). Organic free water was added to fill the reservoir initially and at regular intervals during the experimental run in order to maintain a relatively uniform pressure head. The flow of organic free water to the reactor was initiated and the flow rate was determined (ca 3 mLs/min). Magnetic stirring and sample collection commenced at the same time organic free water flow to the reactor was established. Sampling was conducted by collecting duplicate two (2) mL (approx.) samples in preweighed LSC vials and a single ten (10) mL sample obtained in a preweighed test tube equipped with a Teflon lined screw cap. This sampling

procedure was repeated until the desired number of samples was obtained. The total number of each sample type obtained is presented in tables #4 & #5. The water and sand remaining in the reaction flask at the end of radiation experiment #2 (rad #2) were discarded without further analysis. The water remaining in the reaction flask at the end of radiation experiment #3 (rad #3) was assayed for residual radioactivity (3462 DPM in 54.5 mLs of reactor water). The sand remaining at the end of radiation experiment #3 (rad #3) was partially assayed for remaining radioactivity (see Appendix E).

All glassware used in preparation, transfer, and storage of isotopically labelled ^{14}C -phenanthrene was assayed for residual radioactivity as that portion of the experiment was completed. In general the amount of radioactivity remaining after transfer of sand samples is greater than that observed after transfer of the active carbon/ ^{9-14}C phenanthrene/water indicating the decreased affinity of the sand for the contaminant compared with active carbon.

Table #4: Values of Measured and Calculated Physical Parameters for First Sand/9-¹⁴C Phenanthrene Desorption Experiment:

| Parameter | Value |
|---|--|
| Mass of sand | 1.0007 g (167 particles) |
| Time of equilibration | 16 hrs at 2 ^o C followed by 22 hours at 18-20 ^o C. |
| Amount of radioactivity lost to storage flask | 298 DPM (0.17% of initial radioactive load) |
| *Amount of UL- ¹⁴ C biphenyl added initially | 169,999 DPM (1.04 μg) |

Number of samples obtained:

(1) In scintillation vials - 35 duplicate samples (70 counting samples total)

(2) In test tubes - 35 samples

* See appendix E for DPM to mass conversion calculation

Table #5 : Values of Measured and Calculated Physical Parameters for Second Sand/9-¹⁴C Phenanthrene Desorption Experiment (Rad #3)

| Parameter | Value |
|---|--|
| Mass of sand | 1.0014 g (156 particles) |
| Time of equilibration | 112 hrs at 18-20 ^o C. |
| Amount of radioactivity lost to storage flask | 1044 DPM (0.56% of initial radioactive load) |
| Amount of ¹⁴ C-UL-biphenyl added initially | 184,837 DPM (1.13 μg) |

Number of samples obtained:

(1) In scintillation vials - 40 duplicate samples (80 counting samples total)

(2) In test tubes - 40 samples

* See appendix E for DPM to mass conversion calculation

3.3.3.4 Sonication of UL-¹⁴C biphenyl and biphenyl on glass beads

Five (5) glass bead desorption experiments were performed - radiation experiments #4 through #8 (rad #4-8). The preparation protocol is similar for the sonic and control runs. However, small variations in procedure, especially at the start of the experiments, resulted in significant observable changes during data treatment. Individual method variations for the two experiments are noted below and in appendix E: sections E3 & E5.

All of the glass bead/UL-¹⁴C biphenyl experiments began by preparing a pentane solution of radiolabeled and unlabeled biphenyl. Unlabeled biphenyl was used (3.976 mg in radiation experiment #4 and 3.988 mg in radiation experiments #5-8) to dilute the ¹⁴C labelled biphenyl and obtain a solution of the required specific activity.

Glass beads, prepared previously (section #3.2.6), were placed into the 300 mL reactor vessel (see figure #4 above) and the pentane solution (10 mLs total) of biphenyl was then added. The volumetric transfer flask used to hold the biphenyl was rinsed three (3) times with one (1.0) mL portions of pentane, and these washings were added to the reaction vessel. The reactor was sealed tightly with a rubber cork and the inlet stopcock was closed. A gas inlet

tube was attached to a source of nitrogen gas and the reactor outlet tube was attached through a glass adapter to a cold trap immersed in liquid nitrogen. The cold trap (pictured below) was incorporated to minimize volatilization losses during solvent evaporation while loading isotope onto the substrate.

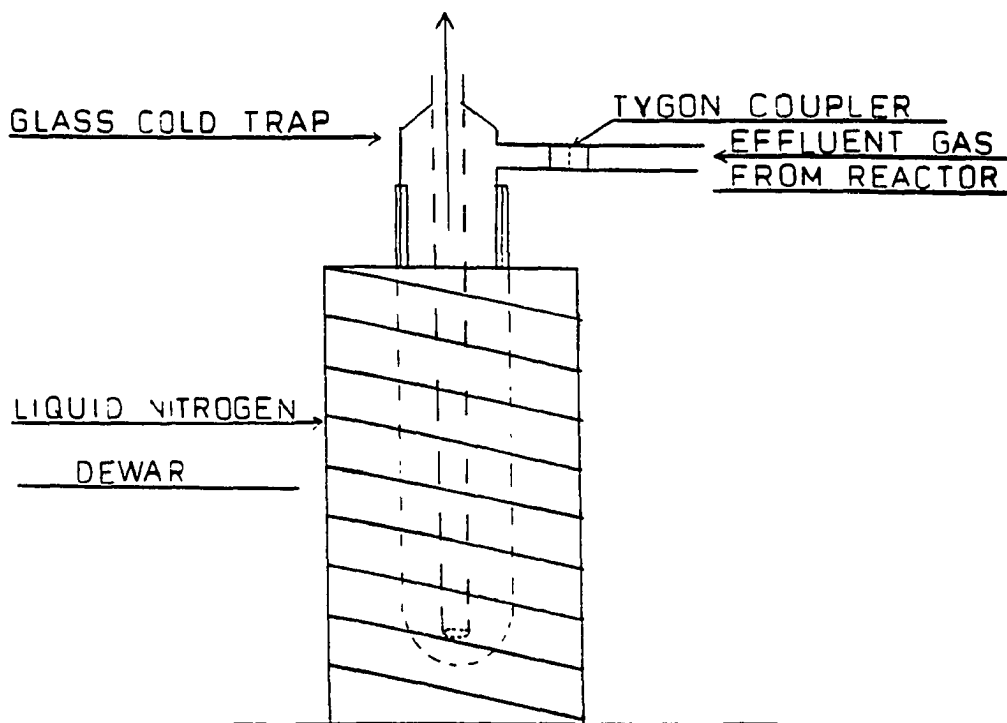


Figure #5: Cold Trap Apparatus

The pentane was evaporated with a steady stream of nitrogen gas at below room temperature. The reaction vessel, glass beads, and precipitated biphenyl were kept cold by applying a cloth dipped in liquid nitrogen to the outside wall of the flask to minimize the volatilization of the radiolabeled biphenyl. When the last of the pentane had been removed the nitrogen infusion was stopped and the reaction flask containing the ^{14}C -UL-biphenyl adsorbed on the surface of the glass beads was cooled further with liquid nitrogen. At this point crystalline biphenyl was visible on the surface of both the beads and the reaction vessel. The seal to the cold trap was then severed and the gas infusion tube was removed from the flask. The stopper was removed from the neck of the flask, a magnetic stir bar was inserted, and the flask was fitted to the ultrasonic horn with the SS Suslick collar. The flask was again cooled with liquid nitrogen and the attachment to the fraction collector was made. A source of organic free water was attached to the inlet and the flow of water was initiated.

The reaction flask was filled rapidly in radiation experiment #4, more slowly in radiation experiment #5, and with a pause in radiation experiments #6, #7, and #8. The pause allowed the magnetic stirrer to disrupt crystalline biphenyl suspended on the surface of the liquid. Sampling was conducted in a fashion similar to previous radiation

experiments with two (2) two (2) mL samples being taken for duplicate liquid scintillation counting and one ten (10) mL sample being taken for further tests. This sampling procedure was repeated (40 times) until all of the required fractions were obtained.

This sampling protocol provided a mechanism by which larger volumes of solution could be run through the reactor without having to discard any effluent liquid. Furthermore, this technique allowed for collection of discrete fractions of effluent for subsequent analysis.

At the end of each experiment all glassware used in preparation, transfer, and storage of isotopically labelled UL-¹⁴C biphenyl was assayed for residual radioactivity. The results of these assays are presented in appendix E.

A loss of cold trap retained material occurred in radiation experiment #4 due to liquid nitrogen boiling within the cold trap after removal of the apparatus from the external dewar of liquid nitrogen. For subsequent experiments (radiation experiments #5-8) the cold trap joint was opened upon removal of the apparatus from the external liquid N₂ bath allowing the condensed N₂ within the trap to volatilize without carrying the trap contents with it.

During the first glass bead/UL-¹⁴C biphenyl trial (radiation exp #4) difficulties were encountered which caused transient peaks of radioactivity to occur in

collected fractions. The presence of these transient peaks had a direct effect on the outcome of a linear regression analysis performed on the combined data from all of the glass beads/UL-¹⁴C biphenyl experiments. The difficulties encountered and techniques utilized to minimize their influence are reviewed more fully in Appendix E: Section E5.

Chapter 4: RESULTS AND DISCUSSION

4.1 Fragmentation

4.1.1 Active Carbon Fragmentation

A study of the breakdown of activated carbon (AC) in an ultrasonic field of varying intensity was conducted because extensive fragmentation could make regeneration of contaminated AC impractical. In addition, extensive fragmentation of AC by high intensity ultrasonic fields may hinder the use of these field strengths to stimulate chemical alteration of surface adsorbed contaminants.

A pictorial representation of the fragmentation apparatus utilized in this investigation is reproduced in figure #1 (page 29).

Minor fragmentation of AC, in aqueous suspensions, was observed at ultrasonic field strengths up to 67 watts/cm² (50 mL reactor - 5 min) and 150 Watts/cm² (310 mL reactor - 30 min). These field strengths were sufficient to establish sustained audible cavitation in the reaction vessels.

Carbon fragmentation was extensive when ultrasonic fields in excess of 85 Watts/cm² (50 mL reactor - 5 min) and 190 Watts/cm² (310 mL reactor - 50 min) were utilized. At these higher energy levels both audible cavitation and visible

circulation of the liquid and carbon by the applied field were observed. Higher rates of fragmentation observed in the smaller (50 mL) reaction vessel indicate that high liquid circulation velocities within the reactor, resulting in impacts of carbon with the walls of the vessel, play a major part in material breakdown. The rate and extent of material breakdown is primarily related to the geometry of the reactor and the ultrasonic field strength, but the duration of treatment also plays a significant role. Evidence of AC fragmentation in the 50 and 310 mL reaction vessels is presented in figures #6-#12 (see also appendix B).

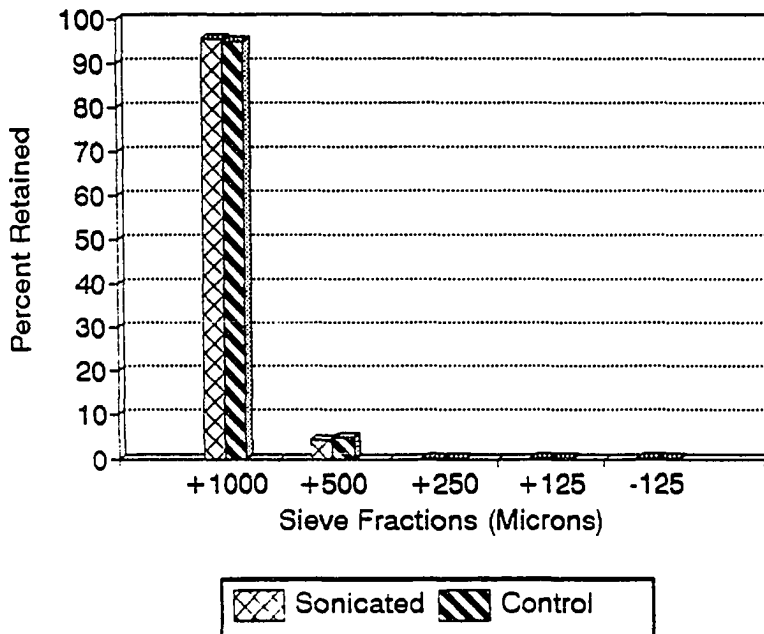


Figure #6: Sieve Analysis of Activated Carbon Subjected To 43 Watts/Sq Cm for 5 Minutes in a 50 mL Reactor

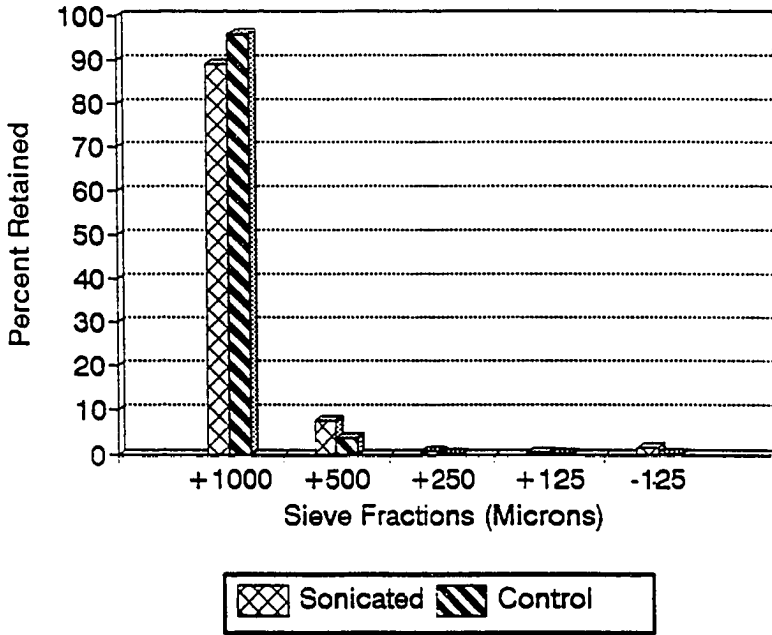


Figure #7: Sieve Analysis of Activated Carbon Subjected To 85 Watts/Sq Cm for 5 Minutes in 50 mL Reactor

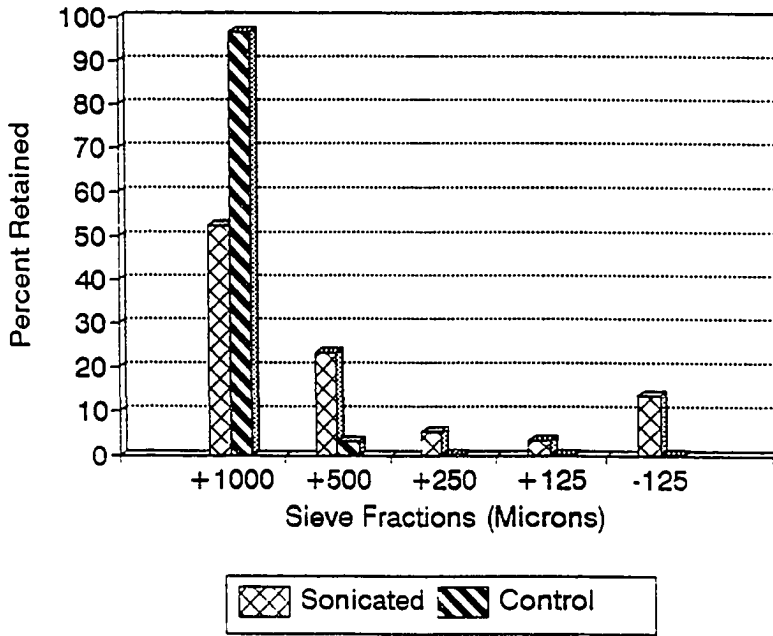


Figure #8: Sieve Analysis of Activated Carbon Subjected To 138 Watts/Sq Cm for 5 Minutes in 50 mL Reactor

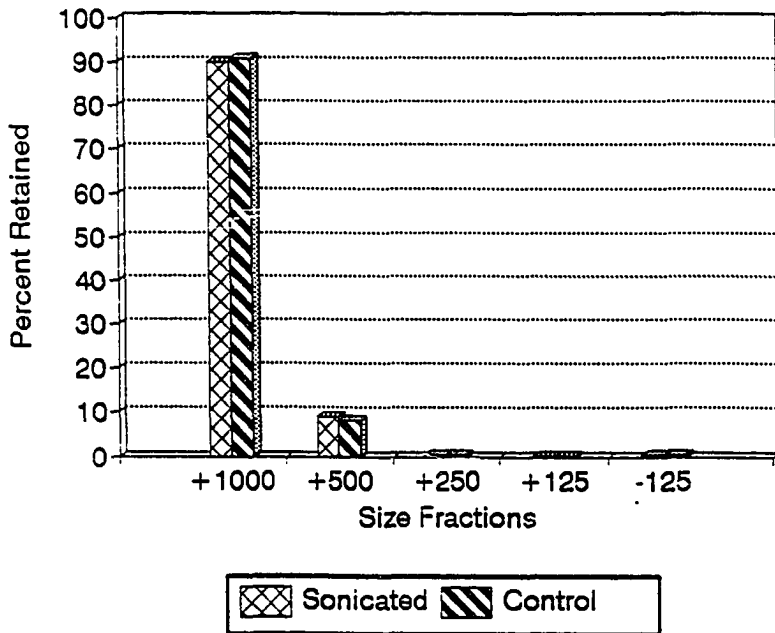


Figure #9: Sieve Analysis of Activated Carbon Subjected to 50 Watts/Sq Cm for 30 Minutes in 310 mL Reactor

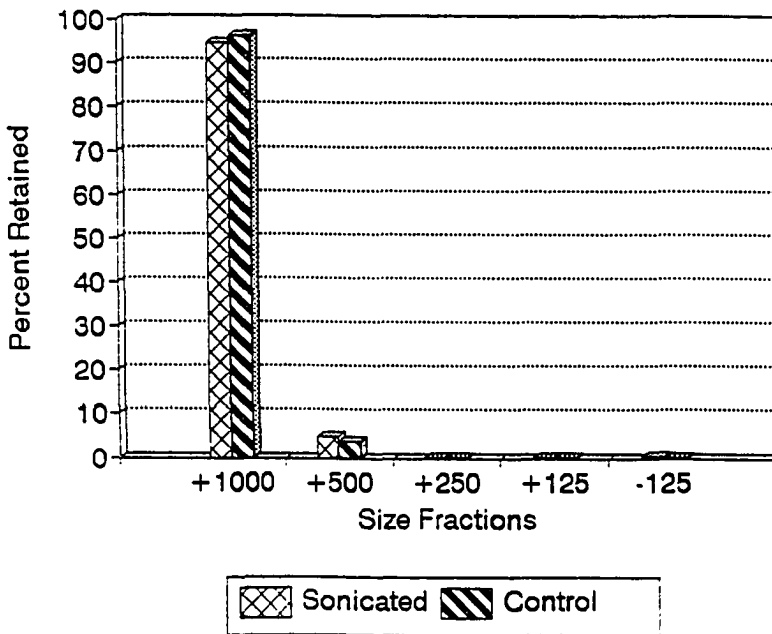


Figure #10: Sieve analysis of Activated Carbon Subjected to 85 Watts/Sq Cm for 25 Minutes in 310 mL Reactor

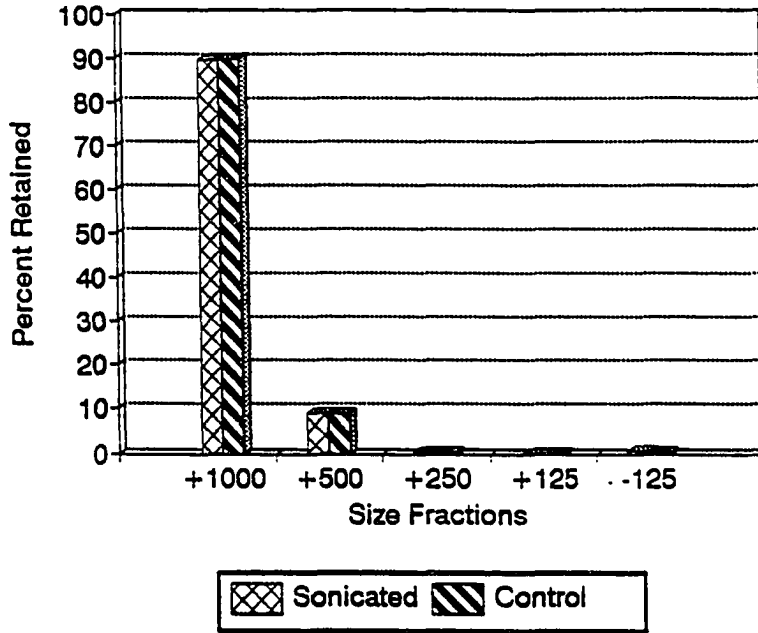


Figure #11: Sieve Analysis of Activated Carbon Subjected to 150 Watts/Sq Cm for 30 minutes in 310 mL Reactor

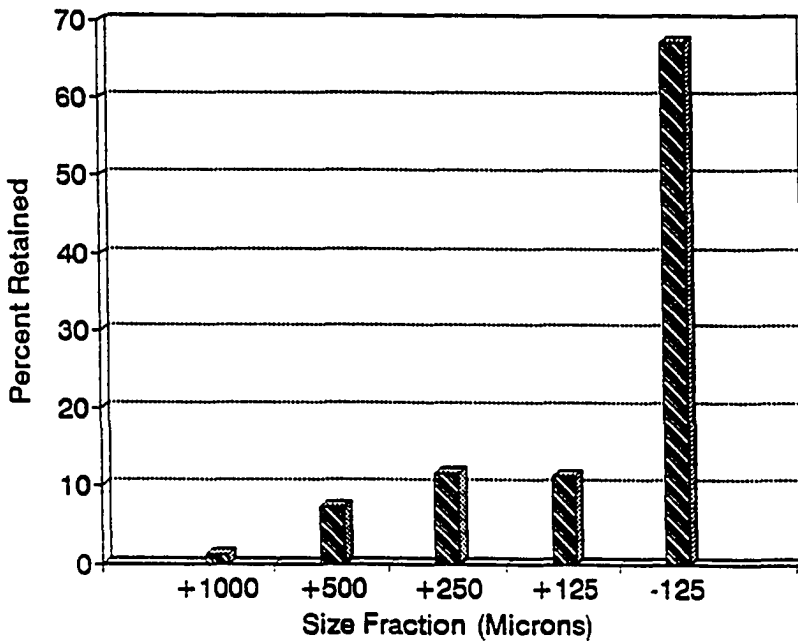


Figure #12: Sieve Analysis of Activated Carbon Subjected to 190 Watts/Sq Cm for 50 minutes in 310 mL Reactor
Single Trial - No Control

The carbon used in these trials was immersed in water just prior to the experimental run. The fragmentation that occurred, therefore, may not be completely representative of the outcome that can be expected when carbon that has been hydrated for a significantly longer time is tested. Time of hydration versus fragmentation rate and extent was not investigated in this study and represents future work.

The outcomes of experiments on AC demonstrate that, in aqueous suspensions, an ultrasonic field of varying intensity can fragment activated carbon extensively. This is not surprising as AC is a relatively soft material whose hardness is measured as an abrasion resistance. However, extensive fragmentation may limit or preclude the use of ultrasound to regenerate AC.

4.1.2 Tanana Valley Sand Fragmentation

Exhaustive fragmentation tests of Tanana Valley sand, a relatively hard natural aggregate material (Beach, 1992), were not conducted in this study. However, a comparison of the results from a single experiment to measure fragmentation of this material in a high intensity ultrasonic field with unreacted starting material demonstrates that the

sand aggregate can undergo fragmentation when exposed to a high intensity ultrasonic field. This comparison reveals a breakdown of sand in the +1000 micron fraction and a subsequent buildup of material in the +500 ml fraction (See figure #13 and #14 below).

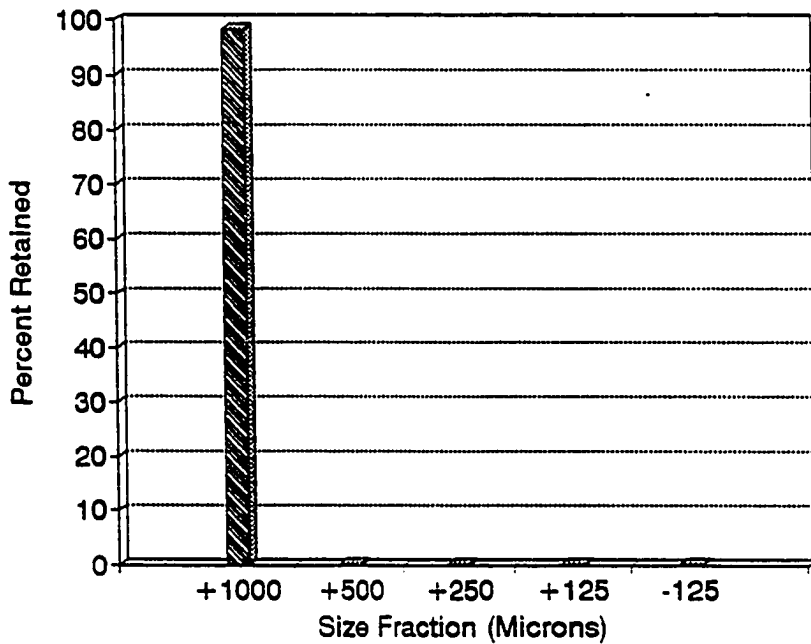


Figure #13: Sieve Analysis of Tanana Valley Sand - Single Trial - Untreated Starting Material

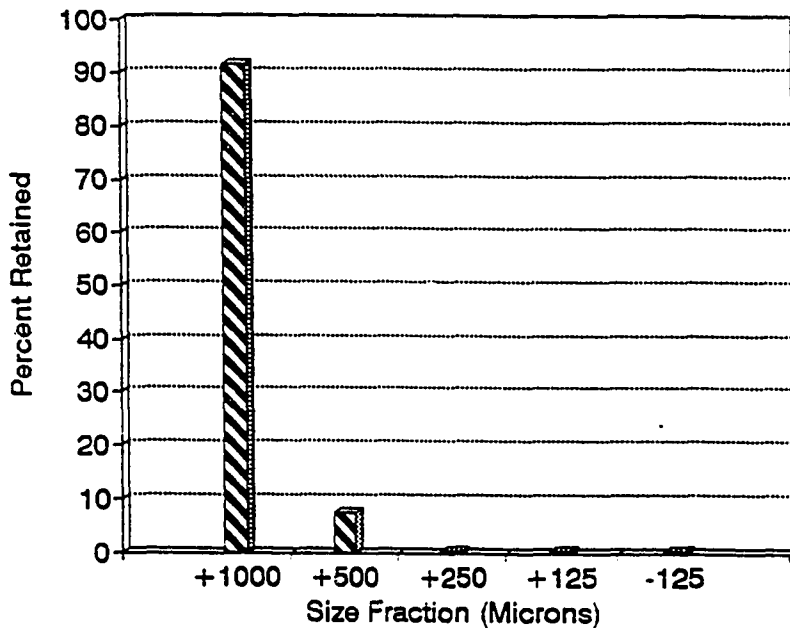


Figure #14: Sieve Analysis of Tanana Valley Sand Subjected to 156 Watts/Sq Cm for 50 Minutes in 310 ml Reaction Vessel - Single Trial

The results obtained for activated carbon and for sand aggregate suggest that attempts to treat contaminated activated carbon and natural aggregate materials with high intensity ultrasonic fields may result in minor or major fragmentation depending on the hardness of the material, reactor geometry, field strength and time of exposure.

4.2 Chemical Alteration

This series of experiments were designed to qualitatively demonstrate chemical alteration of polycyclic aromatic hydrocarbons (PAHs) in aqueous media under the influence of an applied high intensity ultrasonic field. A sample of the changes that occur in parent hydrocarbon (biphenyl and phenanthrene) gas chromatographic (GC) peak area versus total reaction time is presented in Figures #15 & #16 below.

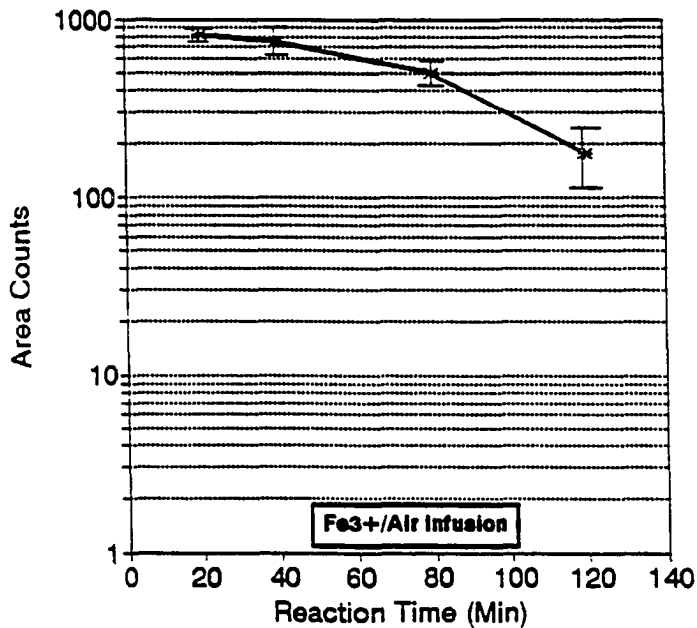


Figure #15: Average Biphenyl Gas Chromatography Peak Area vs Total Reaction Time (90% Confidence Interval Data) - Fe³⁺/Air Infusion

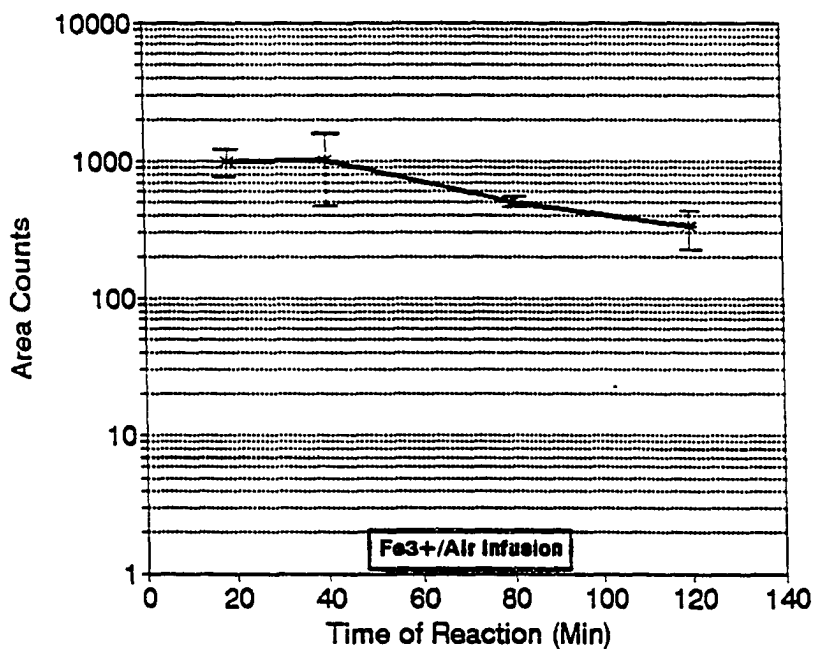


Figure #16: Average Phenanthrene Gas Chromatography Peak Area vs Total Reaction Time (90% Confidence Interval Data) - Fe³⁺/Air Infusion

Similarly, representative variations in total reaction product GC peak area with total reaction time are presented in figures #17 & #18 below.

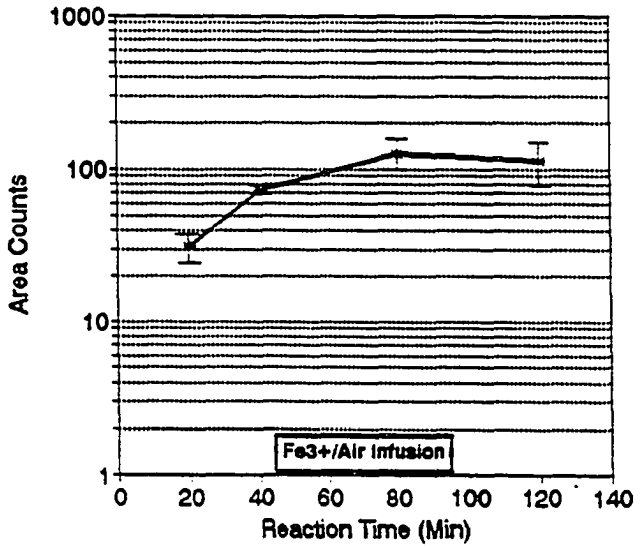


Figure #17: Average Total Biphenyl Reaction Product Gas Chromatography Peak Area vs Total Reaction Time (90% Confidence Interval Data) - Fe³⁺/Air Infusion

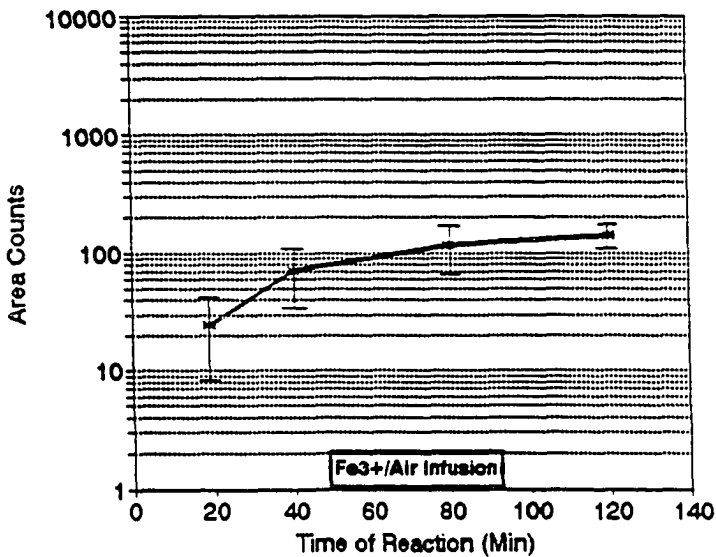


Figure #18: Average Total Phenanthrene Reaction Product Gas Chromatography Peak Area vs Total Reaction Time (90% Confidence Interval Data) Fe³⁺/Air Infusion

Finally, changes in the ratio of parent compound GC peak area to total reaction product GC peak area versus total reaction time are demonstrated in figures #19 and #20 below.

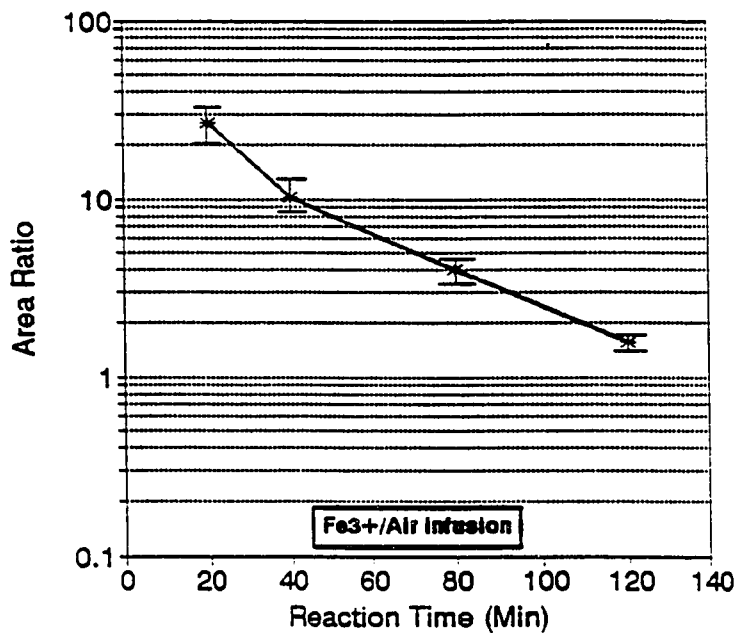


Figure #19: Average Ratio of Biphenyl GC Peak Area to Total Biphenyl Reaction Product GC Peak Area vs Total Reaction Time (90% Confidence Interval Data) - Fe^{3+} /Air Infusion

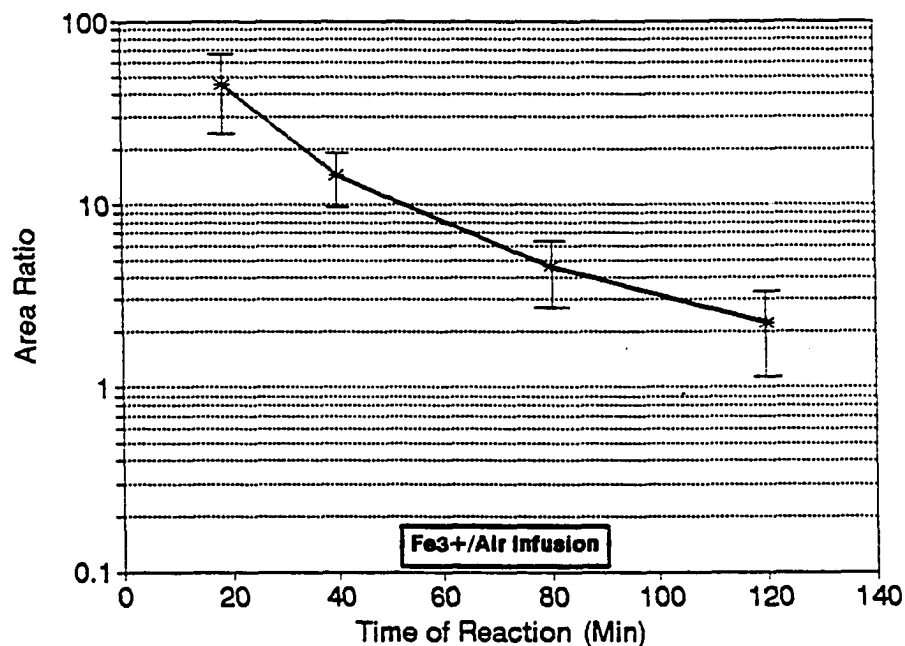


Figure #20: Average Ratio of Phenanthrene GC Peak Area to Total Phenanthrene Reaction Product GC Peak Area vs Total Reaction Time (90% Confidence Interval Data) - Fe³⁺/Air Infusion

Only the reactions in which Fe³⁺ and air infusion were utilized are presented here. A complete listing of all chemical alteration experimental results and plotted data appears in Appendix D.

Gas chromatography peak areas were corrected for background influences through the use of controlled experimental runs in which sonic energy was not applied to the reaction mixture but all other reaction conditions emulated sonic treatment. Figures #15 and #19 for biphenyl and figures #16 and #20 for phenanthrene demonstrate that

the parent peak area and the ratio of parent peak area to total reaction product peak areas decrease with increasing reaction time while figures #17 and #18 show that the total reaction product peak areas generally increases with increasing reaction time.

A statistical analysis of the data was used to construct the confidence intervals presented above. Additional statistical information is presented in Appendix D. Wide variations in parent hydrocarbon GC peak areas and total reaction product GC peak areas gave rise to the large confidence intervals observed in the data. Peak area variations were the result of volatilization upon evaporation both at the start of the reaction and during workup of the reaction mixtures, and a GC column failure during analysis of the samples requiring an additional evaporation step. Large values of the coefficient "T" (see appendix D for an explanation of the "T" coefficient) serve to amplify the size of the confidence intervals. The magnitude of the "T" coefficient increases as the number of sample points obtained at each reaction time interval tested decreases.

4.2.1 Volatility

Evaporative loss of parent compound (biphenyl and phenanthrene) was possible during preparation of the compounds

for reaction. Moreover, loss of parent compound and ultrasound induced reaction products during evaporation of extracts was likely. Future attempts to quantify the extent of reaction will demand techniques which provide a more rigorous control of losses to evaporation. These techniques will require the use of substantially larger quantities of solvent and will subsequently generate significantly larger quantities of hazardous waste.

The volatilization of hydrocarbon was unequivocally identified as a loss mechanism while evaporating radiolabeled biphenyl in preparation for the final series of desorption experiments. When a pentane solution of ^{14}C -UL-biphenyl was evaporated, just to dryness at room temperature, in a scintillation vial the amount of radioactivity decreased from an average of 2995 DPM (standard deviation (s) = 24.5 DPM) to an average of 508 DPM (s = 90.6 DPM); a loss of approximately 83%. It must be noted that distribution of this very small amount of material (ca 2.73 μg) on the relatively large surface area of the scintillation vial will greatly enhance the mass transport of the compound into the nitrogen gas stream.

In order to minimize biphenyl losses during preparation for the subsequent desorption experiments the desorption apparatus was reconstructed. A liquid nitrogen cold trap (see figure #5, page 50) was added to capture effluent vapor

from the evaporation of solvent during the loading of biphenyl onto the glass beads. Analysis of the contents of the cold trap demonstrated that an average of 2.14% ($s = 0.95\%$) of the radioactivity added to the flask was lost from the reactor as vapor during the operation. This occurred in spite of the fact that precautions were taken to minimize volatilization (see section #3.3.3.4). This result emphasizes the importance of volatility considerations during operations in which evaporation, to dryness, of a solution of PAH occurs.

4.2.2 Hydrophobicity

As outlined in section 2.2.4, Henglein and Kormann (1985) have investigated nitrogen and oxygen containing aliphatic, cyclic, and aromatic organic compounds (alcohols, acids, ketones, etc.) and have indicated that a linkage exists between the overall hydrophobicity of a compound and its ability to act as a radical scavenger. The overall hydrophobicity was further related to the tendency of the compound to accumulate at the interface of cavitation bubbles thereby exposing it to the highly reactive free radical species present there. To quantify this relationship Henglein and Kormann formulated a factor "R", based on the ratio of hydrophobic groups to hydrophilic

groups (R = hydrophobic/hydrophilic) in the same molecule, to describe the overall hydrophobicity of a molecular species.

For the polycyclic aromatic hydrocarbons (PAHs) investigated in this study the ratio "R" is undefined since no hydrophilic groups exist on the molecules (i.e. $R = x/0$ where $x =$ any number of hydrophobic groups). In the present study, therefore, the hydrophobic PAHs (biphenyl and phenanthrene) might both be expected to be preferentially present at the reactive interface and exhibit similar reactivities.

The results presented in figures #15 through #20 above as well as figures #D5 through #D18 (see appendix D) show a general similarity between comparable results (air infusion, no gas infusion, and Fe^{3+} /air infusion) obtained for biphenyl and phenanthrene. This similarity may be interpreted as being an indication that variations in PAH hydrophobicity might not play a major part in determining the susceptibility of a species to chemical alteration during ultrasonic treatment. Testing this hypothesis represents an important area for future investigation since many of the PAHs which exhibit the highest potential for carcinogenicity are generally less soluble than either biphenyl or phenanthrene. Experiments to test this

hypothesis have been prepared (i.e. benzo [a] pyrene as contaminant) and more are planned as future work.

4.2.3 The Contribution of Iron (III)

The results of experiments with biphenyl and phenanthrene presented in figures #D11-#D13 and D20-D22 (See Appendix D) indicate that reaction rate enhancement by added Fe^{3+} ions, if present, is not distinct enough to be measurable under the reaction conditions utilized in this work. The expected contribution of the soluble transition metal ion (Fe^{3+}) is partially over-shadowed by the large variation in peak areas for both the parent compound and for the reaction products as is evidenced by the large confidence intervals obtained from the data.

Visual observation of a distinct color change (from clear to a light yellow-brown) during sonication of reaction mixtures containing Fe^{3+} but not during control (no sonic) experiments indicate that Fe^{3+} is undergoing a change during sonic exposure. This color change was evident after 2 minutes of active sonication and appeared to reach a maximum extent after approximately 17 minutes of active sonication. Analogous color changes were not observed in reactions without added iron (i.e. no gas infusion and air infusion without iron). The yellow brown color and the final pH of

the reaction mixtures (pH = 3.0 - 3.4) suggest that ferric hydroxide [Fe(OH)₃] may be forming in the reaction mixture (Snoeyink and Jenkins, 1980), but further tests will be required to evaluate this hypothesis. Rapid formation of ferric hydroxide may limit the ability of Fe³⁺ to act as an efficient single electron transfer agent under these reaction conditions.

A comparison of GC peak patterns indicate that the type of products produced in reactions containing metal ions did not differ significantly from those due to reactions in which metal ions were absent indicating that the same mechanism may be operating in both systems.

4.2.4 Gas Chromatography/Mass Spectrometry (GC/MS)

GC/MS analysis of some reaction mixtures is presented in appendix B. GC/MS analysis of biphenyl reaction mixtures and comparison with fragmentation patterns presented in the literature (Heller, 1978) has yielded insight into the composition of reaction products derived from ultrasonic treatment. The total ion chromatogram of a biphenyl ultrasonic reaction mixture extract is presented in figure #21 below.

By comparison with a literature spectrum (Heller 1978) the biphenyl reaction product peak at 30.33 minutes has been

identified as [1,1 biphenyl]-2-ol. Peaks at 35.93 and 36.20 minutes yielded mass spectral fragmentation patterns that were quite similar. Both spectra are consistent with the two separate literature derived spectra for [1,1 biphenyl]-3-ol and [1,1 biphenyl]-4-ol (Heller, 1978). A more accurate identification of the GC peaks corresponding to [1,1 biphenyl]-3-ol and [1,1 biphenyl]-4-ol cannot be made because of the similarity of the two fragmentation patterns. Absolute identification of the individual reaction products at 35.93 and 36.20 minutes will require comparison of their physical properties with authentic samples of [1,1 biphenyl]-3-ol and [1,1 biphenyl]-4-ol, or through the use of other analytical techniques, and remains as future work.

GC/MS analysis of a phenanthrene reaction extract yielded a mixture of products as is evidenced in figure #22 below.

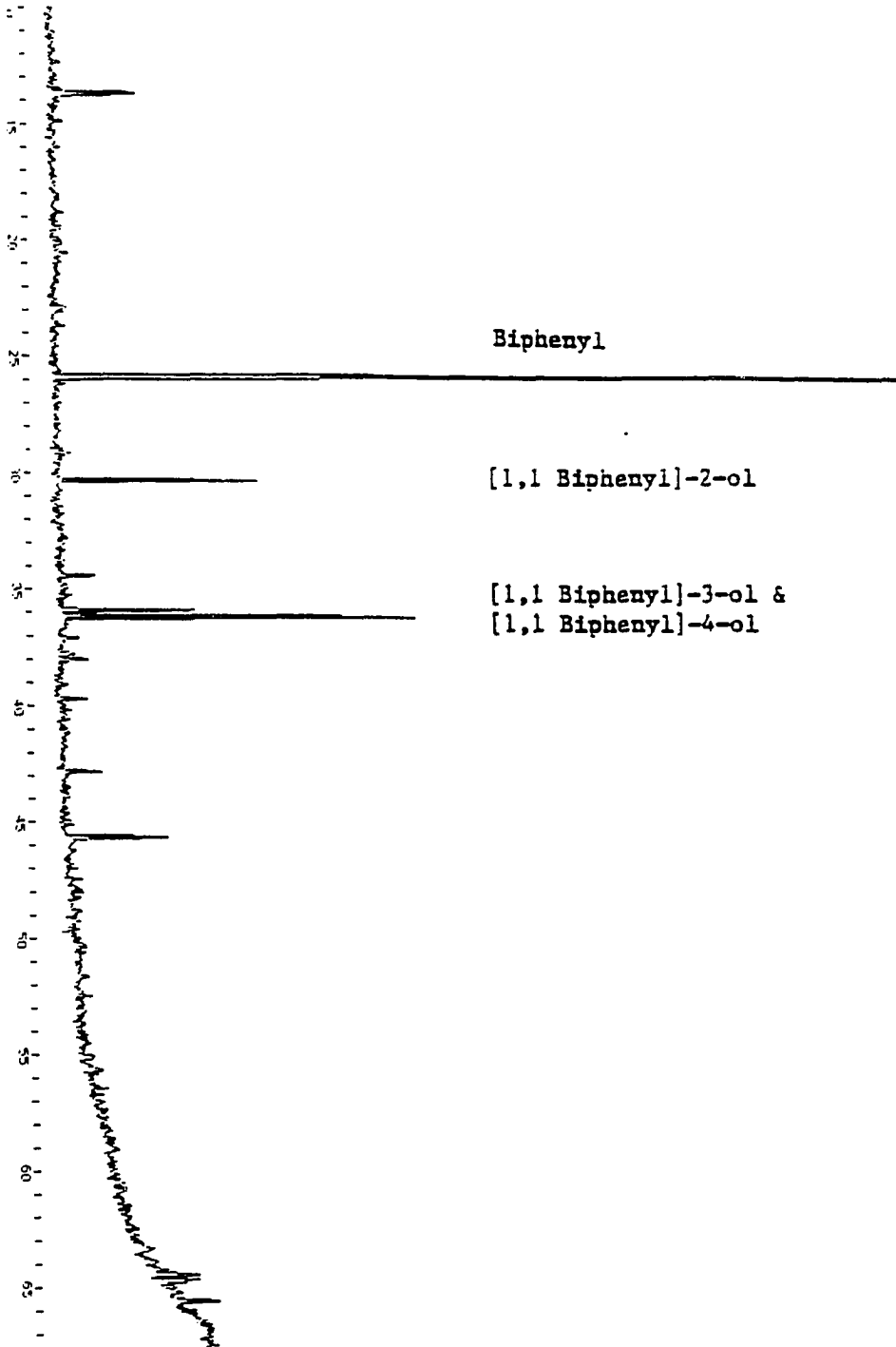


Figure #21: Total Ion Chromatogram of Biphenyl Reaction Mixture

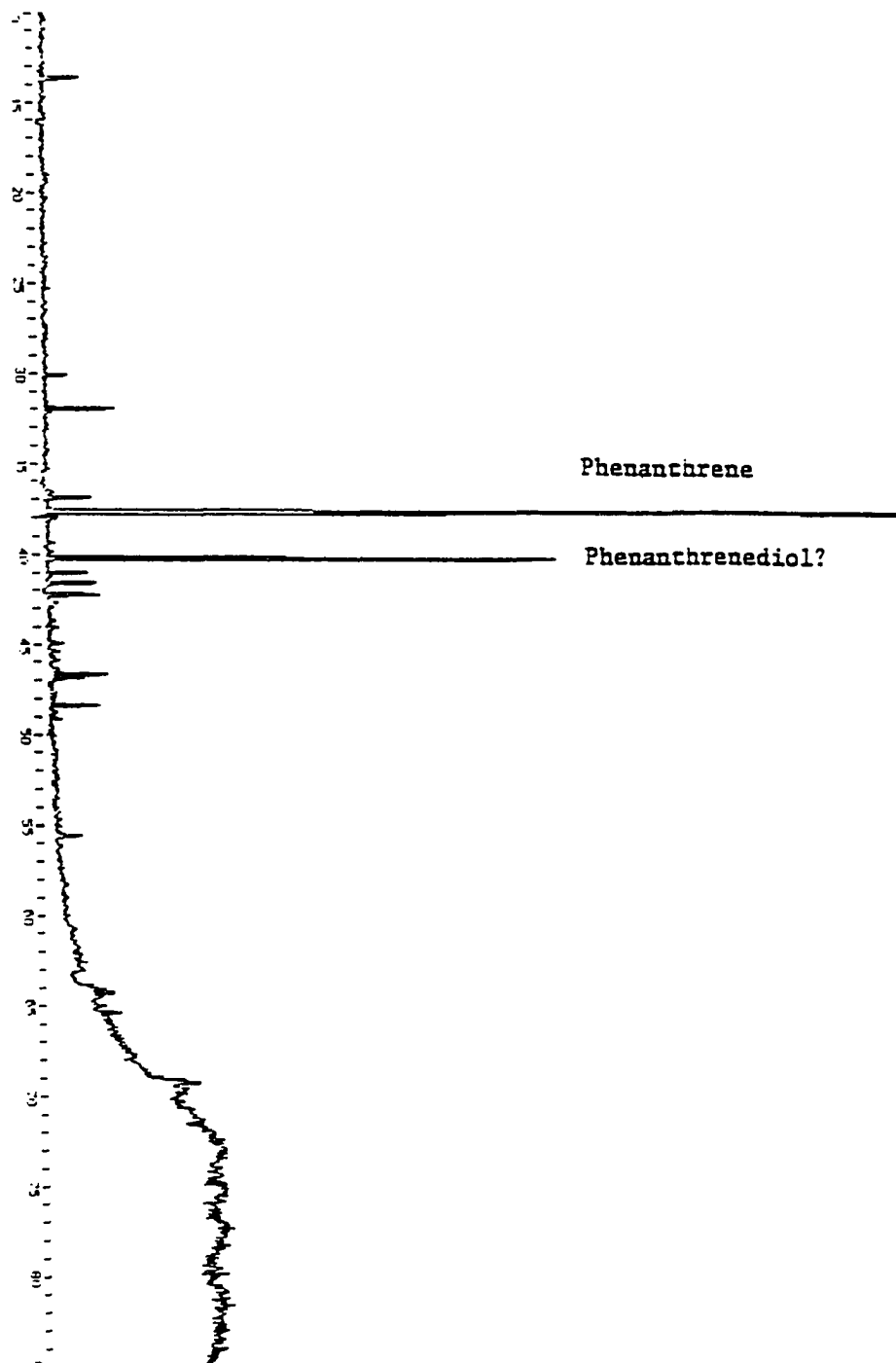


Figure #22: Total Ion Chromatogram of Phenanthrene
Reaction Mixture

In the case of the phenanthrene reaction mixture, identification of individual components by comparison with literature spectra was impaired by the lack of available reference data. The recent literature refers to computer based spectral databases (Fernandez, 1992) which are unavailable at this facility. However, the mass spectrum of the major reaction product at 40.28 mins (Figure #23 below) shows a molecular ion (M^+) of 210 atomic mass units (AMUs) which is consistent with a dihydroxy substituted phenanthrene (phenanthrenediol). The base peak of the major reaction product occurs at 181 AMU resulting from the loss of a fragment of 29 AMU. Comparison with a single literature reference for 9-phenanthrenol (Guidugli, 1986) indicates that loss of a fragment with atomic mass of 29 occurs from this substituted phenanthrene. Based on this evidence, the phenanthrene reaction product at 40.28 minutes is tentatively identified as one of the isomers of phenanthrenediol. Without reference spectra or further chemical tests, however, the substitution pattern of the phenanthrenediol cannot be ascertained at this time.

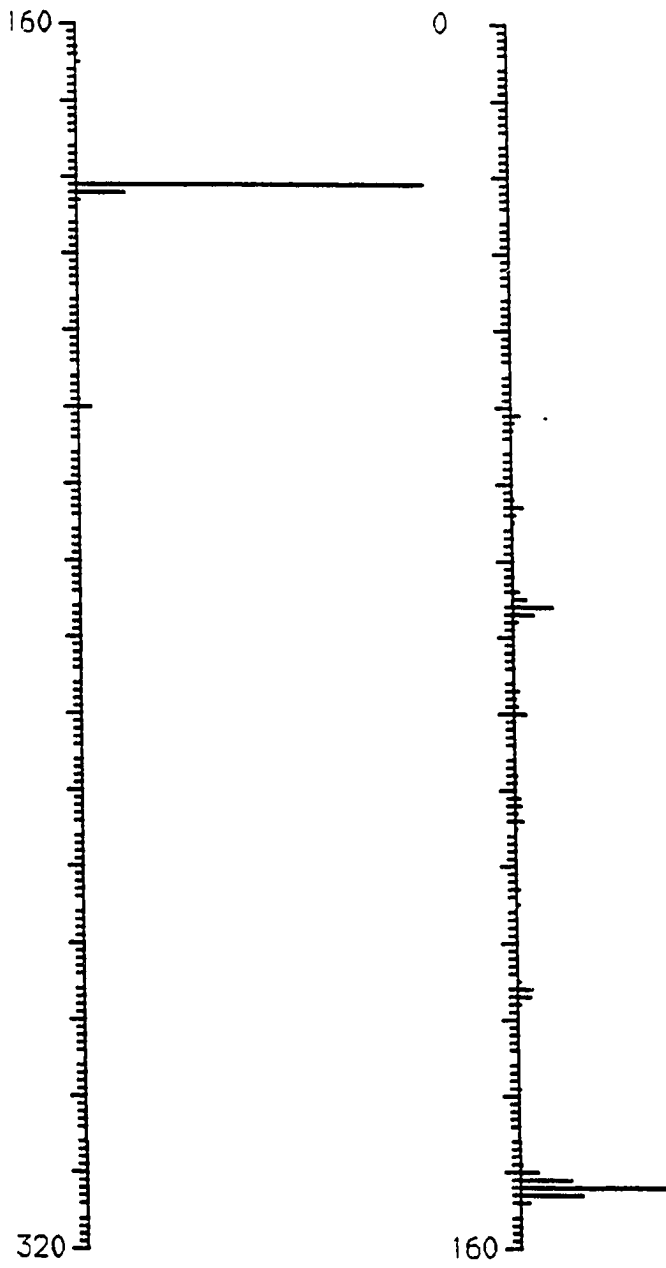


Figure #23: Mass Spectrum of Phenanthrene Reaction Product

For biphenyl, the three proposed reaction products {2,3,4-[1,1 biphenyl]-ol} are all mono-hydroxy substituted species, consistent with an attack by a single hydroxyl free radical ($\text{OH}\cdot$). For phenanthrene, however, the major reaction product appears to be a diol. If similar reaction mechanisms are operational in both systems the predominance of the phenanthrenediol in one system and the mono-hydroxy biphenols in the other must be attributable to subtle mechanistic differences.

One explanation for the production of the phenanthrene diol may be bond fixation present in the phenanthrene molecule (March, 1988). When the five (5) separate resonance structures for phenanthrene are drawn a double bond between carbons 9 and 10 (see figure #2, page #32) is present in four (4) of them. Selective attack by hydroxyl radicals at the 9 and 10 positions of phenanthrene should be favorable because of the increased electron density of this bond and the known electrophilicity of the hydroxyl radical (Walling and Johnson, 1975).

Further analysis of reaction products to provide proof of structure should yield insight into the validity of this hypothesis and mechanistic details of the reaction. These mechanistic considerations should provide direction for future attempts at optimization of ultrasonic treatment.

The gas chromatographic and mass spectral data confirm the hypothesis that chemical alteration of biphenyl and phenanthrene can be induced in the presence of a high intensity ultrasonic field in purely aqueous solutions.

4.2.5 Toxicity Considerations

It has been demonstrated here that polycyclic aromatic hydrocarbons exposed to high intensity ultrasonic fields in aqueous solution undergo reactions to yield a variety of products some of which have been identified as hydroxylated species. Yang and Silverman (1988) have studied the correlation between biological functionalization and carcinogenesis and have found that hydroxylation and epoxidation of polycyclic aromatic hydrocarbons, by biological enzyme systems, can yield ultimate carcinogens from proximate carcinogens. This information implies that the hazard potential of the phenol, and other potential reaction products, relative to the parent PAH, may be increased by ultrasonic treatment. The toxicity of reaction products produced by ultrasonic treatment was not ascertained in this study and remains the subject of a future investigation.

4.3 Desorption

4.3.1 Active Carbon/Phenanthrene Desorption Experiment

After significant fragmentation of the active carbon (AC) was identified (see section 4.1.1) the possibility that low ultrasonic energy levels ($<85 \text{ Watts/cm}^2$), resulting in minimal fragmentation of the carbon, could be used to desorb contaminants from AC still remained. An experiment to desorb radiolabeled PAH (phenanthrene) from the surface of active carbon using a sequence of increasing energy levels, up to and including those which resulted in significant degradation of the carbon matrix, was performed. The results of this experiment are presented in figure #24 below (see also appendix E).

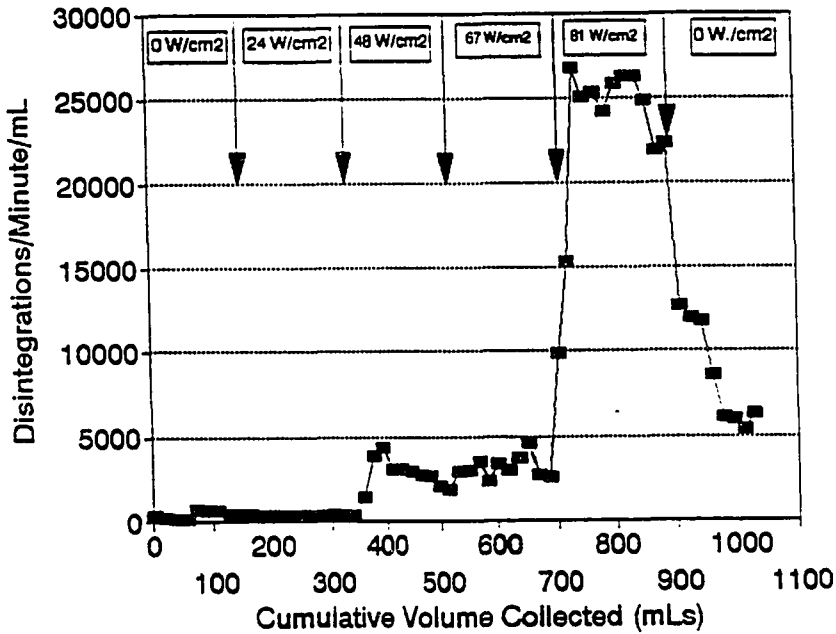


Figure #24: Radiation Experiment #1 (rad #1) - First Trial - Phenanthrene/Active Carbon - Sonic Treatment Background Corrected Disintegrations/Minute/Milliliter vs Cumulative Sample Volume Collected at Indicated Probe Energy Level

The data presented in figure #24 demonstrates the loss of radioactive material from the reactor as a function of effluent volume and ultrasonic intensity. The loss of radioactivity due to desorption of the phenanthrene from the surface of the active carbon is indistinguishable from loss mechanisms due to fragmentation processes using this particular system. Visible particulate material accompanied effluent water from the continuous flow reactor at all energy levels in excess of the audible cavitation threshold

(48 Watts/cm²). Treatment at 48 Watts/cm² and 67 W/cm² were characterized by low to moderately audible cavitation. Elution of fine to medium grained activated carbon particulate matter accompanied the presence of the ¹⁴C radiolabel in the effluent stream of the steady flow reactor. The highest power level attempted with the activated carbon/9-¹⁴C-phenanthrene system was 81 W/cm². At this energy level rapid fragmentation of the activated carbon resulted in significant quantities of carbon particulate matter in the effluent stream. Fragmentation of the active carbon at 81 Watts/cm² was sufficient to make the carbon/water suspension within the reactor opaque. Visual inspection of liquid fractions, prepared for liquid scintillation counting, indicated that a rough correlation existed between the amount of carbon and the level of measured radioactivity.

These preliminary results seem to indicate that the adsorption strength of phenanthrene on activated carbon exceeds the physical strength with which activated carbon granules are bound together. The adsorption strength of phenanthrene on activated carbon is predicted to be quite large (Walters, 1984) and it appears from this initial data that the binding strength may exceed the abrasion resistance of the carbon itself. The great strength with which the polycyclic aromatic hydrocarbon (PAH) is bound to carbon may

prove advantageous if desorption of less tightly bound chemical species in the presence of a adsorbed PAHs is required. The prospect of selective desorption (regeneration) cannot be excluded based on these preliminary findings with the activated carbon/phenanthrene system.

Chemoselective desorption of weakly bound contaminants (for example: low molecular weight halocarbon species) in the presence of a more firmly bound contaminant (i.e. PAHs) was not investigated in this study and represents future work.

4.3.2 Sand/¹⁴C-Phenanthrene desorption experiments

Two sonic treatments of 9-¹⁴C-phenanthrene adsorbed on Tanana Valley alluvial sand resulted in the graphs presented in figure #25 and figure #26 below.

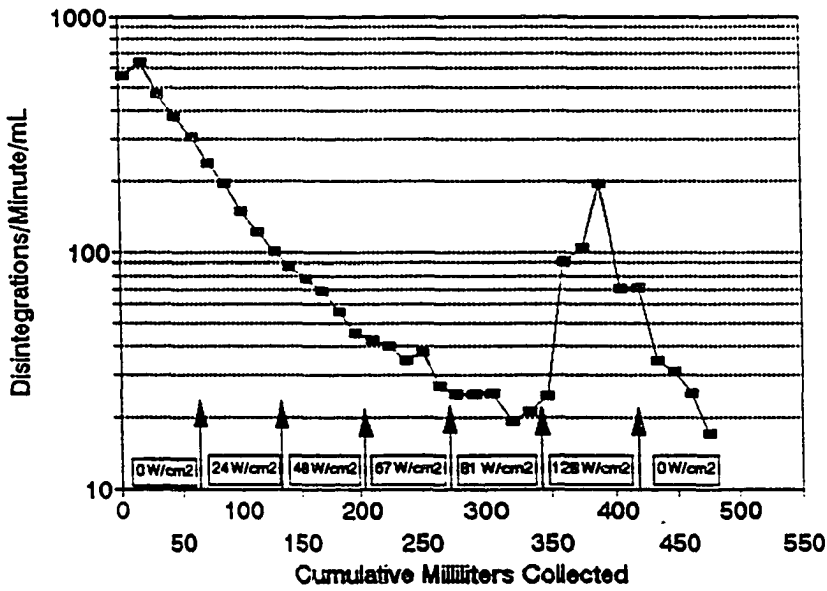


Figure #25: Radiation Experiment #2 (Rad #2) - Phenanthrene/Tanana Valley Sand - Duplicate Averaged Disintegrations/Minute/Milliliter vs Cumulative Sample Volume Collected at Indicated Probe Tip Energy Level

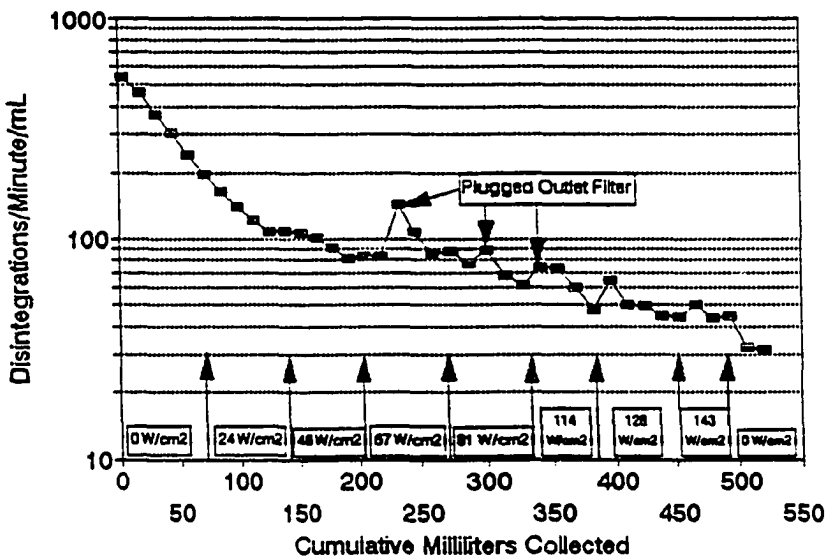


Figure #26: Radiation Experiment #3 (Rad #3) - Phenanthrene/Tanana Valley Sand - Duplicate Average Disintegrations/Minute/Milliliter vs Cumulative Sample Volume Collected at Indicated Probe Tip Energy Level

In both trials slight fragmentation of sand occurred during the experiment as was indicated by fine particulate matter in the collected liquid fractions. Overall, the extent of fragmentation was less pronounced than that observed with active carbon; a finding that is consistent with results obtained in the fragmentation study. As in the case of active carbon, however, fine particulate matter accompanied the radiolabeled species in the effluent leaving the reactor resulting in radioactivity in the collected liquid fractions.

In the first sand experiment (Rad #2) the presence of ^{14}C radiolabel in the effluent stream appeared to be nearly independent of the imposed ultrasonic energy field at 24 Watts/cm², and only slightly dependent at 48, 67, and 81 Watts/cm². Sustained sonication at 128 Watts/cm², however, caused enhanced transport of ^{14}C radiolabeled species into the effluent stream during this run.

In the second sand experiment (rad #3) a glass wool plug (pretreated with neutral phenanthrene to saturate adsorption sites on the glass) was inserted into the outlet line to inhibit the transport of particulate matter by the reactor effluent. This glass wool filter stopped much of the fine particulate matter from leaving the reaction flask but plugged frequently as can be seen in figure #26 above. The

problem of particulate matter produced from sustained sonication at high energy levels will require efficient filtration of effluent water produced from ultrasonic treatment.

Radiation Experiment #3 (rad #3) data indicate that treatment with ultrasound results in an apparent increase in the solution concentration of ^{14}C radiolabel during the interval of sonic treatment. The slope of the line resulting from a semi-log plot of DPM/mL (figure #26) in the collected fractions changes perceptible soon after the field is applied at 48 watts/cm². This result is consistent with findings from later trials where biphenyl adsorbed on glass beads is treated in a similar manner.

The variation that occurred between rad #2 and rad #3 cannot be fully explained at this time. The minimal effect of the applied field at 48-67 Watts/cm² in rad #2 may have been due to some variation in the properties of the aggregate or with the way the sand with adsorbed ^{14}C -phenanthrene was allowed to equilibrate. For radiation experiment #2 (rad #2) the sand was equilibrated for 16 hrs at 2°C and then for 22 hrs at 17°C while sand utilized in radiation experiment #3 (rad #3) was allowed to equilibrate in water for 112 hours at 18-20°C; a significant change in both time of equilibration and in the temperature at which equilibration occurred.

Two tests of the sand aggregate remaining at the end of radiation experiment #3 indicated that the isotope remaining at the end of treatment was non-uniformly distributed on the sand grains and that a large amount of radioactivity was retained on the surface of the material even after exposure to probe energy levels as high as 143 Watts/cm². Numerous liquid scintillation counts were performed on the same samples at increasing times after reaction and the measured radioactivity continued to increase for some time greater than 1.1 hours. The results of this evaluation are presented in figure #27 below and Appendix E.

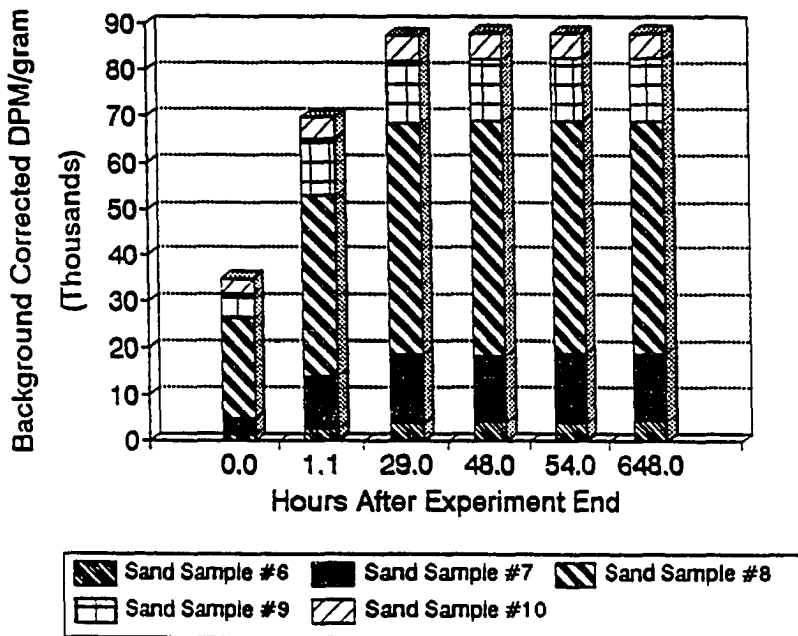


Figure #27: Radiation Experiment #3 - Liquid Scintillation Count of Residual Radioactivity on Surface of Sand After Sonic Treatment - Surface Dried Sand Samples

This result demonstrates two facts:

(1) that the extraction of radiolabeled species from the surface of the sand is a slow process even in organic solvents (liquid scintillation cocktail), proving the tenacity with which the phenanthrene is adsorbed to the surface; and

(2) that significant material remains adhered to the sand even after intense sonication at probe tip intensities of 143 Watts/sq cm.

The production of fine particulate matter during high intensity ultrasonic treatment will probably be a constant feature of this method of treatment. Suslick (1990) has demonstrated that cavitation near surfaces can cause pitting of even very hard materials resulting in the production of microscopic particulate material. This feature of ultrasonic treatment makes the absolute determination of desorption difficult since the contaminant may remain adsorbed on a particle of substrate blasted from the surface of the adsorbent by cavitation.

Based on this fact it may become necessary to develop a "working definition" of desorption, as suggested by Dr. Brown of the advisory committee. Such a definition may state that: "the presence of contaminant on particulate matter passing a 0.45 μ filter will be considered to be desorbed." While such a definition is crude it may yield

sufficient accuracy to make ultrasonic treatment predictable enough for environmental use. Unfortunately, this simplified approach will probably become unrealistic when chemical alteration data is coupled with the desorption data. A general outline of the hypothetical mechanism of desorption showing some of the anticipated complexities of the system is presented in section 4.3.5.

The chemical composition of the sand has been identified as one possible cause of the variations observed in the two sand experiments. In order to minimize the uncertainty associated with variations in aggregate chemical composition a series of experiments with a substrate of more uniform chemical composition were undertaken.

4.3.3 Glass Beads/Biphenyl Desorption Experiments

Borosilicate (Pyrex) glass boiling beads were chosen as an alternative adsorbent to eliminate the uncertainty arising from the chemical composition variations evident in natural aggregates and because of their apparent ability to resist fragmentation under the influence of an applied ultrasonic field. Exposure of glass beads with adsorbed radiolabeled biphenyl in aqueous suspension to ultrasound of varying intensity has been found to increase the solution concentration of radiolabeled species. A graph of the

"sonic interval" data (the sampling interval in which ultrasonic energy is applied to the reactor during sonic treatment: samples #19-107) for an ultrasonic treatment run (figure #28) demonstrate a perceptible change in the slope of the plotted data when compared with a control run in which no sonic energy was applied (Figure #29).

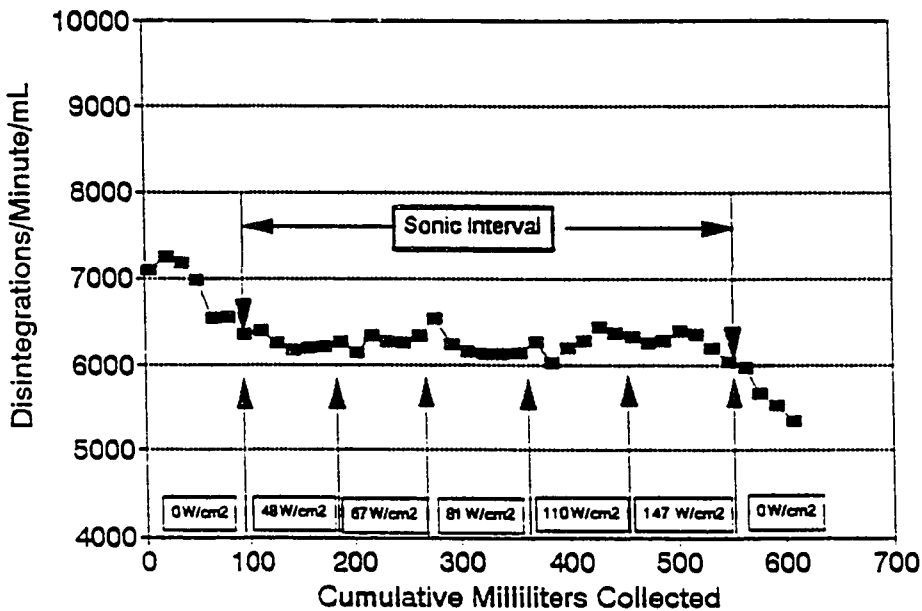


Figure #28: Radiation Experiment #7 (Rad #7) Biphenyl/Glass Beads - Duplicate Averaged DPM/mL vs Cumulative Sample Volume Collected

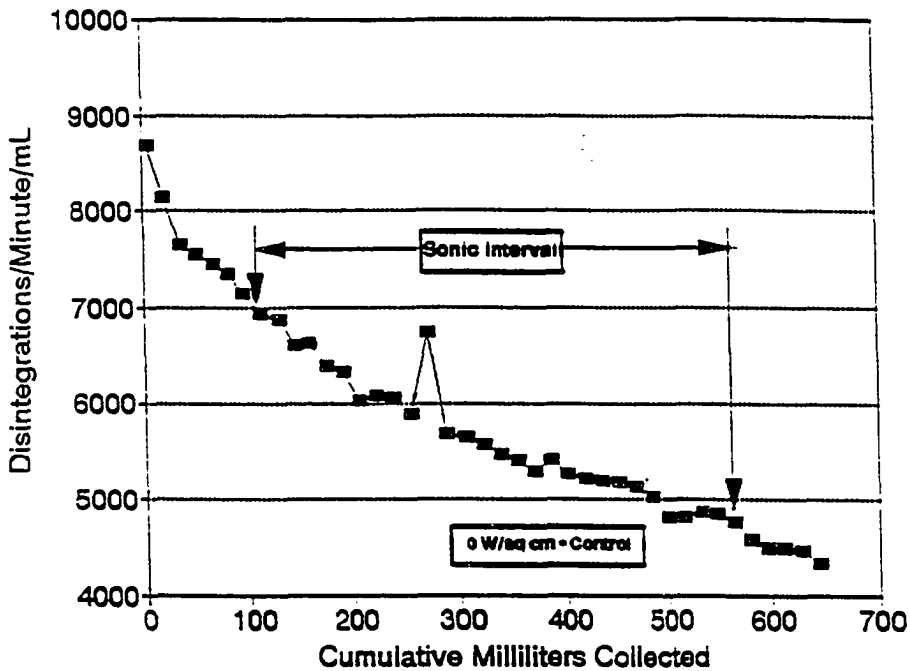


Figure #29: Radiation Experiment #5 (Rad #5) Control (No Sonic) Biphenyl Glass Beads - Duplicate Averaged DPM/mL vs Cumulative Sample Volume Collected

For experiments in which sonic energy is applied the slope of the plotted data is close to zero in the sonic interval while that of the plotted control (no sonic) data exhibit a negative slope in this same interval.

A linear regression analysis of data from the ultrasonic exposure sampling interval (sonic interval: samples #19-107) is presented for both sonic (Rad #6 and #7) and control (Rad #5 and #8) experiments (figures #30 below and appendix E: section E4). The experimental data obtained in Radiation experiment #4 (Rad #4) is excluded from the linear regression analysis. Difficulties incurred during this

method development run make the data inconsistent with that obtained in subsequent sonic treatment experiments (See appendix E, sections E3 and E5.

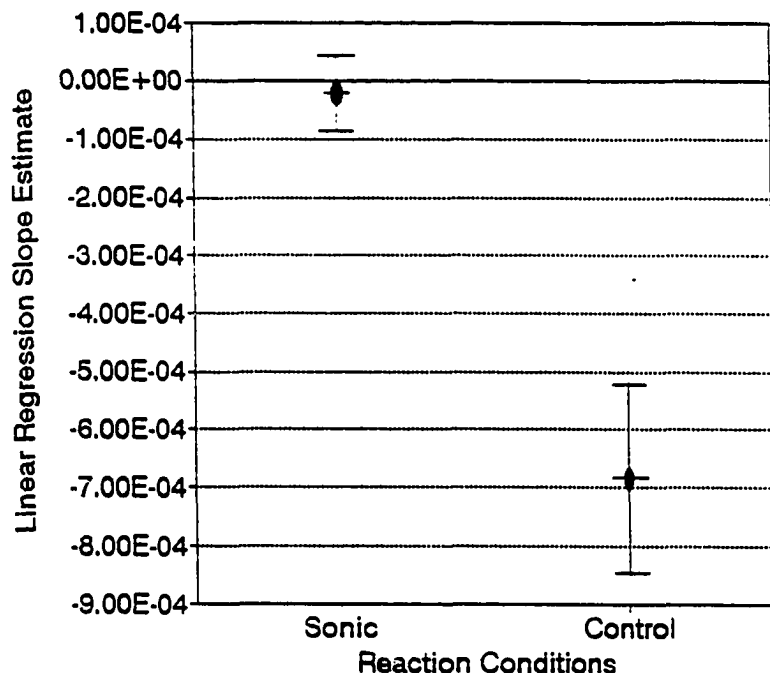


Figure #30: Comparison of Calculated Desorption Linear Regression Slope Estimates for Sonic and Control (No Sonic) Experiments - 99% Confidence Interval

The linear regression analysis demonstrates that the observed slope of the plotted sonic interval data from sonic experiments is significantly different from that obtained in control (no sonic) experiments at the 99% confidence level (see appendix D) using student "t" test values (Kitchens, 1987).

Transient peaks of radioactivity occurred in all data plots in the early stages (samples #1-18) of the desorption

experiments. These transient peaks were probably due to suspended biphenyl crystals eluting from the reactor. The influence of these transient peaks on the shape of the curves was minimized during data treatment by averaging the DPM/mL (concentration) values of contiguous samples and treating them as duplicates.

The problem of suspended particulate matter was caused by two simultaneous requirements of this desorption study. First, the liquid must be saturated with contaminant at the start of the run so that all of the material does not dissolve off the beads before the experiment begins. Second, sufficient contaminant must remain in solution and on the surface of the beads throughout the control (no sonic) experiments so that enhanced desorption can be identified by comparison with results of sonic experiments. For these reasons excess contaminant should be present at the start of the run to assure saturation of liquid and adsorption sites at the finish of sample collection in control runs. The mass of compound necessary to meet these requirements was anticipated from the saturated solution concentration values supplied by Pearlman (1984).

A mass balance comparison between sonic and control reactions was performed and revealed that the overall processes were not significantly different at the 90% confidence level. This fact was largely an outcome of the

limited number of experimental trials (two sonic and two controls) in each set of experiments.

4.3.4 Hypothetical mechanisms of desorption

The interaction of an ultrasonic field with an adsorbed contaminant is anticipated to be complex. A schematic of possible outcomes is presented below:

$ASA \rightarrow ASS \rightarrow \text{outlet}$ (ultrasonic cleaner)

$ASA \rightarrow ASS \rightarrow ADS \rightarrow \text{outlet}$ (clean and dissolve)

$ASA \rightarrow ADS \rightarrow BDS \rightarrow \text{outlet}$ (clean, dissolve and alter)

$ASA \rightarrow BDS \rightarrow \text{outlet}$ (alter & dissolve)

Where:

ASA = Chemical species "A" - surface adsorbed

ASS = Chemical species "A" - suspended in solution

ADS = Chemical species "A" - dissolved in solution

BDS = Chemical species "B" - dissolved in solution

This formulation represents a best "guess" as to the possible mechanisms which are active in the ultrasound/adsorbed crystalline contaminant system.

The first alternative (labelled ultrasonic cleaner) involves the removal of solid material from the surface of the substrate to yield a mixture of "cleaned" substrate, suspended solid material (perhaps still associated with microscopic pieces of glass), and solvent. In this alternative no mechanism to aid in the dissolution and chemical alteration of the material is supplied by the applied ultrasonic field - perhaps because of limited reactor resident times due to high elution rates, or low ultrasonic field strengths.

The second alternative (labelled clean and dissolve) involves a two stage process. In the first stage the substrate is "cleaned" (the contaminant is displaced from the surface) and a suspension of the contaminant is formed. In the second stage, localized microstreaming (Nyborg, 1959), which arises due to the interaction of an ultrasonic field with a suspended solid, may aid in the rapid dissolution of the material, forming a true solution of the contaminant. This alternative assumes that the contaminant remains in the reactor for a sufficient period of time for the combined cleaning and dissolution mechanisms to work.

The third alternative entails cleaning, dissolution, and chemical alteration. As in the second alternative described above, sufficient reactor residence time must be allowed to remove the precipitate from the surface of the substrate and for subsequent enhanced dissolution of the suspended material. An additional requirement of this alternative is that sufficiently intense ultrasonic energy exists in the reactor so that chemical alteration of the dissolved contaminant can be induced. Furthermore, the loss of contaminant from the reactor will become a function of the concentration of both the contaminant and its reaction products.

The fourth alternative has the contaminant being altered directly on the surface of the substrate prior to removal or dissolution. In this case the mineral content of the substrate may play a major role in the chemical alteration of the contaminant. Here again, the loss of contaminant from the reactor will become a function of the concentration of both the contaminant and its reaction products but in addition, the rate of mass transfer from the surface of the substrate may make a contribution to the ultimate rate of contaminant removal.

Chemical alteration of both phenanthrene and biphenyl at 147 Watts/cm^2 has been demonstrated in this investigation. From this fact it can be anticipated that this intensity

level will result in chemical alteration of phenanthrene and biphenyl in the desorption experiments as well. The shape of the curve in figure #28, however, gives no clear indication of increased radiolabel concentration in effluent fractions at any of the individual energy levels tested. If chemical alteration is occurring at energy levels less than 147 Watts/cm^2 to produce hydroxylated aromatic species the solution concentration of radioactivity may be expected to increase in response to the expected water solubility enhancement of the alcohol over the hydrocarbon. Since the curve is essentially flat in the region of sonic treatment this may indicate that chemical alteration is occurring at lower intensity levels (i.e. as low as 48 Watts/cm^2), a fact that will be of economic importance because of decreased loss of transducer material due to cavitation erosion at lower intensity levels.

The ultrasonic intensity at which chemical alteration begins to be observed has not yet been determined, but samples obtained for chemical analysis at the time the desorption experiments were performed (see section #3.3.3.4) may supply an estimate of this threshold. Moreover, analysis of these samples should provide insight into the nature of the chemical species present (parent compound, reactant, or both) in the reactor at each stage of treatment, and the mechanism(s) active in ultrasound

enhanced desorption phenomena. Analysis of these desorption extracts remains as future work.

Chapter 5 Summary and Conclusions

5.1 Conclusions

5.1.1 Fragmentation

The ability of ultrasound to regenerate polycyclic aromatic hydrocarbon (PAH) contaminated active carbon using ultrasonic fields is unlikely based on the low physical strength of this substrate and its high affinity for this class of compounds. The chemoselective desorption of weakly associated chemicals (low molecular weight halocarbons) in the presence of tightly bound aromatic hydrocarbons remains a possibility and a focus for future work. Future attempts to dislodge weakly bound contaminants from the surface of active carbon, however, will require a reactor design which minimizes impacts with the walls of the vessel and with the radiating face of the ultrasonic transducer.

The fragmentation of the sand aggregate suggests that treatment of contaminated material with high intensity ultrasound may require a filtration step or other separation techniques to remove contaminant laden fine particulate material prior to effluent discharge.

5.1.2 Chemical Alteration of Adsorbed Contaminants

Reactions of polycyclic aromatic hydrocarbons (PAHs) occur under the influence of a high intensity (147 Watts/cm²) ultrasonic field in aqueous solution. The ultrasonic intensity threshold at which chemical alteration begins to occur was not investigated by this series of experiments and remains to be demonstrated in future work.

Participation by transition metal ionic species (see section #2.3.5) in ultrasonic reactions may result in a change in the complexed form or oxidation state of the metal while simultaneously enhancing the chemical alteration of an organic contaminant. A color change in response to the applied ultrasonic field clearly indicated that the character of the iron in solution was altered by the applied field, but the qualitative results obtained here were inadequate to prove or disprove an enhancement of PAH reactivity in response to added Fe³⁺. Further quantitative studies will be necessary to accurately measure PAH reactivity enhancement in response to the presence of soluble transition metal complexes and to measure the changes in metal ligand association and oxidation state.

The outlook for PAH chemical alteration in aqueous solution using ultrasound alone, or in conjunction with other treatment techniques, is cautiously optimistic.

However, this optimism may be tempered if toxicity is exhibited by ultrasound derived products. A literature search has begun to ascertain the toxicity of reaction products identified in this work.

5.1.3 Desorption

Enhanced transport of some adsorbed PAHs into water solution can be anticipated. The solution concentration of radiolabeled parent compound or its reaction adducts were increased in the presence of ultrasonic field strengths of 48 Watts/cm² and higher. The amount of contaminant remaining on the surface of a variety of substrates at the end of treatment indicates that the methodology used in this research lacks the ability to remove adsorbed crystalline PAHs exhaustively, but the possibility of linkage to other forms of waste treatment makes the increase in solution concentration of contaminant and/or contaminant derived species a promising finding. The use of ultrasound to clean sediments contaminated with polycyclic aromatic hydrocarbons in purely aqueous solutions is of limited utility, as a stand-alone technology, based on the outcome of experiments presented here.

5.2 Future Work

Historically, reactions of free radical species, generated by various techniques, including ultrasound, have been of limited synthetic utility because of the complex mixture of the reaction products produced. However, when the object is to add functionality to a refractory waste material, thereby enhancing its subsequent degradation by microbial or other means, the use of these highly reactive systems may be justified.

Identification and quantification of the reaction products derived from ultrasonic treatment remains to be investigated. Further tests to ascertain the applicability of ultrasonic treatment to a number of more hazardous organic chemicals {e.g., benzo-[a]-pyrene, PCBs (Arochlors)} and other organic and inorganic chemical species must be performed to measure the broad applicability of the methodology. Moreover, work remains to be done in the area of chemical alteration to optimize performance of the system and to quantify the rate and extent of reaction.

The battery of tests conducted in this investigation (fragmentation, chemical alteration, and desorption) should be extended to contaminants adsorbed on natural aggregate materials to investigate any variations which may occur. Natural aggregate materials are generally much harder than

activated carbon and minor fragmentation of these materials may not seriously impair the ultrasonic treatment outcome. Treatment of colloidal material contaminated with a variety of organic and inorganic contaminants represents a special challenge to be addressed in future work.

Chemoselective desorption of weakly bound contaminants (i.e. low molecular weight halocarbon species) in the presence of a more firmly bound contaminant (i.e., PAHs) was not investigated in this study and also represents future work.

The linkage of ultrasonic treatment techniques developed here with microbiological degradation is a natural and complementary one. Some of the advantages to their linkage are:

(1) initial functionalization of PAHs to increase biodegradation potential; and

(2) concomitant sterilization allowing introduction of acclimated cultures of organisms into media partially or completely sterilized during exposure to high intensity ultrasound, and recycle of carbon and nutrients as organisms are lysed and their cell contents are released through the action of the ultrasonic field.

Evaluation of the biodegradability of ultrasound derived reaction products and the overall response of microbial

organisms to reaction product exposure represent critical objectives of future work.

The toxicity of the products produced by ultrasound induced free radical reactions is a concern. The extent and type of contaminant functionalization is vital information lacking at this time, but based on the findings of Yang and Silverman (1988) increased toxicity due to ultrasonic treatment is plausible. Future work should entail a continuing series of laboratory tests and literature searches to determine the toxicity, teratogenicity, mutagenicity and carcinogenicity of reaction mixtures and individual products. Comparison of these results to risk factors associated with exposure to the unreacted contaminant may yield insight into the validity of this form of hazardous waste treatment.

Bibliography

- Akcay, M.; Elik, A.; Savasci, S. "Effect of Ultrasonication on Extraction Rate and on Recovery of Strontium From River Sediment Using Flame Atomic Absorption Spectrometry"; *Analyst*; 1989; Vol. 114; pp. 1079-1082.
- Alben, K.T.; Kaczmarczyk, J.H. "Ultrasonic Solvent Extraction of Trihalomethanes from Granular Activated Carbon"; *Anal. Chem.*; 1986; Vol. 58; pp. 1817-1822.
- Atchley, A.A.; Crum, L.A. "Acoustic Cavitation and Bubble Dynamics", In: *Ultrasound: Its Chemical, Physical, and Biological Effects*; Suslick, K.S., ed.; VCH Publishers, Inc.; Chapter 1. New York; 1988; pp. 1-64.
- Beach, W. *Arctic Alaska Test Laboratories*; Personal Communication; 1992.
- Bellar, T.A.; Lichtenberg, J.J.; Lonnenman, S.C. "Recovery of Organic Compounds From Environmentally Contaminated Bottom Materials", In: *Contaminants and Sediments: Vol II - Analysis, Chemistry and Biology*; Baker, R.A. Ed.; Ann Arbor Science; 1980; pp. 57-70.
- Borland; *Quattro Pro: @Functions and Macros*; Borland International, Inc.; 1990; p. 9.
- Boudjouk, P. "Heterogeneous Sonochemistry"; In: *Ultrasound: Its Chemical, Physical, and Biological Effects*; Suslick, K.S., Ed.; VCH Publishers; New York; 1988; pp. 165-226.
- Brown, J.F.; Bedard, D.L.; Brennan, M.J.; Carnahan, J.C.; Feng, H.; Wagner, R.E. "Polychlorinate Dechlorination in Aquatic Sediments"; *Science*; 1987; Vol. 36; pp. 709-712.
- Brown, B.; Goodman, J.E. *High Intensity Ultrasonics*; Iliffe Publishers, London; 1965; pp.210-213.
- Champ, D.R. "Observation on the Movement of Colloidal Particles in Saturated Media at the Chalk River Nuclear Laboratories"; *Haz. Mat. Control*; 1990; Vol. 3, #4; pp. 45-46.

Crum, L.A. "Acoustic Cavitation"; *IEEE Ultrasonic Symposium*; 1982; pp. 1-11.

EPA "Sonication Extraction" - Revision #0; Method 3550; Date: 9/86; In: *Test Methods for Evaluating Solid Waste (SW-846) 1986a*.

EPA "Gas Chromatography" - Revision #0; Method 8000-8150; Date: 9/86; In: *Test Methods for Evaluating Solid Waste (SW-846) 1986b*.

EPA "Clean-up" - Revision #0; Method 3600-3660; Date: 9/86; In: *Test Methods for Evaluating Solid Waste (SW-846) 1986c*.

EPA *The Superfund Innovative Technology Evaluation Program: Technology Profiles - Fourth Edition*; EPA/540/5-91/008; 1991a; pp. 14-22.

EPA *Handbook: Remediation of Contaminated Sediments*; EPA/625/6-91/028; 1991b; pp. 21-44.

Esposito, P.; Hessling, J.; Thurnau, R. "Results of Treatment Evaluations of Contaminated Synthetic Soil"; *JAPCA*; 1989; Vol. 39, #3; pp. 294-304.

Fernandez, P.; Grifoll, M.; Solanas, A.M.; Bayona, J.M.; Albalges, J. "Bioassay-Directed Chemical Analysis of Genotoxic Components in Coastal Sediments"; *Environ. Sci Technol.*; 1992; Vol. 26; pp. 817-829.

Fitzgerald, M.E.; Griffing, V.; Sullivan, J. "Chemical Effects of Ultrasonics - 'Hot Spot' Chemistry"; *J. Acoust. Soc. Am.*; 1956; Vol 25, #5; pp. 926-933.

Fogler, H.S. "Colloidally-induced Fines Migration"; *Haz. Mat. Control*; 1990; Vol. 3, #4; p. 53.

Germann, P.F. "Fluid Mechanical Considerations on Colloidal Transport in Porous Media"; *Haz. Mat. Control*; 1990; Vol. 3, #4; p. 52.

Griffing, V. "Theoretical Explanation of the Chemical Effects of Ultrasonics"; *J. Chem. Phys.*; 1950; Vol. 18; pp. 997-998.

Griffing, V. "The Chemical Effects of Ultrasonics"; *J. Chem. Phys.*; 1952; Vol. 20, #6; pp. 939-942.

Grimalt, J.; Marfil, C.; Albaiges, J. "Analysis of Hydrocarbons in Aquatic Sediments"; *Intern. J. Environ. Anal. Chem.*; 1984; Vol. 18; pp. 183 - 194.

Gschwend, P.M. "Formation and Mobilization of Colloidal Particles in Contaminant Plumes"; *Haz. Mat. Control*; 1990; Vol. 3, #4; p. 49.

Guidugli, F.H.; Ardanaz, C.E.; Kavka, J.; Garibay, M.E.; Joseph-Nathan, P. "Further Mass Spectral Studies of Flavones"; *Org. Mass Spectrom.*; 1986; Vol. 21; pp. 117-124.

Harper, S.L.; Walling, J.F.; Holland, D.M.; Pranger, L.J. "Simplex Optimization of Multielement Ultrasonic Extraction of Atmospheric Particulates"; *Anal. Chem.*; 1983; Vol. 55, #9; pp. 1553-1557

Hart, E.J. Henglein, A. "Sonochemistry of Aqueous Solutions: H₂-O₂ Combustion in Cavitation Bubbles"; *J. Phys. Chem.*; 1987; Vol. 91; pp. 3654-3656.

Harvey, E.N.; Barnes, K.K.; McElroy, W.D.; Whitely, A.H.; Pease, D.C.; Cooper, K.W. "Bubble Formation in Animals"; *J. Cell. Comp. Physiol.*; 1944; Vol. 24; pp. 1-22.

Heller, S.R.; Milne, G.W.A. NSRDS-NBS 63; U.S. Dept. of Commerce/National Bureau of Standards - EPA/NIH Mass Spectral Data Base; National Standard Reference Data Service; US Government Printing Office; 1978; Vol. 1, compd # 580-51-8 {[1,1 biphenyl]-3-ol}, p.170; compd #s 90-43-7 {[1,1 biphenyl]-2-ol} and 92-69-3 {[1,1 biphenyl]-4-ol}, p. 4279.

Henglein, A. Kormann, C. "Scavenging of OH Radical Produced in the Sonolysis of Water", *Int. J. Radiat. Biol.*; 1985; Vol. 48, #2; pp. 251-258

Henglein, A. "Sonochemistry: Historical Developments and Modern Aspects"; *Ultrasonics*; 1987; Vol. 25; pp. 6-16.

Heylin, M., Ed. "Quicklime Does Not Decompose PCBs"; *Chemical and Engineering News*; 1991; Vol. 69, #45; p.18

Holoubek, I.; Paasivirta, J.; Maatela, P.; Lahtipera, M.; Holoubkova, I.; Karinek, P.; Bohacek, Z.; Caslavsky, J. "Comparison of Extraction Methods for Polycyclic Aromatic Hydrocarbon Determination in Sediment"; *Toxicol. and Environ.Chem.*; 1990; Vol. 25; pp. 137-154.

Jaffe, B.; Roth, R.S.; Marzullo, S. "Properties of Piezoelectric Ceramics in the Solid-Solution Series Lead Titanate-Lead Zirconate-Lead Oxide: Tin Oxide and Lead Titanate-Lead Hafnate"; *J. of Res. Nat. Bur. Stand.*; 1955; Vol. 55, #5; pp. 239-254.

Jardine, P.M.; Weber, N.; McCarty, J.F. "Chemical and Hydrological Factors Controlling the Transport of Organic Colloids"; *Haz. Mat. Control*; 1990; Vol. 3, #4; p. 44.

Jefcoate, C.R.E.; Norman, R.O.C. "Electron Spin Resonance Studies. Part XIV. Hydroxylation. Part III. Reactions of Anisole, Acetanilide, Fluorobenzene, and some Phenols With the Titanium(III)-Hydrogen Peroxide System"; *J. Chem. Soc. (B - Phys. Org.)*; 1968; pp. 48-53.

Kile, D.E.; Chiou, C.T. "Effect of Some Petroleum Sulfonate Surfactants on the Apparent Water Solubility of Organic Compounds"; *Environ. Sci. Technol.*; 1990; Vol. 24, #24; pp. 205-208.

Kitchens, L.J. *Exploring Statistics: A Modern Introduction to Data Analysis and Inference*; West Publishing Company, New York; 1987; p. 555.

Kostecki, P.T. Calabrese, E.J. *Petroleum Contaminated Soils, Vol. 1*; Lewis Publishers, Inc.; Michigan; 1989; pp. 157-161.

Kotronarou, A.; Mills, G.; Hoffmann, M.R. "Decomposition of Parathion in Aqueous Solution by Ultrasonic Irradiation"; *Environ. Sci. Technol.*; 1992, Vol. 26, #7; pp. 1460-1462.

Krahn, M.M.; Ylitalo, G.M.; Joss, J.; Chan, S. "Rapid, Semi-Quantitative Screening of Sediments for Aromatic Compounds using Sonic Extraction and HPLC/Fluorescence Analysis"; *Marine Environ. Res.*, 1991; Vol. 31; pp. 175-196.

Kruus, P. "Initiation of Polymerization with Ultrasound"; *Ultrasonics*; 1987; Vol. 25; pp. 20-22.

Lake, J.L.; Pruell, R.J.; Osterman, F.A. "An Examination of Dechlorination Processes and Pathways in New Bedford Harbor Sediments"; *Marine Environ. Res.*; 1992; Vol. 33, #1; pp. 31-47.

Lee H.B.; Dookhran, G.; Chau, A.S.Y. "Development and Certification of a Sediment Reference Material for Selected Polynuclear Aromatic Hydrocarbons"; *Analyst*; 1987; Vol. 112; pp. 31-35.

Lindley, J. Mason, T.J. "Sonochemistry: Part 2 - Synthetic Applications"; *Chem. Soc. Rev.*; 1987; Vol. 16; pp. 275-311.

Looney, Brian B.; Newman, M.E.; Elzerman, A.W. "Colloid Facilitated Transport in Groundwater: Laboratory and Field Studies"; *Haz. Mat. Control*, 1990; Vol. 3, #4; pp. 47-48.

Lorimer, J.P.; Mason, T.J.; Mistry, B.P. "Effect of Ultrasound on the Solvolysis of 2-Chloro-2-methylpropane in Aqueous Alcoholic Solvents"; *Ultrasonics*; 1987a; Vol. 25; pp 23-28.

Lorimer, J.P.; Mason, T.J. "Sonochemistry: Part 1- The Physical Aspects"; *Chem Soc Rev.*; 1987b; Vol. 16; pp. 239-274

Makino, K.; Mossoba, M.M.; Riesz, P. *J. Am. Chem. Soc.*; 1982; Vol. 104; pp. 3537-3539.

March, J. *Advanced Organic Chemistry: Reactions, Mechanisms, and Structure*; McGraw-Hill Book Co.; New York; 1968; pp. 38-40.

Marcus, J.M.; Swaringen, G.R.; Williams, A.D.; Heizer, D.D. "Polynuclear Aromatic Hydrocarbons and Heavy Metal Concentrations in Sediments at Coastal South Carolina Marinas"; *Arch. Environ. Contamin. Toxicol.*; 1988; Vol. 17; pp. 103-113.

Margulis, M.A.; Didenko, Yu. T. "Energetics and Mechanism of Acoustochemical Reactions. Sonolysis of solutions of Monochloroacetic Acid in an Argon Atmosphere"; *Rus. J. of Phys. Chem. (Engl. Transl.)*; 1986; Vol. 60, #6; pp. 888-891; *Zh. Fiz. Khim.*; 1986; Vol. 60; 1490-1494

Marshall, J.R., Ed. *Clastic Particles: Scanning Electron Microscopy and Shape Analysis of Sedimentary and Volcanic Clasts*; Van Nostrand Reinhold Co. Inc.; New York; 1987; pp. 1-64.

- McCarthy, J. F.; Zachara, J.M. "Subsurface Transport of contaminants: Mobile Colloids in the Subsurface Environment May Alter The Transport of Contaminants"; *Environ. Sci. Technol.*; **1989**; Vol. 23, #5; pp. 496-502.
- McCarthy, J. F. "The Mobility of Colloidal Particles in the Subsurface"; *Haz. Mat. Control*; **1990**; Vol. 3, #4; p. 38-43.
- Mead, E.L.; Sutherland, R.G.; Verrall, R.E. "The Effect of Ultrasound on Water in the Presence of Dissolved Gases"; *Can. J. Chem.*; **1976**; Vol. 54; pp. 1114-1120.
- Nunno, T.J.; Hyman, J.A.; Pfeiffer, T. "European Approaches to Site Remediation"; *Haz. Mat. Control*; **1989**; Vol. 2, #5; pp. 38-46.
- Nyborg, W.L.; Jackson, F.J. "Small Scale Acoustic Streaming Near a Locally Excited Membrane"; *J. Acoust. Soc. Am.*; **1958**; Vol. 30, #7; pp. 614-619.
- Nyborg, W.L.; Gould, F.J. "Sonically Induced Microstreaming Applied to a Surface Reaction"; *J. Acoust. Soc. Am.*; **1959**; Vol. 31, #6; pp. 706-711.
- Parke, A.V.M. Taylor, D. "The Chemical Action of Ultrasonic Waves"; *J. Chem. Soc.*; **1956**, Part IV; pp. 4442-4450.
- Pearlman, R.S.; Yalkowsky, S.H.; Banerjee, S. "Water Solubilities of Polynuclear Aromatic and Heteroaromatic Compounds"; *J. Phys. Chem. Ref. Data.*; **1984**; Vol. 13, #2; pp. 555-562
- Penrose, W.R.; Polzer, W.L.; Essington, E.H.; Nelson, D.M.; Oriandini, K.A. "Mobility of Plutonium and Americium through A Shallow Aquifer in a Semiarid Region"; *Environ, Sci. Technol.*; **1990**; Vol. 24, #2; pp. 228-234.
- Perrich, J.R. *Activated Carbon Adsorption for Wastewater Treatment*; CRC Press; Boca Raton, Florida; **1981**; pp. 1-46.
- Petrier, C.; Micolle, M.; Merlin, G.; Luche, J.L.; Reverdy, G.; "Characteristics of Pentachlorophenate Degradation in Aqueous Solution by Means of Ultrasound"; *Environ. Sci. Technol.*; **1992**; Vol. 26, #8, pp. 1639-1641.

- Purdhomme, R.O. "Formation D'eau Oxygenee Par Irradiation Ultrasonore De L'eau En Presence Des Differents Gaz Rares"; *Bull. Soc. Chim. Biol.*; 1957; Vol. 39, #4; pp. 425-430.
- Raloff, J. "The Colloid Threat: Small Nontoxic Particles May Enhance Water Pollution"; *Sci. News*; 1990; Vol 137; pp. 169-170.
- Riesz, P.; Kondo, T.; Krishna, M.C. "Sonochemistry of Volatile and Non-Volatile Solutes in Aqueous Solutions: E.P.R. and Spin Trapping Studies"; *Ultrasonics*; 1990; Vol. 28; pp. 295-303.
- Rozin, Yu. P.; Rozina, E. Yu. "Effect of the Gas Content of Liquids on the Physicochemical Processes Stimulated by Cavitation"; *Rus. J. of Phys. Chem. (Engl. Transl.)*; 1986; Vol. 60, #6; pp.891-894; *Zh Fiz. Khim.*; 1986; Vol. 60; pp. 1495-1500.
- Sedlak, D.L.; Andren, A.W. "Aqueous-Phase Oxidation of Polychlorinated Biphenyls by Hydroxyl Radicals"; *Env. Sci and Technol.*; 1991; Vol. 25, #8; pp. 1419-1426.
- Short, A.A.; Lowson, R.T. "²³⁴U/²³⁸U and ²³⁰Th/²³⁴U Activity Ratios in the Colloidal Phases of Aquifers in Lateritic Weathered Zones"; *Geochim. et. Cosmochim. Acta*; 1988; Vol. 52; pp. 2555-2563.
- Smith, J.R.L.; Norman, R.O.C. "Hydroxylation. Part I. The Oxidation of Benzene and Toluene by Fenton's Reagent"; *J. Chem. Soc.*; 1963; pp. 2897-2905.
- Snoeyink, V.L.; Jenkins, D. *Water Chemistry*; John Wiley and Sons, New York.; 1980; p 384
- Sokol'skaya, A.V. "Synthesis of Glycine From Formaldehyde and Molecular Nitrogen in Aqueous Solutions in an Ultrasonic Field"; *J. Evol. Biochem. Physio. (Engl. Transl.)*; 1975; Vol. 11; pp. 446-450; *Zh. Obshch. Khim.*; 1975; Vol. 48, #6; pp. 1407-1410.
- Sprich, J.D. Lewandos, G.S. "Sonochemical Removal of Adsorbed Water and Alcohol from Magnesium Surfaces"; *Inorg. Chem. Acta*; 1983; Vol. 76; pp. L241-L242.
- Suslick, K.S.; Schubert, P.F.; Goodale, J.W. "Chemical Dosimetry of Ultrasonic Cavitation"; *IEEE Ultrasonics Symposium*; 1981; pp. 612-616.

Suslick, K.S. "Determination of Local Temperatures Caused by Acoustic Cavitation"; *IEEE Ultrasonics Symposium - 1985; 1985*; pp. 1116-1121.

Suslick, K.S. "Organometallic Sonochemistry"; *Adv. in Organomet. Chem.*; 1986a; Vol. 25; pp. 73-119.

Suslick, K.S. "Ultrasound in Synthesis"; *Mod. Syn. Meth.*; 1986b; Vol. 4; pp. 1-60.

Suslick, K.S. "Ultrasound Makes a Hit With Metal Powder"; *Adv. Mat. and Processes*; 1990, Vol. 138, #3, pp. 10-37.

Suslick, K.S. "Homogeneous Sonochemistry"; Chapter 4 In: *Ultrasound: Its Chemical, Physical, and Biological Effects*; VCH Publishers, New York; 1988; pp. 125-163.

Suslick, K.S. "The Chemical Effects of Ultrasound"; *Sci. Amer.*; 1989; February; pp. 80-86.

Tanabe, S.; Kannan, N.; Tadaaki, W.; Tatsukawa, R. "Method for the Determination of Three Toxic Non-Orthochlorine substituted Coplanar PCBs in Environmental Samples at Part-Per-Trillion Levels"; *Intern. J. Environ. Anal. Chem.*; 1987; Vol 29; pp. 199-213.

Walling, C.; Johnson, R.A. "Fenton's Reagent. V. Hydroxylation and Side-Chain Cleavage of Aromatics"; *J. Am. Chem. Soc.*; 1975; Vol. 97, #2; pp. 363-367.

Walling, C.; Kato, S. "The Oxidation of Alcohols by Fenton's Reagent. The Effect of Copper Ion"; *J. Am. Chem. Soc.*; 1971; Vol 93, #17; pp. 4275-4281.

Walters, R.W.; Luthy, R.G. "Equilibrium Adsorption of Polycyclic Aromatic Hydrocarbons from Water onto Activated Carbon", *Environ. Sci. Technol.*, 1984; Vol. 18, #6; pp. 395-403.

Weast, R.C., Ed.; "Volume Properties of Water at 1 Atmosphere"; *CRC Handbook of Chemistry and Physics - 68th Edition*; 1987; p. F-4.

Weissler, A.; Cooper, H.W.; Snyder, S. "Chemical Effect of Ultrasonic Waves: Oxidation of Potassium Iodide Solution by Carbon Tetrachloride"; *J. Am. Chem. Soc.*; 1950; Vol. 72; pp. 1769-1775.

- Weissler, A. "Sonochemistry: The Production of Chemical Changes with Sound Waves"; *J. Acoust. Soc. Am.*; 1953; Vol. 25, #4; pp. 651-657.
- Weissler, A. "Production of Nitrous and Nitric Acid by Ultrasonic Cavitation in Water Containing Dissolved Air"; *J. Acoust. Soc. Am.*; 1960; Vol. 32, #10; pp.1208-1212.
- Windholz., M., Ed.; Budavari, S. Assoc. Ed.; Stroumτσos, L.Y. Asst. Ed.; and Fertig, M.N. Asst. Ed. *The Merck Index: Ninth Edition*; 1976; pp. 443 and 934.
- Wood, R.W.; Loomis, A.L. "The Physical and Biological Effects of High Frequency Sound-Waves of Great Intensity"; *Phil. Mag. J. Sci.*; 1927; Series 7; Vol. 4, #22; pp. 417-437.
- Yang, S.K.; Silverman, B.D. *Polycyclic Aromatic Hydrocarbon Carcinogenesis: Structure-Activity Relationships - Volume I*; CRC Press, Inc., Florida; 1988; pp. 2-30.
- Zechmeister, L.; Magoon, E.F. "On the Ultrasonic Cleavage of the Pyridine Ring"; *J. Am. Chem. Soc.*; 1956; Vol. 78; pp. 2149-2150.

Appendix A: Materials and Methods - Supplemental Information

A.1 Instrumentation:

(1) Sonic Processor - Generator: Heat Systems Inc. Model #XL-2020. Transducer: one half (1/2") inch standard taper horn with replaceable titanium tip.

(2) Suslick (1989) reaction cell - modified as depicted in various figures, 50 and 310 ml capacity.

(3) Stainless steel (SS) sealing collar - Suslick (1989) collar - Heat Systems Inc. #100SS.

(4) Perkin Elmer Model #8410 microprocessor controlled gas chromatograph equipped with:

(a) Alltech Heliflex RSL-200 fused silica open tubular (FSOT) column - 30 meter x 0.53 millimeter - 1.2 micrometer thick coating of bonded polydiphenyl - dimethylsiloxane;

(b) flame ionization detector (FID); and

(c) computer controlled chromatographic output analysis software.

(5) Ro-Tap testing sieve shaker - model "B" - equipped with timer.

(6) U.S. Standard brass sieves - both 3 inch and 8 inch diameters.

(7) Rotary evaporator (Rotavapor) - model #RE-111B equipped with an integral heated water bath, Buchi/Brinkmann Corporation.

(8) Mettler model #AE 160 analytical balance, Mettler Instrument Corporation.

(9) Brinkman model #3801 liquid scintillation counter.

(10) Uni Melt - capillary melting point apparatus - Arthur H. Thomas Co.

A.2 Solvents

(1) Water - reverse osmosis (RO) - resistivity <0.5 megohm-cm.

(2) Water - Type I - resistivity >15 megohm-cm, Deionized (designated as "DI" water), "Milli-Q" filtered, no organic removal.

(3) Water - Type I, resistivity >15 megohm-cm, "Milli-Q" filtered, active carbon treated for trace organic removal (designated "organic free" water).

(4) Pentane - C_5H_{12} , Formula Weight (FW) = 72.15 grams/mole, Eastman Kodak Company

(a) refer to methods section for preparation procedure.

(5) Dichloromethane (Methylene Chloride - CH_2Cl_2), FW = 84.93, [CAS #75-09-2] - Baker Resi-Analysed - used as received.

(6) Acetone (CH_3OCH_3), FW = 58.08, [CAS #67-64-1], Omni Solv (HR-GC Grade) - used as received.

A.3 Chemicals

(1) Active Carbon - Calgon 400, received as 14-20 mesh sample - [CAS #7440-44-0], Calgon Corporation.

(2) Biphenyl (Diphenyl - $\text{C}_{12}\text{H}_{10}$), m.p. $69-70^\circ\text{C}$, F.W. 154.2, [CAS# 92-52-4], Sigma Chemical Company.

(3) UL- ^{14}C -Biphenyl ($^{14}\text{C}_6\text{H}_5-^{14}\text{C}_6\text{H}_5$), F.W. 154.2, received as 7.6 mCi/mmole in toluene solution, Sigma Chemical (#29,720-8).

(4) Phenanthrene ($\text{C}_{14}\text{H}_{10}$), F.W. 178.2, m.p. $(98-99^\circ\text{C})$, [CAS #85-01-8] - Eastman Kodak Chemicals - contains maximum 2% anthracene. Recrystallized from EtOH-Water as white platelets, dried in vacuo at 90°C for 24 hours, stored in teflon sealed, opaque container.

(5) Phenanthrene-9- ^{14}C ($\text{C}_6\text{H}_4\text{C}_6\text{H}_4^{14}\text{CHCH}$), F.W. 178.2, received as crystalline solid - 13.1 mCi/mmole - Sigma Chemical Company (#31,528-1).

(6) Drierite - anhydrous calcium sulfate (CaSO_4) dessicant, 8 mesh - regular, [CAS #7778-18-9] - W.A. Hammond Drierite Corporation.

(7) Drierite - anhydrous calcium sulfate (CaSO_4)
dessicant, 8 mesh - indicating, [CAS #7778-18-9] - W.A.
Hammond Drierite Corporation.

(8) Glass beads - Borosilicate glass boiling beads,
approximately three (3) millimeters in diameter

(a) refer to methods section for preparation procedure:

(9) Type 4A activated molecular sieves (8-12 mesh) -
Baker Chemical

(a) reactivated at 500°C for 2 hours, cooled in
dessicator with Drierite, stored in brown bottle with teflon
lined cap.

(10) calcium hydride (CaH_2) - F.W. 42.096, [CAS #7789-78-
8], powder, Fischer Scientific, Inc.

(11) anhydrous sodium sulfate (Na_2SO_4) - FW. 142.04, [CAS
#7757-82-6], 'Baker analysed', 12-60 mesh powder

(12) ferric chloride ($\text{FeCl}_3\cdot 6\text{H}_2\text{O}$) - FW = 270.30 - [CAS
#10025-77-1],
Supplied as small lumps, ground into powder as needed.

(13) fumed silica (silicon dioxide) thixotropic gelling
agent - type m-5, Cab-O-Sil, Cab-O-Sil Corporation.

(14) liquid scintillation cocktail - Biosafe II -
Research Products International Corporation Inc. Used as
received or mixed with 30 grams/liter of Cab-O-Sil gelling
agent to form suspensions of particles from carbon and sand
experiments.

A.4 Gases

Helium carrier gas used for gas chromatography analysis was scrubbed to remove both water (Hydropurge II - indicating molecular sieve pre-column gas moisture trap - Alltech Associates) and oxygen (oxytrap and indicating oxy-trap - Alltech Associates) prior to introduction into the chromatography column.

Hydrogen (H_2) and breathing quality compressed air were used as combustion gases for the gas chromatograph flame ionization detector without further treatment.

Evaporation/concentration was conducted under a stream of nitrogen (N_2) gas.

All gases were obtained from the University of Alaska physical plant.

Appendix B: Supplemental Experimental Data - Active Carbon and Tanana Valley Sand Fragmentation:

Included in this section are plots and tabular listings of sieve data that resulted from the analysis of fragmentation studies on active carbon (AC) (figure #B4 through #B12) and Tanana Valley alluvial sand (figure #B14). Sieve analyses of the untreated active carbon and sand starting material are presented in figure #B1-B3 and #B13, respectively.

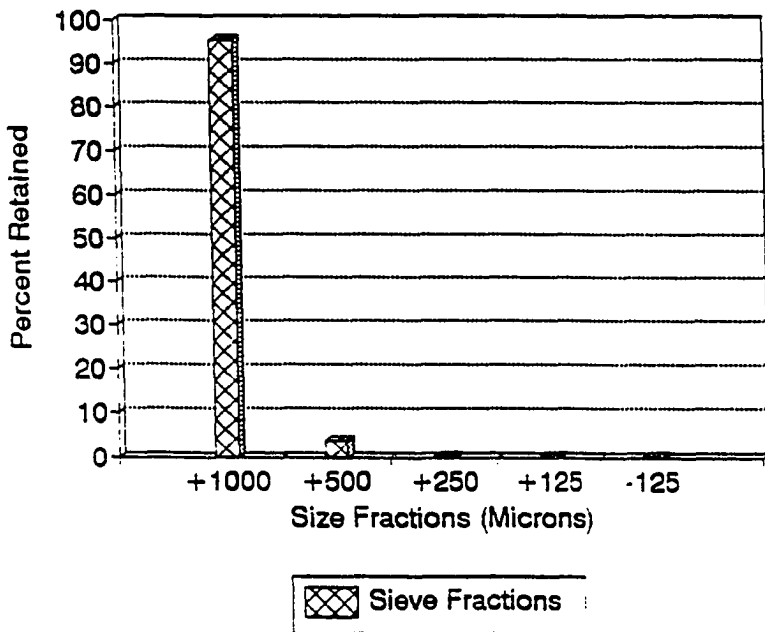


Figure #B1: Active Carbon Sieve Analysis - 1/16/91 - Untreated Starting Material

Table #B1: Active Carbon Sieve Analysis - 1/16/91 -
Untreated Starting Material

Note: B - Value at 90% Confidence Level

| Size Fraction (Microns) | Mean % of Total | Variance (Var) | B - Value $2.132[(\text{var}/5)^{0.5}]$ |
|----------------------------|--------------------|-------------------|--|
| +1000 | 95.6539 | 0.1404 | 0.3572 |
| +500 | 3.9012 | 0.1170 | 0.3262 |
| +250 | 0.0200 | 0.0002 | 0.0138 |
| +125 | 0.0200 | 0.0001 | 0.0083 |
| -125 | 0.1099 | 0.0001 | 0.0090 |

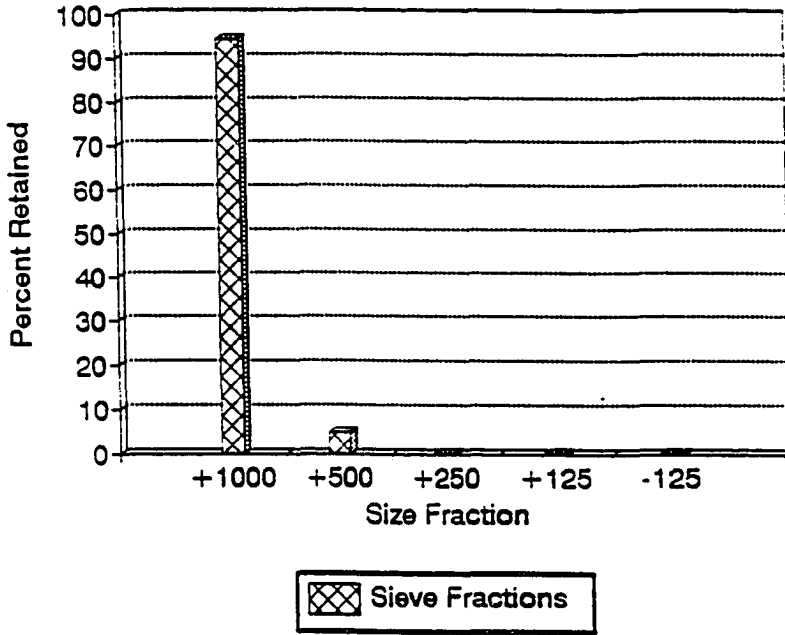


Figure #B2: Active Carbon Sieve Analysis - 2/1/91 - Untreated Starting Material

Table #B2 : Active Carbon Sieve Analysis - 2/1/91 Untreated Starting Material

Note: (B - Value at 90% confidence Level)

| Size Fractions (Microns) | Mean % of Total | Variance (Var) | B -Value $2.132 \{ (Var/5)^{0.5} \}$ |
|-----------------------------|--------------------|-------------------|---|
| +1000 | 94.6548 | 0.0993 | 0.3004 |
| +500 | 4.9159 | 0.0723 | 0.2563 |
| +250 | 0.0133 | 0.0000 | 0.0067 |
| +125 | 0.0003 | 0.0000 | 0.0001 |
| -125 | 0.0019 | 0.0006 | 0.0234 |

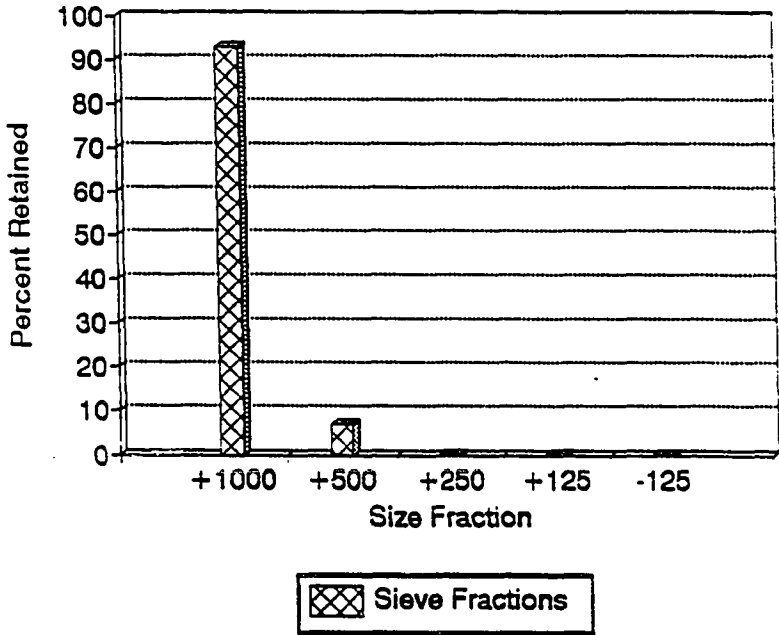


Figure #B3: Active Carbon Sieve Analysis 2/28/91 - Untreated Starting Material

Table #B3: Active Carbon Sieve Analysis - 2/28/91 Untreated Starting Material

Note: (B - Value at 90% Confidence Level)

| Size Fractions (Microns) | Mean % of Total | Variance (Var) | B - Value $2.132[(\text{Var}/5)^{0.5}]$ |
|--------------------------|-----------------|----------------|---|
| +1000 | 92.9523 | 0.0505 | 0.2143 |
| +500 | 6.8944 | 0.0484 | 0.2097 |
| +250 | 0.0267 | 0.0003 | 0.0162 |
| +125 | 0.0003 | 0.0000 | 0.0001 |
| -125 | 0.0019 | 0.0000 | 0.0005 |

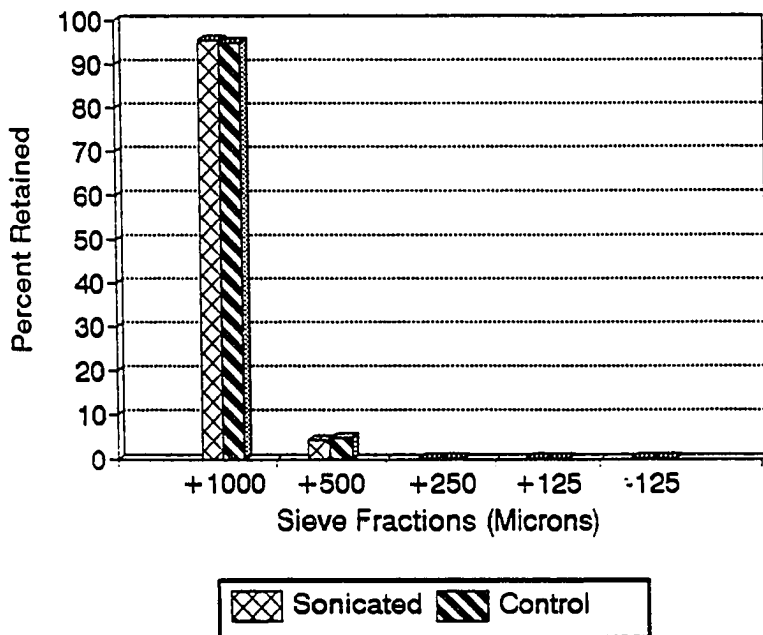


Figure #B4: Sieve Analysis of Active Carbon Subjected To 43 Watts/Cm² for 5 Minutes in a 50 mL Reactor

Table #B4: Sieve Analysis of Active Carbon Subjected To 43 Watts/Cm² for 5 Minutes in a 50 mL Reactor

=====
Sonic - 6 Trials (B - Value at 90% Confidence Level)

| Size Fractions (Microns) | Mean % of Total | Variance (Var) | B - Value $2.015[(\text{Var}/6)^{0.5}]$ |
|--------------------------|-----------------|----------------|--|
| +1000 | 95.5424 | 1.2611 | 0.9238 |
| +500 | 4.3868 | 0.8656 | 0.7654 |
| +250 | 0.0321 | 0.0021 | 0.0376 |
| +125 | 0.0300 | 0.0004 | 0.0164 |
| -125 | 0.1659 | 0.0047 | 0.0562 |

=====
Control - 4 Trials (No Sonic) B - Value at 90% Confidence Level

| Size Fractions (Microns) | Mean % of Total | Variance (Var) | B - Value $2.353[(\text{Var}/4)^{0.5}]$ |
|--------------------------|-----------------|----------------|--|
| +1000 | 94.9446 | 0.1737 | 0.4903 |
| +500 | 4.7411 | 0.1257 | 0.4170 |
| +250 | 0.0166 | 0.0000 | 0.0062 |
| +125 | 0.0116 | 0.0000 | 0.0044 |
| -125 | 0.1178 | 0.0006 | 0.0294 |

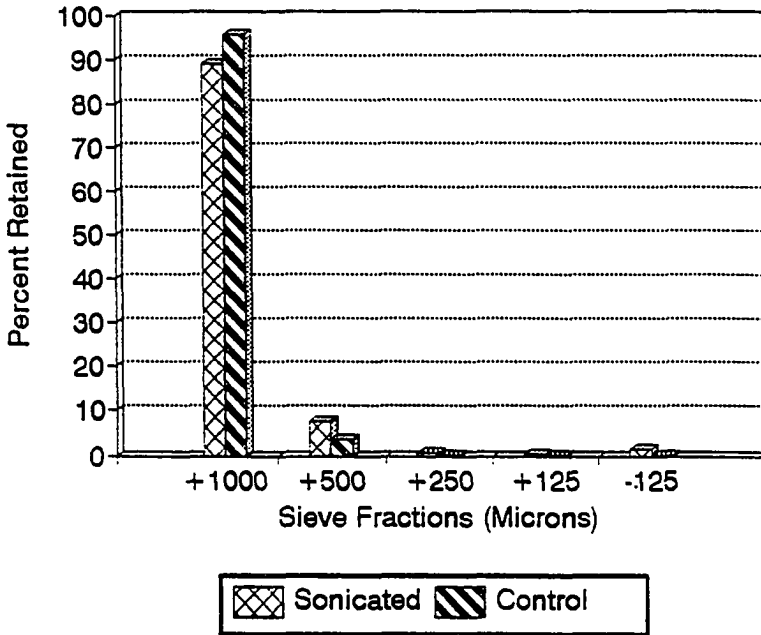


Figure #B5: Sieve Analysis of Active Carbon Subjected To 85 Watts/Cm² for 5 Minutes in 50 mL Reactor

Table #B5: Sieve Analysis of Active Carbon Subjected To 85 Watts/Cm² for 5 Minutes in 50 mL Reactor

=====
Sonic - 6 Trials (B - Value at 90% Confidence Interval)

| Size Fractions (Microns) | Mean % of Total | Variance (Var) | B - Value $2.015[(Var/6)^{0.5}]$ |
|--------------------------|-----------------|----------------|-------------------------------------|
| +1000 | 89.3088 | 0.8201 | 0.7450 |
| +500 | 7.5632 | 0.7225 | 0.6992 |
| +250 | 0.8151 | 0.0068 | 0.0676 |
| +125 | 0.5578 | 0.0029 | 0.0441 |
| -125 | 1.3667 | 0.0292 | 0.1407 |

=====
Control - 4 Trials (No Sonic) B-Value at 90% Confidence Interval

| Size Fractions (Microns) | Mean % of Total | Variance (Var) | B - Value $2.353[(Var/4)^{0.5}]$ |
|--------------------------|-----------------|----------------|-------------------------------------|
| +1000 | 95.8687 | 0.5449 | 0.8685 |
| +500 | 0.8222 | 0.4951 | 0.8278 |
| +250 | 0.0166 | 0.0000 | 0.0024 |
| +125 | 0.0166 | 0.0000 | 0.0035 |
| -125 | 0.1451 | 0.0033 | 0.0676 |

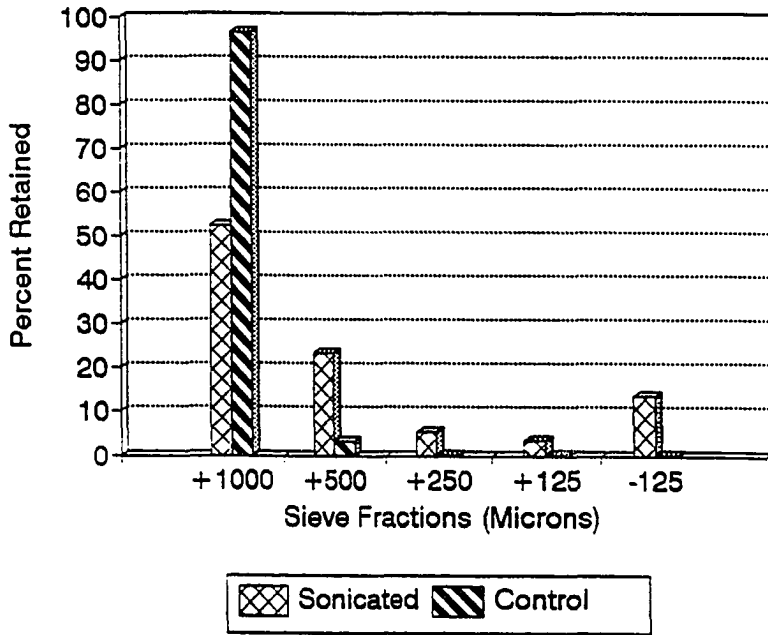


Figure #B6: Sieve Analysis of Active Carbon Subjected To 138 Watts/Cm² for 5 Minutes in 50 mL Reactor

Table # B6: Sieve Analysis of Active Carbon Subjected To 138 Watts/Cm² for 5 Minutes in 50 mL Reactor

=====
Sonic - 6 Trials (B-Value at 90% Confidence Interval)

| Size Fractions (Microns) | Mean % of Total | Variance (Var) | B - Value $2.132[(Var/6)^{0.5}]$ |
|--------------------------|-----------------|----------------|----------------------------------|
| +1000 | 52.5675 | 11.8008 | 2.9900 |
| +500 | 23.4419 | 5.0772 | 1.9612 |
| +250 | 5.5401 | 0.2184 | 0.4067 |
| +125 | 3.3373 | 0.0676 | 0.2263 |
| -125 | 13.6331 | 1.0965 | 0.9114 |

=====
Control - 4 Trials (No Sonic) B - Value at 90% Confidence Level

| Size Fractions (Microns) | Mean % of Total | Variance (Var) | B - Value $2.353[(Var/4)^{0.5}]$ |
|--------------------------|-----------------|----------------|----------------------------------|
| +1000 | 96.5951 | 0.8336 | 1.0742 |
| +500 | 3.2422 | 0.6489 | 0.9477 |
| +250 | 0.0324 | 0.0001 | 0.0105 |
| +125 | 0.0224 | 0.0000 | 0.0080 |
| -125 | 0.1162 | 0.0002 | 0.0184 |

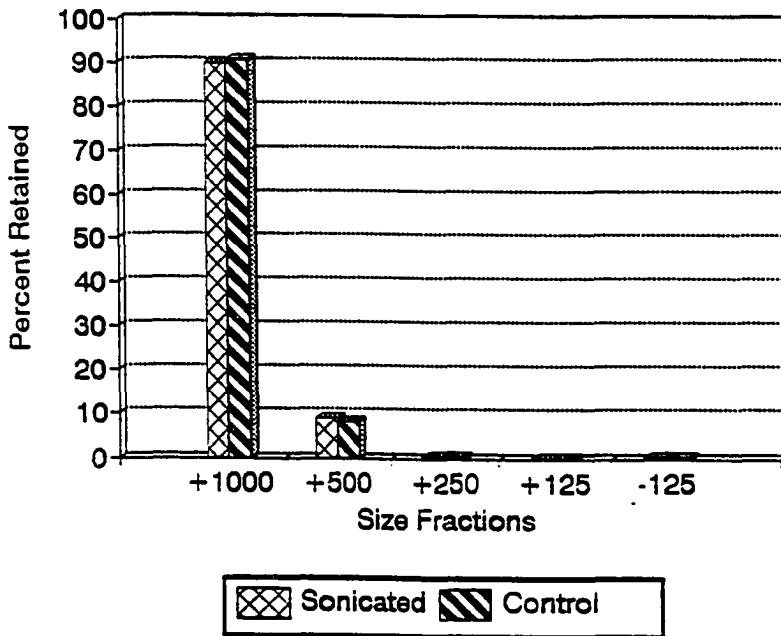


Figure #B7: Sieve Analysis of Active Carbon Subjected to 50 Watts/Cm² for 30 Minutes in 310 mL Reactor

Table #B7: Sieve Analysis of Active Carbon Subjected to 50 Watts/Cm² for 30 Minutes in 310 mL Reactor

Sonic - 6 Trials (B-Value at 90% Confidence Level)

| Size Fractions (Microns) | Mean % of Total | Variance (Var) | B - Value $2.015[(\text{Var}/6)^{0.5}]$ |
|--------------------------|-----------------|----------------|---|
| +1000 | 90.1600 | 0.8814 | 0.7723 |
| +500 | 9.0580 | 0.6702 | 0.6734 |
| +250 | 0.3343 | 0.0039 | 0.0512 |
| +125 | 0.0946 | 0.0002 | 0.0127 |
| -125 | 0.3470 | 0.0020 | 0.0367 |

Control - 3 Trials - (No Sonic) B-Value at 90% Confidence Level

| Size Fractions (Microns) | Mean % of Total | Variance (Var) | B - Value $2.92[(\text{Var}/3)^{0.5}]$ |
|--------------------------|-----------------|----------------|--|
| +1000 | 90.8826 | 5.1454 | 3.8241 |
| +500 | 8.3909 | 4.1773 | 3.4456 |
| +250 | 0.2869 | 0.0196 | 0.2360 |
| +125 | 0.0698 | 0.0010 | 0.0533 |
| -125 | 0.3045 | 0.0025 | 0.0829 |

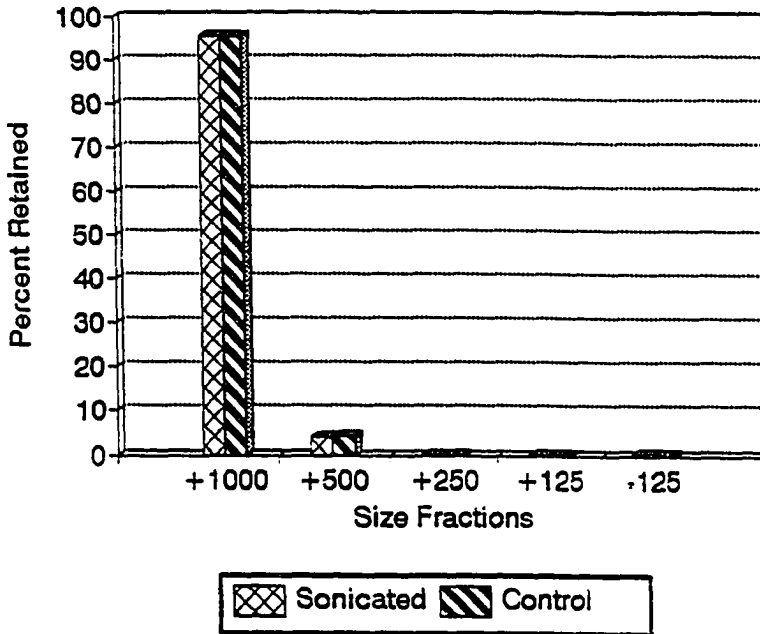


Figure #B8: Sieve Analysis of Active Carbon Subjected to 85 Watts/Cm² for 5 Minutes in a 310 mL Reactor

Table #B8: Sieve Analysis of Active Carbon Subjected to 85 Watts/Cm² for 5 Minutes in a 310 mL Reactor

Sonic - 6 Trials (B - Value at 90% Confidence Level)

| Size Fractions (Microns) | Mean % of Total | Variance (Var) | B - Value $2.015[(\text{Var}/6)^{0.5}]$ |
|-----------------------------|--------------------|-------------------|--|
| +1000 | 95.5252 | 0.0903 | 0.2472 |
| +500 | 4.1660 | 0.0438 | 0.1722 |
| +250 | 0.0498 | 0.0004 | 0.0154 |
| +125 | 0.0338 | 0.0002 | 0.0121 |
| -125 | 0.2730 | 0.0118 | 0.0893 |

Control - 3 Trials (No Sonic) B - Value at 90% Confidence Level

| Size Fractions (Microns) | Mean % of Total | Variance (Var) | B - Value $2.92[(\text{Var}/3)^{0.5}]$ |
|-----------------------------|--------------------|-------------------|---|
| +1000 | 95.3700 | 0.1723 | 0.6999 |
| +500 | 4.2917 | 0.1581 | 0.6704 |
| +250 | 0.0310 | 0.0001 | 0.0147 |
| +125 | 0.0254 | 0.0000 | 0.0027 |
| -125 | 0.1515 | 0.0001 | 0.0186 |

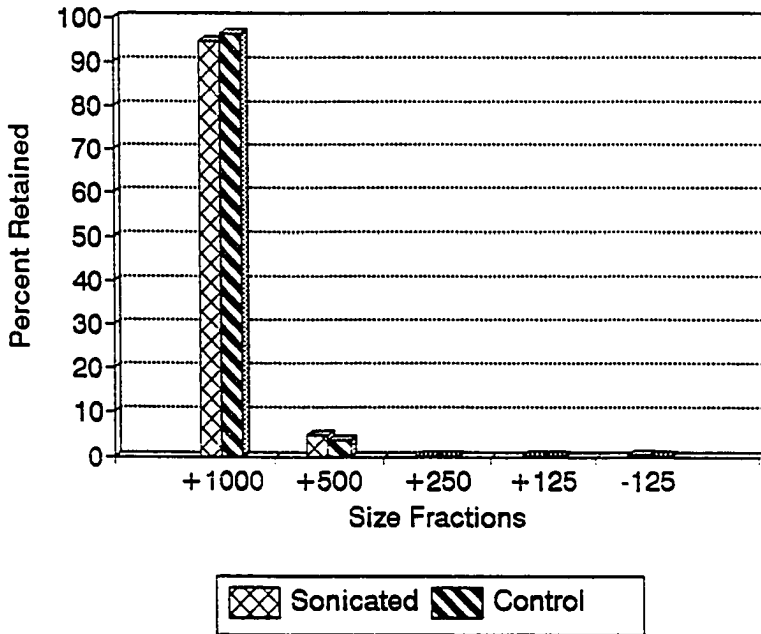


Figure #B9: Sieve Analysis of Active Carbon Subjected to 85 Watts/Cm² for 25 Minutes in 310 mL Reactor

Table #B9: Sieve Analysis of Active Carbon Subjected to 85 Watts/Cm² for 25 Minutes in 310 mL Reactor

=====
 Sonic - 6 Trials (B - Value at 90% confidence Level)

| Size Fractions (Microns) | Mean % of Total | Variance (Var) | B - Value $2.015[(Var/6)^{0.5}]$ |
|--------------------------|-----------------|----------------|----------------------------------|
| +1000 | 94.8886 | 0.1910 | 0.3595 |
| +500 | 4.9787 | 0.4446 | 0.5485 |
| +250 | 0.0678 | 0.0011 | 0.0269 |
| +125 | 0.0295 | 0.0001 | 0.0089 |
| -125 | 0.2904 | 0.0053 | 0.0601 |

=====
 Control - 3 Trials (No Sonic) B - Value at 90% confidence Level

| Size Fractions (Microns) | Mean % of Total | Variance (Var) | B - Value $2.92[(Var/3)^{0.5}]$ |
|--------------------------|-----------------|----------------|---------------------------------|
| +1000 | 96.2344 | 0.2970 | 0.9188 |
| +500 | 3.7811 | 0.5071 | 1.2006 |
| +250 | 0.0356 | 0.0003 | 0.0297 |
| +125 | 0.0278 | 0.0000 | 0.0071 |
| -125 | 0.1890 | 0.0012 | 0.0576 |

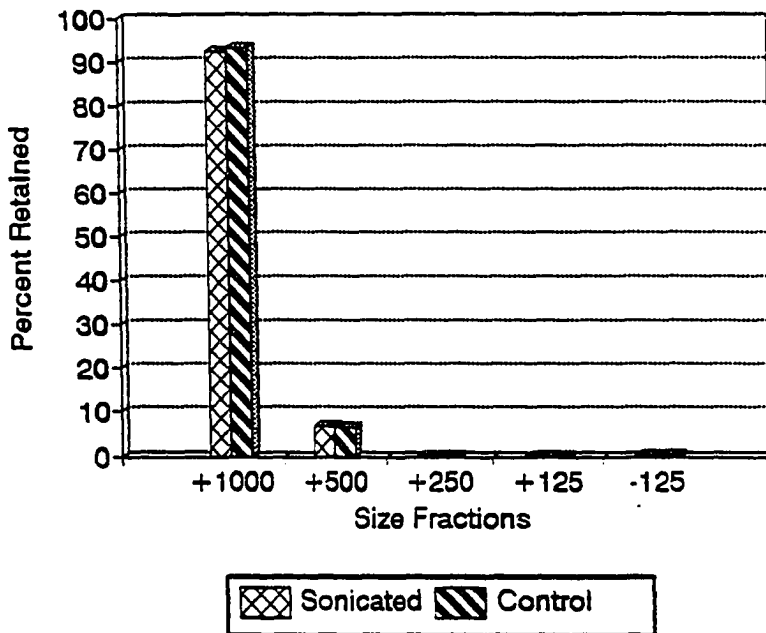


Figure #B10: Sieve Analysis of Active Carbon Subjected to 100 Watts/Cm² for 30 Minutes in 310 mL Reactor

Table #B10: Sieve Analysis of Active Carbon Subjected to 100 Watts/Cm² for 30 Minutes in 310 mL Reactor

Sonicated - 6 Trials (B-Value at 90% Confidence Level)

| Size Fractions (Microns) | Mean % of Total | Variance (Var) | B - Value $2.015[(\text{Var}/6)^{0.5}]$ |
|--------------------------|-----------------|----------------|--|
| +1000 | 92.5729 | 3.6451 | 1.5706 |
| +500 | 6.8551 | 2.6598 | 1.3416 |
| +250 | 0.2029 | 0.0311 | 0.1451 |
| +125 | 0.0543 | 0.0017 | 0.0339 |
| -125 | 0.3752 | 0.0159 | 0.1037 |

Control - 3 Trials (No Sonic) B-Value at 90% Confidence Level

| Size Fractions (Microns) | Mean % of Total | Variance (Var) | B - Value $2.92[(\text{Var}/3)^{0.5}]$ |
|--------------------------|-----------------|----------------|---|
| +1000 | 93.2456 | 0.3398 | 0.9827 |
| +500 | 6.5937 | 0.0941 | 0.5172 |
| +250 | 0.1354 | 0.0247 | 0.2650 |
| +125 | 0.0422 | 0.0022 | 0.0797 |
| -125 | 0.2397 | 0.0049 | 0.1180 |

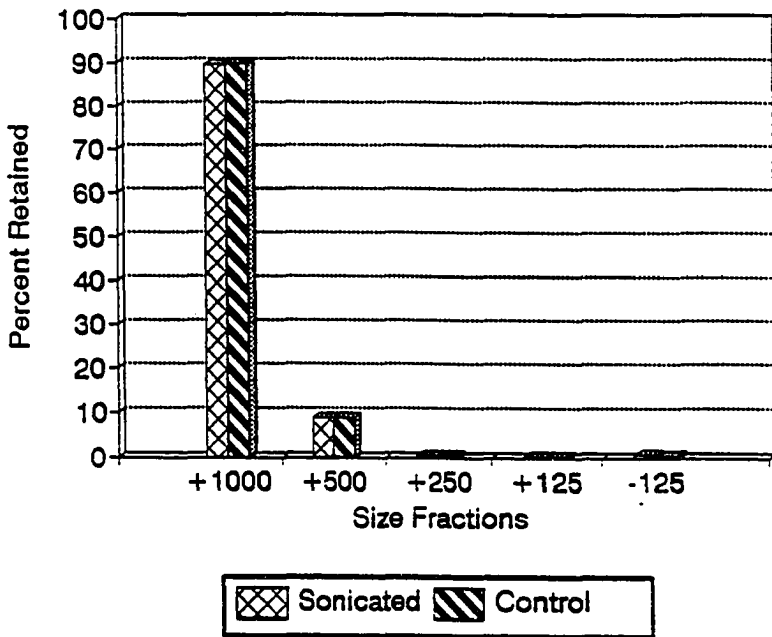


Figure #B11: Sieve Analysis of Active Carbon Subjected to 150 Watts/Cm² for 30 minutes in 310 mL Reactor

Table #B11: Sieve Analysis of Active Carbon Subjected to 150 Watts/Cm² for 30 minutes in 310 mL Reactor

Sonic - 6 Trials (B - Value at 90% Confidence Level)

| Size Fractions (Microns) | Mean % of Total | Variance (Var) | B - Value $2.015[(Var/6)^{0.5}]$ |
|--------------------------|-----------------|----------------|----------------------------------|
| +1000 | 89.6285 | 0.5116 | 0.5884 |
| +500 | 9.0705 | 0.2261 | 0.3912 |
| +250 | 0.3606 | 0.0160 | 0.1042 |
| +125 | 0.1153 | 0.0066 | 0.0668 |
| -125 | 0.7953 | 0.0197 | 0.1155 |

Control - 3 Trials (No sonic) B - Value at 90% Confidence Level

| Size Fractions (Microns) | Mean % of Total | Variance (Var) | B - Value $2.92[(Var/3)^{0.5}]$ |
|--------------------------|-----------------|----------------|---------------------------------|
| +1000 | 90.1929 | 1.0812 | 1.7529 |
| +500 | 9.0340 | 0.7916 | 1.5000 |
| +250 | 0.3456 | 0.0047 | 0.1152 |
| +125 | 0.0864 | 0.0005 | 0.0390 |
| -125 | 0.3345 | 0.0022 | 0.0791 |

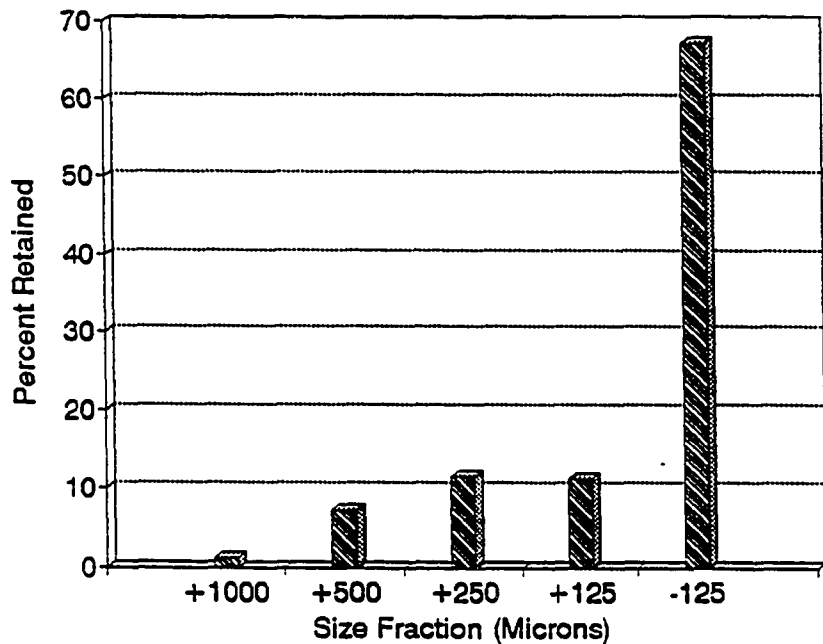


Figure #B12: Sieve Analysis of Active Carbon Subjected to 190 Watts/Cm² for 50 minutes in 310 mL Reactor Single Trial - No Control

Table #B12: Sieve Analysis of Active Carbon Subjected to 190 Watts/Cm² for 50 minutes in 310 mL Reactor Single Trial - No Control

| Size Fraction | Percent Retained (%) |
|---------------|----------------------|
| +1000 | 1.2300 |
| +500 | 7.3600 |
| +250 | 11.6400 |
| +125 | 11.2500 |
| -125 | 67.2300 |

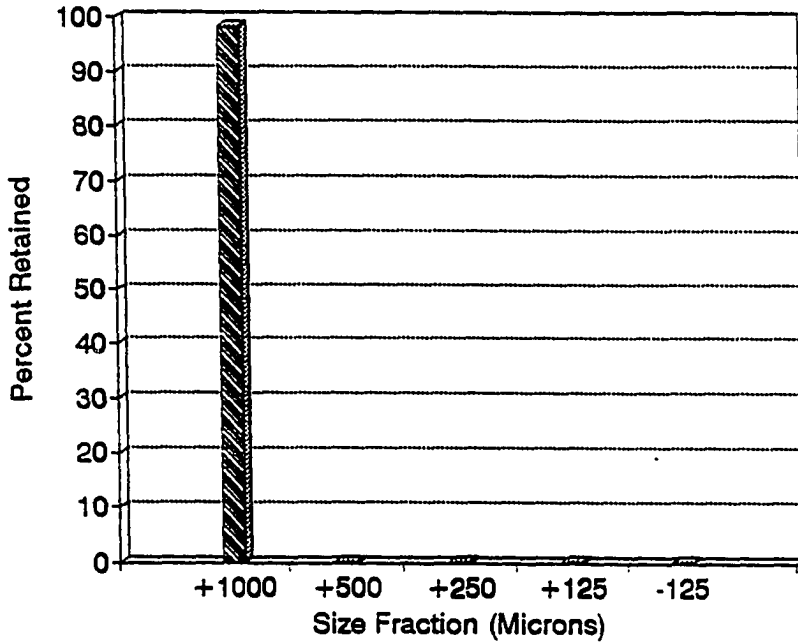


Figure #B13: Sieve Analysis of Tanana Valley Sand - Single Trial - Untreated Starting Material

Table #B13: Sieve Analysis of Tanana Valley Sand - Single Trial - Untreated Starting Material

| Size Fraction | Percent Retained (%) |
|---------------|----------------------|
| +1000 | 98.2814 |
| +500 | 0.0100 |
| +250 | 0.0600 |
| +125 | 0.0600 |
| -125 | 0.0600 |

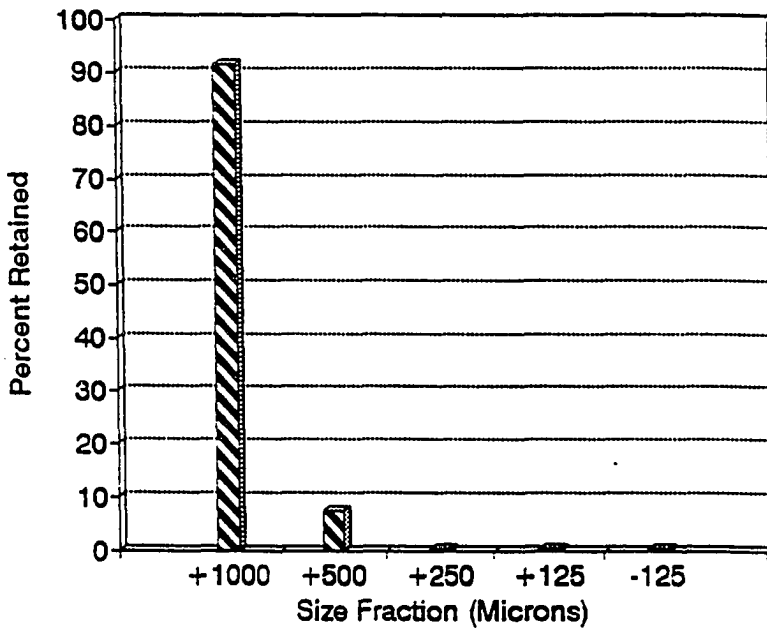


Figure #B14: Sieve Analysis of Tanana Valley Sand Subjected to 156 Watts/Cm² for 50 Minutes in 310 mL Reaction Vessel - Single Trial

Table #B14: Sieve Analysis of Tanana Valley Sand Subjected to 156 Watts/Cm² for 50 Minutes in 310 mL Reaction Vessel - Single Trial

| Size Fraction | Percent Retained % |
|---------------|-----------------------|
| +1000 | 91.5690 |
| +500 | 7.4523 |
| +250 | 0.2004 |
| +125 | 0.2547 |
| -125 | 0.2547 |

Appendix C: Gas Chromatography and Mass Spectrometry Data

Included in this section is information related to the acquisition of gas chromatography (GC) and combined gas chromatography/mass spectrometry (GC/MS) data. Equipment descriptions, materials utilized and operating condition are presented in tables #C1 through #C3. Sample chromatograms of control (no sonic - figures #C1 and #C6) and sonic treatment (figures #C2 and #C7) reaction mixtures obtained through the use of a the flame ionization detector (FID) for both biphenyl and phenanthrene are included. The ion chromatograms of selected biphenyl and phenanthrene reaction mixtures are also included (figure #C3 and C8). Mass spectra, and associated ion abundances, of selected reaction products from sonic treatment of both biphenyl and phenanthrene are also presented.

C.1 Gas Chromatography Programs

Table #C1: Gas Chromatography Program for Perkin Elmer Gas Chromatograph With FID Detector - Biphenyl

| Parameter | Value |
|---------------------------------|------------------------|
| Injector temperature | 320 degrees Centigrade |
| Detector temperature | 350 degrees Centigrade |
| Temperature program: | |
| Initial oven temperature | 120 degrees Centigrade |
| Initial temperature time | 2 minutes |
| Temperature ramp rate | 5 degrees Centigrade |
| Final temperature | 280 degrees Centigrade |
| Time at final temperature | 10 minutes |
| FID sensitivity | high |
| Detector zero | on |
| Carrier gas | Helium (He) |
| Carrier gas flow rate | 36 mL/min |
| Equilibration time | 0.5 min |
| Total run time | 44.0 min |
| Section Two: Timed events | |
| Valley base point | 8.00 minutes |
| Section Three: Data Acquisition | |
| Start time | 0.00 minutes |
| End time | 44.00 minutes |
| Width | 5 |
| Skim sensitivity | 9 |
| Baseline correction | B-B |
| Area sensitivity | 50 |
| Base sensitivity | 4 |
| Calculation type | % |
| Area/Height calculation | area |

Table #C2: Gas Chromatography Program for Perkin Elmer Gas Chromatograph With FID Detector Phenanthrene

| Parameter | Value |
|---------------------------------|------------------------|
| Injector temperature | 320 degrees Centigrade |
| Detector temperature | 350 degrees Centigrade |
| Temperature program: | |
| Initial oven temperature | 120 degrees Centigrade |
| Initial temperature time | 2 minutes |
| Temperature ramp rate | 5 degrees Centigrade |
| Final temperature | 280 degrees Centigrade |
| Time at final temperature | 10 minutes |
| FID sensitivity | high |
| Detector zero | on |
| Carrier gas | Helium (He) |
| Carrier gas flow rate | 36 mL/min |
| Equilibration time | 0.5 min |
| Total run time | 44.0 min |
| Section Two: Timed Events | |
| Valley base point | 10.00 minutes |
| Valley base point | 25.00 minutes |
| Skim sensitivity (9) | 25.01 minutes |
| Valley base point | 34.00 minutes |
| Section Three: Data Acquisition | |
| Start time | 0.00 minutes |
| End time | 44.00 minutes |
| Width | 5 |
| Skim sensitivity | 9 |
| Baseline correction | B-B |
| Area sensitivity | 50 |
| Base sensitivity | 4 |
| Calculation type | % |
| Area/Height calculation | area |

Table #C3: Data Acquisition and Operating Parameters for Hewlett Packard Gas Chromatograph With Mass Selective Detector - Biphenyl and Phenanthrene

| Parameter | Value |
|-----------------------------|--|
| Gas Chromatograph | Hewlett Packard Model 5700A |
| Column | HP-5 (5% crosslinked phenyl methyl silicone) |
| Column length | 25 meters |
| Column internal diameter | 0.2 millimeters |
| coating film thickness | 0.33 micrometers |
| carrier gas | Helium |
| carrier gas pressure | 25 PSI |
| Temperature Program: | |
| Initial temperature | 40 degrees Centigrade |
| Initial time | 2 minutes |
| Temperature ramp rate | 2 degrees per minute |
| Final temperature | 300 degrees Centigrade (Biphenyl) |
| Final temperature | 320 degrees Centigrade (Phenanthrene) |
| Mass spectroscopy | |
| Instrument | Hewlett-Packard model 5930A |
| Operation mode | Electron impact |
| Electron energy | 70 Electron Volts |
| Scan interval | 50 to 400 Daltons |

C.2 Gas Chromatography (GC) and Combined Gas Chromatography/Mass Spectrometry (GC/MS) Data

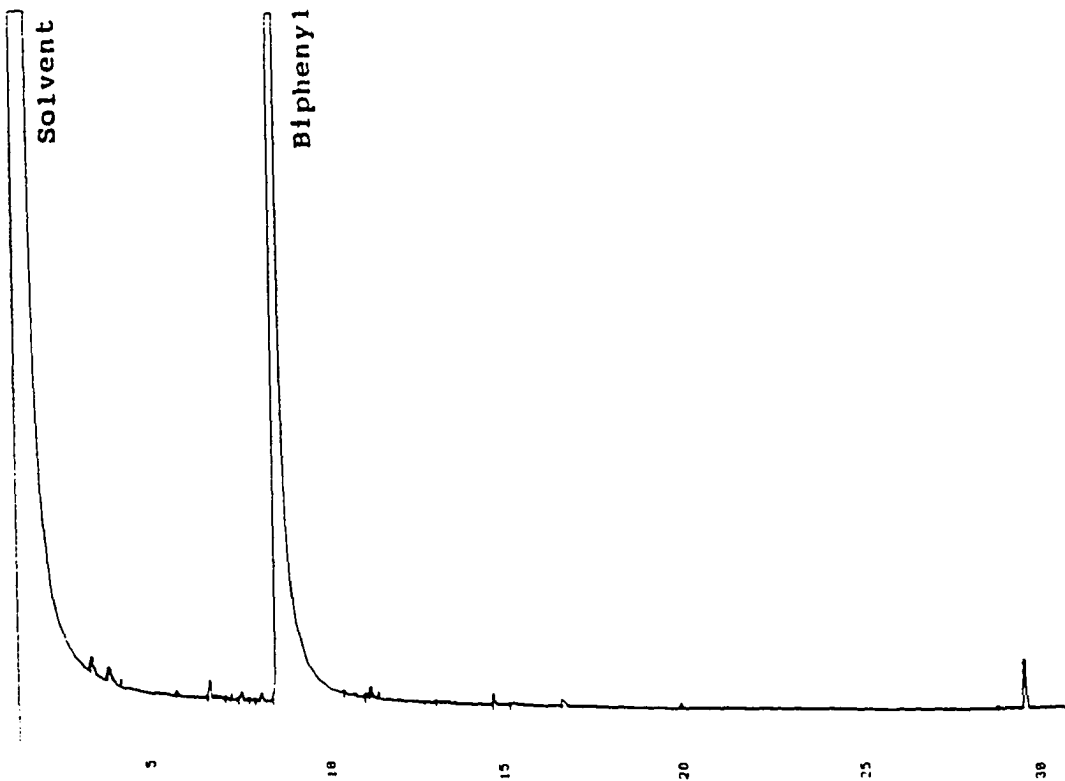


Figure #C1: Gas Chromatography Plot of Biphenyl Control (No Sonic) Reaction Mixture - FID Detector

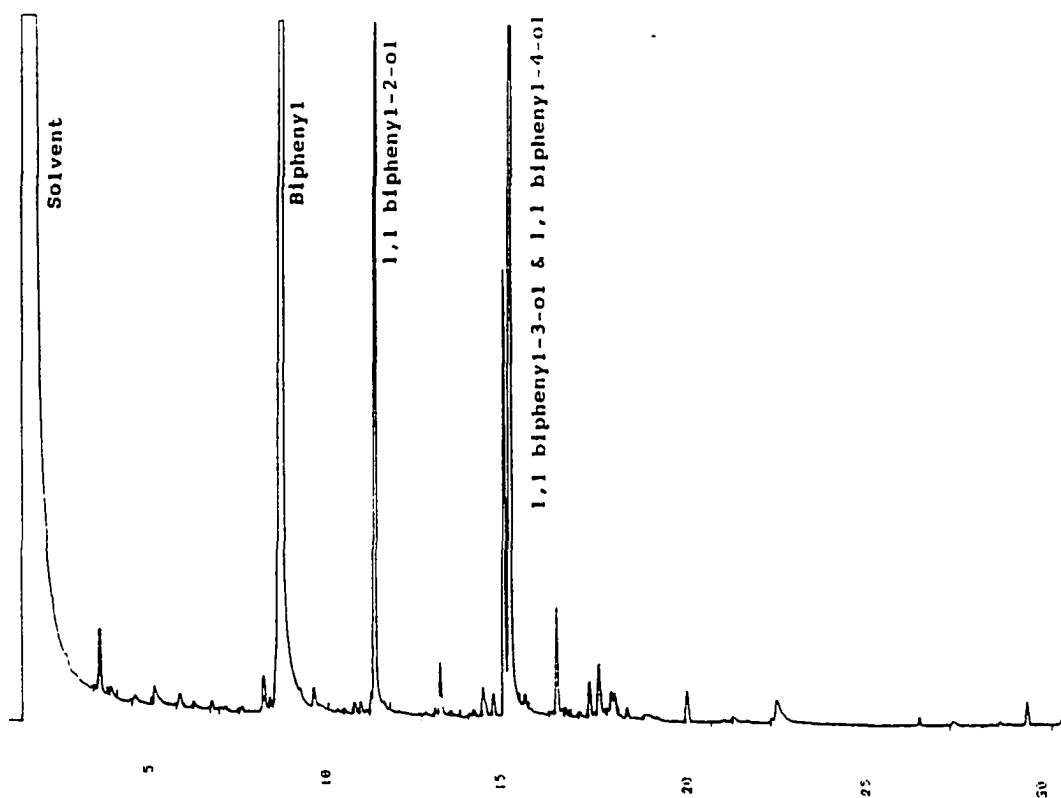


Figure #C2: Gas Chromatography Plot of Biphenyl Ultrasonic Reaction Mixture - FID Detector

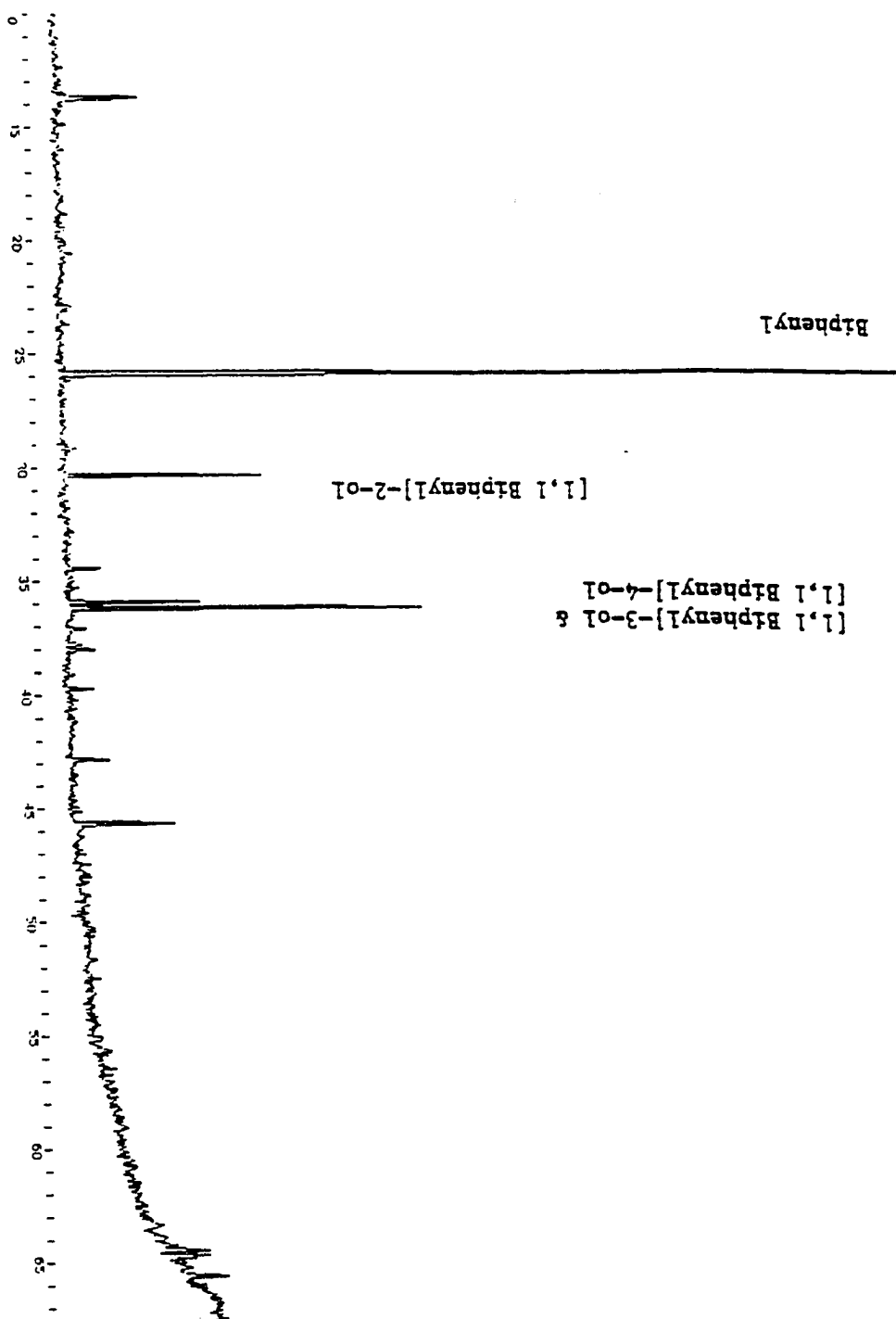


Figure #C3: Total Ion Chromatogram of Biphenyl Ultrasonic Reaction Mixture - Mass Selective Detector

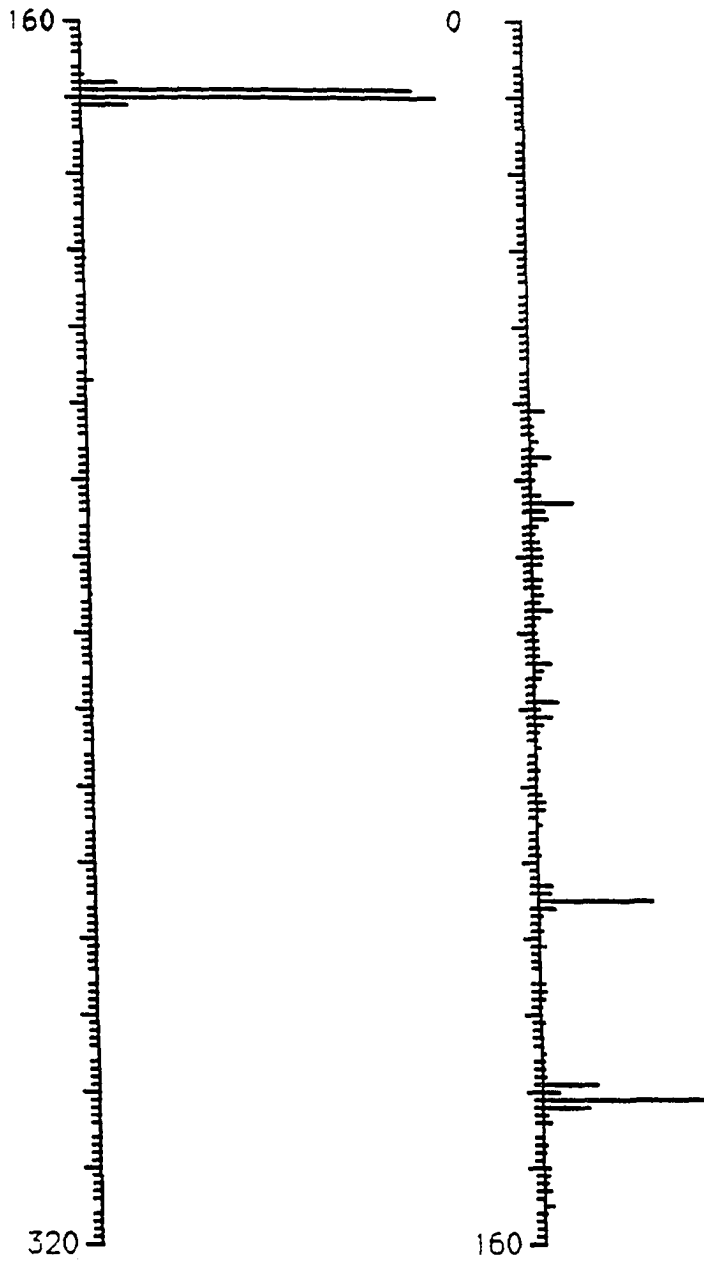


Figure #C4: Mass Spectrum of ortho-Hydroxy Biphenyl - Peak at Time 30.33 Minutes in Total Ion Chromatogram (See Figure #C3)

Table #C4: Mass Spectrum of Biphenyl Ultrasonic Reaction Product with Retention Time of 30.33 Minutes (See Figure #C3) - o-Hydroxy Biphenyl

| Mass Number | Ion Abundance (Threshold 1%) | Mass Number | Ion Abundance (Threshold 1%) |
|-------------|------------------------------|-------------|------------------------------|
| 51.0 | 4.4 | 91.1 | 4.9 |
| 53.3 | 1.1 | 91.9 | 2.3 |
| 53.8 | 1.1 | 93.0 | 1.1 |
| 54.9 | 2.2 | 94.6 | 1.1 |
| 57.0 | 5.8 | 95.0 | 1.3 |
| 57.5 | 3.4 | 100.8 | 1.5 |
| 58.0 | 2.0 | 102.0 | 2.7 |
| 58.6 | 1.3 | 102.9 | 2.2 |
| 60.5 | 1.1 | 104.9 | 1.3 |
| 62.0 | 2.7 | 113.0 | 3.9 |
| 63.0 | 12.0 | 114.1 | 3.4 |
| 63.9 | 4.1 | 115.1 | 33.3 |
| 65.0 | 4.8 | 116.1 | 4.7 |
| 66.2 | 1.7 | 117.0 | 1.1 |
| 68.1 | 2.2 | 118.9 | 1.1 |
| 69.0 | 2.6 | 119.1 | 1.1 |
| 69.4 | 2.3 | 121.0 | 1.7 |
| 70.0 | 3.1 | 126.3 | 1.3 |
| 70.5 | 1.5 | 127.1 | 1.9 |
| 71.0 | 2.8 | 128.0 | 1.5 |
| 73.0 | 2.7 | 139.1 | 15.7 |
| 73.5 | 2.6 | 140.1 | 4.6 |
| 74.1 | 2.4 | 141.1 | 47.8 |
| 75.0 | 3.0 | 142.1 | 13.2 |
| 76.0 | 2.0 | 143.1 | 1.3 |
| 77.0 | 5.3 | 144.0 | 2.3 |
| 78.0 | 1.8 | 150.1 | 1.7 |
| 81.0 | 1.3 | 151.1 | 1.6 |
| 82.2 | 1.5 | 153.0 | 2.0 |
| 83.4 | 1.2 | 155.2 | 2.8 |
| 84.0 | 4.6 | 168.1 | 10.4 |
| 85.2 | 2.8 | 169.1 | 93.5 |
| 86.0 | 1.9 | 170.2 | 100.0 |
| 89.0 | 6.5 | 171.1 | 13.0 |
| 90.0 | 1.2 | 207.2 | 1.8 |

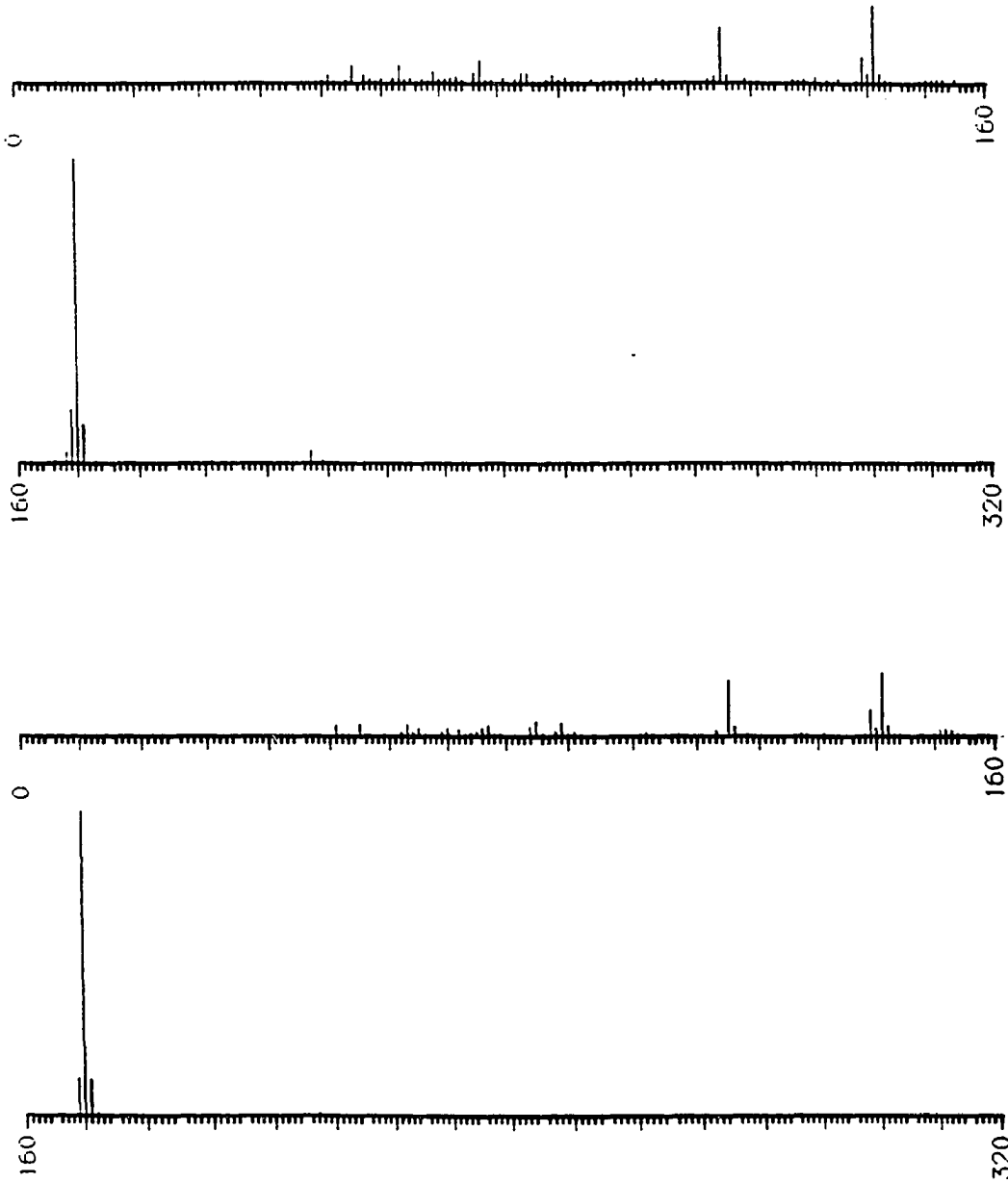


Figure #C5: Mass Spectra of meta- & para-Hydroxy Biphenyl - Peaks With Retention Times of 35.93 and 36.20 Minutes in Ion Chromatogram (See Figure #C3)

Table #C5: Mass Spectrum of Biphenyl Reaction Product with Retention Time of 35.93 Minutes (See Figure #C3) m- or p-Hydroxy Biphenyl

| Mass Number | Ion Abundance (Threshold 1%) | Mass Number | Ion Abundance (Threshold 1%) |
|-------------|------------------------------|-------------|------------------------------|
| 50.9 | 2.6 | 95.1 | 1.4 |
| 55.0 | 6.0 | 102.0 | 2.0 |
| 55.5 | 1.7 | 103.3 | 2.0 |
| 56.9 | 2.6 | 105.0 | 1.2 |
| 58.0 | 1.2 | 113.0 | 1.5 |
| 60.0 | 1.5 | 114.1 | 2.1 |
| 61.9 | 1.8 | 115.1 | 18.0 |
| 63.0 | 5.9 | 116.1 | 2.5 |
| 63.9 | 1.3 | 119.0 | 1.6 |
| 65.1 | 1.7 | 127.0 | 1.5 |
| 66.8 | 1.3 | 129.0 | 1.8 |
| 69.0 | 4.1 | 131.1 | 2.2 |
| 69.5 | 1.7 | 135.2 | 1.3 |
| 70. | 1.3 | 139.1 | 8.8 |
| 70.5 | 1.1 | 140.1 | 3.1 |
| 70.9 | 1.3 | 141.2 | 25.5 |
| 72.1 | 1.7 | 142.2 | 3.2 |
| 73.1 | 2.2 | 150.1 | 1.7 |
| 75.9 | 3.5 | 151.3 | 1.3 |
| 77.0 | 7.5 | 152.1 | 1.3 |
| 81.0 | 1.9 | 153.1 | 1.3 |
| 83.1 | 1.4 | 155.1 | 1.6 |
| 84.1 | 3.3 | 168.1 | 3.6 |
| 84.9 | 3.7 | 169.1 | 17.6 |
| 87.6 | 1.2 | 170.2 | 100.0 |
| 89.1 | 2.7 | 171.1 | 12.7 |
| 91.0 | 1.7 | 207.1 | 3.9 |

Table #C6: Mass Spectrum of Biphenyl Reaction Product with Retention Time of 36.20 Minutes(See Figure #C3) m- or p-Hydroxy Biphenyl

| Mass Number | Ion Abundance (Threshold 1%) | Mass Number | Ion Abundance (Threshold 1%) |
|-------------|------------------------------|-------------|------------------------------|
| 50.9 | 3.4 | 91.1 | 1.4 |
| 55.0 | 4.0 | 102.0 | 1.4 |
| 62.0 | 1.5 | 113.1 | 1.8 |
| 63.0 | 4.0 | 115.1 | 18.7 |
| 64.0 | 1.5 | 116.1 | 3.2 |
| 65.0 | 2.7 | 127.1 | 1.1 |
| 68.9 | 1.4 | 131.1 | 1.1 |
| 69.5 | 1.5 | 139.0 | 8.8 |
| 70.0 | 2.6 | 140.0 | 2.7 |
| 72.1 | 2.2 | 141.1 | 20.9 |
| 74.0 | 1.1 | 142.1 | 3.5 |
| 75.0 | 1.3 | 151.1 | 2.1 |
| 75.5 | 1.5 | 152.1 | 2.4 |
| 76.0 | 2.7 | 153.1 | 1.7 |
| 77.0 | 3.4 | 169.1 | 12.2 |
| 84.0 | 2.9 | 170.1 | 100.0 |
| 85.0 | 5.3 | 171.2 | 11.6 |
| 88.1 | 1.2 | 172.2 | 1.1 |
| 89.0 | 4.1 | | |

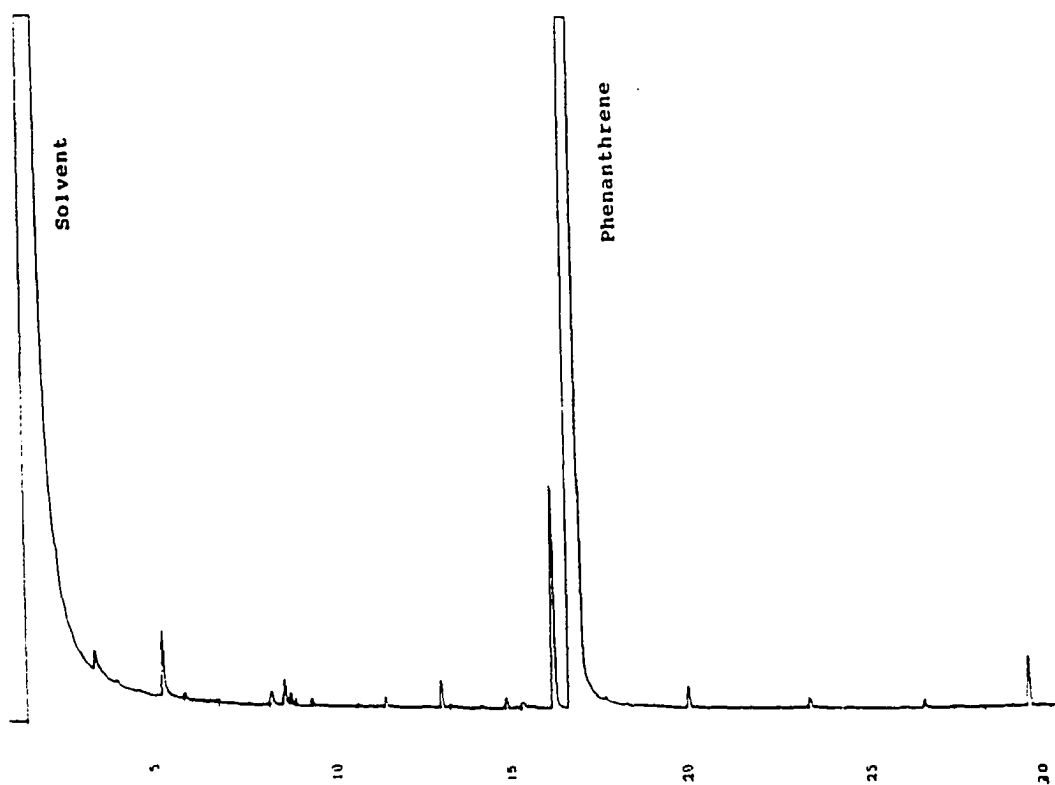


Figure #C6: Sample Gas Chromatography Plot of a Phenanthrene Control
(No Sonic) Reaction Mixture - FID Detector

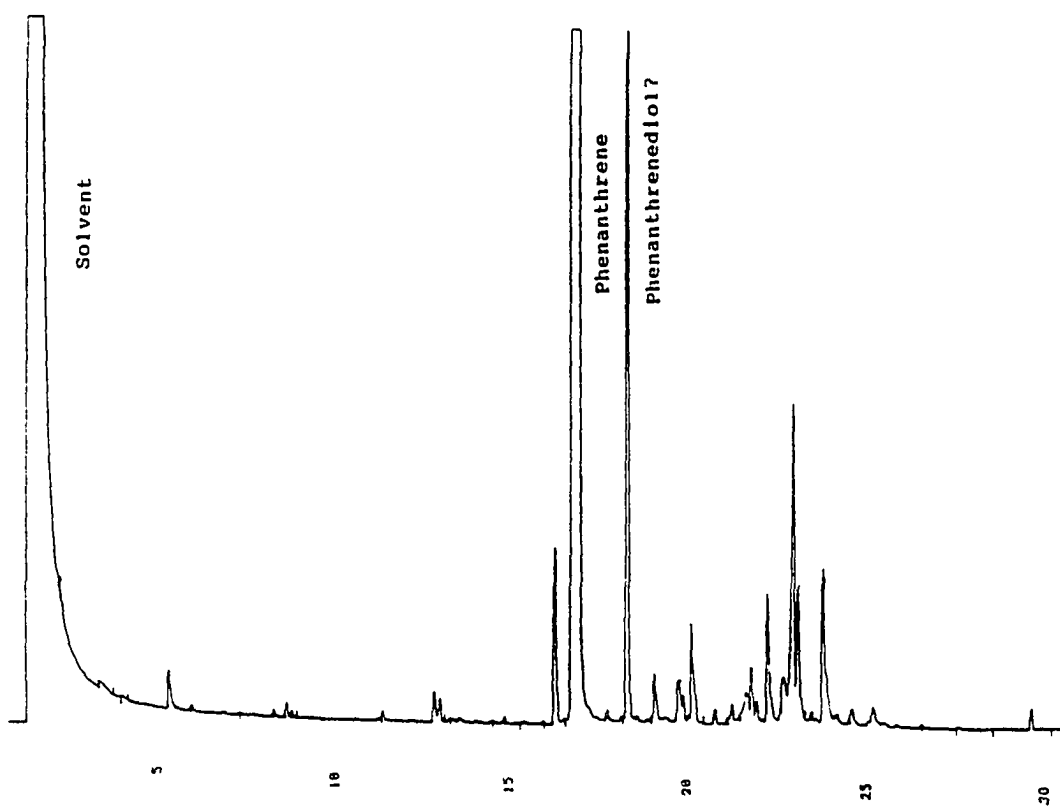


Figure #C7: Sample Gas Chromatography Plot of Phenanthrene Ultrasonic Reaction Mixture - FID Detector

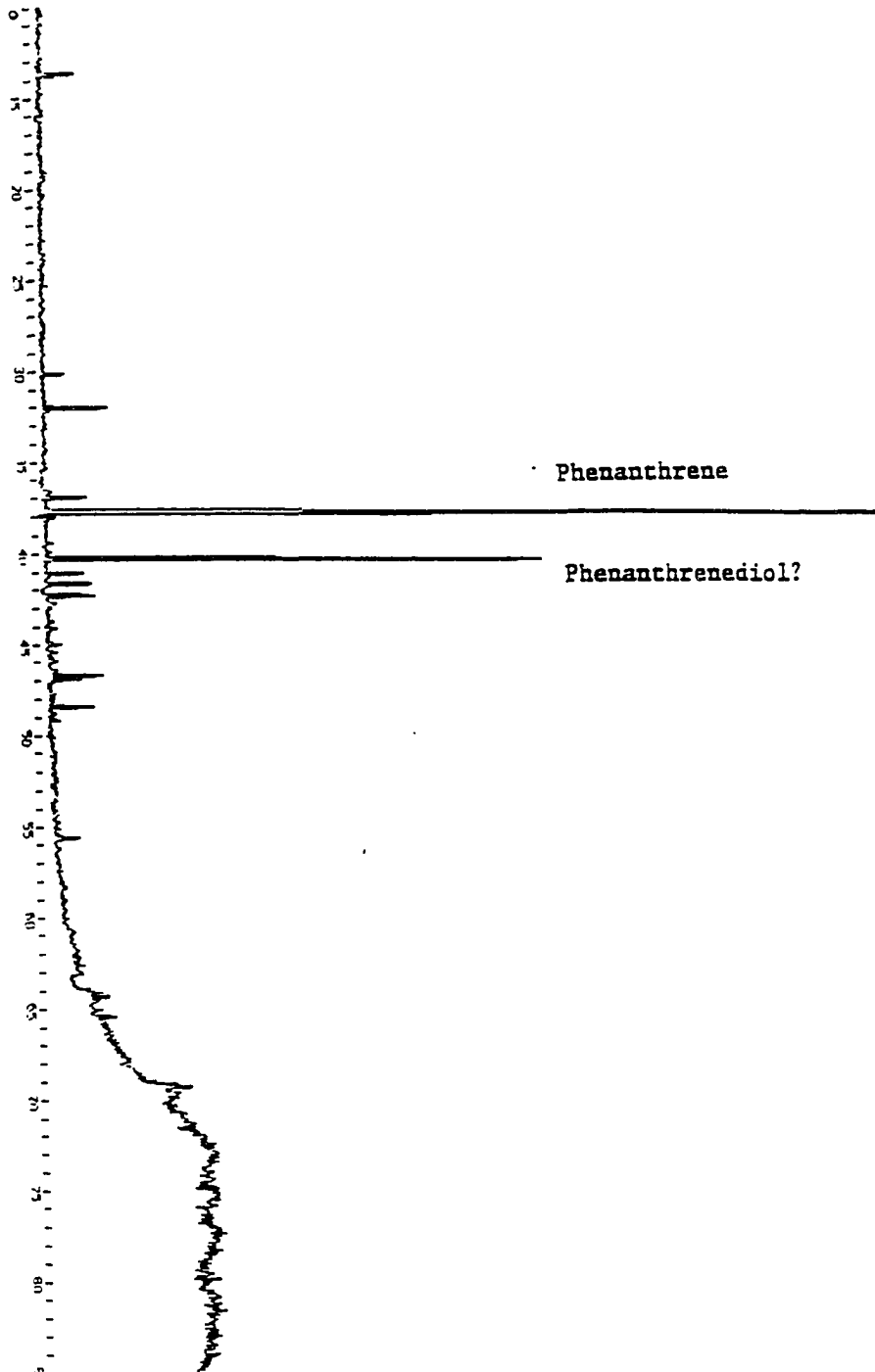


Figure #C8: Ion Chromatogram of Phenanthrene Ultrasonic Reaction Mixture

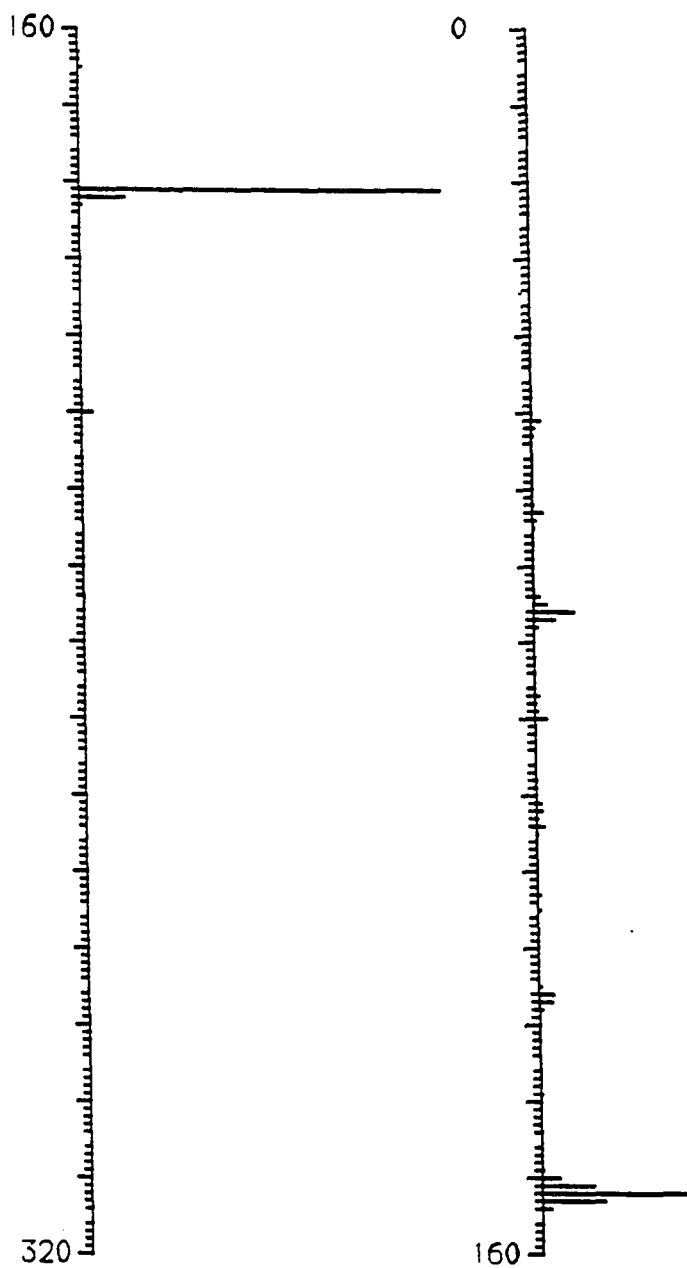


Figure #C9: Mass Spectrum of Phenanthrene Ultrasonic Reaction Product at 40.28 Minutes (Figure #C8)

Table #C7: Mass Spectrum of Phenanthrene Reaction Product With Retention Time of 40.28 Minutes

| Mass Number | Ion Abundance (Threshold 1%) |
|-------------|------------------------------|
| 77.0 | 6.2 |
| 78.1 | 1.3 |
| 87.0 | 1.3 |
| 90.5 | 3.4 |
| 101.0 | 1.5 |
| 102.0 | 1.7 |
| 104.1 | 2.1 |
| 115.1 | 1.2 |
| 125.1 | 1.1 |
| 126.1 | 4.5 |
| 127.1 | 3.8 |
| 150.1 | 5.2 |
| 151.1 | 14.8 |
| 152.2 | 41.2 |
| 153.1 | 17.5 |
| 154.2 | 2.6 |
| 165.2 | 1.6 |
| 181.2 | 100.0 |
| 182.2 | 14.1 |
| 183.2 | 1.2 |
| 210.2 | 3.3 |

Appendix D: Supplemental Experimental Data - Chemical Alteration

This section contains data from a series of experiments designed to demonstrate chemical alteration of polycyclic aromatic hydrocarbons (PAHs) in aqueous solution with high intensity ultrasound.

Gas chromatography peak areas were obtained as a direct output from the Perkin Elmer chromatographic data station. The peak area of the "parent compound" is that of the unreacted starting product, either biphenyl or phenanthrene. The total reaction product peak area was obtained for reactions in which biphenyl was utilized, by first obtaining the total area of GC peaks (retention time equal to 10 mins to 22 mins) in the spectrum from the control run spectrum. In the next step the area of GC peaks over the same time interval (10 to 22 mins) in the spectrum from the sonic treatment run were ascertained. The total peak areas from the sonic and control (no sonic) runs were then normalized using their solvent peak areas to minimize the variation due to injection volume. Finally, the normalized total product area from the control run is subtracted from the total product area from the sonic run; resulting in a corrected total reaction product peak area. In schematic form:

| Sonic Total Reaction Product (-) GC Peak Area | Normalized Control Total Reaction Product (=) GC Peak Area | Corrected Sonic Total Reaction Product GC Peak Area |
|---|--|---|
|---|--|---|

A similar operation was performed for phenanthrene reactions, however, the area of GC peaks from 17.5 minutes to 26 minutes were utilized for this compound. In general, the magnitude of the peak area corrections for both biphenyl and phenanthrene were small because of the lack of measurable impurity peak areas in the control reaction mixture spectrums. Small impurity peak areas were the direct result of the use of high purity solvents and chemicals.

Sample GC spectra of biphenyl and phenanthrene control (no sonic) reaction mixtures are presented in figures #D1 and #D3 below. Similarly, GC spectra of biphenyl and phenanthrene sonic treatment reaction mixtures are presented in figures #D2 and #D4 below.

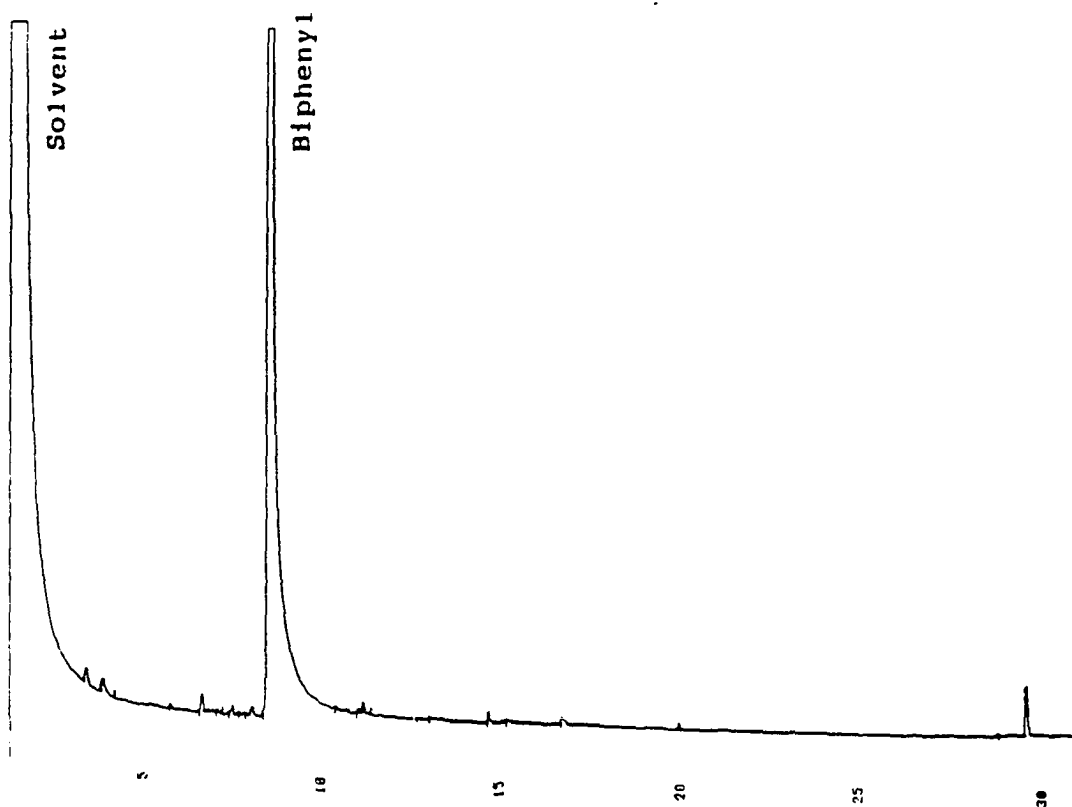


Figure #D1: Gas Chromatography Plot of Biphenyl Control (No Sonic) Reaction Mixture - (FID) Detector

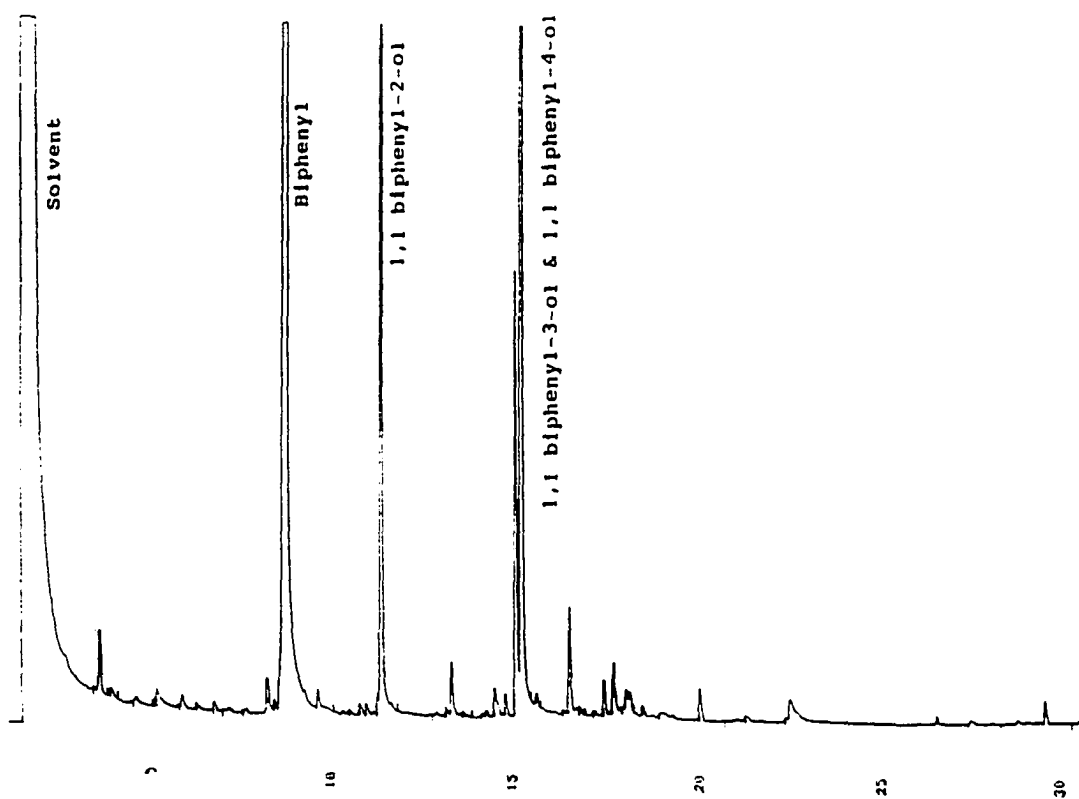


Figure #D2: Gas Chromatography Plot of Biphenyl Ultrasonic Reaction Mixture - (FID) Detector

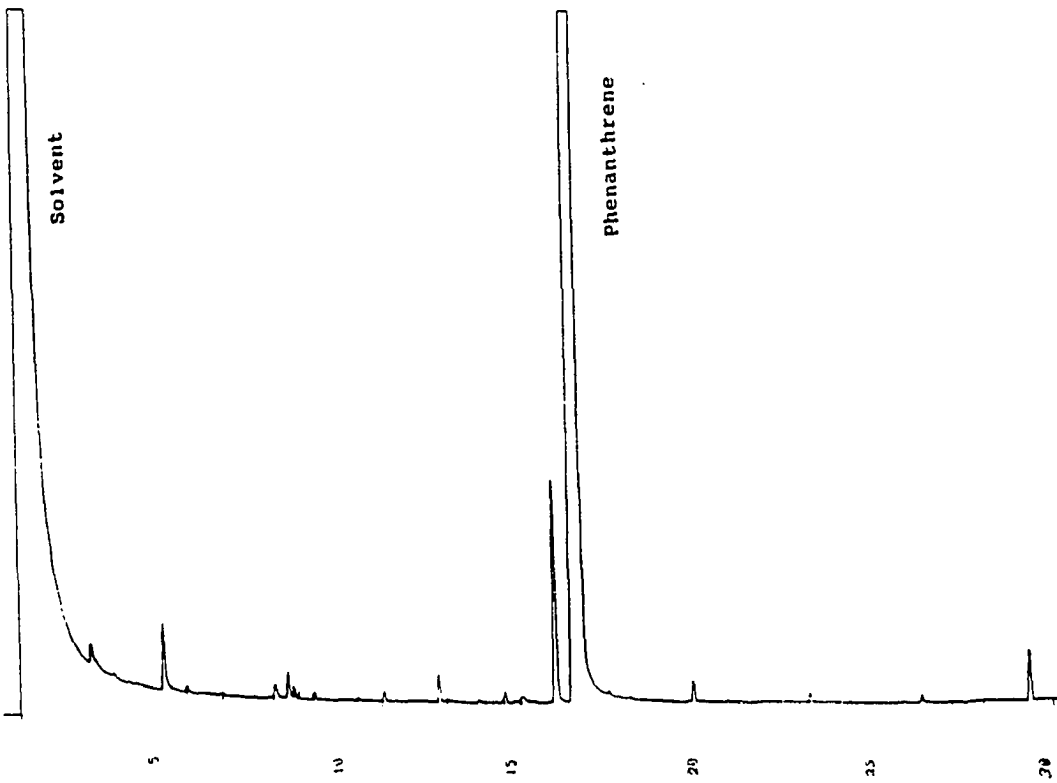


Figure #D3: Gas Chromatography Plot of Phenanthrene Control
(No Sonic) Reaction mixture - (FID) Detector

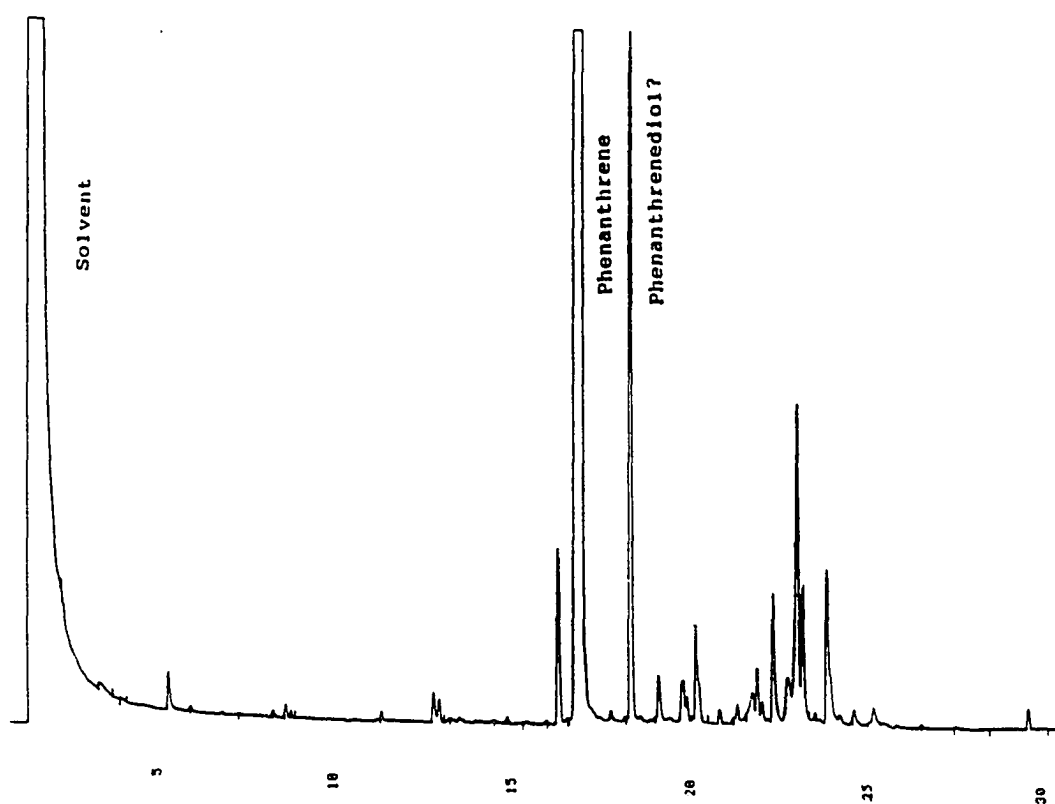


Figure #D4: Gas Chromatography Plot of Phenanthrene
Ultrasonic Reaction Mixture - (FID) Detector

The results obtained from three or more separate experimental trials were averaged to obtain parent hydrocarbon GC peak areas, reaction product GC peak areas, and the ratio of parent GC peak area to total reaction product GC peak areas at each indicated time along the x-axis (See figures D5-D22 below). A statistical analysis was performed on the three or more data points at each individual total reaction time interval (20, 40, 80, and 120 minutes) and confidence intervals at the 90% confidence level were constructed. The statistical analysis involved calculating the mean (avg value) plus or minus (+/-) an interval value (B-value) using the relationship (Borland, 1990):

$$\text{Confidence interval} = \text{Average} \pm (T) \left(\frac{\text{variance}}{n} \right)^{0.5}$$

where:

$$\text{variance} = (X_1 - \text{Average})^2 + \dots + (X_n - \text{Average})^2$$

n = number of samples

X_n = nth sample value

Avg = (sum X_j) / n, and

The values of "T" were obtained from a student "t" table of values at the 90% confidence interval (Kitchens, 1987). For data sets containing three values (n = 3) and two degrees of freedom the value of "T" is 2.92. A value for "T" of 2.353, derived from the same source, is used as a

multiplier if four trials (3 degrees of freedom) were performed.

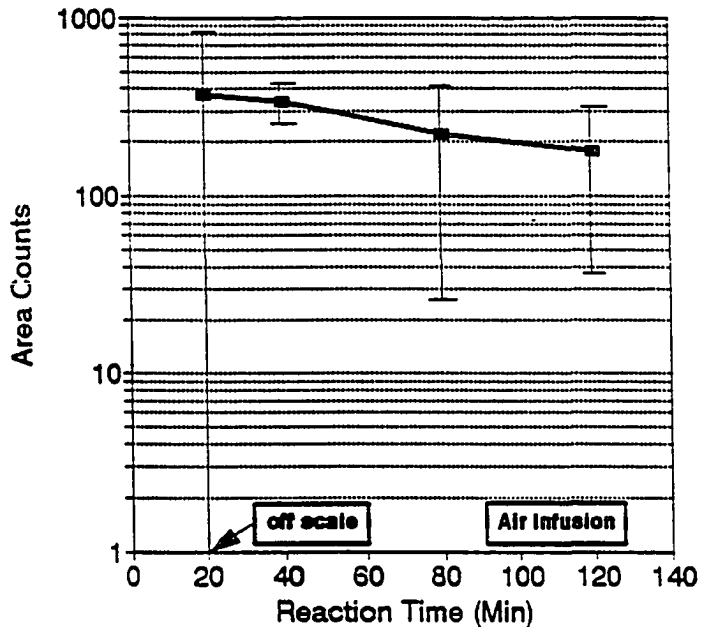


Figure #D5: Average Biphenyl Gas Chromatography Peak Area vs Total Reaction Time (90% Confidence Interval Data) - Air Infusion

Table #D1: Average Biphenyl GC Peak Area As a Function of Reaction Time 90% Confidence Interval Data - Air Infusion

| Time of Reaction (Min) | Low Interval Point | Average Biphenyl Peak Area <-(90% Confidence Interval)-> | High Interval Point |
|------------------------|--------------------|---|---------------------|
| 20 | -77.0056 | 370.2364 | 817.4783 |
| 40 | 256.2432 | 342.4236 | 428.6040 |
| 80 | 25.9275 | 221.9709 | 418.0143 |
| 120 | 38.2675 | 177.8575 | 317.4475 |

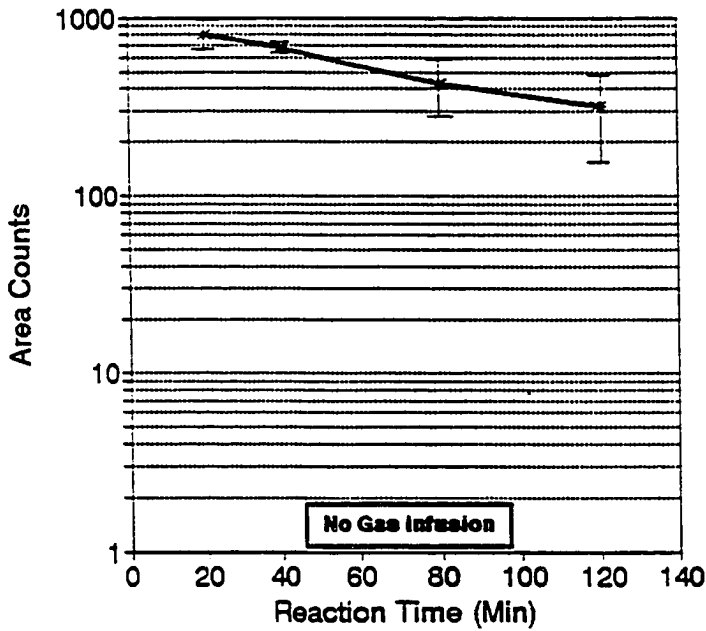


Figure #D6: Average Biphenyl Gas Chromatography Peak Area vs Total Reaction Time (90% Confidence Interval Data) - No Gas Infusion

Table #D2: Average Biphenyl Peak Area As a Function of Reaction Time 90% Confidence Interval Data - No Gas Infusion

| Time of Reaction (Min) | Low Interval Point | Average Biphenyl Peak Area <-(90% Confidence Interval)-> | High Interval Point |
|------------------------|--------------------|---|---------------------|
| 20 | 675.6075 | 816.5084 | 957.4093 |
| 40 | 630.1293 | 679.1931 | 728.2569 |
| 80 | 283.7144 | 428.1727 | 572.6310 |
| 120 | 154.6958 | 319.8606 | 485.0254 |

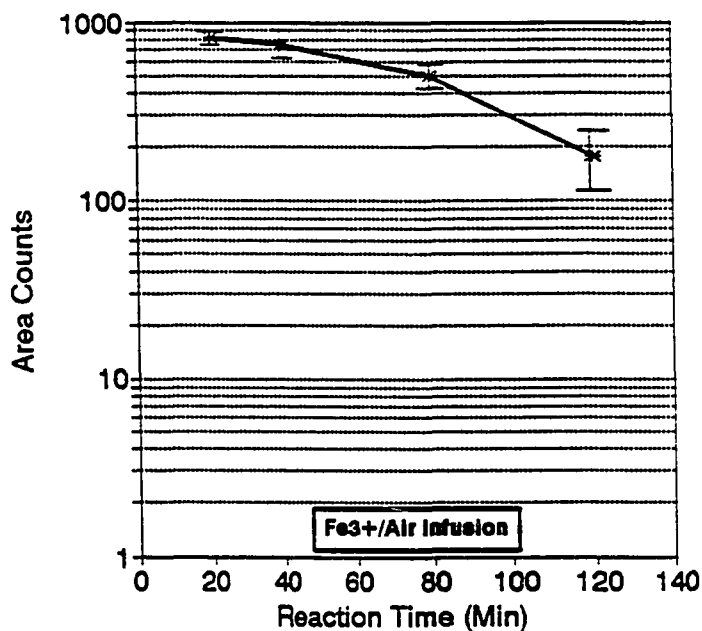


Figure #D7: Average Biphenyl Gas Chromatography Peak Area vs Total Reaction Time (90% Confidence Interval Data) - Fe³⁺/Air Infusion

Table #D3: Average Biphenyl GC Peak Area As a Function of Reaction Time 90% Confidence Interval Data - Fe³⁺/Air Infusion

| Time of Reaction (Min) | Low Interval Point | Average Biphenyl Peak Area <-(90% Confidence Interval)-> | High Interval Point |
|------------------------|--------------------|---|---------------------|
| 20 | 763.2712 | 820.9691 | 878.6671 |
| 40 | 639.1826 | 756.3762 | 873.5697 |
| 80 | 421.2414 | 499.8627 | 578.4840 |
| 120 | 115.1698 | 178.6493 | 242.1288 |

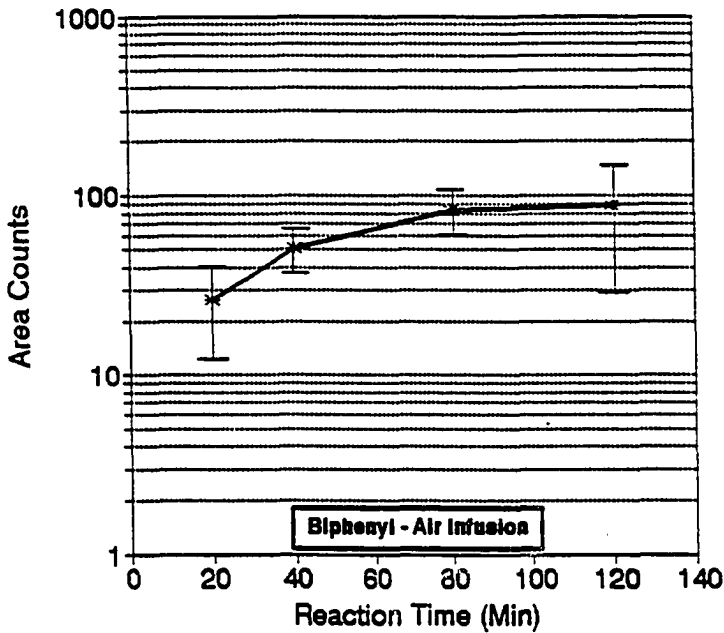


Figure #D8: Average Total Biphenyl Reaction Product Gas Chromatography Peak Area vs Total Reaction Time (90% Confidence Interval Data) - Air Infusion

Table #D4: Average Total Biphenyl Reaction Product Area As a Function of Reaction Time - 90% Confidence Interval Data - Air Infusion

| Time of Reaction (Min) | Low Interval Point | Average Total Biphenyl Reaction Product Peak Area <-(90% Confidence Interval)-> | High Interval Point |
|------------------------|--------------------|--|---------------------|
| 20 | 12.4599 | 26.5593 | 40.6587 |
| 40 | 37.7908 | 50.8771 | 63.9634 |
| 80 | 60.9329 | 82.8731 | 104.8132 |
| 120 | 29.1490 | 88.1293 | 54.1000 |

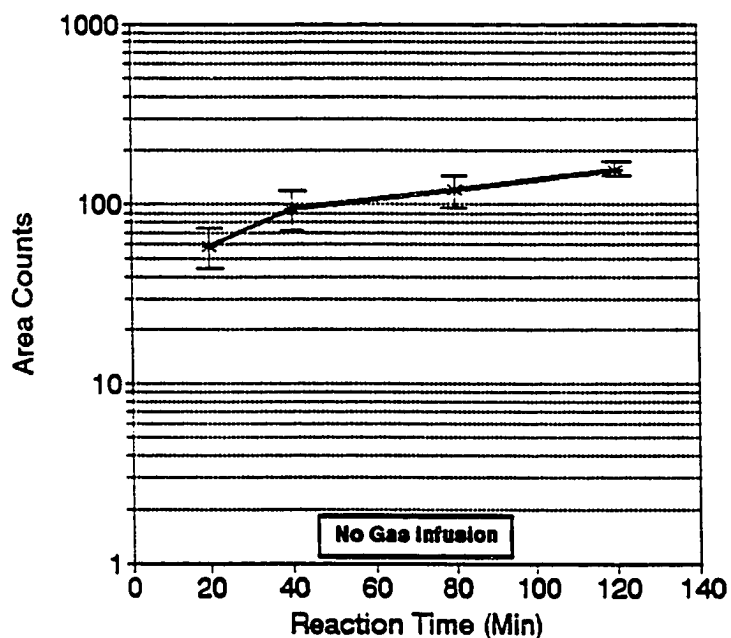


Figure #D9: Average Total Biphenyl Reaction Product Gas Chromatography Peak Area vs Total Reaction Time (90% Confidence Interval Data) - No Gas Infusion

Table #D5: Average Total Biphenyl Reaction Product Peak Area As a Function of Reaction Time - 90% Confidence Interval Data - No Gas Infusion

| Time of Reaction (Min) | Low Interval Point | Average Total Biphenyl Reaction Product Peak Area <-(90% Confidence Interval)-> | High Interval Point |
|------------------------|--------------------|--|---------------------|
| 20 | 44.0410 | 58.7495 | 73.4579 |
| 40 | 72.6402 | 94.9210 | 117.2018 |
| 80 | 98.0891 | 120.6609 | 143.2326 |
| 120 | 145.2436 | 156.6924 | 168.1412 |

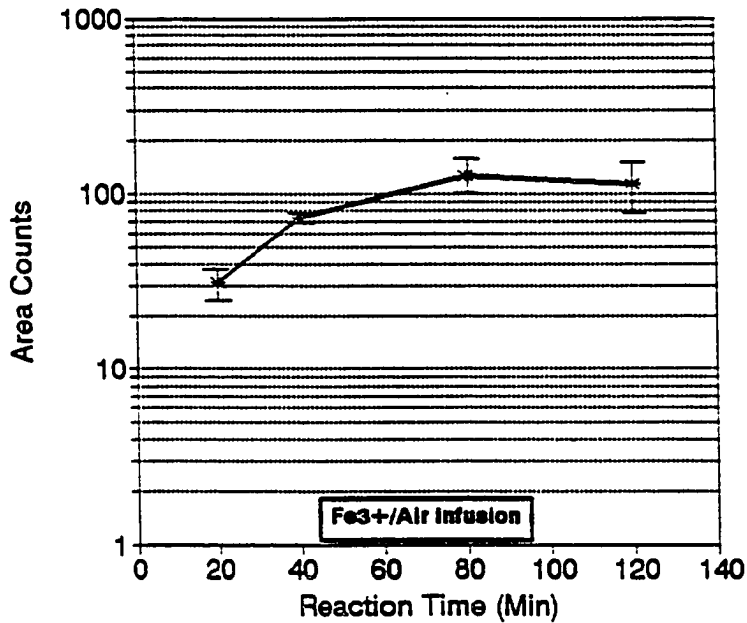


Figure #D10: Average Total Biphenyl Reaction Product Gas Chromatography Peak Area vs Total Reaction Time (90% Confidence Interval Data) - Fe³⁺/Air Infusion

Table #D6: Average Total Biphenyl Reaction Product Peak Area As a Function of Reaction Time - 90% Confidence Interval Data - Fe³⁺/Air Infusion

| Time of Reaction (Min) | Low Interval Point | Average Total Biphenyl Reaction Product Peak Area <-(90% Confidence Interval)-> | High Interval Point |
|------------------------|--------------------|--|---------------------|
| 20 | 24.8740 | 31.2037 | 37.5334 |
| 40 | 68.8274 | 73.3696 | 77.9118 |
| 80 | 100.8339 | 126.1836 | 151.5333 |
| 120 | 77.8951 | 113.8275 | 149.7599 |

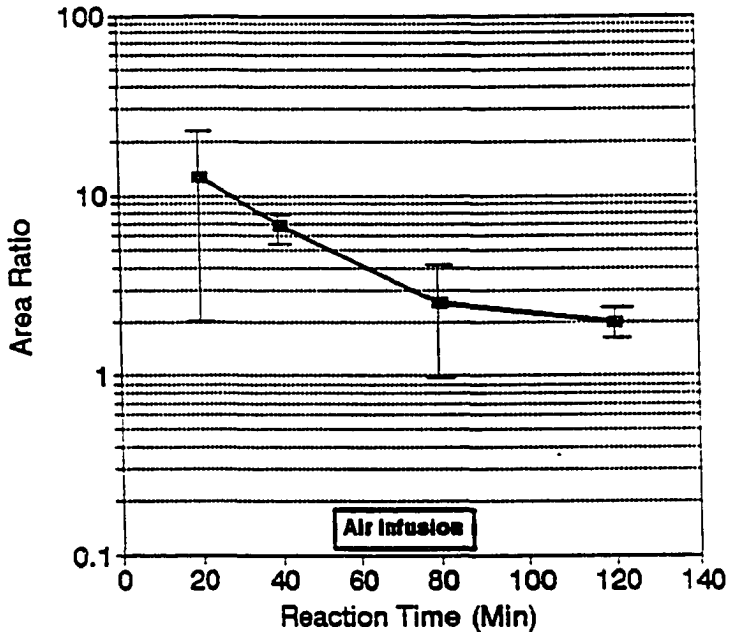


Figure #D11: Average Ratio of Biphenyl GC Peak Area to Total Biphenyl Reaction Product Gas Chromatography Peak Area vs Total Reaction Time (90% Confidence Interval Data) - Air Infusion

Table #D7: Average Ratio of Biphenyl Peak Area To Corrected Total Product Peak Area as a Function of Reaction Time - 90% Confidence Interval Data - Air Infusion

| Time of Reaction (Min) | Low Interval Point | Average Ratio of Biphenyl Area To Corrected Total Product Area <-(90% Confidence Interval)-> | High Interval Point |
|------------------------|--------------------|--|---------------------|
| 20 | 2.0662 | 12.5624 | 23.0585 |
| 40 | 5.4842 | 6.7776 | 8.0711 |
| 80 | 0.9765 | 2.5491 | 4.1218 |
| 120 | 1.6188 | 2.0188 | 2.4188 |

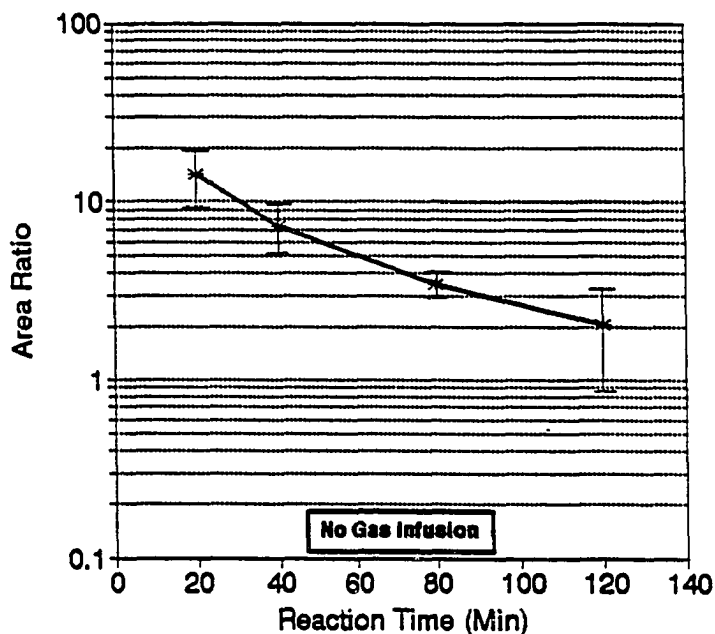


Figure #D12: Average Ratio of Biphenyl GC Peak Area to Total Biphenyl Reaction Product Gas Chromatography Peak Area vs Total reaction Time (90% Confidence Interval Data) - No Gas Infusion

Table #D8: Average Ratio of Biphenyl Peak Area To Corrected Total Product Peak Area as a Function of Reaction Time - 90% Confidence Interval Data - No Gas Infusion

| Time of Reaction (Min) | Low Interval Point | Average Ratio of Biphenyl Area To Corrected Total Product Area <-(90% Confidence Interval)-> | High Interval Point |
|------------------------|--------------------|--|---------------------|
| 20 | 9.3448 | 14.2739 | 19.2031 |
| 40 | 5.0698 | 7.3429 | 9.6159 |
| 80 | 3.0055 | 3.5154 | 4.0253 |
| 120 | 0.8624 | 2.0670 | 3.2716 |

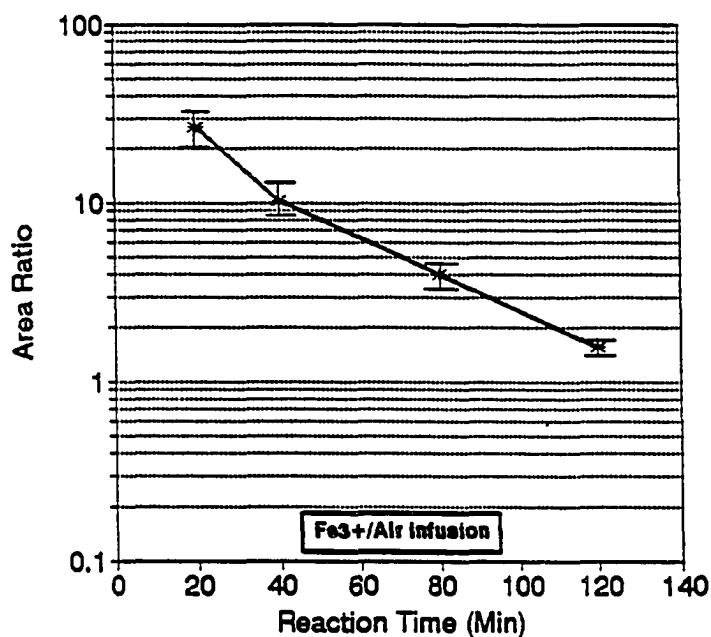


Figure #D13: Average Ratio of Biphenyl GC Peak Area to Total Biphenyl Reaction Product Gas Chromatography Peak Area vs Total reaction Time (90% Confidence Interval Data) - Fe³⁺/Air Infusion

Table #D9: Average Ratio of Biphenyl Peak Area To Corrected Total Product Peak Area as a Function of Reaction Time - 90% Confidence Interval Data - Fe³⁺/Air Infusion

```
=====
```

| Time of Reaction (Min) | Low Interval Point | Average Ratio of Biphenyl Area To Corrected Total Product Area <-(90% Confidence Interval)-> | High Interval Point |
|------------------------|--------------------|--|---------------------|
| 20 | 20.7050 | 26.7251 | 32.7451 |
| 40 | 8.3101 | 10.3452 | 12.3804 |
| 80 | 3.4137 | 3.9896 | 4.5654 |
| 120 | 1.4046 | 1.5648 | 1.7251 |

```
=====
```

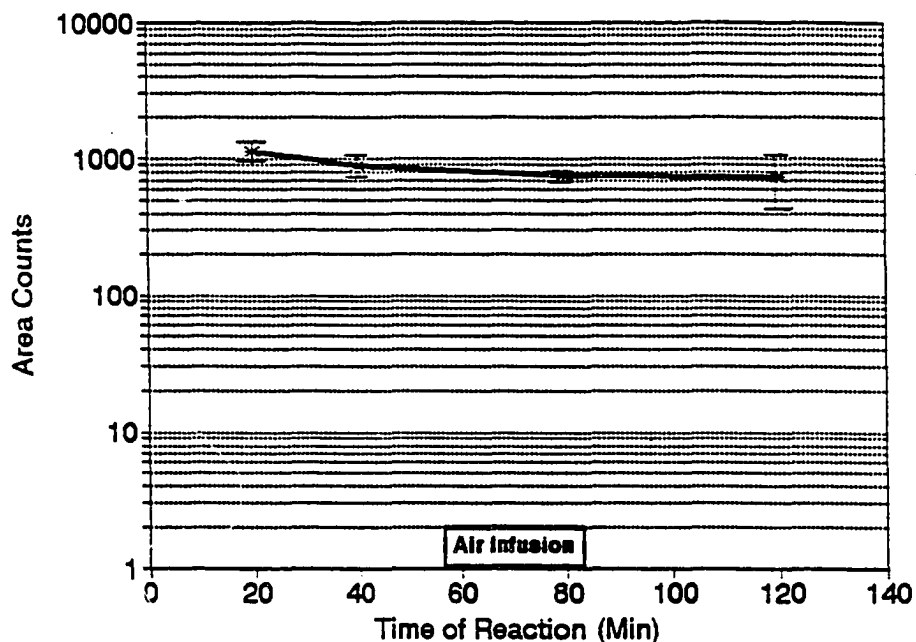



Figure #D14: Average Phenanthrene Gas Chromatography Peak Area vs Total Reaction Time (90% Confidence Interval Data) - Air Infusion

Table #D10: Average Phenanthrene Peak Area As a Function of Total Reaction Time - 90% Confidence Interval - Air Infusion

| Time of Reaction (Min) | Low Interval Point | Phenanthrene Peak Area <-(90% Confidence Interval)-> | High Interval Point |
|------------------------|--------------------|---|---------------------|
| 20 | 954.3165 | 1127.6972 | 1301.0779 |
| 40 | 728.8306 | 876.6912 | 1024.5317 |
| 80 | 666.7884 | 743.6126 | 820.4368 |
| 120 | 411.5736 | 736.4102 | 1061.2468 |

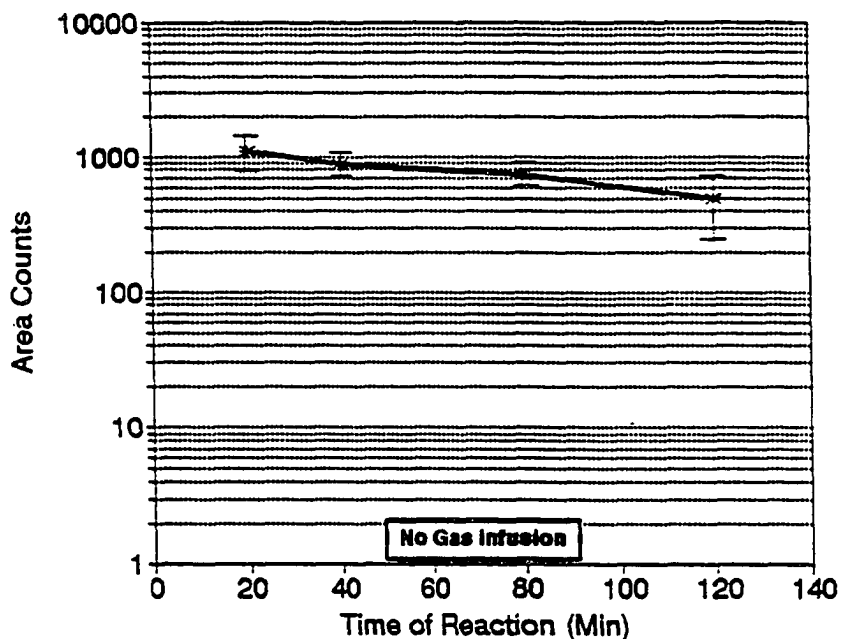


Figure #D15: Average Phenanthrene Gas Chromatography Peak Area vs Total Reaction Time (90% Confidence Interval Data) - No Gas Infusion

Table #D11: Average Phenanthrene Peak Area As a Function of Total Reaction Time - 90% Confidence Interval - No Gas Infusion

| Time of Reaction (Min) | Low Interval Point | Phenanthrene Peak Area <-(90% Confidence Interval)-> | High Interval Point |
|------------------------|--------------------|---|---------------------|
| 20 | 777.1089 | 1105.7167 | 1434.3245 |
| 40 | 712.2468 | 875.0824 | 1037.9180 |
| 80 | 600.8499 | 756.8144 | 912.7789 |
| 120 | 249.5168 | 487.8547 | 726.1926 |

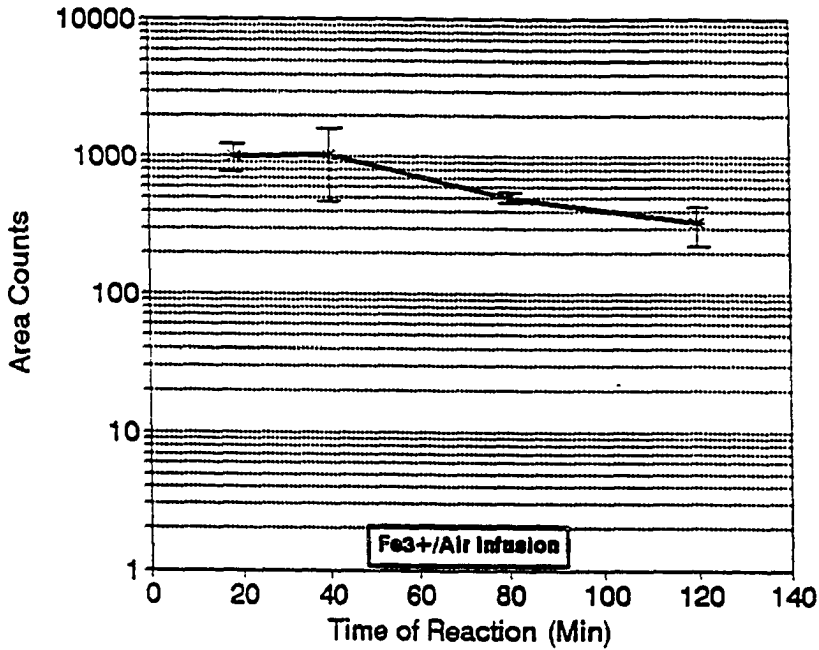


Figure #D16: Average Phenanthrene Gas Chromatography Peak Area vs Total Reaction Time (90% Confidence Interval Data) - Fe³⁺/Air Infusion

Table #D12: Average Phenanthrene Peak Area As a Function of Total Reaction Time - 90% Confidence Interval - Air/Fe³⁺ Infusion

| Time of Reaction (Min) | Low Interval Point | Phenanthrene Peak Area <-(90% Confidence Interval)-> | High Interval Point |
|------------------------|--------------------|---|---------------------|
| 19 | 753.8686 | 998.0526 | 1242.2366 |
| 40 | 455.3174 | 1023.0012 | 1590.6850 |
| 80 | 475.7557 | 504.9575 | 534.1593 |
| 120 | 245.8434 | 329.1208 | 412.3982 |

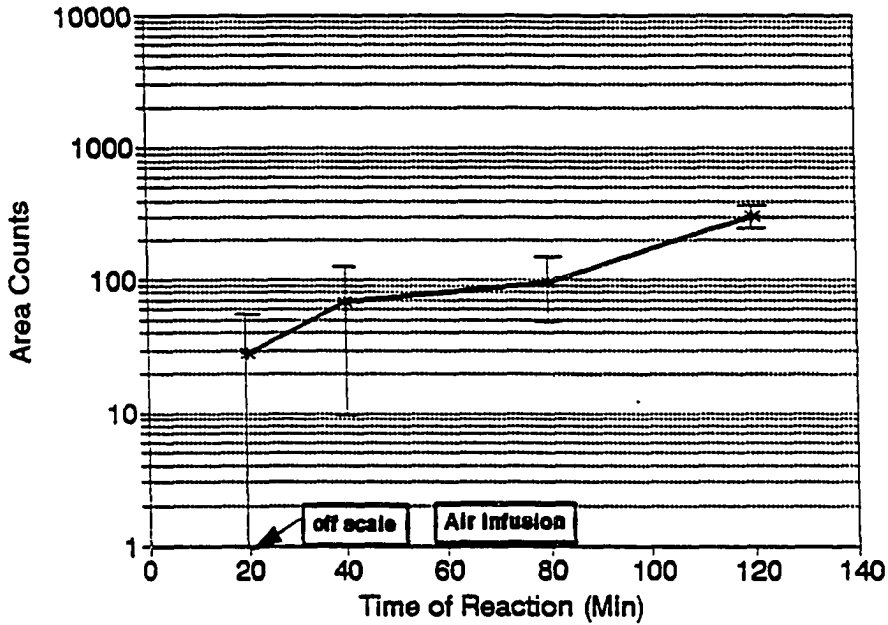


Figure #D17: Average Total Phenanthrene Reaction Product Gas Chromatography Peak Area vs Total Reaction Time (90% Confidence Interval Data) - Air Infusion

Table #D13: Average Phenanthrene Product Peak Area As a Function of Total Reaction Time - 90% Confidence Interval - Air Infusion

| Time of Reaction (Min) | Low Interval Point | Total Corrected Phenanthrene Reaction Product Peak Area <-(90% Confidence Interval)-> | High Interval Point |
|------------------------|--------------------|--|---------------------|
| 20 | 0.9047 | 28.1206 | 55.3366 |
| 40 | 9.6477 | 69.2893 | 128.9309 |
| 80 | 48.8457 | 97.4664 | 146.0871 |
| 120 | 242.7935 | 305.2338 | 367.6742 |

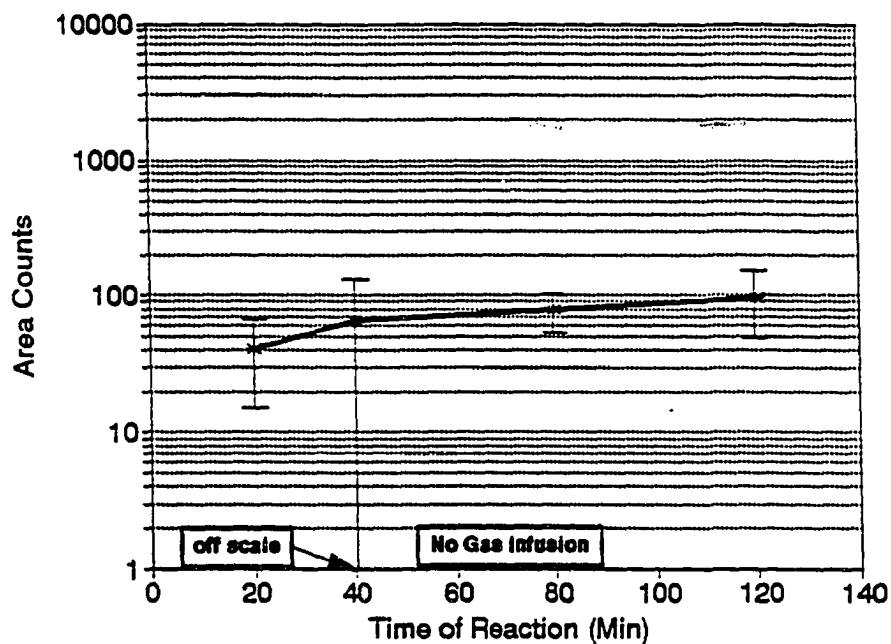


Figure #D18: Average Total Phenanthrene Reaction Product Gas Chromatography Peak Area vs Total Reaction Time (90% Confidence Interval Data) No Gas Infusion

Table #D14: Average Phenanthrene Product Peak Area As a Function of Total Reaction Time - 90% Confidence Interval - No Gas Infusion

| Time of Reaction (Min) | Low Interval Point | Total Corrected Phenanthrene Reaction Product Peak Area <-(90% Confidence Interval)-> | High Interval Point |
|------------------------|--------------------|--|---------------------|
| 20 | 15.0308 | 41.2518 | 67.4728 |
| 40 | -1.2342 | 65.7042 | 132.6425 |
| 80 | 54.7516 | 77.6083 | 100.4649 |
| 120 | 48.6187 | 97.2983 | 145.9779 |

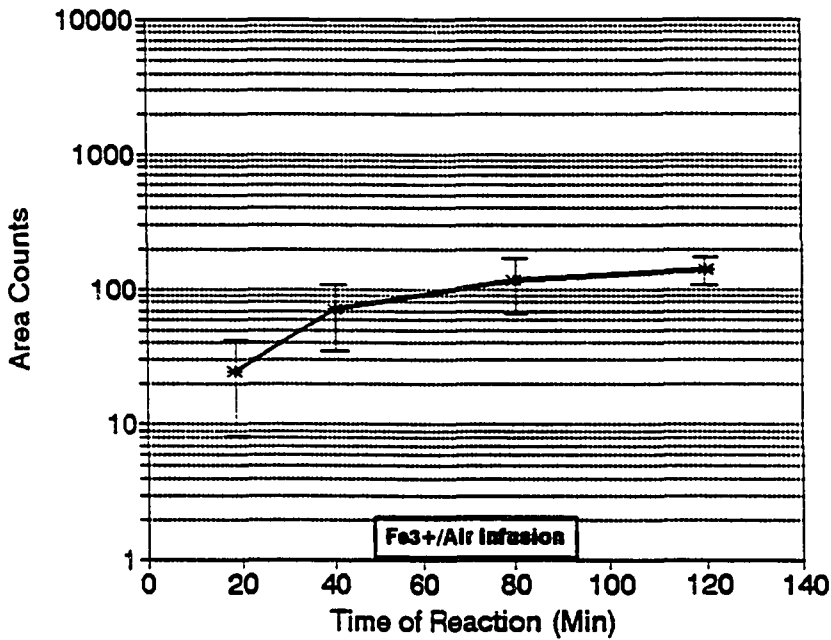


Figure #D19: Average Total Phenanthrene Reaction Product Gas Chromatography Peak Area vs Total Reaction Time (90% Confidence Interval Data) Fe³⁺/Air Infusion

Table #D15: Average Phenanthrene Product Peak Area As a Function of Total Reaction Time - 90% Confidence Interval - Fe³⁺/Air Infusion

| Time of Reaction (Min) | Low Interval Point | Total Corrected Phenanthrene Reaction Product Peak Area <-(90% Confidence Interval)-> | High Interval Point |
|------------------------|--------------------|--|---------------------|
| 19 | 8.1053 | 24.3714 | 40.6374 |
| 40 | 34.1273 | 71.8015 | 109.4758 |
| 80 | 67.2478 | 117.9928 | 168.7377 |
| 120 | 115.1407 | 141.7711 | 168.4015 |

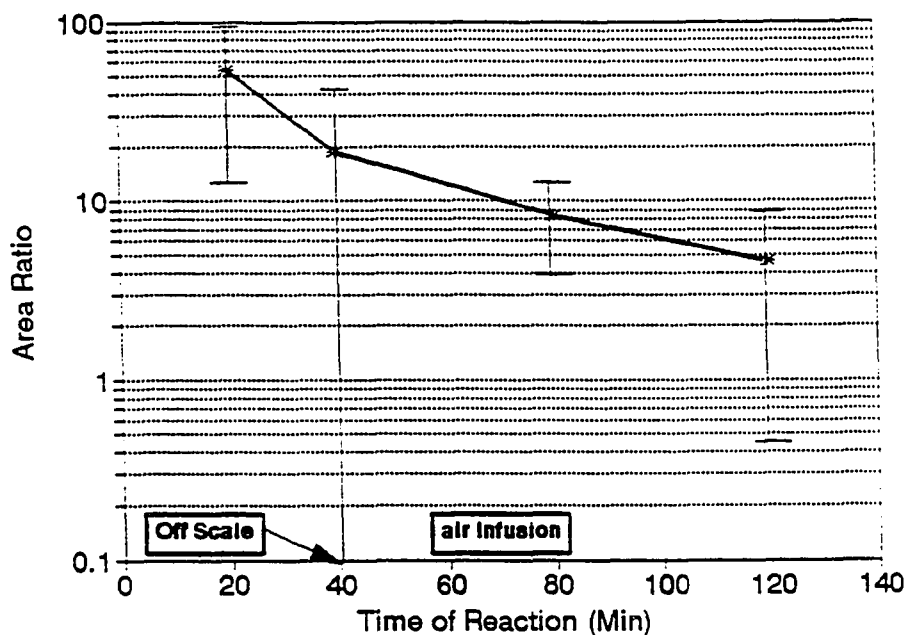


Figure #D20: Average Ratio of Phenanthrene GC Peak Area to Total Phenanthrene Reaction Product Gas Chromatography Peak Area vs Total Reaction Time (90% Confidence Interval Data) - Air Infusion

Table #D16: Average Ratio of Phenanthrene Peak Area to Total Reaction Product Area As Function of Total Reaction Time - 90% Confidence Interval Data - Air Infusion

| Time of Reaction (Min) | Low Interval Point | Average Ratio Phenanthrene Area To Total Product Area <-(90% Confidence Interval)-> | High Interval Point |
|------------------------|--------------------|--|---------------------|
| 20 | 12.7564 | 54.2202 | 95.6840 |
| 40 | -3.4981 | 18.8664 | 41.2308 |
| 80 | 4.0294 | 8.3243 | 12.6192 |
| 120 | 0.4528 | 4.6351 | 8.8174 |

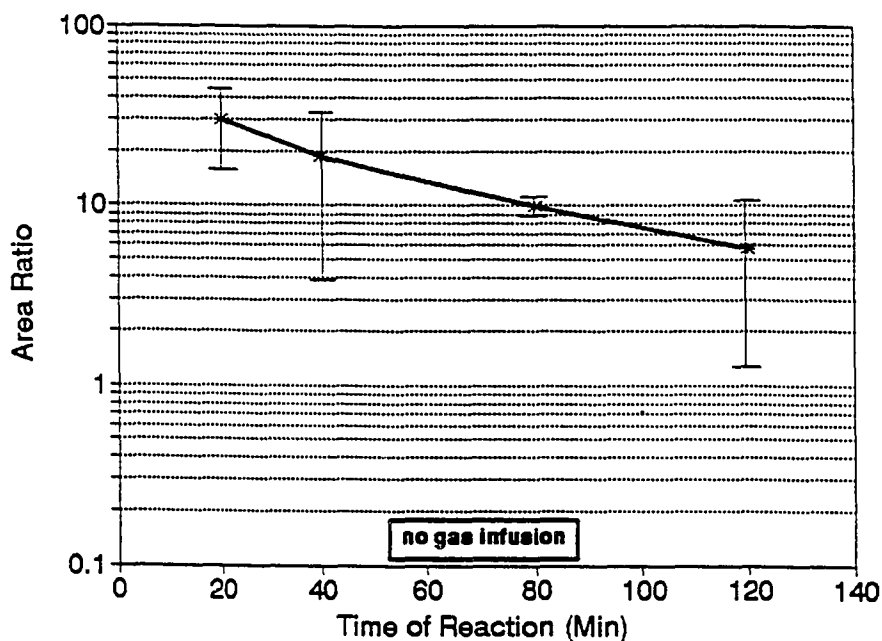


Figure #D21: Average Ratio of Phenanthrene GC Peak Area to Total Phenanthrene Reaction Product Gas Chromatography Peak Area vs Total Reaction Time (90% Confidence Interval Data) No Gas Infusion

Table #D17: Average Ratio of Phenanthrene Peak Area to Total Reaction Product Area As Function of Total Reaction Time - 90% Confidence Interval Data - No Gas Infusion

| Time of Reaction (Min) | Low Interval Point | Average Ratio Phenanthrene Area To Total Product Area <-(90% Confidence Interval)-> | High Interval Point |
|------------------------|--------------------|--|---------------------|
| 20 | 15.9523 | 29.8637 | 43.7752 |
| 40 | 3.8078 | 18.5926 | 33.3774 |
| 80 | 8.7787 | 9.8428 | 10.9068 |
| 120 | 1.3003 | 5.8012 | 10.3020 |

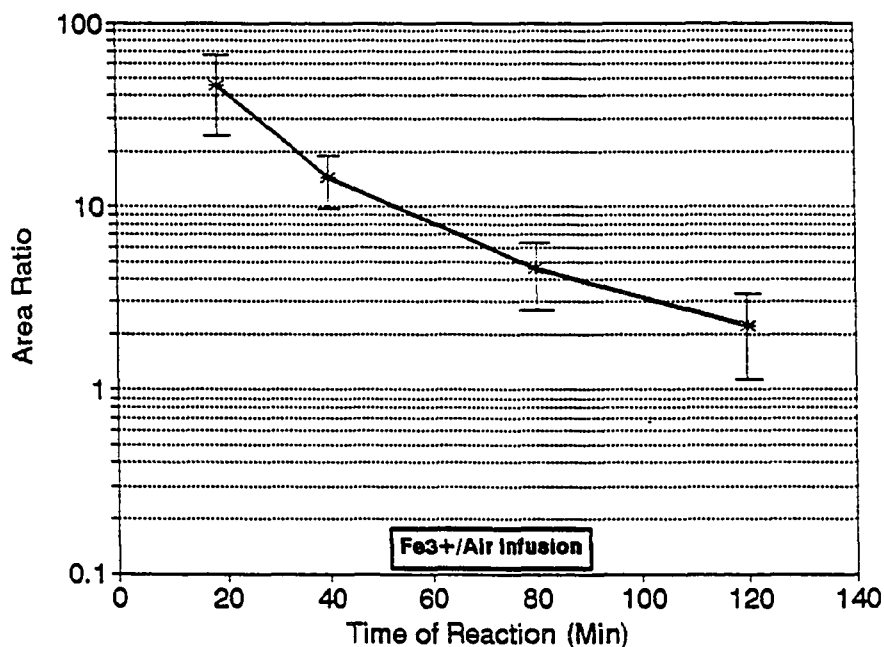


Figure #D22: Average Ratio of Phenanthrene GC Peak Area to Total Phenanthrene Reaction Product Gas Chromatography Peak Area vs Total Reaction Time (90% Confidence Interval Data) Fe³⁺/Air Infusion

Table #D18: Average Ratio of Phenanthrene Peak Area to Total Reaction Product Area As Function of Total Reaction Time - 90% Confidence Interval Data - Fe³⁺/Air Infusion

| Time of Reaction (Min) | Low Interval Point | Average Ratio Phenanthrene Area To Total Product Area <-(90% Confidence Interval)-> | High Interval Point |
|------------------------|--------------------|---|---------------------|
| 19 | 24.0905 | 45.7123 | 67.3341 |
| 40 | 9.9043 | 14.4581 | 19.0119 |
| 80 | 2.7250 | 4.5484 | 6.3718 |
| 120 | 1.3765 | 2.2489 | 3.1213 |

Appendix E: Supplemental Experimental Data - Radioisotope Studies

This section contains tabular and graphical data derived from a number of desorption experiments outlined in table E1.

Table #E1 : Overview of Desorption Experiments

| Experiment # | Contaminant ID | Substrate ID |
|--|----------------------------------|---------------|
| Radiation Experiment #1 Trial #1 (Rad #1 - Trial #1) | Phenanthrene (Sonic) | Active Carbon |
| Radiation Experiment #1 Trial #2 (Rad #1 - Trial #2) | Phenanthrene (Sonic) | Active Carbon |
| Radiation Experiment #2 (Rad #2) | Phenanthrene (Sonic) | Sand |
| Radiation Experiment #3 (Rad #3) | Phenanthrene (Sonic) | Sand |
| Radiation Experiment #4 (Rad #4) | Biphenyl (Sonic) | Glass Beads |
| Radiation Experiment #5 (Rad #5) | Biphenyl (No Sonic-Control) | Glass Beads |
| Radiation Experiment #6 (Rad #6) | Biphenyl (Sonic) | Glass Beads |
| Radiation Experiment #7 (Rad #7) | Biphenyl (Sonic) | Glass Beads |
| Radiation Experiment #8 (Rad #8) | Biphenyl (No Sonic - Control) | Glass Beads |

E.1: Data from Active Carbon/⁹⁻¹⁴C Phenanthrene Experiment
(Radiation Experiment #1 - Rad #1)

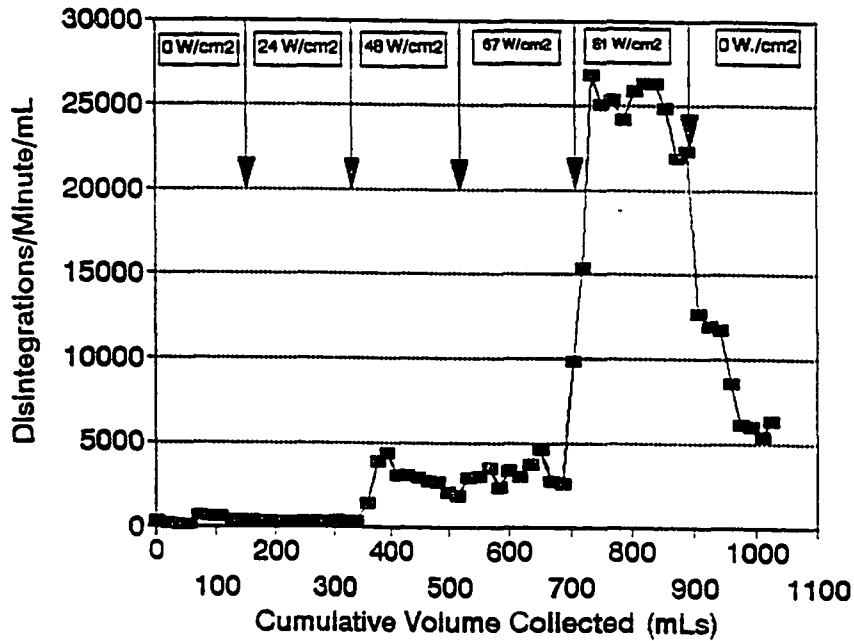


Figure #E1: Radiation Experiment #1 (Rad #1) - First Trial -
Phenanthrene/Active Carbon - Sonic Treatment - Background
Corrected Disintegrations/Minute/Milliliter vs Cumulative
Sample Volume Collected at Indicated Probe Energy Level

Table #E2: Radiation Experiment #1 (Rad #1) - First Trial - Phenanthrene/ Active Carbon - Sonic Treatment - Background Corrected Disintegrations/Minute/Milliliter vs Cumulative Sample Volume Collected at Indicated Probe Energy Level

| Sample ID | Conditions | Cumulative Milliliters (mL) | H# and Background Corrected DPM/mL |
|-----------|----------------|-----------------------------|------------------------------------|
| 1 A | 0 Watts/Sq Cm | 2.3 | 394 |
| 2 A | 0 Watts/Sq Cm | 20.2 | 193 |
| 3 A | 0 Watts/Sq Cm | 38.1 | 155 |
| 4 A | 0 Watts/Sq Cm | 54.9 | 125 |
| 5 A | 0 Watts/Sq Cm | 72.7 | 726 |
| 6 A | 0 Watts/Sq Cm | 90.5 | 638 |
| 7 A | 0 Watts/Sq Cm | 108.4 | 578 |
| 8 A | 0 Watts/Sq Cm | 126.2 | 448 |
| 9 A | 0 Watts/Sq Cm | 144.0 | 415 |
| 10 A | 0 Watts/Sq Cm | 161.8 | 425 |
| 11 A | 24 Watts/Sq Cm | 179.8 | 361 |
| 12 A | 24 Watts/Sq Cm | 197.5 | 390 |
| 13 A | 24 Watts/Sq Cm | 215.2 | 373 |
| 14 A | 24 Watts/Sq Cm | 232.9 | 345 |
| 15 A | 24 Watts/Sq Cm | 250.6 | 313 |
| 16 A | 24 Watts/Sq Cm | 268.2 | 306 |
| 17 A | 24 Watts/Sq Cm | 285.9 | 326 |
| 18 A | 24 Watts/Sq Cm | 303.7 | 408 |
| 19 A | 24 Watts/Sq Cm | 321.6 | 305 |
| 20 A | 24 Watts/Sq Cm | 339.4 | 325 |
| 21 A | 41 Watts/Sq Cm | 357.5 | 1412 |
| 22 A | 41 Watts/Sq Cm | 375.3 | 3887 |
| 23 A | 41 Watts/Sq Cm | 392.9 | 4376 |
| 24 A | 41 Watts/Sq Cm | 410.9 | 3080 |
| 25 A | 41 Watts/Sq Cm | 428.3 | 3084 |
| 26 A | 41 Watts/Sq Cm | 445.7 | 2974 |
| 27 A | 41 Watts/Sq Cm | 463.0 | 2768 |
| 28 A | 41 Watts/Sq Cm | 480.2 | 2658 |
| 29 A | 41 Watts/Sq Cm | 497.5 | 2119 |
| 30 A | 41 Watts/Sq Cm | 514.5 | 1878 |
| 31 A | 67 Watts/Sq Cm | 531.9 | 2926 |
| 32 A | 67 Watts/Sq Cm | 548.9 | 3055 |
| 33 A | 67 Watts/Sq Cm | 566.3 | 3503 |
| 34 A | 67 Watts/Sq Cm | 583.4 | 2382 |
| 35 A | 67 Watts/Sq Cm | 600.5 | 3382 |
| 36 A | 67 Watts/Sq Cm | 617.5 | 3040 |
| 37 A | 67 Watts/Sq Cm | 634.6 | 3741 |
| 38 A | 67 Watts/Sq Cm | 651.6 | 4573 |
| 39 A | 67 Watts/Sq Cm | 669.0 | 2717 |
| 40 A | 67 Watts/Sq Cm | 686.2 | 2587 |

(table #E2 continued next page)

Table #E2 Continued: Radiation Experiment #1 (Rad #1) - First Trial
Phenanthrene/ Active Carbon - Sonic Treatment - Background
Corrected Disintegrations/Minute/Milliliter vs Cumulative
Sample Volume Collected at Indicated Probe Energy Level

| Sample ID | Conditions | Cumulative Milliliters (mL) | H# and Background Corrected DPM/mL |
|-----------|----------------|-----------------------------|------------------------------------|
| 41 A | 81 Watts/Sq Cm | 703.2 | 9817.9 |
| 42 A | 81 Watts/Sq Cm | 720.1 | 15382.3 |
| 43 A | 81 Watts/Sq Cm | 737.1 | 26875.4 |
| 44 A | 81 Watts/Sq Cm | 754.0 | 25046.2 |
| 45 A | 81 Watts/Sq Cm | 771.2 | 25377.8 |
| 46 A | 81 Watts/Sq Cm | 788.2 | 24212.9 |
| 47 A | 81 Watts/Sq Cm | 805.3 | 25849.9 |
| 48 A | 81 Watts/Sq Cm | 822.3 | 26350.4 |
| 49 A | 81 Watts/Sq Cm | 839.5 | 26341.2 |
| 50 A | 81 Watts/Sq Cm | 856.8 | 24921.8 |
| 51 A | 0 Watts/Sq Cm | 873.8 | 21935.5 |
| 52 A | 0 Watts/Sq Cm | 890.9 | 22377.1 |
| 53 A | 0 Watts/Sq Cm | 907.9 | 12678.8 |
| 54 A | 0 Watts/Sq Cm | 924.8 | 11959.7 |
| 55 A | 0 Watts/Sq Cm | 941.7 | 11733.1 |
| 56 A | 0 Watts/Sq Cm | 958.6 | 8581.7 |
| 57 A | 0 Watts/Sq Cm | 975.7 | 6078.2 |
| 58 A | 0 Watts/Sq Cm | 992.5 | 5977.5 |
| 59 A | 0 Watts/Sq Cm | 1009.3 | 5376.0 |
| 60 A | 0 Watts/Sq Cm | 1026.1 | 6330.4 |

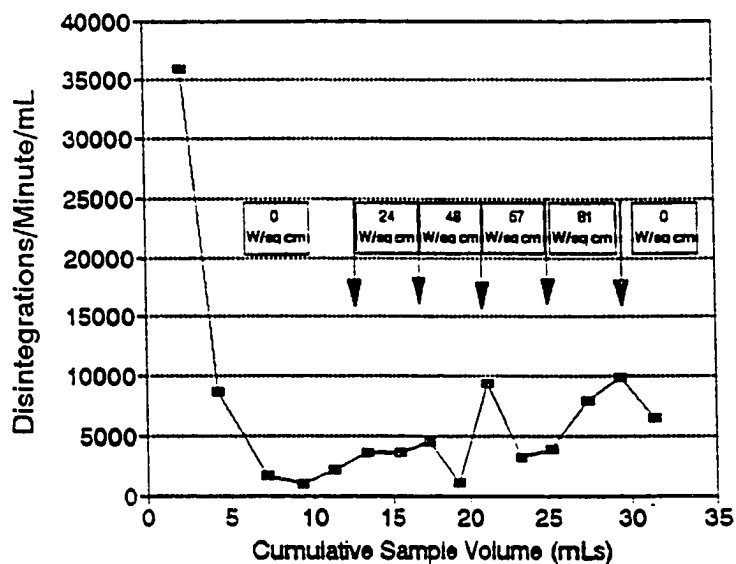


Figure #E2: Radiation Experiment #1 (Rad #1) Second Trial
Phenanthrene/Active Carbon - Sonic Treatment - Background
Corrected Disintegrations/Minute/Milliliter vs Cumulative
Sample Volume Collected at Indicated Probe Tip Energy Level

Table #E3: Radiation Experiment #1 (Rad #1) Second Trial
Phenanthrene/Active Carbon - Sonic Treatment - Background
Corrected Disintegrations/Minute/Milliliter vs Cumulative
Sample Volume Collected at Indicated Probe Tip Energy Level

| Sample ID | Probe Energy Level | Cumulative Milliliters (mL) | H# and Background Corrected DPM/mL |
|-----------|--------------------|-----------------------------|------------------------------------|
| #1 Alpha | 0 Watts/Sq Cm | 2.2 | 35848.6 |
| #2 Alpha | 0 Watts/Sq Cm | 4.2 | 8740.1 |
| #3 Alpha | 0 Watts/Sq Cm | 7.2 | 1681.7 |
| 61 A | 0 Watts/Sq Cm | 9.3 | 979.0 |
| 62 A | 0 Watts/Sq Cm | 11.3 | 2274.6 |
| 63 A | 24 Watts/Sq Cm | 13.3 | 3702.7 |
| 64 A | 24 Watts/Sq Cm | 15.4 | 3657.0 |
| 65 A | 41 Watts/Sq Cm | 17.4 | 4543.6 |
| 66 A | 41 Watts/Sq Cm | 19.2 | 1031.0 |
| 67 A | 67 Watts/Sq Cm | 21.2 | 9441.1 |
| 68 A | 67 Watts/Sq Cm | 23.3 | 3233.9 |
| 69 A | 81 Watts/Sq Cm | 25.2 | 3958.9 |
| 70 A | 81 Watts/Sq Cm | 27.4 | 7886.2 |
| 71 A | 0 Watts/Sq Cm | 29.3 | 9878.5 |
| 72 A | 0 Watts/Sq Cm | 31.4 | 6477.0 |

E.2 Data from Tanana Valley Sand/¹⁴C Phenanthrene Experiments (Radiation Experiments #2 & #3 - Rad #2 and #3)

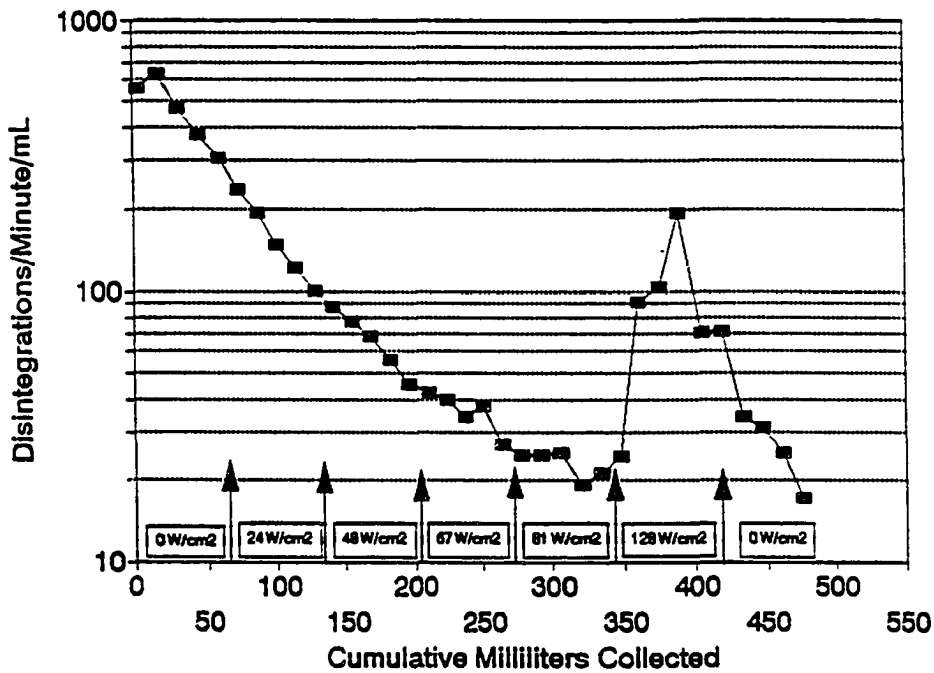


Figure #E3: Radiation Experiment #2 (Rad #2) - Phenanthrene/Tanana Valley Sand - Duplicate Averaged Disintegrations/Minute/Milliliter vs Cumulative Sample Volume Collected at Indicated Probe Tip Energy Level

Table #E4: Radiation Experiment #2 (Rad #2) - 9-¹⁴C Phenanthrene/Tanana Valley Sand - Duplicate Averaged Disintegrations/Minute/ Milliliter vs Cumulative Sample Volume Collected at Indicated Probe Tip Energy Level

| Sample ID | Probe Energy Level | Duplicate Avg DPM/mL | Average Cumulative Milliliters Collected |
|-----------|--------------------|----------------------|--|
| Alpha 1 A | 0 Watts/Sq Cm | 564 | 3.6 |
| Alpha 2 A | 0 Watts/Sq Cm | 638 | 17.1 |
| Alpha 3 A | 0 Watts/Sq Cm | 469 | 30.9 |
| Alpha 4 A | 0 Watts/Sq Cm | 375 | 45.0 |
| Alpha 5 A | 0 Watts/Sq Cm | 310 | 59.2 |
| Alpha 6 A | 24 Watts/Sq Cm | 237 | 73.2 |
| Alpha 7 A | 24 Watts/Sq Cm | 195 | 87.1 |
| Alpha 8 A | 24 Watts/Sq Cm | 148 | 100.7 |
| Alpha 9 A | 24 Watts/Sq Cm | 121 | 114.3 |
| Alpha 10A | 24 Watts/Sq Cm | 100 | 127.9 |
| Alpha 11A | 48 Watts/Sq Cm | 88 | 141.3 |
| Alpha 12A | 48 Watts/Sq Cm | 77 | 154.8 |
| Alpha 13A | 48 Watts/Sq Cm | 69 | 168.5 |
| Alpha 14A | 48 Watts/Sq Cm | 56 | 182.6 |
| Alpha 15A | 48 Watts/Sq Cm | 45 | 196.2 |
| Alpha 16A | 67 Watts/Sq Cm | 42 | 210.1 |
| Alpha 17A | 67 Watts/Sq Cm | 40 | 223.9 |
| Alpha 18A | 67 Watts/Sq Cm | 35 | 237.5 |
| Alpha 19A | 67 Watts/Sq Cm | 38 | 250.8 |
| Alpha 20A | 67 Watts/Sq Cm | 27 | 264.6 |
| Alpha 21A | 81 Watts/Sq Cm | 25 | 278.6 |
| Alpha 22A | 81 Watts/Sq Cm | 25 | 292.4 |
| Alpha 23A | 81 Watts/Sq Cm | 25 | 305.8 |
| Alpha 24A | 81 Watts/Sq Cm | 19 | 320.1 |
| Alpha 25A | 81 Watts/Sq Cm | 21 | 333.4 |
| Alpha 26A | 128 Watts/Sq Cm | 25 | 347.1 |
| Alpha 27A | 128 Watts/Sq Cm | 92 | 360.6 |
| Alpha 28A | 128 Watts/Sq Cm | 104 | 375.0 |
| Alpha 29A | 128 Watts/Sq Cm | 194 | 389.0 |
| Alpha 30A | 128 Watts/Sq Cm | 70 | 404.6 |
| Alpha 31A | 0 Watts/Sq Cm | 71 | 419.3 |
| Alpha 32A | 0 Watts/Sq Cm | 35 | 433.1 |
| Alpha 33A | 0 Watts/Sq Cm | 31 | 447.4 |
| Alpha 34A | 0 Watts/Sq Cm | 25 | 461.4 |
| Alpha 35A | 0 Watts/Sq Cm | 17 | 475.5 |

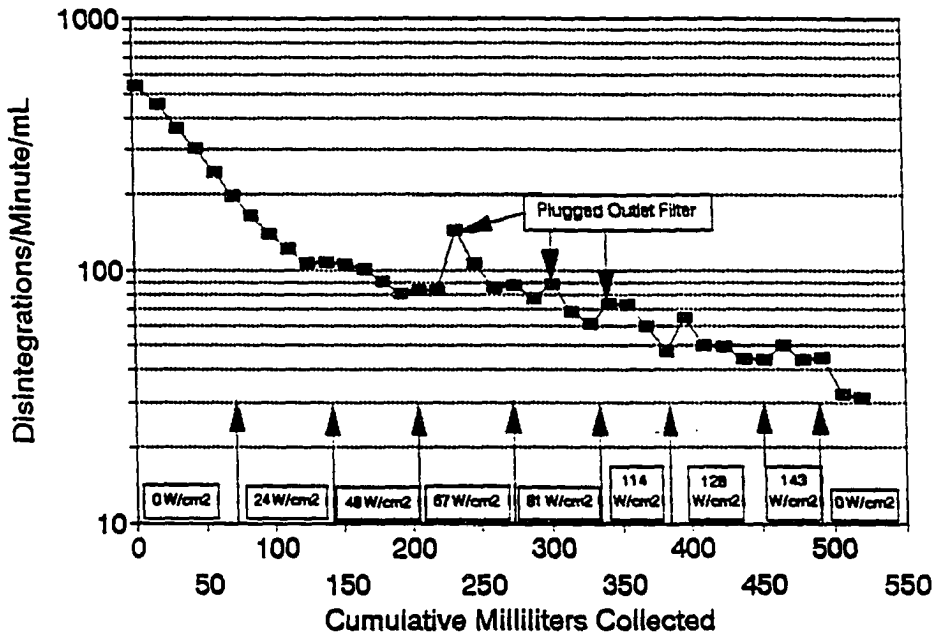


Figure #E4: Radiation Experiment #3 (Rad #3) -Phenanthrene/Tanana Valley Sand Duplicate Average Disintegrations/Minute/Milliliter vs Cumulative Sample Volume Collected at Indicated Probe Tip Energy Level

Table #E5: Radiation Experiment #3 (Rad #3) -Phenanthrene/Tanana Valley Sand Duplicate Average Disintegrations/Minute/Milliliter vs Cumulative Sample Volume Collected at Indicated Probe Tip Energy Level

| Sample Id | Probe energy Watts/Cm ² | Duplicate Avg DPM/ml | Avg Cumulative Milliliters |
|-----------|------------------------------------|----------------------|----------------------------|
| Beta 1A | 0 Watts/Sq Cm | 539 | 3.0 |
| Beta 2A | 0 Watts/Sq Cm | 461 | 17.7 |
| Beta 3A | 0 Watts/Sq Cm | 369 | 31.3 |
| Beta 4A | 0 Watts/Sq Cm | 303 | 44.6 |
| Beta 5A | 0 Watts/Sq Cm | 243 | 57.9 |
| Beta 6A | 24 Watts/Sq Cm | 196 | 71.2 |
| Beta 7A | 24 Watts/Sq Cm | 165 | 84.7 |
| Beta 8A | 24 Watts/Sq Cm | 140 | 98.2 |
| Beta 9A | 24 Watts/Sq Cm | 123 | 111.8 |

(table #E5 continued next page)

Table #E5 Continued: Radiation Experiment #3 (Rad #3) -
Phenanthrene/Tanana Valley Sand Duplicate Average
Disintegrations/Minute/Milliliter vs Cumulative Sample
Volume Collected at Indicated Probe Tip Energy Level

| Sample Id | Probe energy Watts/Cm ² | Average Corrected DPM/mL | Average Cumulative Milliliters |
|-----------|------------------------------------|--------------------------|--------------------------------|
| Beta 10A | 24 Watts/Sq Cm | 107 | 125.1 |
| Beta 11A | 48 Watts/Sq Cm | 109 | 139.3 |
| Beta 12A | 48 Watts/Sq Cm | 106 | 152.7 |
| Beta 13A | 48 Watts/Sq Cm | 101 | 166.1 |
| Beta 14A | 48 Watts/Sq Cm | 91 | 179.4 |
| Beta 15A | 48 Watts/Sq Cm | 82 | 192.4 |
| Beta 16A | 67 Watts/Sq Cm | 84 | 205.2 |
| Beta 17A | 67 Watts/Sq Cm | 84 | 218.9 |
| Beta 18A | 67 Watts/Sq Cm | 144 | 232.6 |
| Beta 19A | 67 Watts/Sq Cm | 107 | 245.9 |
| Beta 20A | 67 Watts/Sq Cm | 86 | 259.7 |
| Beta 21A | 81 Watts/Sq Cm | 88 | 273.8 |
| Beta 22A | 81 Watts/Sq Cm | 77 | 287.9 |
| Beta 23A | 81 Watts/Sq Cm | 89 | 301.7 |
| Beta 24A | 81 Watts/Sq Cm | 68 | 315.2 |
| Beta 25A | 81 Watts/Sq Cm | 61 | 328.8 |
| Beta 26A | 114 Watts/Sq Cm | 74 | 342.0 |
| Beta 27A | 114 Watts/Sq Cm | 73 | 355.2 |
| Beta 28A | 114 Watts/Sq Cm | 60 | 369.0 |
| Beta 29A | 128 Watts/Sq Cm | 47 | 383.1 |
| Beta 30A | 128 Watts/Sq Cm | 65 | 396.6 |
| Beta 31A | 128 Watts/Sq Cm | 50 | 410.3 |
| Beta 32A | 128 Watts/Sq Cm | 50 | 424.0 |
| Beta 33A | 128 Watts/Sq Cm | 45 | 437.9 |
| Beta 34A | 143 Watts/Sq Cm | 44 | 451.8 |
| Beta 35A | 143 Watts/Sq Cm | 51 | 465.1 |
| Beta 36A | 143 Watts/Sq Cm | 44 | 478.7 |
| Beta 37A | 0 Watts/Sq Cm | 45 | 492.2 |
| Beta 38A | 0 Watts/Sq Cm | 32 | 506.4 |
| Beta 39A | 0 Watts/Sq Cm | 31 | 520.0 |

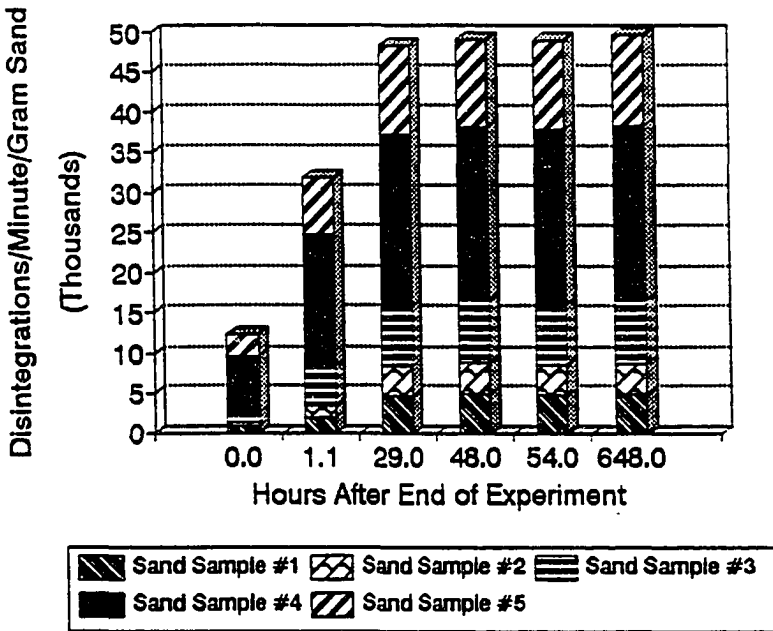


Figure #E5: Radiation Experiment #3 - Liquid Scintillation Count of Residual Radioactivity on Surface of Sand After Sonic Treatment - Wet Sand Samples

Table #E6: Radiation Experiment #3 - Liquid Scintillation Count of Residual Radioactivity on Surface of Sand After Sonic Treatment - Wet Sand Samples

| Sample # | 1 | 2 | 3 | 4 | 5 |
|--------------------|--------|--------|--------|--------|--------|
| Status | wet | wet | wet | wet | wet |
| Weight | 0.1001 | 0.0800 | 0.0832 | 0.0747 | 0.0640 |
| DPM 0.0 Hours AEE* | 889 | 563 | 1,262 | 7,095 | 2,766 |
| DPM 1.1 Hours AEE | 1,968 | 1,588 | 4,988 | 16,386 | 7,094 |
| DPM 29 Hours AEE | 4,625 | 3,850 | 7,500 | 21,553 | 10,984 |
| DPM 48 Hours AEE | 4,885 | 4,050 | 7,680 | 21,714 | 10,984 |
| DPM 54 Hours AEE | 4,755 | 3,863 | 7,584 | 21,995 | 11,125 |
| DPM 648 Hours AEE | 4,904 | 3,914 | 7,913 | 21,854 | 11,363 |

* AEE = After End of Experiment

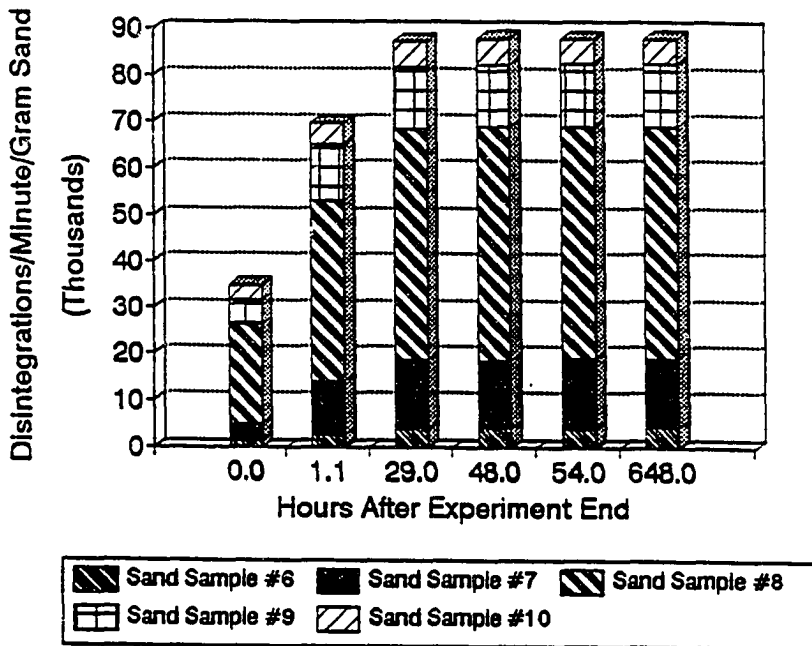


Figure #E6: Radiation Experiment #3 - Liquid Scintillation Count of Residual Radioactivity on Sand Surface After Sonic Treatment - Surface Dried Sand Samples

Table #E7: Radiation Experiment #3 - Liquid Scintillation Count of Residual Radioactivity on Sand Surface After Sonic Treatment - Surface Dried Sand Samples

| Sample # | 1 | 2 | 3 | 4 | 5 |
|--------------------|--------|--------|--------|--------|--------|
| Status | dry | dry | dry | dry | dry |
| Weight | 0.0541 | 0.0630 | 0.0558 | 0.0469 | 0.0413 |
| DPM 0.0 Hours AEE* | 1,442 | 3,650 | 21,362 | 5,501 | 3,341 |
| DPM 1.1 Hours AEE | 2,514 | 11,524 | 39,104 | 12,217 | 4,625 |
| DPM 29 Hours AEE | 3,919 | 14,921 | 49,928 | 13,603 | 5,569 |
| DPM 48 Hours AEE | 4,011 | 14,603 | 50,627 | 13,433 | 5,690 |
| DPM 54 Hours AEE | 3,956 | 15,111 | 50,358 | 13,561 | 5,400 |
| DPM 648 Hours AEE | 4,273 | 14,985 | 50,231 | 13,498 | 5,558 |

* AEE = After End of Experiment

E.3 Data from Glass Beads/UL-¹⁴C Biphenyl Experiments
(Radiation Experiments #4 thru #8 - Rad #4 through #8)

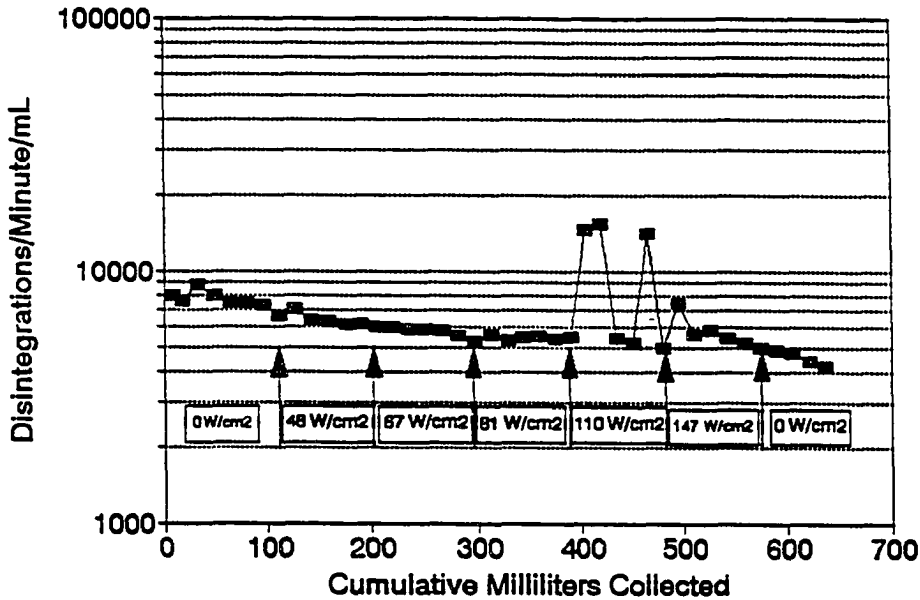


Figure #E7: Radiation Experiment #4 (Rad #4)- Biphenyl Glass Beads - Duplicate Averaged DPM/mL vs Cumulative Sample Volume Collected at Indicated Probe Tip Energy Level

Table #E8: Radiation Experiment #4 (Rad #4) Biphenyl/Glass Bead - Duplicate Averaged Data - Liquid Scintillation Counting Results

| Power Level At Probe Tip | Sample ID | Averaged Cumulative Volume (mLs) | Background and H Number Corrected Averaged DPM/mL |
|-----------------------------|---------------|---|--|
| 0 Watts/Sq Cm | Sample 1-5 | 8.2 | 8304.1 |
| 0 Watts/Sq Cm | A-Gamma 1-2 | 17.6 | 7024.8 |
| 0 Watts/Sq Cm | A-Gamma 4-5 | 33.3 | 8516.9 |
| 0 Watts/Sq Cm | A-Gamma 7-8 | 48.5 | 8118.8 |
| 0 Watts/Sq Cm | A-Gamma 10-12 | 64.2 | 7033.5 |
| 0 Watts/Sq Cm | A-Gamma 13-14 | 80.1 | 7515.3 |
| 0 Watts/Sq Cm | A-Gamma 16-17 | 95.8 | 7328.9 |

(table #E8 continued next page)

Table #E8 Continued: Radiation Experiment #4 (Rad #4)
Biphenyl/Glass Bead - Duplicate Averaged Data -
Liquid Scintillation Counting Results

| Power Level At Probe Tip | Sample ID | Averaged Cumulative Volume (mLs) | Background and H Number Corrected Averaged DPM/mL |
|-----------------------------|-----------------|---|--|
| 48 Watts/Sq Cm | A-Gamma 19-20 | 111.6 | 6704 |
| 48 Watts/Sq Cm | A-Gamma 22-23 | 126.8 | 7100 |
| 48 Watts/Sq Cm | A-Gamma 25-26 | 143.4 | 6341 |
| 48 Watts/Sq Cm | A-Gamma 28-29 | 159.0 | 6340 |
| 48 Watts/Sq Cm | A-Gamma 31-32 | 174.5 | 6220 |
| 48 Watts/Sq Cm | A-Gamma 34-35 | 189.8 | 6315 |
| 67 Watts/Sq Cm | A-Gamma 37-38 | 203.8 | 5994 |
| 67 Watts/Sq Cm | A-Gamma 40-41 | 219.3 | 6098 |
| 67 Watts/Sq Cm | A-Gamma 43-44 | 234.5 | 5823 |
| 67 Watts/Sq Cm | A-Gamma 46-47 | 250.1 | 5829 |
| 67 Watts/Sq Cm | A-Gamma 49-50 | 265.4 | 5915 |
| 67 Watts/Sq Cm | A-Gamma 52-53 | 280.6 | 5528 |
| 81 Watts/Sq Cm | A-Gamma 55-56 | 296.1 | 5216 |
| 81 Watts/Sq Cm | A-Gamma 58-59 | 313.0 | 5521 |
| 81 Watts/Sq Cm | A-Gamma 61-62 | 328.2 | 5334 |
| 81 Watts/Sq Cm | A-Gamma 64-65 | 343.4 | 5597 |
| 81 Watts/Sq Cm | A-Gamma 67-68 | 358.7 | 5596 |
| 81 Watts/Sq Cm | A-Gamma 70-71 | 373.9 | 5319 |
| 110 Watts/Sq Cm | A-Gamma 73-74 | 389.3 | 5504 |
| 110 Watts/Sq Cm | A-Gamma 76-77 | 404.5 | 21599 |
| 110 Watts/Sq Cm | A-Gamma 79-80 | 419.7 | 5642 |
| 110 Watts/Sq Cm | A-Gamma 82-83 | 434.7 | 5537 |
| 110 Watts/Sq Cm | A-Gamma 85-86 | 451.0 | 5480 |
| 110 Watts/Sq Cm | A-Gamma 88-89 | 466.0 | 5458 |
| 147 Watts/Sq Cm | A-Gamma 91-92 | 481.0 | 4773 |
| 147 Watts/Sq Cm | A-Gamma 94-95 | 496.0 | 8326 |
| 147 Watts/Sq Cm | A-Gamma 97-98 | 511.4 | 5667 |
| 147 Watts/Sq Cm | A-Gamma 100-101 | 527.3 | 5825 |
| 147 Watts/Sq Cm | A-Gamma 103-104 | 543.1 | 5442 |
| 147 Watts/Sq Cm | A-Gamma 106-107 | 559.2 | 5360 |
| 0 Watts/Sq Cm | A-Gamma 109-110 | 574.0 | 4962 |
| 0 Watts/Sq Cm | A-Gamma 112-113 | 589.6 | 4925 |
| 0 Watts/Sq Cm | A-Gamma 115-116 | 605.3 | 4667 |
| 0 Watts/Sq Cm | A-Gamma 118-119 | 622.1 | 4450 |
| 0 Watts/Sq Cm | A-Gamma 121-122 | 637.3 | 4201 |

**Table #E9: Radiation Exp #4 (Rad #4) Sonic Treatment - Glass Beads/
Biphenyl - Experimental Parameters and Recovery Data**

| | | |
|--|-----------------------|-----------------------|
| Amount of Radioactivity Added Originally | (DPM) (Micrograms) | 6,641,564.00 60.60 |
| Radioactivity Remaining on Glass Beads and Stir Bar | (DPM) (Micrograms) | 118,785.20 1.08 |
| Radioactivity Remaining in Water at End of Run | (DPM) (Micrograms) | 1,252,605.00 11.43 |
| Radioactivity Remaining on Reactor & Fraction Collector Walls at End of Experiment | (DPM) (Micrograms) | 1,440.00 0.01 |
| Radioactivity Remaining at End of Run on Beads, Spin Bar, and Reactor Walls | (DPM) (Micrograms) | 120185.6 1.097 |
| Total Radioactivity Remaining At End of Run in Water, on Spin Bar, on Reactor Walls and on Beads | (DPM) (Micrograms) | 1,372,830.00 12.53 |
| Total Remaining Radioactivity as a % of Initial Load | (%) | 20.56 |
| Radioactivity on Glass Beads, Stir Bar, and Vessel Walls as a % of Load | (%) | 1.81 |
| Radioactivity Captured in Cold Trap | (DPM) (Micrograms) | 68,340.00 0.62 |
| Radioactivity in Analyzed Sample Fractions | (DPM) (Micrograms) | 1,590,927 14.52 |
| Estimated Radioactivity in Remaining Liquid Fractions | (DPM) (Micrograms) | 2,696,722 24.61 |
| Estimated Overall Recovery | (%) | 86.30 |
| Total mass of Radioactive & Neutral Biphenyl Remaining in the Water and on the Surfaces of the Glass Beads, Reactor Vessel, and Spin Bar | (Micrograms) | 832.44 |

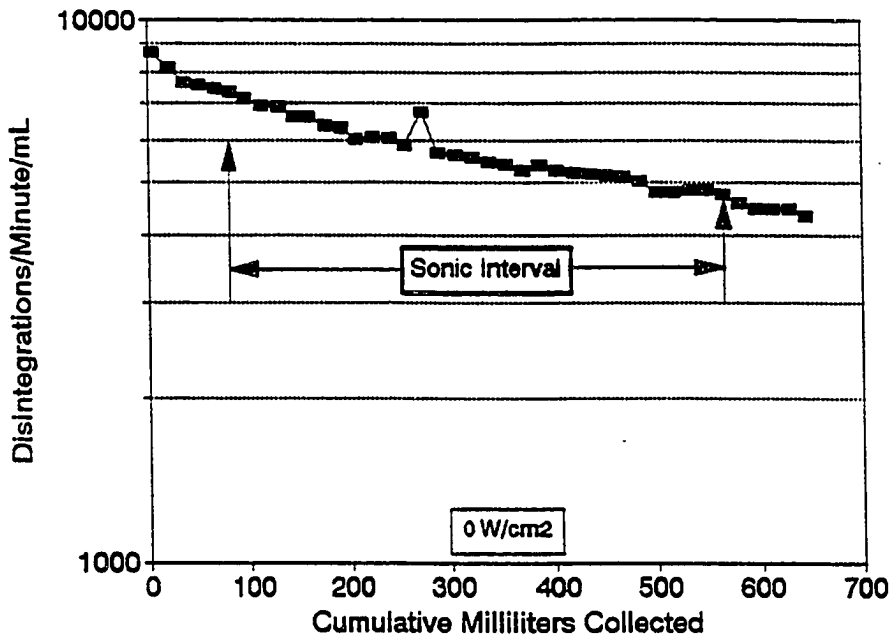


Figure #E8: Radiation Experiment #5 (Rad #5) Control (No Sonic) Biphenyl Glass Beads - Duplicate Averaged DPM/mL vs Cumulative Sample Volume Collected

Table #E10: Radiation Experiment #5 (Rad #5) Biphenyl/Glass Beads - Control - Duplicate Averaged Data - Liquid Scintillation Counting Results

| Power Level At Probe Tip | Sample ID | Averaged Cumulative Volume (mLs) | Background and H Number Corrected Average DPM/mL |
|-----------------------------|---------------|---|---|
| 0 Watts/Sq Cm | B-Gamma 1-2 | 4.5 | 8691 |
| 0 Watts/Sq Cm | B-Gamma 4-5 | 19.5 | 8143 |
| 0 Watts/Sq Cm | B-Gamma 7-8 | 34.9 | 7654 |
| 0 Watts/Sq Cm | B-Gamma 10-11 | 50.3 | 7567 |
| 0 Watts/Sq Cm | B-Gamma 13-14 | 65.7 | 7450 |
| 0 Watts/Sq Cm | B-Gamma 16-17 | 80.8 | 7350 |
| 0 Watts/Sq Cm | B-Gamma 19-20 | 96.1 | 7150 |
| 0 Watts/Sq Cm | B-Gamma 22-23 | 112.6 | 6934 |

(table #E10 continued next page)

Table #E10 Continued: Radiation Experiment #5 (Rad #5)
Biphenyl/ Glass Beads Duplicate Averaged Data -
Liquid Scintillation Counting Results

| Power Level At Probe Tip | Sample ID | Averaged Cumulative Volume (mLs) | Background and H Number Corrected Average DPH/mL |
|-----------------------------|-----------------|---|---|
| 0 Watts/Sq Cm | B-Gamma 25-26 | 129.5 | 6874 |
| 0 Watts/Sq Cm | B-Gamma 28-29 | 145.2 | 6604 |
| 0 Watts/Sq Cm | B-Gamma 31-32 | 158.8 | 6625 |
| 0 Watts/Sq Cm | B-Gamma 34-35 | 175.2 | 6385 |
| 0 Watts/Sq Cm | B-Gamma 37-38 | 190.8 | 6321 |
| 0 Watts/Sq Cm | B-Gamma 40-41 | 206.9 | 6030 |
| 0 Watts/Sq Cm | B-Gamma 43-44 | 223.1 | 6075 |
| 0 Watts/Sq Cm | B-Gamma 46-47 | 240.0 | 6057 |
| 0 Watts/Sq Cm | B-Gamma 49-50 | 256.3 | 5883 |
| 0 Watts/Sq Cm | B-Gamma 52-53 | 272.7 | 6751 |
| 0 Watts/Sq Cm | B-Gamma 55-56 | 289.4 | 5694 |
| 0 Watts/Sq Cm | B-Gamma 58-59 | 305.9 | 5655 |
| 0 Watts/Sq Cm | B-Gamma 61-62 | 322.2 | 5575 |
| 0 Watts/Sq Cm | B-Gamma 64-65 | 337.8 | 5469 |
| 0 Watts/Sq Cm | B-Gamma 67-68 | 354.1 | 5408 |
| 0 Watts/Sq Cm | B-Gamma 70-71 | 369.6 | 5297 |
| 0 Watts/Sq Cm | B-Gamma 73-74 | 385.8 | 5421 |
| 0 Watts/Sq Cm | B-Gamma 76-77 | 401.8 | 5267 |
| 0 Watts/Sq Cm | B-Gamma 79-80 | 417.8 | 5220 |
| 0 Watts/Sq Cm | B-Gamma 82-83 | 433.9 | 5198 |
| 0 Watts/Sq Cm | B-Gamma 85-86 | 449.9 | 5189 |
| 0 Watts/Sq Cm | B-Gamma 88-89 | 466.3 | 5135 |
| 0 Watts/Sq Cm | B-Gamma 91-92 | 482.4 | 5029 |
| 0 Watts/Sq Cm | B-Gamma 94-95 | 498.7 | 4811 |
| 0 Watts/Sq Cm | B-Gamma 97-98 | 515.1 | 4810 |
| 0 Watts/Sq Cm | B-Gamma 100-101 | 532.0 | 4868 |
| 0 Watts/Sq Cm | B-Gamma 103-104 | 547.7 | 4849 |
| 0 Watts/Sq Cm | B-Gamma 106-107 | 563.6 | 4757 |
| 0 Watts/Sq Cm | B-Gamma 109-110 | 579.9 | 4588 |
| 0 Watts/Sq Cm | B-Gamma 112-113 | 595.5 | 4489 |
| 0 Watts/Sq Cm | B-Gamma 115-116 | 611.5 | 4489 |
| 0 Watts/Sq Cm | B-Gamma 118-119 | 628.4 | 4474 |
| 0 Watts/Sq Cm | B-Gamma 121-122 | 644.6 | 4345 |

**Table #E11: Radiation Exp #5 (Rad #5) Control (No Sonic) - Glass Beads/
Biphenyl - Experimental Parameters and Recovery Data**

| | | |
|--|-----------------------|-----------------------|
| Amount of Radioactivity Added Originally | (DPM) (Micrograms) | 6,596,803.90 60.21 |
| Radioactivity Remaining on Glass Beads and Stir Bar | (DPM) (Micrograms) | 500,809.00 4.57 |
| Radioactivity Remaining in Water at End of Run | (DPM) (Micrograms) | 1,439,197.00 13.14 |
| Radioactivity Remaining on Reactor & Fraction Collector Walls at End of Experiment | (DPM) (Micrograms) | 54,588.80 0.498 |
| Radioactivity Remaining at End of Run on Beads, Spin Bar, and Reactor Walls | (DPM) (Micrograms) | 555,461 5.07 |
| Total Radioactivity Remaining At End of Run in Water, on Spin Bar, on Reactor Walls And on Beads | (DPM) (Micrograms) | 1,994,595.00 18.21 |
| Total Remaining Radioactivity as a % of Load | (%) | 30.24 |
| Radioactivity on Glass Beads, Stir Bar, and Vessel Walls as a % of Load | (%) | 8.42 |
| Radioactivity Captured in Cold Trap | (DPM) (Micrograms) | 154,345 1.41 |
| Radioactivity in Analyzed Sample Fractions | (DPM) (Micrograms) | 1,415,706 12.92 |
| Estimated Radioactivity in Remaining Liquid Fractions | (DPM) (Micrograms) | 2,410,254 22.00 |
| Estimated Overall Recovery | (%) | 90.95 |
| Total Mass of Radioactive & Neutral Biphenyl Remaining in the Water and on the Surfaces of the Glass Beads, Reactor Vessel, and Spin Bar | (Micrograms) | 1,224.03 |

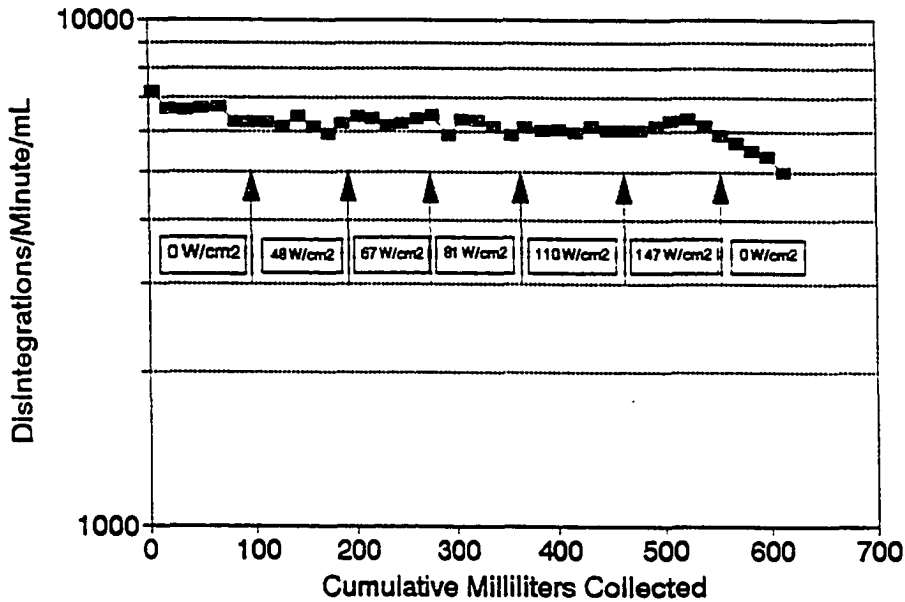


Figure #E9: Radiation Experiment #6 (Rad #6) Sonic Treatment Biphenyl Glass Beads - Duplicate Averaged DPM/mL vs Cumulative Sample Volume Collected at Indicated Probe Tip Energy Level

Table #E12: Radiation Experiment #6 (Rad #6) Sonic Treatment Biphenyl/Glass Beads - Duplicate Averaged Data - Liquid Scintillation Counting Results

| Power Level At Probe Tip | Sample ID | Averaged Cumulative Volume (mLs) | Background and H Number Corrected Average DPM/mL |
|-----------------------------|---------------|---|---|
| 0 Watts/Sq Cm | C-Gamma 1-2 | 3.8 | 7179 |
| 0 Watts/Sq Cm | C-Gamma 4-5 | 18.9 | 6664 |
| 0 Watts/Sq Cm | C-Gamma 7-8 | 34.2 | 6647 |
| 0 Watts/Sq Cm | C-Gamma 10-11 | 49.1 | 6689 |
| 0 Watts/Sq Cm | C-Gamma 13-14 | 65.7 | 6768 |
| 0 Watts/Sq Cm | C-Gamma 16-17 | 81.7 | 6258 |

(table #E12 continued next page)

Table #E12 Continued: Radiation Experiment #6 (Rad #6)
Biphenyl/Glass Beads/Sonic - Duplicate Averaged
Data - Liquid Scintillation Counting Results

| Power Level At Probe Tip | Sample ID | Averaged Cumulative Volume (mLs) | Background and H Number Corrected Average DPM/mL |
|-----------------------------|-----------------|---|---|
| 48 Watts/Sq Cm | C-Gamma 19-20 | 95.8 | 5279 |
| 48 Watts/Sq Cm | C-Gamma 22-23 | 111.0 | 6270 |
| 48 Watts/Sq Cm | C-Gamma 25-26 | 126.8 | 6132 |
| 48 Watts/Sq Cm | C-Gamma 28-29 | 141.9 | 6445 |
| 48 Watts/Sq Cm | C-Gamma 31-32 | 157.2 | 6123 |
| 48 Watts/Sq Cm | C-Gamma 34-35 | 172.4 | 5932 |
| 67 Watts/Sq Cm | C-Gamma 37-38 | 186.1 | 6252 |
| 67 Watts/Sq Cm | C-Gamma 40-41 | 201.0 | 6452 |
| 67 Watts/Sq Cm | C-Gamma 43-44 | 215.6 | 6387 |
| 67 Watts/Sq Cm | C-Gamma 46-47 | 230.6 | 6160 |
| 67 Watts/Sq Cm | C-Gamma 49-50 | 245.4 | 6246 |
| 67 Watts/Sq Cm | C-Gamma 52-53 | 260.4 | 6383 |
| 81 Watts/Sq Cm | C-Gamma 55-56 | 276.6 | 6505 |
| 81 Watts/Sq Cm | C-Gamma 58-59 | 292.6 | 5911 |
| 81 Watts/Sq Cm | C-Gamma 61-62 | 307.4 | 6349 |
| 81 Watts/Sq Cm | C-Gamma 64-65 | 322.5 | 6292 |
| 81 Watts/Sq Cm | C-Gamma 67-68 | 339.1 | 6123 |
| 81 Watts/Sq Cm | C-Gamma 70-71 | 355.4 | 5907 |
| 110 Watts/Sq Cm | C-Gamma 73-74 | 370.3 | 6141 |
| 110 Watts/Sq Cm | C-Gamma 76-77 | 386.3 | 6041 |
| 110 Watts/Sq Cm | C-Gamma 79-80 | 402.0 | 6080 |
| 110 Watts/Sq Cm | C-Gamma 82-83 | 417.8 | 5974 |
| 110 Watts/Sq Cm | C-Gamma 85-86 | 432.6 | 6166 |
| 110 Watts/Sq Cm | C-Gamma 88-89 | 448.8 | 6051 |
| 147 Watts/Sq Cm | C-Gamma 91-92 | 463.4 | 6017 |
| 147 Watts/Sq Cm | C-Gamma 94-95 | 478.6 | 6028 |
| 147 Watts/Sq Cm | C-Gamma 97-98 | 493.6 | 6197 |
| 147 Watts/Sq Cm | C-Gamma 100-102 | 507.9 | 6334 |
| 147 Watts/Sq Cm | C-Gamma 103-104 | 523.3 | 6366 |
| 147 Watts/Sq Cm | C-Gamma 106-107 | 538.5 | 6167 |
| 0 Watts/Sq Cm | C-Gamma 109-110 | 552.8 | 5908 |
| 0 Watts/Sq Cm | C-Gamma 112-113 | 567.5 | 5699 |
| 0 Watts/Sq Cm | C-Gamma 115-116 | 582.8 | 5532 |
| 0 Watts/Sq Cm | C-Gamma 118-119 | 597.1 | 5375 |
| 0 Watts/Sq Cm | C-Gamma 121-122 | 613.1 | 5005 |

Table #E13: Radiation Exp #6 (Rad #6) Sonic Treatment - Glass Beads/
Biphenyl - Experimental Parameters and Recovery Data

| | | |
|--|-----------------------|--------------------|
| Amount of Radioactivity Added Originally | (DPM) (Micrograms) | 6,529,764 59.60 |
| Radioactivity Remaining on Glass Beads and Stir Bar | (DPM) (Micrograms) | 85,034 0.78 |
| Radioactivity Remaining in Water at End of Run | (DPM) (Micrograms) | 1,278,990 11.67 |
| Radioactivity Remaining on Reactor & Fraction Collector Walls at End of Experiment | (DPM) (Micrograms) | 372 0.034 |
| Radioactivity Remaining at End of Run on Beads, Spin Bar, and Reactor Walls | (DPM) (Micrograms) | 8,742 0.81 |
| Total Radioactivity Remaining At End of Run in Water, on Spin Bar, on Reactor Walls and on Beads | (DPM) (Micrograms) | 1,367,751 12.48 |
| Total Remaining Radioactivity as a % of Load | (%) | 20.95 |
| Radioactivity on Glass Beads, Stir Bar, and Vessel Walls as a % of Load | (%) | 1.36 |
| Radioactivity Captured in Cold Trap | (DPM) (Micrograms) | 223,333 2.04 |
| Radioactivity in Analyzed Sample Fractions | (DPM) (Micrograms) | 1,366,779 12.48 |
| Estimated Radioactivity in Remaining Liquid Fractions | (DPM) (Micrograms) | 2,432,318 22.20 |
| Estimated Overall Recovery | (%) | 82.50 |
| Total mass of Radioactive & Neutral Biphenyl Remaining in the Water and on the Surfaces of the Glass Beads, Reactor Vessel, and Spin Bar | (Micrograms) | 835.33 |

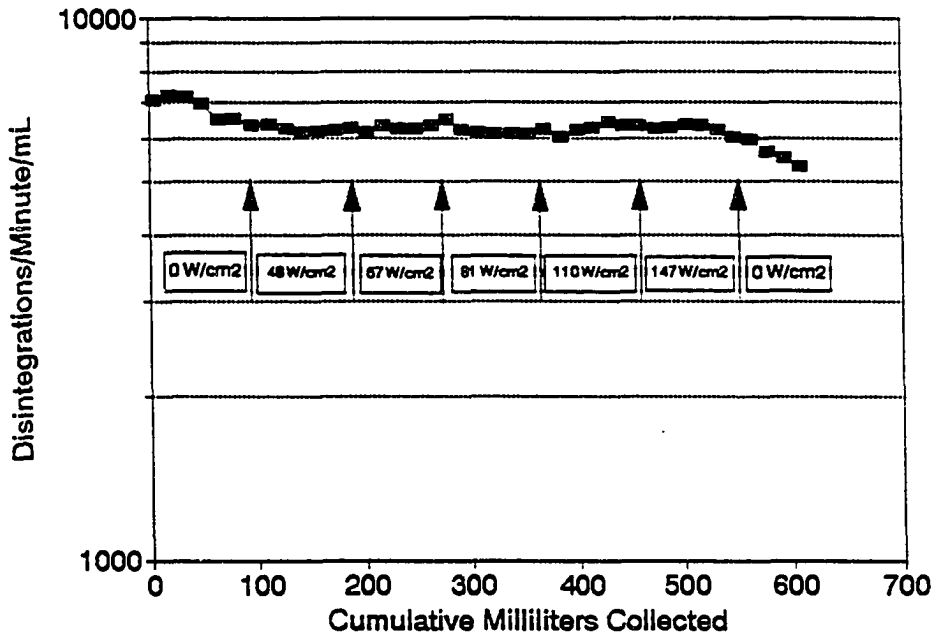


Figure #E10: Radiation Experiment #7 (Rad #7) Biphenyl/Glass Beads
Averaged DPM/mL vs Cumulative Sample Volume Collected at
Indicated Probe Tip Energy Level

Table #E14: Radiation Experiment #7 (Rad #7) Biphenyl/Glass
Beads - Sonic Treatment - Duplicate Averaged Data - Liquid
Scintillation Counting Results

| Power Level At Probe Tip | Sample ID | Averaged Cumulative Volume (mLs) | Background and H Number Corrected Average DPM/mL |
|-----------------------------|---------------|---|---|
| 0 Watts/Sq Cm | D-Gamma 1-2 | 3.9 | 7088.9 |
| 0 Watts/Sq Cm | D-Gamma 4-5 | 18.8 | 7247.3 |
| 0 Watts/Sq Cm | D-Gamma 7-8 | 34.3 | 7176.8 |
| 0 Watts/Sq Cm | D-Gamma 10-11 | 49.0 | 6974.0 |
| 0 Watts/Sq Cm | D-Gamma 13-14 | 64.2 | 6532.0 |
| 0 Watts/Sq Cm | D-Gamma 16-17 | 79.5 | 6549.9 |

(table #E14 continued next page)

Table #E14 Continued: Radiation Experiment #7 (Rad #7)
Sonic Treatment - Biphenyl/Glass Beads -
Duplicate Averaged Data - Liquid Scintillation
Counting Results

| Power Level At Probe Tip | Sample ID | Averaged Cumulative Volume (mLs) | Background and H Number Corrected Average DPM/mL |
|-----------------------------|-----------------|---|---|
| 48 Watts/Sq Cm | D-Gamma 19-20 | 95.5 | 6349 |
| 48 Watts/Sq Cm | D-Gamma 22-23 | 112.3 | 6390 |
| 48 Watts/Sq Cm | D-Gamma 25-26 | 127.7 | 6261 |
| 48 Watts/Sq Cm | D-Gamma 28-29 | 143.2 | 6168 |
| 48 Watts/Sq Cm | D-Gamma 31-32 | 157.7 | 6186 |
| 48 Watts/Sq Cm | D-Gamma 34-35 | 172.9 | 6211 |
| 67 Watts/Sq Cm | D-Gamma 37-38 | 188.2 | 6275 |
| 67 Watts/Sq Cm | D-Gamma 40-41 | 203.0 | 6150 |
| 67 Watts/Sq Cm | D-Gamma 43-44 | 217.8 | 6337 |
| 67 Watts/Sq Cm | D-Gamma 46-47 | 232.9 | 6271 |
| 67 Watts/Sq Cm | D-Gamma 49-50 | 248.0 | 6256 |
| 67 Watts/Sq Cm | D-Gamma 52-53 | 262.6 | 6336 |
| 81 Watts/Sq Cm | D-Gamma 55-56 | 277.5 | 6525 |
| 81 Watts/Sq Cm | D-Gamma 58-59 | 292.8 | 6239 |
| 81 Watts/Sq Cm | D-Gamma 61-62 | 308.1 | 6158 |
| 81 Watts/Sq Cm | D-Gamma 64-65 | 323.4 | 6126 |
| 81 Watts/Sq Cm | D-Gamma 67-68 | 338.7 | 6127 |
| 81 Watts/Sq Cm | D-Gamma 70-71 | 354.1 | 6141 |
| 110 Watts/Sq Cm | D-Gamma 73-74 | 369.2 | 6268 |
| 110 Watts/Sq Cm | D-Gamma 76-77 | 384.5 | 6035 |
| 110 Watts/Sq Cm | D-Gamma 79-80 | 400.2 | 6198 |
| 110 Watts/Sq Cm | D-Gamma 82-83 | 414.1 | 6278 |
| 110 Watts/Sq Cm | D-Gamma 85-86 | 429.3 | 6442 |
| 110 Watts/Sq Cm | D-Gamma 88-89 | 443.7 | 6360 |
| 147 Watts/Sq Cm | D-Gamma 91-92 | 458.6 | 6329 |
| 147 Watts/Sq Cm | D-Gamma 94-95 | 474.2 | 6259 |
| 147 Watts/Sq Cm | D-Gamma 97-98 | 488.0 | 6278 |
| 147 Watts/Sq Cm | D-Gamma 100-101 | 502.7 | 6399 |
| 147 Watts/Sq Cm | D-Gamma 103-104 | 517.3 | 6353 |
| 147 Watts/Sq Cm | D-Gamma 106-107 | 532.0 | 6200 |
| 0 Watts/Sq Cm | D-Gamma 109-110 | 547.2 | 6038 |
| 0 Watts/Sq Cm | D-Gamma 112-113 | 562.3 | 5965 |
| 0 Watts/Sq Cm | D-Gamma 115-116 | 577.2 | 5667 |
| 0 Watts/Sq Cm | D-Gamma 118-119 | 592.5 | 5539 |
| 0 Watts/Sq Cm | D-Gamma 121-122 | 608.0 | 5338 |

**Table #E15: Radiation Exp #7 (Rad #7) Sonic Treatment - Glass Beads/
Biphenyl - Experimental Parameters and Recovery Data**

| | | |
|--|-----------------------|--------------------|
| Amount of Radioactivity Added Originally | (DPM) (Micrograms) | 7,022,695 64.10 |
| Radioactivity Remaining on Glass Beads and Stir Bar | (DPM) (Micrograms) | 308,297 2.81 |
| Radioactivity Remaining in Water at End of Run | (DPM) (Micrograms) | 1,685,987 15.39 |
| Radioactivity Remaining on Reactor & Fraction Collector Walls at End of Experiment | (DPM) (Micrograms) | 5,971 0.055 |
| Radioactivity Remaining at End of Run on Beads, Spin Bar, and Reactor Walls | (DPM) (Micrograms) | 314,433 2.87 |
| Total Radioactivity Remaining At End of Run in Water, on Spin Bar, on Reactor Walls And on Beads | (DPM) (Micrograms) | 2,000,255 18.26 |
| Total Remaining Radioactivity as a % of Load | (%) | 28.48 |
| Radioactivity on Glass Beads, Stir Bar, and Vessel Walls as a % of Load | (%) | 4.48 |
| Radioactivity Captured in Cold Trap | (DPM) (Micrograms) | 99,385 0.91 |
| Radioactivity in Analyzed Sample Fractions | (DPM) (Micrograms) | 1,353,561 12.35 |
| Estimated Radioactivity in Remaining Liquid Fractions | (DPM) (Micrograms) | 2,487,822 22.71 |
| Estimated Overall Recovery * | (%) | 84.60 |
| Total mass of Radioactive & Neutral Biphenyl Remaining in the Water and on the Surfaces of the Glass Beads, Reactor Vessel, and Spin Bar | (Micrograms) | 1,136 |

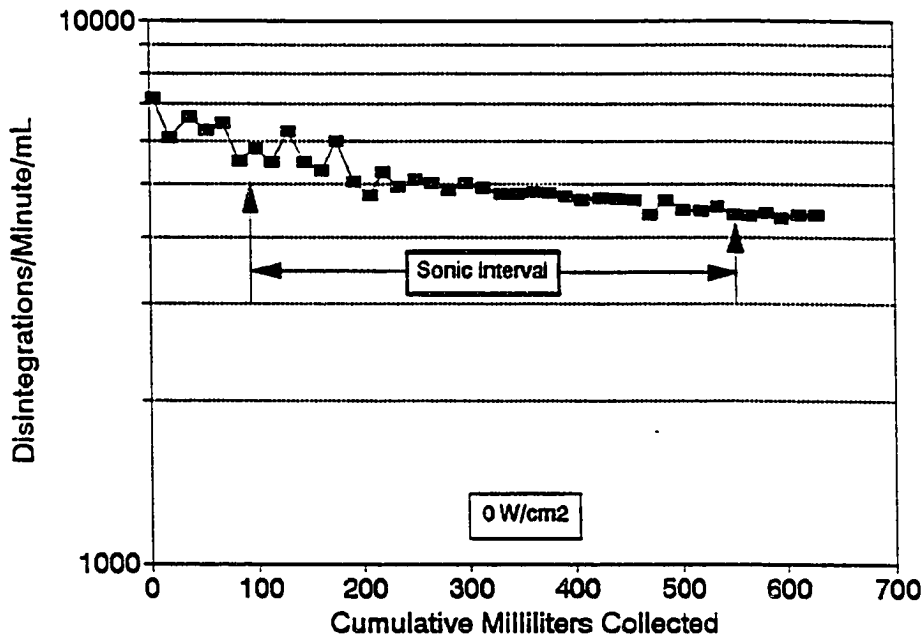


Figure #E11: Radiation Experiment #8 (Rad #8) - Control (No Sonic)
Biphenyl Glass Beads - Averaged DPM/mL vs Cumulative
Sample Volume Collected

Table #E16: Radiation Experiment #8 (Rad #8) - Control
(No Sonic) Biphenyl/Glass Beads/Control -
Duplicate Averaged Data - Liquid Scintillation
Counting Results

| Power Level At Probe Tip | Sample ID | Averaged Cumulative Volume (mLs) | Background and H Number Corrected Average DPM/mL |
|-----------------------------|---------------|---|---|
| 0 Watts/Sq Cm | E-Gamma 1-2 | 4.2 | 7208 |
| 0 Watts/Sq Cm | E-Gamma 4-5 | 19.7 | 6110 |
| 0 Watts/Sq Cm | E-Gamma 7-8 | 37.7 | 6667 |
| 0 Watts/Sq Cm | E-Gamma 10-11 | 53.1 | 6281 |
| 0 Watts/Sq Cm | E-Gamma 13-14 | 68.5 | 6471 |
| 0 Watts/Sq Cm | E-Gamma 16-17 | 83.7 | 5532 |

(table #E16 continued next page)

Table #E16 Continued: Radiation Experiment #8 (Rad #8) -
Control (No Sonic) Biphenyl/Glass Beads/Control -
Duplicate Averaged Data - Liquid Scintillation
Counting Results

| Power Level At Probe Tip | Sample ID | Averaged Cumulative Volume (mLs) | Background and H Number Corrected Average DPM/mL |
|-----------------------------|-----------------|---|---|
| 0 Watts/Sq Cm | E-Gamma 19-20 | 99.0 | 5804 |
| 0 Watts/Sq Cm | E-Gamma 22-23 | 114.7 | 5485 |
| 0 Watts/Sq Cm | E-Gamma 25-26 | 130.2 | 6266 |
| 0 Watts/Sq Cm | E-Gamma 28-29 | 145.8 | 5515 |
| 0 Watts/Sq Cm | E-Gamma 31-32 | 161.2 | 5318 |
| 0 Watts/Sq Cm | E-Gamma 34-35 | 176.2 | 6003 |
| 0 Watts/Sq Cm | E-Gamma 37-38 | 192.0 | 5046 |
| 0 Watts/Sq Cm | E-Gamma 40-41 | 207.6 | 4783 |
| 0 Watts/Sq Cm | E-Gamma 43-44 | 219.6 | 5253 |
| 0 Watts/Sq Cm | E-Gamma 46-47 | 234.6 | 4979 |
| 0 Watts/Sq Cm | E-Gamma 49-50 | 249.9 | 5108 |
| 0 Watts/Sq Cm | E-Gamma 52-53 | 265.4 | 5021 |
| 0 Watts/Sq Cm | E-Gamma 55-56 | 280.7 | 4888 |
| 0 Watts/Sq Cm | E-Gamma 58-59 | 297.1 | 5025 |
| 0 Watts/Sq Cm | E-Gamma 61-62 | 314.1 | 4927 |
| 0 Watts/Sq Cm | E-Gamma 64-65 | 330.8 | 4810 |
| 0 Watts/Sq Cm | E-Gamma 67-68 | 345.7 | 4807 |
| 0 Watts/Sq Cm | E-Gamma 70-71 | 360.9 | 4864 |
| 0 Watts/Sq Cm | E-Gamma 73-74 | 376.3 | 4831 |
| 0 Watts/Sq Cm | E-Gamma 76-77 | 392.0 | 4740 |
| 0 Watts/Sq Cm | E-Gamma 79-80 | 407.3 | 4684 |
| 0 Watts/Sq Cm | E-Gamma 82-83 | 424.0 | 4724 |
| 0 Watts/Sq Cm | E-Gamma 85-86 | 439.3 | 4717 |
| 0 Watts/Sq Cm | E-Gamma 88-89 | 454.7 | 4692 |
| 0 Watts/Sq Cm | E-Gamma 91-92 | 469.9 | 4412 |
| 0 Watts/Sq Cm | E-Gamma 94-95 | 485.6 | 4695 |
| 0 Watts/Sq Cm | E-Gamma 97-98 | 502.3 | 4501 |
| 0 Watts/Sq Cm | E-Gamma 100-101 | 519.0 | 4476 |
| 0 Watts/Sq Cm | E-Gamma 103-104 | 535.2 | 4560 |
| 0 Watts/Sq Cm | E-Gamma 106-107 | 551.1 | 4415 |
| 0 Watts/Sq Cm | E-Gamma 109-110 | 565.5 | 4381 |
| 0 Watts/Sq Cm | E-Gamma 112-113 | 580.5 | 4442 |
| 0 Watts/Sq Cm | E-Gamma 115-116 | 595.6 | 4331 |
| 0 Watts/Sq Cm | E-Gamma 118-119 | 610.8 | 4407 |
| 0 Watts/Sq Cm | E-Gamma 121-122 | 627.2 | 4412 |

Table #E17: Radiation Exp #8 (Rad #8) Control (No Sonic) - Glass Beads/
Biphenyl - Experimental Parameters and Recovery Data

| | | |
|--|-----------------------|-----------------------|
| Amount of Radioactivity Added Originally | (DPM) (Micrograms) | 6,965,504 63.58 |
| Radioactivity Remaining on Glass Beads and Stir Bar | (DPM) (Micrograms) | 547,843.97 5.00 |
| Radioactivity Remaining in Water at End of Run | (DPM) (Micrograms) | 1,690,974.80 15.43 |
| Radioactivity Remaining on Reactor & Fraction Collector Walls at End of Experiment | (DPM) (Micrograms) | 196,974.30 1.79 |
| Radioactivity Remaining at End of Run on Beads, Spin Bar, and Reactor Walls | (DPM) (Micrograms) | 743,901.80 6.79 |
| Total Radioactivity Remaining At End of Run in Water, on Spin Bar, on Reactor Walls And on Beads | (DPM) (Micrograms) | 2,434,894.00 22.23 |
| Total Remaining Radioactivity as a % of Load | (%) | 34.96 |
| Radioactivity on Glass Beads, Stir Bar, and Vessel Walls as a % of Load | (%) | 10.68 |
| Radioactivity Captured in Cold Trap | (DPM) (Micrograms) | 174,730 1.59 |
| Radioactivity in Analyzed Sample Fractions | (DPM) (Micrograms) | 1,135,272 10.36 |
| Estimated Radioactivity in Remaining Liquid Fractions | (DPM) (Micrograms) | 2,048,256 18.70 |
| Estimated Overall Recovery | (%) | 83.10 |
| Total mass of Radioactive & Neutral Biphenyl Remaining in the Water and on the Surfaces of the Glass Beads, Reactor Vessel, and Spin Bar | (Micrograms) | 1,394.09 |

E.4 Linear Regression Analysis of Plotted Data from Radiation Experiments Number Five Through Eight (Rad #5 Through Rad #8)

This section contains tabular and graphical data; the product of a linear regression analysis of the logarithm of disintegrations/minute/milliliter (DPM/mL - ordinate) vs cumulative collected sample volume (mLs - abscissa) at various ultrasonic field strengths. The data interval analyzed included those samples taken while active ultrasonic treatment occurred during experiments when sonic energy was applied to the system. The interval containing these sample points is referred to as the "sonic interval" and occurs in the range of samples numbered 19 through 107 in both the ultrasound and control (no ultrasound) experiments. The two data sets for control runs (rad #5 and #8) were combined prior to regression analysis. Similarly, sonic interval data sets from sonic runs (rad #6 and #7) were also combined prior to regression analysis. Because of difficulties encountered during method development (see section E5) the data from radiation experiment #4 was not included in the formulation of the linear regression slope estimate comparison presented below.

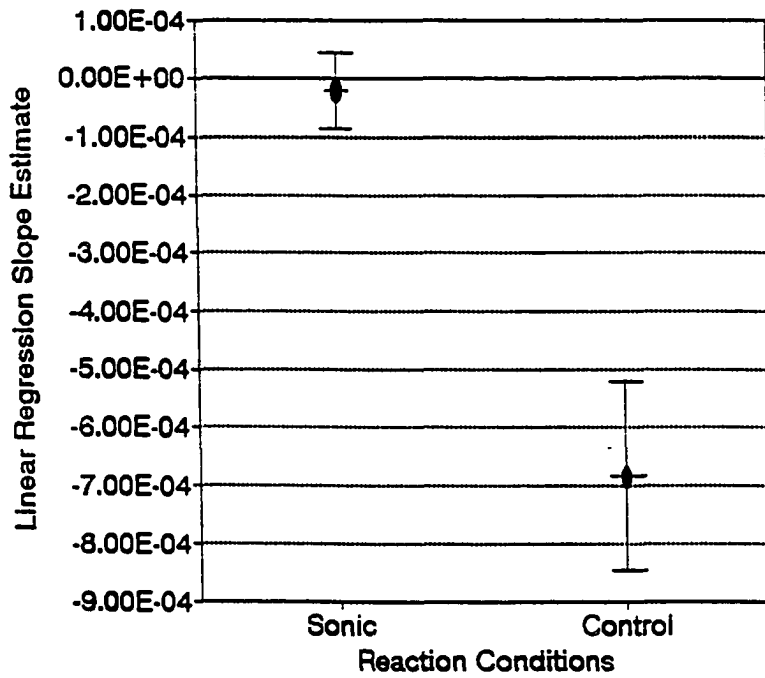


Figure #E12: Comparison of Calculated Desorption Linear Regression Slope Estimates for Sonic and Control (No Sonic) Experiments - 99% Confidence Interval

Table #E18: 99% Confidence Intervals of Calculated Desorption Linear Regression Slope Data - Sonic and Control (No Ultrasound) Sonic Interval Data

| Rad # | 99% Confidence <-----Interval-----> | | |
|-----------------|--|---------------|-------------------------------|
| | Low Slope Interval Points | Average Slope | High Slope Interval Points |
| 6 & 7 Sonic | 4.2922E-05 | -2.1124E-05 | -8.5170E-05 |
| #5 & #8 Control | -5.1933E-04 | -6.8390E-04 | -8.4847E-04 |

E.5 Method Development for Glass Beads/UL-¹⁴C Biphenyl Experiments

Development of a methodology to study the desorption of UL-¹⁴C biphenyl from the surface of glass beads resulted in difficulties during the first experimental trial of the sequence (rad #4). Because of these difficulties the data from radiation experiment #4 was not directly comparable to subsequent ultrasonic treatment experiments (rad #6 and #7) and was not used in the construction of the linear regression slope estimates used to compare control (no sonic) and sonic experiments. However, since a comparison of the slopes of plotted data was used to validate the enhanced transport of UL-¹⁴C biphenyl from the surface of the glass beads a more complete summary of the experimental difficulty encountered and its impact on the outcome of data analysis is presented here.

During the first glass bead/UL-¹⁴C biphenyl experiment (Rad #4) a few of the glass beads with adsorbed contaminant floated to the surface of the water as the flask was being filled. In addition, small crystals were also observed floating on the surface of the liquid. This material was presumably undissolved biphenyl. An attempt to submerge the crystals and dislodge the glass beads from the surface by varying the speed of the magnetic stirrer was unsuccessful. Filling was continued in an attempt to dissolve more

biphenyl from the surface of the liquid and from the surface of the beads; causing the latter to fall to the bottom of the flask. When the flask had been filled completely to the outlet level, however, the beads and some of the crystalline material remained at the surface. The liquid was allowed to stir for approximately 15 minutes without significant change in the status of the system. At the end of this time the solution was heated with hot water in the external water bath, to aid dissolution of the biphenyl. After a few minutes at approximately 40°C the beads became dislodged from the surface of the liquid but a small amount of the crystalline material remained floating on the surface. This crystalline material remained at the surface of the liquid throughout the early stages of the experiment. When 81 watts/cm² of ultrasonic energy was applied to the reactor, however, the liquid circulation pattern changed. This caused some of the crystalline material to be ejected, with bubbles of gas, from the flask through the outlet line and into the collection vials. The result of this problem can be observed at cumulative sample volumes (389 - 560 mLs) in figure E7.

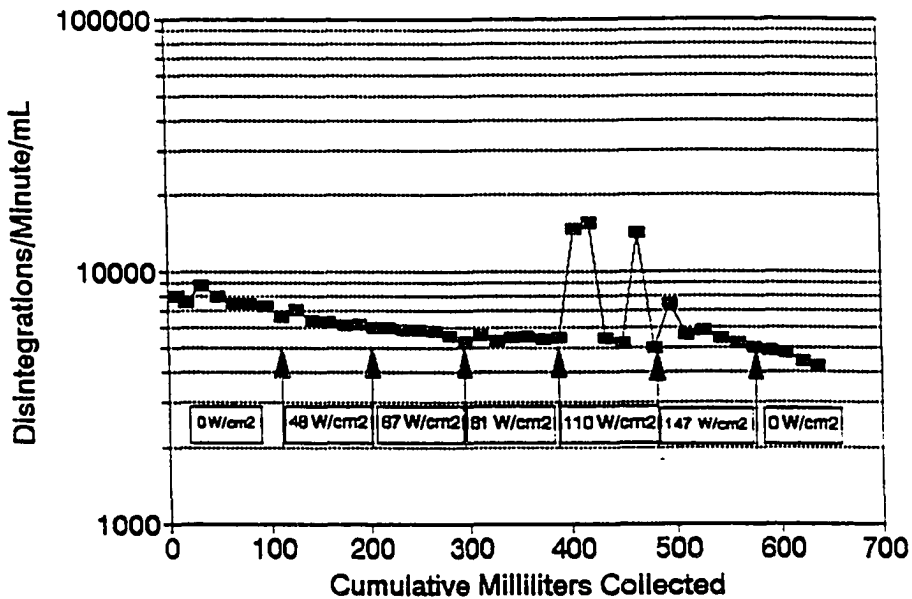


Figure #E7: Radiation Experiment #4 (Rad #4) - Biphenyl/Glass Beads - Averaged DPM/mL vs Cumulative Sample Volume Collected

A similar problem with floating material occurred in radiation experiment #5 (Rad #5), a control run without applied sonic energy. However, in this case the situation was somewhat alleviated by filling the reaction vessel more slowly with liquid. Glass beads with adsorbed biphenyl did not float to the surface of the liquid but crystalline material remained at the surface throughout the experiment. No major change in circulation patterns occurred in this reaction to cause bubbles to form in the outlet line, as had occurred in the radiation exp #4 in response to the applied field, and only one transient peak of radioactivity occurred

after 265 cumulative milliliters of sample had been collected
(See figure E8 below).

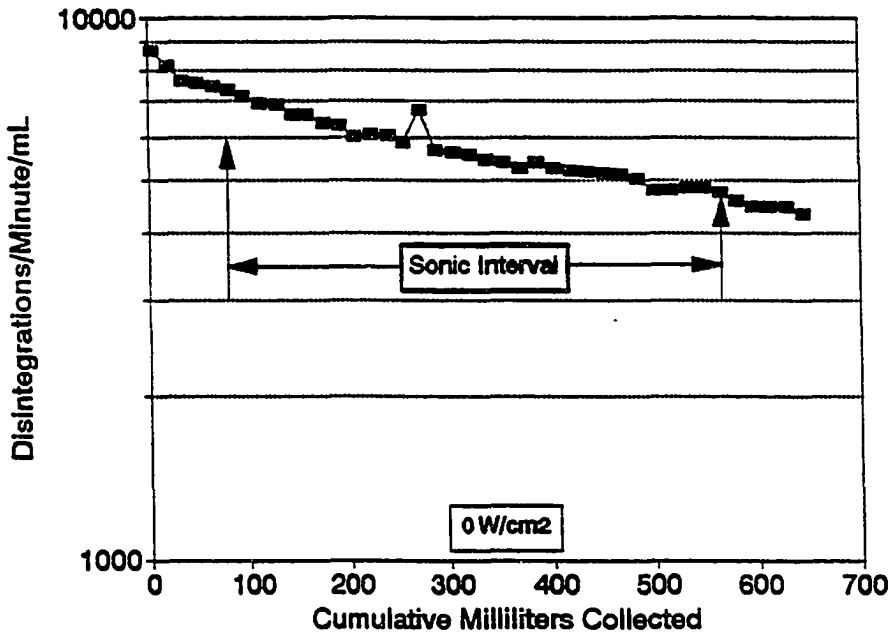


Figure #E8: Radiation Experiment #5 (Rad #5) Control (No Sonic) Biphenyl Glass Beads - Averaged DPM/mL vs Cumulative Sample Volume Collected

This single peak was probably due to a small crystal being swept into the outlet line. The crystalline material remaining on the surface of the liquid throughout the length of the run appears to indicate that the reaction mixture remained saturated with biphenyl throughout the experimental procedure.

Experimental runs Rad #6 through Rad #8 were treated somewhat differently. In these procedures the reaction

flask was filled with water to approximately the half full level (ca 150 mL) and vigorous stirring was then initiated. This procedure resulted in two major changes to the system:

(1) The crystalline material on the surface of the liquid was dispersed throughout the liquid; and

(2) The floating glass beads, with adsorbed contaminant, were forced to the bottom of the flask by the vortexing action of the magnetic stirrer. These changes gave rise to an apparent increase in dispersed crystalline material throughout the reaction vessel. The presence of this dispersed crystalline material is evident in the data plot of control (no sonic) Radiation experiment #8 (Rad #8).

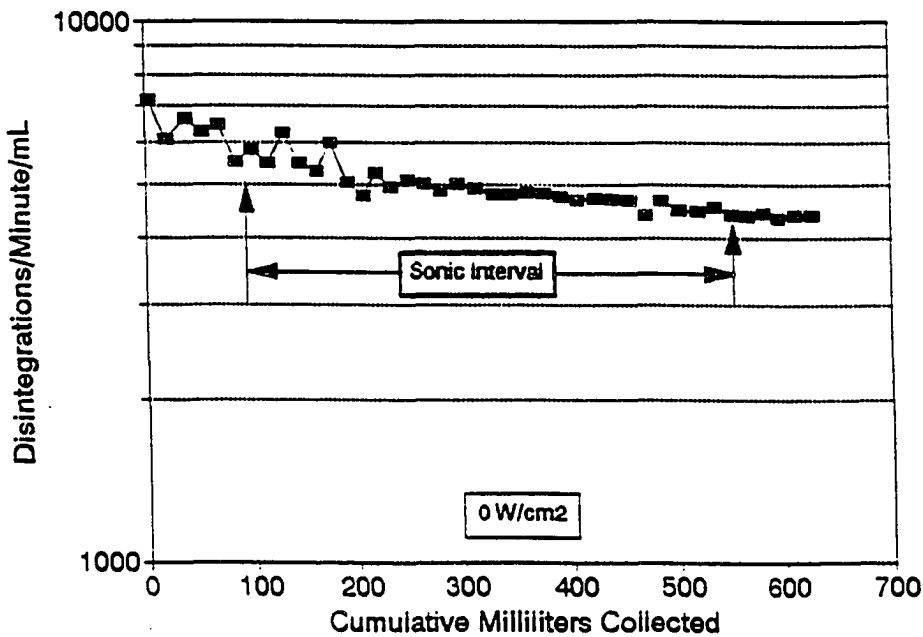


Figure #E11: Radiation Experiment #8 (Rad #8) - Control (No Sonic)
Biphenyl/Glass Beads - Duplicate Averaged DPM/mL vs
Cumulative Sample Volume Collected

E.6 Conversion from disintegrations per minute to mass measure

Generalized conversion calculation from Disintegrations per minute for 9-¹⁴C phenanthrene to mass of Phenanthrene

| X DPM | 1 micro- curie | 1 milli- curie | 1 milli- mole | 178 milli- grams | = Y milligrams |
|----------|-------------------|----------------------|----------------------|---------------------|----------------|
| | 2,220,000 DPM | 1000 micro- curie | 13.1 milli- curie | milli- mole | |

Generalized conversion calculation from Disintegrations per minute for UL-¹⁴ biphenyl to mass of biphenyl

| X DPM | 1 micro- curie | 1 milli- curie | 1 milli- mole | 154 milli- grams | = Y milligrams |
|----------|-------------------|----------------------|---------------------|---------------------|----------------|
| | 2,220,000 DPM | 1000 micro- curie | 7.6 milli- curie | milli- mole | |